

imperial College of Science and Technology
(University of London)

**TRANSIENT RESPONSE OF
MECHANICAL STRUCTURES
USING MODAL ANALYSIS
TECHNIQUES.**

BY

ANGELA BURGESS

A thesis submitted in partial fulfilment for the
degree of Doctor of Philosophy, and for the
Diploma of Imperial College.

Department of Mechanical Engineering,
imperial College, London SW7.
J a n u a r y 1 9 8 8 .

Research at a public
research establishment.
ARE(Portland)

ABSTRACT

The use of experimental modal analysis techniques together with Fourier transform methods is considered for their application to the transient response analysis of structures. The limitations and validity of this approach are examined for linear structures, and a relationship derived that describes the errors involved due to time aliasing within the inverse discrete Fourier transform. The method is demonstrated with a simple beam using several experimental modal analysis procedures.

The applicability of the same analysis and prediction techniques to non-linear structures is explored. The use of constant-force stepped-sine excitation and subsequent circle-fit modal analysis procedures for identifying non-linearities is reviewed. Also, the reciprocal-of-receptance analysis is extended for classifying and quantifying the non-linearity present.

Results from non-linear systems subjected to impulse excitation are examined using various analyses. It is found that clear trends are evident for different non-linearities, but they do not correspond to those from a constant-force stepped-sine test.

Techniques for predicting the transient response for non-linear systems using data from experimental tests are examined, with the result that several different approaches are recommended depending on the non-linearity, the initial conditions and the type and accuracy required of the results. These prediction methods include using a specific linear model and developing non-linear models that accurately describe the transient response.

Multi-degree-of-freedom systems with one non-linear element are also examined, as in many practical structures the non-linearity tends to be concentrated in a single component. The trends exhibited in the individual non-linear elements subjected to experimental modal analysis are found to correspond to those trends found in the resonances of the multi-degree-of-freedom systems. Similarly, the recommended techniques for transient response prediction of a non-linear structure correspond to those for non-linear elements under the same conditions.

CONTENTS

| | Page |
|---|------|
| Abstract. | 2 |
| List of tables. | 8 |
| List of figures. | 10 |
| Acknowledgements. | 16 |
| 1 INTRODUCTION. | |
| 1.1 Background and overview. | 17 |
| 1.2 Objectives. | 18 |
| 1.3 Contents of the thesis. | 18 |
| 2 A REVIEW OF TRANSIENT RESPONSE ANALYSIS METHODS. | |
| 2.0 Introduction. | 21 |
| 2.1 Time domain methods. | 22 |
| 2.1 .1 Numerical methods. | 22 |
| 2.1.2 Duhamet's integral. | 23 |
| 2.1.3 Graphical methods. | 25 |
| 2.2 Frequency domain methods. | 26 |
| 2.2.1 Shock response spectra. | 26 |
| 2.2.2 Fourier transform methods. | 29 |
| 2.3 Discussion. | 31 |

| | Page |
|---|------|
| 3 A REVIEW OF FREQUENCY RESPONSE METHODS FOR STRUCTURAL MODELLING. | |
| 3.0 Introduction. | 32 |
| 3.1 Summary of essential modal theory. | 33 |
| 3.2 Experimental testing for frequency response of structures. | 37 |
| 3.3 Extracting modal properties from experimental frequency response data. | 41 |
| 3.3.1 Single-degree-of-freedom (SDOF) analysis. | 41 |
| 3.3.2 Multi-degree-of-freedom (MDOF) analysis. | 43 |
| 3.3.3 Time domain analysis. | 45 |
| 3.4 Application of frequency response data and modal parameters. | 46 |
| 3.4.1 From modal model to spatial model. | 46 |
| 3.4.2 Response prediction in the frequency domain. | 47 |
| 3.4.3 Frequency response coupling for structural assemblies. | 47 |
| 3.5 Discussion. | 49 |
| Figures for chapter 3. | 50 |
| 4 REQUIREMENTS FOR TRANSIENT RESPONSE ANALYSIS USING FREQUENCY RESPONSE. | |
| 4.0 Introduction. | 56 |
| 4.1 Fourier transform - from theory to practice. | 58 |
| 4.2 Limitations of using the 'Fourier transform method within the DFT. | 61 |
| 4.2.1 Frequency aliasing and windowing. | 61 |
| 4.2.2 Errors due to time aliasing. | 62 |
| 4.3 Limitations of using the 'Fourier transform method. resulting from errors in experimental data. | 65 |
| 4.3.1 Consequences of linear damping model. | 65 |
| 4.3.2 Accuracy of experimental data. | 66 |
| 4.3.3 Effect of the out-of-range modes. | 68 |
| 4.4 Case study - Transient response analysis of a beam. | 70 |
| 4.5 Discussion. | 73 |
| Tables for chapter 4. | 75 |
| Figures for chapter 4. | 78 |

| | Page |
|---|------|
| 5 RESPONSE CHARACTERISTICS OF NON-LINEAR ELEMENTS USING MODAL TESTING TECHNIQUES. | |
| 5.0 Introduction. | 101 |
| 5.1 Some examples of non-linear elements found in practice. | 103 |
| 5.1.1 Stiffness type non-linearities. | 103 |
| 5.1.2 Damping type non-linearities. | 105 |
| 5.2 Frequency response measurement of non-linear elements. | 107 |
| 5.3 Frequency response characteristics from sine tests. | 109 |
| 5.3.1 Characteristics in the measured Bode plot. | 110 |
| 5.3.2 Modal parameters obtained from SDOF analysis. | 112 |
| 5.3.3 Hilbert transform. | 115 |
| 5.3.4 Characteristics using 'standard' sine excitation. | 115 |
| 5.4 Response characteristics from impulse tests. | 116 |
| 5.4.1 Characteristics of the time-histories. | 116 |
| 5.4.2 Data trends in the frequency domain from impulse excitation. | 118 |
| 5.5 Comparison of response characteristics in the time domain. | 121 |
| 5.6 Discussion. | 123 |
| Tables for chapter 5. | 125 |
| Figures for chapter 5. | 136 |

| | Page |
|---|------|
| 6 TRANSIENT RESPONSE PREDICTION OF NON-LINEAR ELEMENTS USING DATA FROM MODAL TESTS. | |
| 6.0 Introduction. | 181 |
| 6.1 Summary of routes for transient response prediction. | 182 |
| 6.2 Transient response prediction for a cubic stiffness element. | 184 |
| 6.3 Transient response prediction for a system with backlash. | 187 |
| 6.4 Transient response prediction for a system with bi-linear stiffness. | 190 |
| 6.5 Transient response prediction for a system with friction. | 192 |
| 6.6 Transient response prediction for an element with quadratic viscous damping. | 194 |
| 6.7 Discussion. | 196 |
| Tables for chapter 6. | 197 |
| Figures for chapter 6. | 198 |
| | |
| 7 RESPONSE ANALYSIS OF MDOF SYSTEMS WITH A NON-LINEAR ELEMENT. | |
| 7.0 Introduction. | 211 |
| 7.1 System definition. | 212 |
| 7.2 Application of prediction techniques for transient response of MDOF non-linear systems. | 213 |
| 7.3 Modal analysis of non-linear systems. | 215 |
| 7.4 Transient response of non-linear systems via the frequency domain. | 218 |
| 7.4 Discussion. | 220 |
| Tables for chapter 7. | 222 |
| Figures for chapter 7. | 232 |

| | Page | |
|---|--|-----|
| 8 CONCLUDING DISCUSSION. | | |
| 8.0 Introduction. | 252 | |
| 8.1 Discussion. | 252 | |
| 8.2 Recommendations for transient response predictions. | 256 | |
| 8.3 Suggestions for further research. | 260 | |
| | | |
| 9 REFERENCES. | 261 | |
| | | |
| 10 APPENDICES. | | |
| Appendix 1 | Summary of essential modal theory. | 279 |
| Appendix 2 | Summary of SDOF modal analysis methods. | 284 |
| Appendix 3 | MDOF curve fitting for lightly damped structures. | 289 |
| Appendix 4 | Basic impedance coupling theory. | 291 |
| Appendix 5 | Free decay for systems with viscous or hysteretic damping. | 292 |
| Appendix 6 | Determination of friction damping from reciprocal-of-receptance analysis. | 294 |
| Appendix 7 | Development of a non-linear model for the transient response prediction of a friction element. | 296 |

List of tables

| | Page | |
|------------|---|-----------|
| 4.1 | Modal parameters for theoretical 12 mode structure. | 75 |
| 4.2 | Modal parameters from FRF data obtained using stepped-sine excitation. | 76 |
| 4.3 | Modal parameters from FRF data obtained using random and impulse excitations. | 77 |
| 5.1 | Trends in frequency domain displays from non-linear systems subjected to sine testing. | 125 |
| 5.2 | Various parameters evaluated from a single constant-force stepped-sine test of a system with cubic stiffness. | 126 |
| 5.3 | Various parameters evaluated from a single constant-force stepped-sine test of a system with backlash. | 127 |
| 5.4 | Various parameters evaluated from a single constant-force stepped-sine test of a system with friction. | 128 |
| 5.5 | Various parameters evaluated from a single constant-force stepped-sine test of a system with quadratic viscous damping. | 129 |
| 5.6 | Trends in frequency domain displays from non-linear systems subjected to impulse excitation. | 130 |
| 5.7 | Various parameters evaluated from a single impulse test of a system with cubic stiffness. | 131 |
| 5.8 | Various parameters evaluated from a system with backlash subjected to an impulse. | 132 |
| 5.9 | Parameters from the 'modes' of a bi-linear system subjected to a single impulse. | 133 |
| 5.10 | Various parameters evaluated from a system with friction subjected to an impulse. | 134 |
| 5.11 | Various parameters evaluated from a system with quadratic viscous damping subjected to an impulse. | 135 |

| | Page |
|---|------|
| 6.1 Data from analysis of systems with backlash type non-linearity subjected to constant-force stepped-sine tests and reciprocal-of-receptance analysis using data either above or below resonance and averaging the two results. | 197 |
| 7.1 Physical description of each 2 degree-of-freedom system. | 222 |
| 7.2 Parameters from mode 1 point 1,1. | 223 |
| 7.3 Parameters from mode 2 point 1,1. | 224 |
| 7.4 Parameters from mode 1 point 1,2. | 225 |
| 7.5 Parameters from mode 2 point 1,2. | 226 |
| 7.6 Parameters from mode 1 point 2,1. | 227 |
| 7.7 Parameters from mode 2 point 2,1. | 228 |
| 7.8 Parameters from mode 1 point 2,2. | 229 |
| 7.9 Parameters from mode 2 point 2,2. | 230 |
| 7.10 Results from using 'Ident' type analysis of point (2,2) of the 2 degree-of-freedom system with bi-linear stiffness. | 231 |

List of figures

| | Page |
|--|------|
| 2.1 Shock response spectra for a half-sine pulse. | 28 |
| 3.1 Bode plot using linear frequency axis and log response. | 50 |
| 3.2 Nyquist display with frequency information included. | 50 |
| 3.3 Data from sine test - Coarse log frequency sweep followed by fine linear frequency sweeps around resonance. | 51 |
| 3.4 Measured FRF from random excitation on a structure, linear frequency spacing over the full frequency range. | 51 |
| 3.5 Nyquist analysis. | 52 |
| 3.6 reciprocal-of-receptance analysis. | 53 |
| 3.7 Effect of MDOF extension to SDOF analysis. | 54 |
| 3.8 Effect of residuals on regenerated FRF data. | 55 |
| 4.1 Common windows and their frequency components. | 78 |
| 4.2 Comparison of time-histories transformed from SDOF modal models with equivalent linear damping. | 79 |
| 4.3 Comparison of time-histories transformed from SDOF modal models with equivalent linear damping. | 80 |
| 4.4 Effect of errors in natural frequency on the predicted time-history of a theoretical 12 mode system. | 81 |
| 4.5 Effect of errors in the magnitude of the modal constant on the predicted time-history of a theoretical 12 mode system. | a2 |
| 4.6 Effect of errors in the phase of the modal constant on the predicted time-history of a theoretical 12 mode system. | 83 |
| 4.7 Effect of errors in the damping estimate on the predicted time-history of a theoretical 12 mode system. | 84 |
| 4.8 Displacement time-histories from a theoretical 12 mode system. | 85 |
| 4.9 Velocity time-histories from a theoretical 12 mode system. | 86 |
| 4.10 Acceleration time-histories from a theoretical 12 mode system. | 87 |
| 4.11 Displacement time-histories from a theoretical 12 mode system: effect of high frequency modes. | 88 |

| | Page |
|--|------|
| 4.12 Velocity time-histories from a theoretical 12 mode system: effect of high frequency modes. | 89 |
| 4.13 Acceleration time-histories from a theoretical 12 mode system: effect of high frequency modes. | 90 |
| 4.14 Solution routes for the 'Fourier transform method' of transient response prediction. | 91 |
| 4.15 Experimental setups for aluminium beam. | 92 |
| 4.16 Measured input force signal. | 93 |
| 4.17 Measured acceleration time-history from point (3,1). | 93 |
| 4.18 Predicted acceleration time-histories from point (3,1). | 94 |
| 4.19 Comparison of initial predictions (with extra damping) from point (3,1) | 97 |
| 5.1 Stiffness-type non-linearities. | 136 |
| 5.2 Damping-type non-linearities. | 137 |
| 5.3 Examples of the differences in the Bode plots due to changing input force level. | 138 |
| 5.4 Trends in Bode plots from a system with cubic stiffness. | 139 |
| 5.5 Trends in Bode plots from a systems with backlash. | 140 |
| 5.6 Trends in Bode plots from a systems with bi-linear stiffness. | 141 |
| 5.7 Trends in Bode plots from a systems with friction. | 142 |
| 5.8 Detail of trends near resonance in Bode plots from systems with quadratic viscous damping. | 143 |
| 5.9 Trends in the frequency domain from a system with hardening cubic stiffness. | 144 |
| 5.10 Trends in the frequency domain from a system with backlash. | 145 |
| 5.11 Trends in the frequency domain from a system with bi-linear stiffness. | 146 |
| 5.12 Trends in the frequency domain from the first harmonic of a system with bi-linear stiffness. | 147 |
| 5.13 Trends in the frequency domain from a system with friction. | 148 |
| 5.14 Trends in the frequency domain from a system with quadratic viscous damping. | 149 |

| | Page |
|--|------|
| 5.15 Time-histories from a linear system. | 150 |
| 5.16 Time-histories from systems with cubic stiffness. | 152 |
| 5.17 Time-histories from a system with backlash. | 154 |
| 5.18 Time-histories from a system with bi-linear stiffness. | 156 |
| 5.19 Time-histories from a system with friction. | 158 |
| 5.20 Time-histories from a system with quadratic viscous damping. | 160 |
| 5.21 Trends in the frequency domain from systems with cubic stiffness subjected to impulse excitation. | 162 |
| 5.22 Trends in the frequency domain from the first harmonic resonance of fig (5.21 a). | 163 |
| 5.23 Trends in the frequency domain from systems with backlash subjected to impulse excitation. | 164 |
| 5.24 Trends in the frequency domain from the first harmonic resonance of fig (5.23a). | 165 |
| 5.25 Bode plot from a system with bi-linear stiffness (ratio 4:1) subjected to an impulse. | 166 |
| 5.26 Nyquist, 3-D damping and reciprocal-of-receptance plots of the resonances of fig (5.25). | 167 |
| 5.27 Trends in the frequency domain from systems with friction subjected to impulse excitation. | 172 |
| 5.28 Trends in reciprocal-of-receptance plots from systems with friction subjected to impulse excitation. | 173 |
| 5.29 Trends in the frequency domain from systems with quadratic viscous damping subjected to impulse excitation. | 174 |
| 5.30 Comparison of time-histories from a linear system using data from an impulse test and transformed sine test data. | 175 |
| 5.31 Comparison of time-histories from a system with cubic stiffness using data from an impulse test and transformed sine test data. | 176 |
| 5.32 Comparison of time-histories from a system with backlash using data from an impulse test and transformed sine test data. | 177 |

| | Page |
|--|-------------|
| 5.33 Comparison of time-histories from a system with bi-linear stiffness using data from an impulse test and transformed sine test data. | 178 |
| 5.34 Comparison of time-histories from a system with friction using data from an impulse test and transformed sine test data. | 179 |
| 5.35 Comparison of time-histories from a system with quadratic viscous damping using data from an impulse test and transformed sine test data. | 180 |
| 6.1 Solution routes for impulse response functions (IRFs) of non-linear systems. | 198 |
| 6.2 Exact and predicted transient response of a system with cubic stiffness; $v(0)=1.0$ m/s. | 199 |
| 6.3 Exact and predicted transient response of a system with cubic stiffness. | 200 |
| 6.4 Exact and predicted transient response of a system with backlash; gap is approx. 1% of max. disp. | 201 |
| 6.5 Exact and predicted transient response of a system with backlash; gap is approx. 10% of max. disp. | 202 |
| 6.6 Exact and predicted transient response of a system with backlash: gap is approx. 5% of max. disp. | 203 |
| 6.7 Examples of the IRF of a system with bi-linear stiffness; Spring ratio 1 :16. | 204 |
| 6.8 Exact and predicted transient response of a system with friction; using a linear model; $v(0)=1.0$ m/s. | 205 |
| 6.9 Exact and predicted transient response of a system with friction; using a linear model. | 206 |
| 6.10 Exact and predicted transient response of a system with friction: using a non-linear model. | 207 |
| 6.11 Exact and predicted transient response of a system with quadratic viscous damping. | 208 |
| 6.12 Exact and predicted transient response of a system with quadratic viscous damping; using a linear model. | 209 |

| | Page |
|--|------|
| 6.13 Solution routes for transient response predictions of various non-linear systems. | 210 |
| 7.1 FRFs from a linear system. | 232 |
| 7.2 FRFs from a system with cubic stiffness subjected to a constant-force sine test (force amplitude 75). | 233 |
| 7.3 FRFs from a system with backlash subjected to a constant-force sine test (force amplitude 1). | 234 |
| 7.4 FRFs from a system with bi-linear stiffness subjected to a constant-force sine test. | 235 |
| 7.5 FRFs from a system with friction subjected to a constant-force sine test (force amplitude 0.1). | 236 |
| 7.6 FRFs from a system with quadratic viscous damping subjected to a constant-force sine test (force amplitude 2). | 237 |
| 7.7 IRFs from a system with cubic stiffness and a linear system; $v(0)=1.0$ m/s. | 238 |
| 7.8 IRFs from a system with cubic stiffness and a linear system; $v(0)=5.0$ m/s. | 239 |
| 7.9 IRFs from a system with cubic stiffness and a linear system; $v(0)=10.0$ m/s. | 240 |
| 7.10 IRFs from a system with backlash and a linear system; $v(0)=1.0$ m/s. | 241 |
| 7.11 IRFs from a system with backlash and a linear system; $v(0)=5.0$ m/s. | 242 |
| 7.12 IRFs from a system with backlash and a linear system; $v(0)=0.1$ m/s. | 243 |
| 7.13 IRFs from a system with backlash and a linear system; $v(0)=0.05$ m/s. | 244 |
| 7.14 IRF from a system with bi-linear stiffness. | 245 |
| 7.15 Predicted IRF for a system with bi-linear stiffness using a linear model with the softer of the two springs. | 245 |
| 7.16 Predicted IRF for a system with bi-linear stiffness using a linear model with the stiffer of the two springs. | 246 |

| | Page |
|--|------|
| 7.17 Predicted IRF for a system with bi-linear stiffness using a linear model with the average of the two springs. | 246 |
| 7.18 IRFs from a system with friction and a linear system; $v(0)=0.5$ m/s. | 247 |
| 7.19 IRFs from a system with friction and a linear system; $v(0)=0.1$ m/s. | 248 |
| 7.20 IRFs from a system with friction and a linear system; $v(0)=0.05$ m/s. | 249 |
| 7.21 IRFs from a system with quadratic viscous damping and a linear system; $v(0)=1.0$ m/s. | 250 |
| 7.22 IRFs from a system with quadratic viscous damping and a linear system; $v(0)=5.0$ m/s. | 251 |

ACKNOWLEDGEMENTS

The work in this thesis was carried out with the support of the Ministry of Defence, who entirely funded this research project.

The author wishes to thank her supervisors, Professor D. J. Ewins (Imperial College) and Dr. D. A. C. Parkes (Admiralty Research Establishment, Portland), for their continued help and enthusiasm throughout the duration of this project. Thanks are also due to colleagues in the Imperial College Dynamics Group, both past and present, and at the Admiralty Research Establishment, Portland, particularly Dr. R. M. Thompson and Mr R. W. Windell, for their advice and encouragement over the years. The author also thanks Mrs P. J. Thompson for her help in typing this thesis.

1 INTRODUCTION

1.1 Background and overview

Shock loading of a submarine may cause damage to important on-board systems. This damage ranges in severity depending on the level of shock but in extreme cases may render the submarine unserviceable, or unable to return safely to base. Shock protection of critical on-board systems is therefore essential, and it is necessary to be able to predict the transient response of these systems to the expected shock loading in order to determine the shock protection requirements.

One obvious approach to this requirement is shock testing of the systems of interest to a standard specified by relevant interested parties. There are several problems in the shock testing of structures, including the expense and availability of full-size models and the logistics of running such a test. Using scale models is an alternative, but there are still problems in scaling the required parameters and in extrapolating the results to the required shock standard on a full-size system. Also, it is usual to have only a few of the full size components to test, with scale models of some of the other systems and analytical models of the remaining components, and the subsequent mathematical models all require combining in some form to provide a complete description of the total structure.

Several techniques exist for the transient response prediction of structures, but all the methods require a mathematical description of the structure. In situations where mathematical models do not exist there is a requirement to construct such a model from experimental tests. Experimental modal analysis methods are an alternative route for evaluating mathematical models. Experimental modal analysis covers the testing of the structure - eg by stepped-sine excitation, random excitation or impact testing - and the subsequent analysis of the data - in either the frequency or the time domain - to obtain a frequency response model of a structure. As some of the sub-structures of a submarine are too complex to be modelled theoretically, and models for these will need to be obtained from experimental data, the use of

transient response prediction methods with experimental data is an important topic.

All systems are to some degree non-linear; therefore, the use of transient response prediction methods for non-linear structures with mathematical models derived by modal analysis techniques is an important area for investigation as it is reasonable to assume that most of the on-board systems of a submarine are non-linear.

1.2 Objectives

As experimental modal analysis methods can be used to determine mathematical models of structures far more easily, and at less expense, than by calculating a model from shock tests, a primary objective of this research is to explore the potential for using experimental modal analysis data to evaluate suitable parameters for the prediction of the response of the structure to a shock input. An essential component of this study is to determine the limitations and restrictions placed on the experimental analysis techniques and the transient response prediction methods used, and the subsequent accuracy of the results. In particular, the special problems in predicting the transient response of structures with non-linear components using models derived from experimental modal analysis are to be addressed as these conditions represent the closest to real-life applications.

1.3 Contents of the thesis

Initially, methods available for transient response prediction are reviewed. All the techniques, whether working in the time or in the frequency domains, require a mathematical model of the structure. The Fourier transform approach uses a frequency response model of the structure, and as such is perhaps the most appropriate method for use with experimental data. Frequency response models are often determined using modal analysis methods, and experimental modal analysis techniques are reviewed in chapter 3, including both the testing and the data analysis procedures. Also included in that

chapter is a section on the process of coupling together frequency response measurements on separate components in order to evaluate the response characteristics of the complete structure formed by their assembly.

The Fourier transform method is considered in detail in chapter 4, with a brief review of Fourier theory followed by an examination of the requirements of the frequency response data for accurate transient response predictions. These requirements have implications for the experimental and analytical procedures used to obtain the frequency response data as it is found that errors in the modal parameters can result in large deviations of the predicted transient response from the true response. In terms of the data used in the transform, the usual criterion of a sample rate of twice the maximum frequency content avoid frequency aliasing is mentioned, and also a maximum frequency spacing for any given system to avoid time aliasing when transforming from the frequency to the time domain has been developed. Both forms of aliasing are considered. This technique for transient response prediction is suitable for linear systems provided that certain constraints are observed in the quality of data, and in the digitisation of the frequency response for the transform.

Attention is then turned to the problems associated with non-linear structures. In chapter 5 the application of modal analysis techniques to non-linear structures is examined in terms of the ability of the techniques to identify and quantify a non-linearity. Of particular interest is the *reciprocal-of-receptance* method which is found to be a powerful tool in distinguishing between damping and stiffness type non-linearities, and the method is easily adapted for some non-linearities to enable specific non-linear parameters to be evaluated.

Examination of the results in the frequency response data from transient excitation again shows distinct trends for each non-linearity considered, but these are not generally the same as the trends seen in frequency response data for the same non-linearity but measured via a constant-force sine test. As the results of the frequency response data vary considerably, the impulse response functions from the two excitation techniques are compared, and again there is found to be very little agreement.

Predictions for the impulse response functions of non-linear elements are examined in chapter 6. Two approaches are considered; using the frequency response functions from modal analysis, or developing a non-linear model from experimental data specifically for use in transient response predictions. The linear approach is suitable for several applications, but generally using a specific set of modal parameters (several different sets of modal parameters can be evaluated from a single measurement of a non-linear structure). The modal parameters recommended so as to ensure acceptable results are derived for various non-linearities. The limitations on the validity and accuracy of any prediction is examined and it is found that for some non-linearities the linear approach generates good predictions, whilst for others a non-linear model must be developed if accurate predictions are required. However, non-linear models can be very complex: a separate model needs to be developed for each type of non-linearity, and the resulting non-linear model will only be valid for transient response predictions and would generate large errors if used for steady-state response predictions. Therefore, non-linear models should only be used where necessary, and not as standard practice.

In chapter 7 the extension of these techniques for application to multi-degree-of-freedom systems is considered. The trends for identifying the presence and type of non-linearity remain unchanged from the corresponding single-degree-of-freedom element. The transient response predictions using the linear parameters evaluated as recommended from the single-degree-of-freedom elements are also examined.

Finally, the results of the work are summarised in the form of recommendations of how to use experimental modal analysis in transient response predictions, for both linear and non-linear structures. For linear structures, future developments in modal analysis techniques may enable parameters to be evaluated that are a closer approximation to those of the real structure and hence result in a better transient response prediction. However, further research is envisaged into many aspects of the transient response prediction of non-linear structures using experimental data.

2 A REVIEW OF TRANSIENT RESPONSE ANALYSIS METHODS

2.0 Introduction

The requirements for a transient structural response analysis vary from one application to another. For some analyses a single-degree-of-freedom (SDOF) model is sufficient, whilst in other cases a more detailed multi-degree-of-freedom (MDOF) model is necessary. Further, the need for an approach to non-linearities in the system ranges from ignoring them altogether to attempting to model the non-linearity in detail. To satisfy this range of requirements, many different transient response analysis methods have been developed, working in both the time and the frequency domains. The presentation of results also differs with the analysis and application from showing only the maximum response to displaying the full time history. The aim of this chapter is to review the methods available for transient response analysis of theoretical and real structures. In considering the various alternatives, the primary concern is the applicability of each method for the prediction of transient responses of complex structures using experimental data as a means of describing their properties.

The first part of the chapter is concerned with time domain methods, including time-marching solutions, Duhamel's integral method and graphical techniques. Frequency domain methods are then examined. Shock spectra are used when only the maximum values of response are of interest, and the Fourier transform approach is examined in detail for use with frequency response data.

Many engineering structures that are subjected to transient loading are often too complex to be theoretically modelled in full. For these structures, some or all of the components may need to be described by experimental data. In these situations the experimental description of the structure is usually in the frequency domain as frequency response functions or modal data, in which case the most appropriate technique for transient response analysis is to use a Fourier transform-based approach.

2.1 Time domain methods

This section reviews the techniques available for transient response analysis in the time domain. The first group of methods considered solve the equations of motion of the structure numerically. These types of analysis are suitable for SDOF or MDOF components, and can also be adapted for non-linear systems. Duhamel's integral method is considered next: this is based on the principle of convolution and is primarily applicable to linear models whose impulse response functions can be expressed analytically. Finally in this section, graphical approaches are mentioned: these analyses are performed on SDOF elements or individual modes of vibration of a structure and, when the non-linearity in a system is known, graphical analysis can easily be adapted to include the effect.

All of the methods in this section require a knowledge of the properties of the system. This makes the time domain techniques better suited to the transient response analysis of structures that can easily be modelled theoretically than those that need to be described by experimental data. Duhamel's integral and graphical approaches are developed for SDOF systems: these techniques can be applied to MDOF systems but the accuracy of the solution is less than for the SDOF example. Numerical solutions are attractive for real structures as the solutions are for MDOF systems and several of the methods can be adapted for non-linear components - the problem being that in our case not all the structures are analytic and therefore the form of any non-linearity is not known. This means that the equations of motion can not be formulated theoretically.

2.1.1 Numerical methods

Many different algorithms exist for the step-by-step solution of differential equations. The choice of method for use in a particular case depends on many factors including, the form and type of the equations, the known boundary conditions and the speed or accuracy required. Chan and Newmark [1] assess many of them, and methods are well documented by other authors (eg [2] to [7]). The Newmark- β method (refs [8] to [11]) is a general numerical procedure that has been developed for transient structural response analysis.

The choice of β in the equation determines the variation of acceleration within the time step, so that stability and convergence of the calculation is dependent on the value of β . Use of the **Newmark- β** - or any numerical solution - requires a knowledge of the system parameters (ie mass and stiffness). If the structure is too complex to be modelled theoretically a description of the component can be obtained by using experimental modal analysis. There are also other types of numerical solution for MDOF systems which provide an approximate response using only a few of the modes (eg mode superposition method [12]). These methods are more efficient when - as is often the case in shock response - the first few modes contribute the majority of the response.

The **Newmark- β** method has been extended to include non-linear elements and, once the non-linear parameters have been obtained, solves the equations without linearisation. A finite difference method [13] has been developed that is similar to the **Newmark- β** method but is in a form that will accept any form of non-linearity. Also, Lyons et al [14] suggested using a two stage solution for non-linear systems. The first stage is to solve the equations of motion directly using a numerical method to calculate an equivalent non-linear force. This calculation is performed using only the non-linear components and a small number of low frequency linear modes - as the response of non-linear elements is primarily affected by those linear modes of vibration. In the second stage, this equivalent non-linear force is substituted into the equations of motion for the non-linear terms and the equations for the full system are solved using the more efficient transform analysis.

2.1.2 Duhamel's Integral

Duhamel's Integral method and the Superposition Integral are two names that are used to describe the convolution integral when it is applied to structural dynamics. Convolution is an important operation in linear systems theory, and the theory of convolution and its applications are well covered in the many text books available that examine linear systems (eg [15] to [25]).

The convolution integral as applied to transient vibration analysis is an exact solution for the linear system. The integral treats the input ($f(t)$) as a series of impulses of various magnitudes, and assumes that the response ($x(t)$) is given by the sum of responses to all the impulses. The response can be written as:

$$x(t) = \int_0^t f(\tau)h(t-\tau)d\tau$$

where $h(t)$ is the impulse response function of the system.

To perform Duhamel's integral, the impulse response function of the system needs to be determined. This can be calculated by several different methods:

(i) for a simple system whose equation of motion is known, the equation can be solved using the initial conditions of an impulse ($x(0)=0$, $\dot{x}(0)=\text{impulse/mass}$) to give the impulse response function.

(ii) the impulse response function can also be found by taking the inverse Laplace transform of the system transfer function ($H(s)$).

$$h(t)=L^{-1}(H(s))$$

In practice, the impulse response function can be obtained by:

(iii) applying a step forcing function to the system, and differentiating the consequent response to obtain the impulse response function;

(iv) applying a high-level pulse whose duration is short compared with the upper cut-off frequency of the system so as to simulate an impulse. The response is taken as $h(t)$;

(v) a random noise input, whose spectral density is flat, is applied to the system and the cross correlation function between the input and the output is computed. This is $H(\omega)$, the system frequency response function, and $h(t)$ is obtained by inverse Fourier transforming $H(\omega)$.

Often, the response is required to transient inputs applied simultaneously at several different sites on the structure. To extend this method for multi-site excitation requires a knowledge of how the point of interest responds to an impulse at each point of excitation. The total response at point i is then given by a summation of the integrals at the response point of interest with the M excitation points.

$$x_i(t) = \sum_{j=1}^M \int_0^t f_j(t') h_{ij}(t-t') dt'$$

The integrals can become complicated for MDOF systems resulting in the need for numerical integration. The major advantage of a closed-form solution is then lost and the restrictions on accuracy are now similar to those for other numerical techniques.

2.1.3 Graphical methods

Graphical methods are time-consuming as a complete construction is needed at every frequency of interest. Sometimes, the particular quantity required (eg maximum displacement) can be recognised from a graphical construction more quickly than it can be calculated. The most useful graphical technique is the Phase-Plane method (ref [23] to [28]) which can be developed for non-linear equations and is then often referred to as the Phase-Plane-Delta method. The Phase-Plane techniques are basically intended for SDOF systems, or for analysing isolated modes that are expressed analytically as SDOF systems, but these approaches can be applied to MDOF systems using superposition if the relationship between the individual modes is known.

These techniques are basically graphical approaches to a numerical solution - a time-stepping method that relies on previous time data and an estimate as to how one of the parameters varies over the time step. Graphical methods have an advantage over numerical analysis in that the response is seen at each time step and the process can be stopped when enough of the solution has been calculated, and the technique may also be quicker in obtaining the maximum response.

2.2 Frequency domain methods

In **this** section the methods available for transient response analysis in the frequency domain are reviewed. Shock response spectra are examined followed by the Fourier transform method. Both approaches assume that the system is linear, shock spectra being for SDOF systems whilst the Fourier transform method can be applied to any system. As in SDOF time domain methods, results from any shock response spectrum can be superimposed for MDOF systems if the relationship between the modes is known or can be approximated. There is also a difference in the presentation of results from these analyses, shock response spectra present only the maximum response of SDOF systems to a pulse, whilst the Fourier transform provides the full response for the system.

2.2.1 Shock response spectra

The concept of the shock response spectrum was originally developed in order to examine the effects of earthquakes on structures when, since it was the maximum responses that was causing most of the damage, it was decided that the full response time-history was not required. These maximum responses tend to occur during, or shortly after, the initial response from the earthquake.

Shock response spectra present the maximum response of several SDOF systems to a pulse, the axes of the plot being the natural frequency of the SDOF system along the x-axis and maximum response in the y-direction. Often, shock spectra have non-dimensionalised axes: the response axis is non-dimensionalised to maximum static displacement, and the frequency axis non-dimensionalised by the pulse duration. Shock response spectra for undamped SDOF systems are well covered by several authors (eg [29] to [36]). Spectra for damped SDOF systems are also discussed by a few (eg [24] and [37] to [39]), but the variation in the maximum response with damping is small and undamped spectra, which are considered conservative estimates for the damped systems, are generally used for any system.

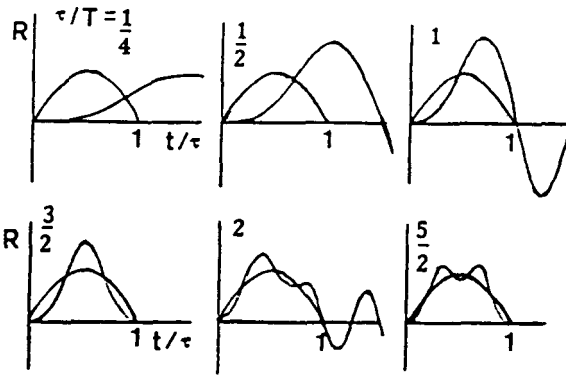
There are three types of shock response spectrum: maximax, residual and initial. The **maximax response spectrum** is the maximum response of the system to the pulse, the residual response spectrum is the maximum response of the system after the pulse has finished, and the initial **response spectrum** is the maximum response of the system during the pulse. Examples of the spectra for a half sine pulse are shown overleaf in fig (2.1).

When designing against malfunction or fracture, the maximax spectrum is of particular interest. If fatigue is the likely mode of failure then the residual spectrum is of interest. Any of the three types of spectrum may be the absolute response of the mass or the relative response of the mass to another point on the structure. Damage may occur to the structure, for instance, if a critical relative displacement is exceeded - a maximum stress level may be reached, or the system may collide with another damage-prone element.

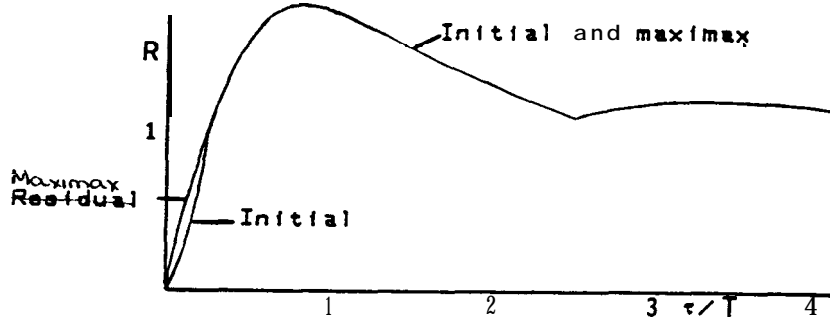
Several methods are available for generating shock response spectra. The original method used a reed gauge where the reeds are tuned to prescribed frequencies. This can also be synthesised by using a series of filters. If the equation of motion is known analytically then it can be solved for a range of natural frequencies and the maximum values obtained. Shock response spectra can be constructed from experimental data, using the maximum response of the system from different duration pulses (rather than changing the natural frequency of the system). There are also methods available for maximax estimation eg ref [30] which may be quicker than exact evaluation.

One restriction on the use of shock response spectra is that they relate to SDOF systems only, whereas very few real structures can be represented by SDOF models. This problem has been examined in several references, including [34] where the general trends of shock response spectra are also examined, [35] where estimating, rather than calculating, maximax response for discrete MDOF systems is considered, and [36] where it is developed in the field of earthquakes.

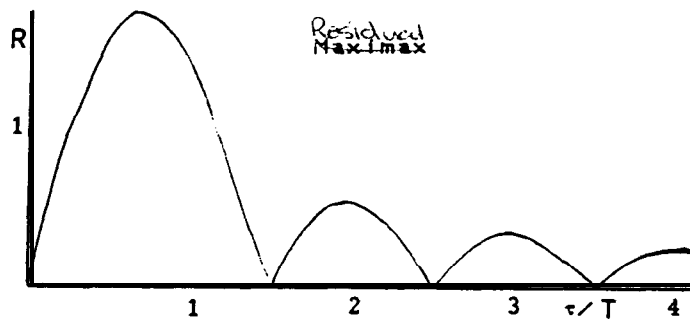
a



b



c



T is natural period of responding system
 R is response divided by maximum of pulse
 τ is time length of pulse

- 2.1a Time-response curves resulting from a single half-sine pulse
- 2.1b Initial and maximax shock response spectra
- 2.1c Residual shock response spectrum

The need for non-linear analysis has been mentioned by several authors (eg [32] and [36]) including the problems of using superposition with non-linear systems. Ref [36] also notes that in some cases the response of the non-linear system can be greater than the corresponding linear system; hence, using estimates from linear shock response spectra might not be conservative.

Nevertheless, shock response spectra have their uses in predicting the maximum response of a system to a transient input. In order to be able to combine the predicted maximum response for MDOF systems, the relative contribution of each mode needs to be known. This information can be obtained by experimental modal analysis if the system cannot be modelled theoretically. Using shock response spectra does not enable a time history of the response to be calculated, and is therefore only useful when the criterion under consideration is that of maximum response.

2.2.2 Fourier transform methods

The Fourier transform is a method of analysis that is used on linear systems to recast a problem in a format that can be solved more readily than is possible in the original format. For the application of transient response prediction of structures, the Fourier transform is widely used. More specifically, a version known as the discrete Fourier transform (DFT) is often used, as this can very readily be implemented by using an efficient set of algorithms on computers, known as the 'fast Fourier transform' (FFT). Information on Fourier transform methods and the application to transient response prediction of structures is available in the literature on the subject which includes refs [40] to [45].

The basic principle for transient response prediction in structural dynamics using the FFT is to apply the Fourier transform to the convolution integral. This recasts the time domain integration expression into a frequency domain multiplication. Fourier transforms are useful tools for predicting the transient response of a linear, or linearised system. Performing multiplications in the frequency domain is more efficient than integration in the time domain.

In practical situations, a time domain transient input can be transformed into the frequency domain. This is then multiplied by the frequency response function of the system under analysis, and the result transformed back into the time domain to obtain the time history of the response.

In experimental modal analysis, the information most readily available about the structure is a set of frequency responses. These frequency response data are in the form required for convolution in the frequency domain with the input signal. No analysis needs to be done to available experimental data - such as extracting the modal parameters - before using these data for transient response prediction. However, if modal parameters are available, either from experimental data or from a theoretical model, the frequency response functions can then be regenerated up to the required frequency of interest. This can then be treated as the- experimentally-obtained frequency response functions.

The limitations and approximations are in the DFT process, both in transforming the input signal to the frequency domain, and transforming the results back to the time domain. Most of the limitations, such as frequency aliasing, are well documented. Some limitations specific to structural dynamics, such as incomplete or badly-defined frequency response data, need careful consideration and will be examined in more detail later in this thesis.

2.3 Discussion

For structural transient response analysis the frequency domain methods can be applied equally well using both theoretical data and with experimental data. The time domain approaches, however, are better suited to theoretical systems where the equations of motion are known.

The Fourier transform and the time-marching methods are more suited to MDOF systems than are the other methods, although formation of the equations for the time-marching algorithms becomes harder with increasing numbers of degrees of freedom. Duhamel's integral method, graphical techniques and shock spectra apply primarily to SDOF systems but can be adapted for MDOF systems with some approximations to the contribution of each mode to the total response.

Methods that take account of non-linearity in systems include the time-marching solutions - notably, Newmark- β - and graphical methods. In the latter case the responses from several modes are combined using superposition and normal mode contributions, thereby assuming linearity. The time-marching solutions require the non-linearity to be defined mathematically and this is often only a rough approximation. None of the methods mentioned provides exact transient response solutions using non-linear experimental data.

The Fourier transform method is more efficient than direct solution of the equations of motion and, if the structure cannot be modelled and has to be measured experimentally, the digitised frequency response functions can easily be multiplied by any forcing function to provide a transient response prediction.

For these reasons this thesis concentrates on the use of Fourier transforms for transient response analysis from experimental data. These data can take the form of raw frequency response measurements, (such as are measured in typical modal test procedures) or the modal parameters obtained from experimental data. One of the methods of evaluating the required parameters of the system from the experimental data is by using modal analysis.

3 A REVIEW OF FREQUENCY RESPONSE METHODS FOR STRUCTURAL MODELLING

3.0 Introduction

The technique known as modal analysis is often used to create a frequency domain model of structures of interest. In this instance, experimental modal analysis covers the experimental testing of structures and the subsequent analysis of the measured data to extract the modal parameters (natural frequencies, mode shapes, and damping) that form the frequency domain model. The information obtained from these tests and analyses can be used in several applications - one of which is response prediction to any input force condition including transient excitation. The aim of this chapter is to review current testing procedures for measuring the frequency response function (FRF) properties of structures, and the analysis methods for evaluating the modal parameters from these FRF data. In the review of analysis methods attention is focused on techniques that will be used in later sections. Some applications of these FRF data and modal parameters will also be considered.

The present chapter starts by briefly examining the essential theory of modal analysis necessary for the subsequent analysis of experimental data. Some of the methods for experimentally measuring the frequency response of the structure will then be discussed and various methods for analysing the data will be examined. The advantages and limitations of the experimental techniques and analysis methods will also be considered. In the last part of the chapter some of the applications of data obtained from experimental modal tests - either raw FRF data or modal parameters - are reviewed. The topics discussed in this chapter are extensively covered in the available literature on modal analysis. The work by Ewins (ref [46]) on modal testing includes information on most of the subjects.

3.1 Summary of essential modal theory

The theoretical route to vibration analysis generally starts with a spatial model, which is a description of the physical properties - ie mass, stiffness and damping - of the system. Next, the spatial model equations are solved for a modal description of the system consisting of a set of natural frequencies, mode shape vectors and modal damping of the system, together known as the modal model. Finally, in the theoretical analysis, a response model can be generated to describe how the structure responds under given force excitation conditions. The theoretical development from spatial to modal to response model is reviewed in Appendix 1.

One convenient form of response model for a structure can be expressed as a set of frequency response functions (FRFs) for the points of interest on the structure. Each FRF in this case is the ratio of the response to a unit amplitude sinusoidal force applied at a single point over the frequency range of interest. The general form of the for displacement FRF (receptance) is:-

$$\alpha_{jk}(\omega) = \frac{x_j e^{i\omega t}}{f_k e^{i\omega t}} = \sum_{r=1}^N \frac{C_r}{\omega_r^2 - \omega^2 + iD_r}$$

where $\alpha_{jk}(\omega)$ is the receptance FRF at point (jk)

x_j is the response at point j

f_k is the input force at point k

N is the number of modes of vibration.

C_r is the r^{th} modal constant - which is the product of the mode shape vectors from the excitation and response point. C_r may or may not be frequency dependent and can be either real or complex depending on the damping model used.

ω_r is the r^{th} natural frequency.

D_r is the r^{th} damping term - which may or may not be frequency dependent and can be either real or complex depending on the damping model used.

The FRFs for velocity (mobility) or acceleration (accelerance) responses are related to receptance by (io) or $(-\omega^2)$ respectively. The reciprocal relationships of force per unit response are also used. These relationships are more often associated with other fields of application - eg sound propagation - but, if the inverse FRFs are applied to structural dynamics, then it is important that their significance be fully understood, as considerable errors occur when they are incorrectly applied to multi-degree-of-freedom (MDOF) systems.

It is worth mentioning here the two common models of linear damping (refs [47] & [48]). These are:-

- (i) viscous damping, where the damping force is proportional to velocity.
- (ii) hysteretic (or structural) damping, which is defined for sinusoidal excitation, is where the damping force is proportional to displacement but takes the sign of velocity.

The theoretical development of the FRFs of a system with viscous damping is rigorous - the differential equations of motion are first solved for a complementary solution, then for the particular integral for sinusoidal excitation. Inspection of the FRFs for these systems reveals that the effect of the damper is dependent upon frequency. In practical structures, damping is usually found to be relatively independent of frequency so, to take this into account, the hysteretic (or structural) damping model is used. Hysteretic damping is defined as a dissipation mechanism whose damping coefficient is inversely proportional to frequency, and this results in frequency-independent damping terms in the FRF. However, the analysis with hysteretic damping is not strictly valid for free vibration, as the damping model is only defined for forced sinusoidal excitation and does not apply for $\omega=0$. Even so, hysteretic damping is an acceptable model of damping for forced harmonic vibration. Also, as it is always possible to express an FRF as a series of simpler terms, each of which may be identified with one of the 'modes' of a system so the individual terms may be considered genuine characteristics of the system.

When examining systems with hysteretic damping models the damping quantity is usually expressed as a 'loss factor' (η), which is the ratio of the energy lost per cycle (ΔE) to the maximum potential energy stored in the system during that cycle (\hat{V}). This can be expressed as:-

$$\eta = \frac{1}{2\pi} \frac{\Delta E}{\hat{V}}$$

In systems with viscous damping, the 'damping ratio' (ζ) is often referred to, which is the ratio of the actual viscous damping in the system to the critical damping (c_c) of the system (critical damping is when there is just no oscillations).

$$\zeta = c / c_c$$

Using energy considerations, the expression for the damping loss factor can be used to calculate equivalent damping loss factors for other damping mechanisms. In the case of viscous damping this leads to:-

$$\eta_e = 2\zeta (\omega / \omega_0)$$

This means that at resonance $\eta = 2\zeta$. This relationship will be used later in the thesis when the damping ratio is required from calculated damping loss factors.

Presentation of results

The FRF data are complex, hence there are three quantities - two parts to the complex FRF, and the frequency - that need to be displayed. To present all these data requires two plots, as a standard plot can only show two of the three quantities. There are several different forms of presentation used depending on the requirements from the measured data. Two of the more common forms of presentation for structural analysis are mentioned here, one of which is only suitable for damped systems.

The first form of presentation is the Bode type. This consists of two plots - modulus (of the FRF) vs frequency and phase vs frequency. To encompass the wide range of values associated with FRFs, the plots often make use of logarithmic axes for the frequency and modulus scales. An example of this type of display is shown in **fig (3.1)**.

The Nyquist (or Argand plane) plot is the second type of presentation in widespread use. This is a single plot of the real part of the FRF against the imaginary part. The frequency information is not readily available from this type of display, but can be marked on the plot as shown in the example in **fig (3.2)**. The Nyquist plot is particularly suitable for focusing attention to the detail around the resonance region.

Both the Bode and the Nyquist plots contain interesting geometric properties that are related to the modal parameters. This is particularly useful in the experimental approach to modal analysis as given the frequency response data the modal parameters can generally be calculated from detailed analysis of the actual plotted curves.

Figures are at the end of the chapter.

3.2 Experimental testing for frequency response of structures

The experimental testing procedure starts where the theoretical route finishes - the frequency response data. In this approach, the FRF is measured experimentally from the structure, modal parameters evaluated from the FRF and finally a spatial model may be reconstructed from the modal model. In this section the measurement techniques used for obtaining the frequency response will be summarised.

The type of structural measurement required for experimental modal analysis needs both the input and the response to be measured simultaneously. The amplitude ratio and the phase relationship of the two signals then needs to be evaluated in the frequency domain to obtain the FRF. If care and attention are paid to the details of preparing a structure for test then the measured data should be an accurate frequency response description of the structure. However, large errors can be introduced if, for instance, the mass of the measuring transducers is significant compared with the effective mass of the structure, or resonances can be added to the system through the suspension of the structure.

There are several experimental testing methods available that are in common usage. These can broadly be split into two types:-

- (i) Single-point excitation, as the name suggests, has only one point of excitation at a time and corresponds closely to the theoretical derivation for frequency response functions; and
- (ii) Multi-point excitation, where several sites are chosen to be excited simultaneously (eg refs [49] to [52]).

For a linear structure, where the relationship between input and response is constant at any given frequency, the excitation method makes no difference to the measured frequency response and can consist of sinusoidal, random, periodic or transient inputs. The single-point excitation techniques, which are the methods more commonly used for experimental modal analysis, are now examined in more detail.

Sine excitation

Stepped-sine testing is the classical excitation method involving a discrete sinusoid with fixed amplitude and frequency as the input excitation signal. The frequency is stepped from one frequency to another to provide the range of data required. At each frequency it is necessary to ensure that the response is steady - ie that all the transients have decayed away - to obtain a true steady state measurement. This method is quite slow to measure the full frequency response, but has the advantage that the frequency points can be chosen where required, closely-spaced around the rapidly changing region of resonance and more widely spaced where the change is less rapid. Also, for many structures there are less problems associated with the measurement of the more widely spaced data, and these data are less likely to be required with as great an accuracy for later analysis than the data in the critical regions. It follows from this that the time spent in measuring can be optimised. Typical FRF data from a sine test are shown in fig (3.3).

As an extension to stepped-sine testing is the slow-sine sweep method where the excitation frequency is slowly varied through the range of interest. It is necessary to ensure that the sweep rate is not too fast, otherwise distortions will occur in the FRF plot. There are guidelines as to the maximum sweep rate through resonance in the ISO standard for 'Methods for the experimental determination of Mechanical Mobility' (ref [53]).

Random excitation

This technique uses statistical relationships between the input and output signals. The theory for this type of response measurement can be found in literature on signal processing as well as on modal testing (eg refs [44] & [54] to [58]). A random signal is used to excite the system, and the relationship between the cross spectrum of the input and response and the auto spectrum of the input is usually used to estimate the FRF. There are other estimations of the FRF which are occasionally used and which should theoretically produce the same results, but there are several reasons why they may differ including noise on one or both the signals, secondary input to the structure and poor frequency resolution. It is therefore important to use the most appropriate estimation for the FRF in any situation. The advantage of random excitation is the speed with which the FRF can be produced. However, to obtain data as good as that obtained using stepped-sine excitation may involve many averages, and zoom measurements around resonances, making the total time to obtain analysable data much the same as for stepped-sine testing. An example of FRF from random data is shown in fig (3.4).

Periodic excitation

A group of excitation techniques, referred to as periodic excitation, use similar analysis to random with periodic input force signals consisting of many frequencies. These techniques include; periodic excitation - frequencies of known amplitude and phase relationship; pseudo-random - frequencies with a random mixture of amplitudes and phases; periodic-random - using a pseudo-random sequence for one response measurement then changing the pseudo sequence for the next measurement and the process repeated until sufficient averages have been obtained; and burst signals, either random or sine (eg ref [59]) - where the time length of the input signal is short, but not impulsive-like, and there is sufficient time between bursts for the response to have decayed away. The FRF can be calculated from the ratio of the Fourier transforms of both the input and output signal as well as using cross and auto spectra. In these four methods, problems such as leakage do not occur as the signals are periodic in the analyser bandwidth. Periodic random, in particular, increases the measurement time over true random due to the amount of data not used.

Transient excitation

There are two major types of transient excitation: impact testing (ref [50]) and rapid sweep (refs [61] to [63]). Both forms can be analysed either using the ratio of the Fourier series description of the input and output, or in the same manner as random signals. Often, in both sets of tests, the results are averaged over several transient inputs. Impact testing, from a hammer blow for instance, has the frequency content limited by the length of the impact: the shorter the pulse the higher the frequency range. Rapid sweep testing has control over the frequency and amplitudes present in the signal. The advantage of impact testing over all the other methods mentioned is that it does not require an exciter or power amplifier, and so the problems of attaching the source of excitation to the structure do not exist. Also, the excitation site can be rapidly moved around the structure.

3.3 Extracting modal properties from experimental frequency response data

Having obtained raw frequency response data, the next step in the processing is to derive the parameters of the modal model. The task is to find the coefficients in the theoretical expressions for FRF which are the best approximation to the experimental data. These coefficients correspond closely to the modal properties of the system. This section examines some of the procedures that are available for this 'modal analysis' part of the test.

There are two main types of analysis of the FRF - the first involves analysing individual modes of vibration while the second type analyses all of the modes in one stage. There is an extension to the second type that is used; that of simultaneously fitting several FRF curves from the same structure. This procedure uses the fact that for linear structures the natural frequencies and modal dampings are global parameters - ie for a given mode of vibration those parameters are independent of excitation or response sites. There are also a few procedures available which calculate the modal parameters from response data in the time domain. These methods either fit all the modes from one time history or solve for several curves simultaneously. Most of the frequency and the time domain methods are referred to in ref [64] and further specific references available from the surveys and bibliographies available (eg refs [65], [66] & [137]).

3.3.1 Single-degree-of-freedom (SDOF) analysis

The SDOF methods assume that in the vicinity of resonance the total response is dominated by the contribution of the local mode. Some of the methods allow for the contribution of other modes by approximating their effect on the resonance region of interest to a constant. There are several types of analysis in this category (refs [67] to [72]) but the two that are outlined here are the more common methods in use and are the ones that will be used in future analysis in this thesis. The theoretical background to these two methods is provided in Appendix 2.

Nyquist or circle-fit method

This method uses the geometric properties of the Nyquist circle to calculate the modal parameters. The natural frequency is located first by identifying the point of maximum sweep rate. From this, several damping estimates can be calculated using different combinations of points above and below resonance. Ideally, all these estimates should be identical, but by presenting the values on an isometric (or 3-D) damping plot, rather than giving a single averaged value, information can be gained about the source of the discrepancy - incorrect location of the natural frequency, 'noisy' data or non-linear data. The final parameter to be calculated is the modal constant and this is obtained from the diameter of the circle. The approximate effects of the other modes can be evaluated from the offset of the circle. As a final check on the parameters, a theoretical curve can be regenerated and compared with the experimental data. An example of this type of analysis is shown in fig (3.5). Further information can be obtained from the general literature on modal analysis and ref [69].

Reciprocal-of-receptance

This method also uses data around resonance, but uses the plots of the inverse of the FRF. This usually results in two plots, the real part and the imaginary part - in both plots the x-axis is frequency squared. From the real part, the resonance frequency and the modal constant can be evaluated. The damping value can then be read from the imaginary plot. An example of this type of analysis is shown in fig (3.6). This inverse method is mentioned in a few of the general references and also in refs [71] & [72].

This method assumes that the modes are real and is best used with well separated modes. The advantages over the Nyquist method are that the least-squares fitting routine is based on a straight line rather than a circle, and that the points close to resonance - which are more likely to be in error - are not weighted more than the other points used in the analysis. It may also be possible to use this method to estimate parameters when there are insufficient data between the half power points for a Nyquist analysis. Dobson [67] has developed this technique to account for the complexity of the modes whilst still retaining the straight line curve fits.

3.3.2 Multi-degree-of-freedom (MDOF) analysis

There are several methods of MDOF analysis depending on the application. For lightly-damped structures, where there is insufficient measured data around resonance, an appropriate MDOF analysis has been developed, whilst the MDOF techniques that are extensions of the SDOF analysis methods are suitable for refining modal data from FRFs with strong coupling effects between the modes. There are several numerical algorithms available for fitting data points to the theoretical FRF and then calculating all the modal properties of the system. The global methods of simultaneously fitting several FRF curves include the widely used rational fraction method (refs [73] & [74]) and the simultaneous frequency domain technique (refs [75] & [76]). However, in this section two of the simpler MDOF analyses - for lightly damped structures, and iterations on the SDOF analysis methods - will be discussed.

Extension to SDOF **analysis**

The first MDOF method is a simple extension to the SDOF analysis. In this analysis the contribution from the other modes is evaluated at each frequency point and results in an iterative procedure between the modes until satisfactory modal parameters have been obtained. This type of approach is necessary on closely-coupled modes, but even on weakly coupled modes the improvement may be noticeable. An example using Nyquist analysis with and without iterations is shown in fig (3.7).

A method for lightly-damped structures

This second technique is suited to lightly damped structures where the light damping does not allow sufficient data of acceptable quality to be collected around resonance. This method is also often used for frequency response data that have been collected using random excitation where the frequency spacing around resonance is too great for a Nyquist analysis. For this MDOF method the analysis is performed using an undamped FRF model, picking the peak values as resonance points and a selection of off-resonance points to solve the undamped frequency response equations. Damping is then estimated from the measured peak values at resonance. This full procedure is often referred to as the 'IDENT' technique. The values of natural frequency and modal constant evaluated from this method are generally good when the system is such that the resonance frequency is a close approximation to the natural frequency, but the damping values are usually overestimated as the measured peak value is usually below the true maximum value. The general theory behind this approach is shown in Appendix 3 and is found in the general literature on modal analysis and ref [77].

Residuals

In this section it is also worth mentioning the problem of residuals. These are the effects of the modes that are out of the range of measurement, both high-frequency and low-frequency, but which influence the measured data points. All the low-frequency modes can be approximated by a single term similar to those in the FRF series. This term is mass-like in its effect on the regenerated FRF and is sometimes referred to as the 'mass residual'. The high-frequency modes can also be represented by a single term whose effect is stiffness-like on the regenerated FRF, hence is known as the 'stiffness residual'. The effect of the residuals varies significantly from structure to structure, and indeed with different FRFs from the same structure. The effect is usually most noticeable on the point measurements (response and excitation at the same site) of the structure. This effect cannot be calculated for FRFs that have not been measured (ref [78]) and is often a major source of error in predicted responses as shown in fig (3.8). This figure shows a complete FRF of a theoretical system, and compares the central portion when regenerated with and without residuals.

3.3.3 Time domain analysis

There exist several analysis techniques for extracting modal parameters from time domain data (refs [79] to [90]). Most of the methods for single curve analysis are derived from the complex exponential technique where sampled impulse response data are used to set up an eigenvalue problem whose solution, via the Prony method (eg ref [79]), leads to the damping ratios and the natural frequencies. To obtain good estimates of the resonance modes in noisy data, many more resonances than exist have to be estimated to allow 'computational modes' to be evaluated separately so as not to contaminate the true modes. These computational modes are easily distinguishable, with low modal constants and high damping ratios. From the measured data, an initial guess to the number of modes has to be made and usually at least one other attempt made to verify that enough resonances were chosen. The damping estimates are often in error (ref [79]) as they are evaluated from the data points at the start of the exponential curve where the slope and the rate of change of slope is often large.

Many of these time domain techniques have been developed for global parameter estimation, in which case the solution is often calculated in two parts. The first is to evaluate the damping and natural frequencies in the time domain and the second part is to evaluate the mode shapes. This second part of the analysis is performed on individual curves, and it is recommended (ref [83]) that the frequency domain is used to estimate the modal constants where allowance can be made for the 'out-of-range' modes. The analysis of data in the frequency domain is limited by the need to transform measured time data to the frequency domain and the subsequent frequency spacing which is dictated by the time length of the sample. As in most time domain analysis methods, the damping estimates tend to be poor.

3.4 Application of frequency response data and modal parameters

There are many applications for the measured experimental data and the calculated modal parameters (eg refs [91] to [94]). The application of the data will often dictate the type of test performed and the analysis used. If using data to compare with a theoretical model, only the resonance frequencies and approximate mode shapes are required, whilst if the model will be used to couple the structure into a larger system, accurate resonance frequencies mode shapes and damping are required in rotation as well as in translation. Apart from the applications mentioned in this section, others include force determination, correlation of experimental and theoretical data, structural modification and non-destructive testing.

3.4.1 From modal model to spatial model

Unfortunately, the transformation from modal model to spatial model is not as easy as it first appears. From the definition of the mass-normalised mode shapes, the spatial mass and stiffness matrices would be:-

$$[M] = [\phi]^{-T}[\phi]^{-1}$$
$$[K] = [\phi]^{-T}[-\lambda_r^2][\phi]^{-1}$$

where $[\phi]$ are the mass-normalised eigenvectors

and $[-\lambda_r^2]$ are the complex eigenvalues

However, the inverting of matrices is only possible if they are square - ie in this case if there are as many modes as coordinates - and, even then, the results are only valid if all the modes have been measured. 'Pseudo' flexibility and inverse-mass matrices (eg ref [95]) can be constructed with rectangular eigenvector and eigen value matrices. These 'pseudo' inverse matrices can be useful in correcting theoretical models so long as the spatial mass and stiffness matrices from the theoretical model are restricted to the same coordinates as those used in the modal test.

3.4.2 Response prediction in the frequency domain

Having obtained accurate modal models, these can now be used to predict the response of the structure to more complicated excitation conditions than can be simulated in laboratory tests.

The procedure uses the standard response-force equation:-

$$\{x\}e^{i\omega t} = [\alpha(\omega)]\{f\}e^{i\omega t}$$

where $[\alpha(\omega)]$ is the receptance matrix - the elements of which have been derived from the modal test.

The force excitation matrix may have more than one non-zero value, and the amplitude and phase relationship may change at each frequency. Apart from the quality of the models, a constraint on the accuracy of this method is the number of measured coordinates. In practice, this method is capable of producing good results provided that the modal model used to generate the FRF contains sufficient modes.

3.4.3 Frequency response coupling for structural assemblies

There are many cases when a complex structure is best described as an assembly of simpler components. These components can be individually analysed for their modal model, or FRF, using the most appropriate method - either analytical or experimental. These sub-system models then require to be combined to provide the frequency response or modal model of the complete structure.

There are several different methods of approaching the problem of sub-structure coupling, but the method of interest is the impedance coupling method or the 'stiffness' method, which provides the frequency response of the coupled structure and uses the FRF data of each of its individual components. The method requires that the FRF properties of each sub-structure are known, either from model or test, at the points of coupling. The basic theory is shown in Appendix 4. There are several references on the subject of impedance coupling (eg [96] to [98]) and the problems that are involved. One problem area that particularly effect the results from coupled structure analysis is that

of rotational coordinates - they are difficult to measure but their omission can cause large errors on the resulting FRF. Also, with impedance coupling the incompleteness of a model from experimental data may make modal models from different origins (eg from measured data and from finite element models) incompatible, and hence restrict the applications. A coupling method using FRF data has been examined (ref [99]) to overcome this problem of incomplete models as FRFs are compatible irrespective of origin. However, this technique of coupling FRF data only ensures that data used are compatible, and other possible sources of error, such as measurement of rotational coordinates, exist in both types of coupling techniques.

3.5 Discussion

There are many excitation and analysis techniques available for experimental modal analysis - none of which provide the 'best' solution in all situations. The choice of excitation technique will depend on the structure, the application and quality required of measured data and any future analysis on the data. The choice of analysis method will depend on the use and the accuracy required of the modal parameters and also the quality and quantity of measured data.

Once good measured data have been obtained, the main differences in the analysis methods are in the complexity of the solution and in the quality of the damping estimate. All the methods can provide good natural frequency estimates and modal constants, but only a limited number of frequency domain analyses allow for complex modes. From the mentioned analyses, the best damping estimate can be obtained using Nyquist analysis ensuring that there are sufficient measured data points between the half power points.

Having evaluated modal parameters, the response to a transient excitation can be calculated in the frequency domain using response prediction, with the transient input expressed in the frequency domain. The response to a transient is usually required in the time domain as a time-history. To change working domains from the time to the frequency for the input, and from frequency to time domain for the predicted response, Fourier analysis methods are usually used in structural dynamics.

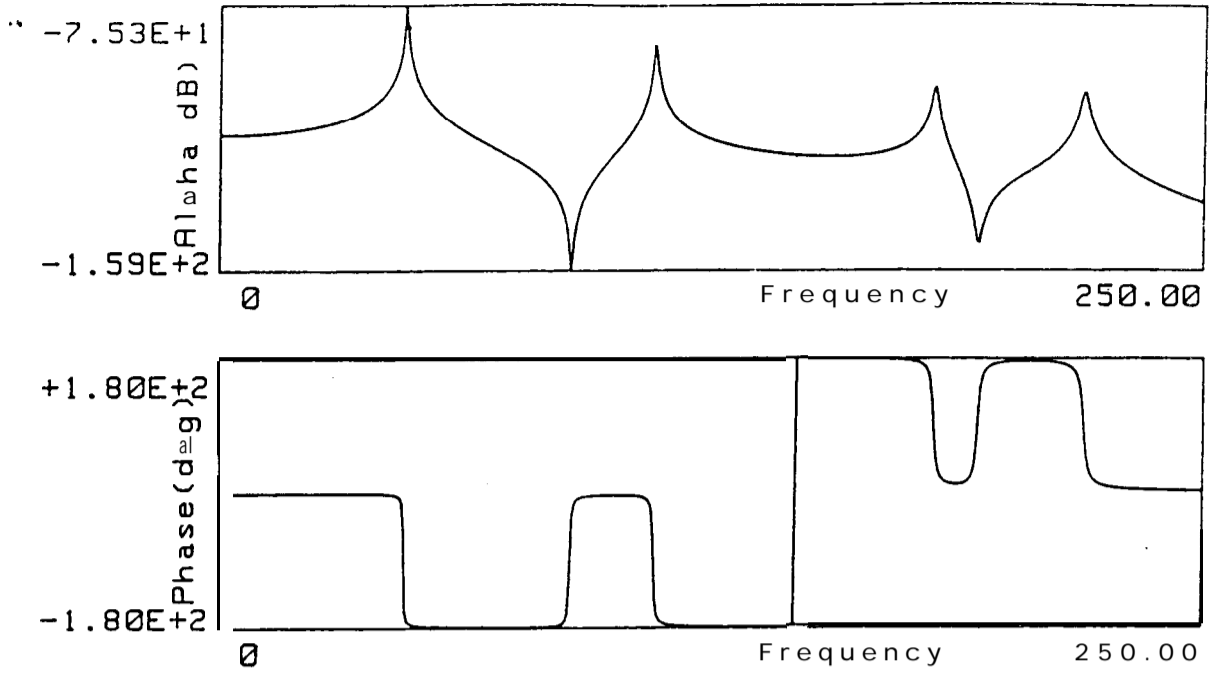


Fig 3.1 Bode plot using linear frequency axis and log response

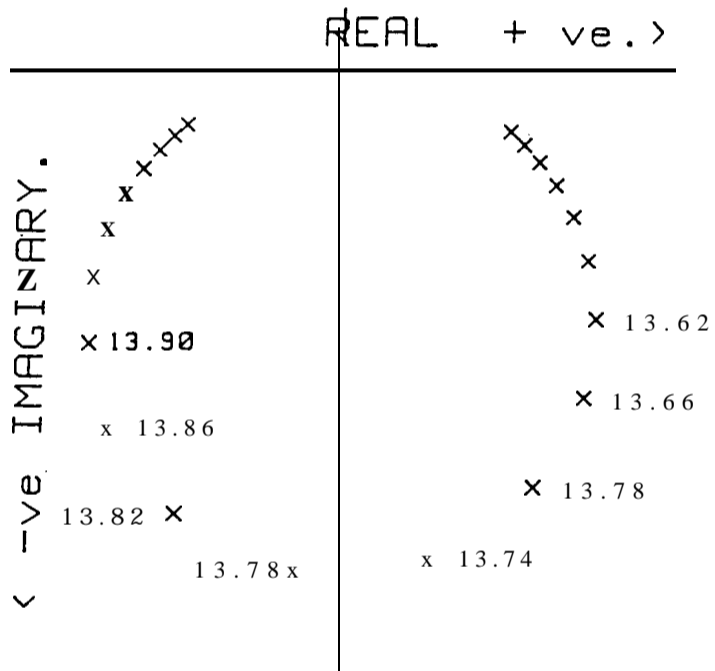


Fig 3.2 Nyquist display with frequency information included

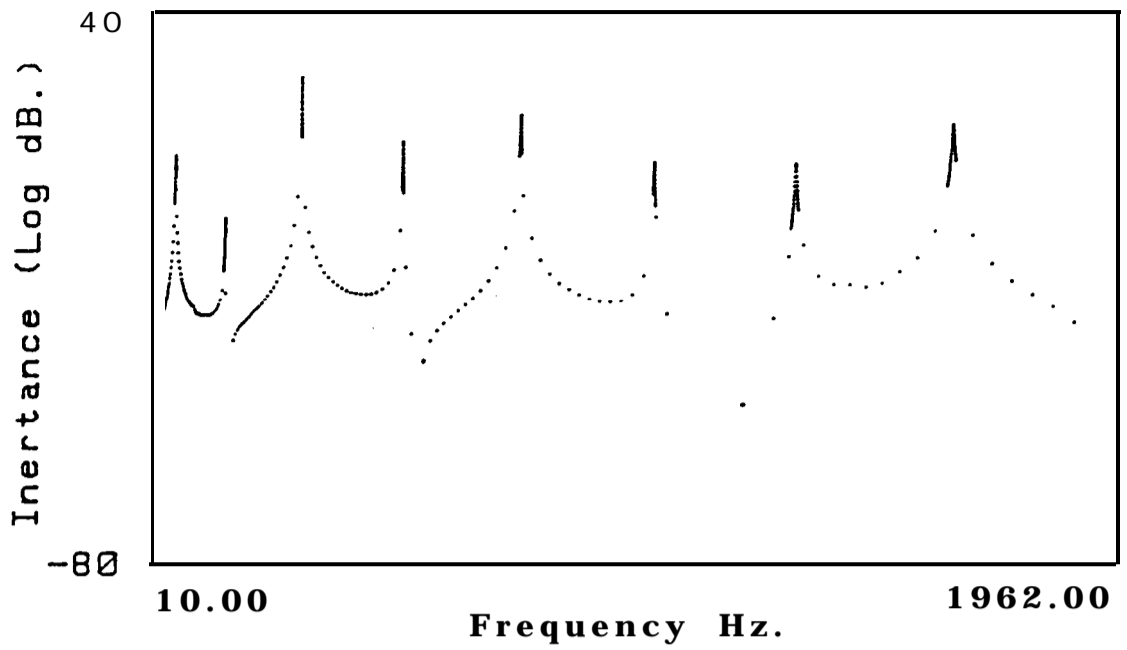


Fig 3.3 Data from sine test - Coarse log frequency sweep followed by fine linear frequency sweeps around resonances

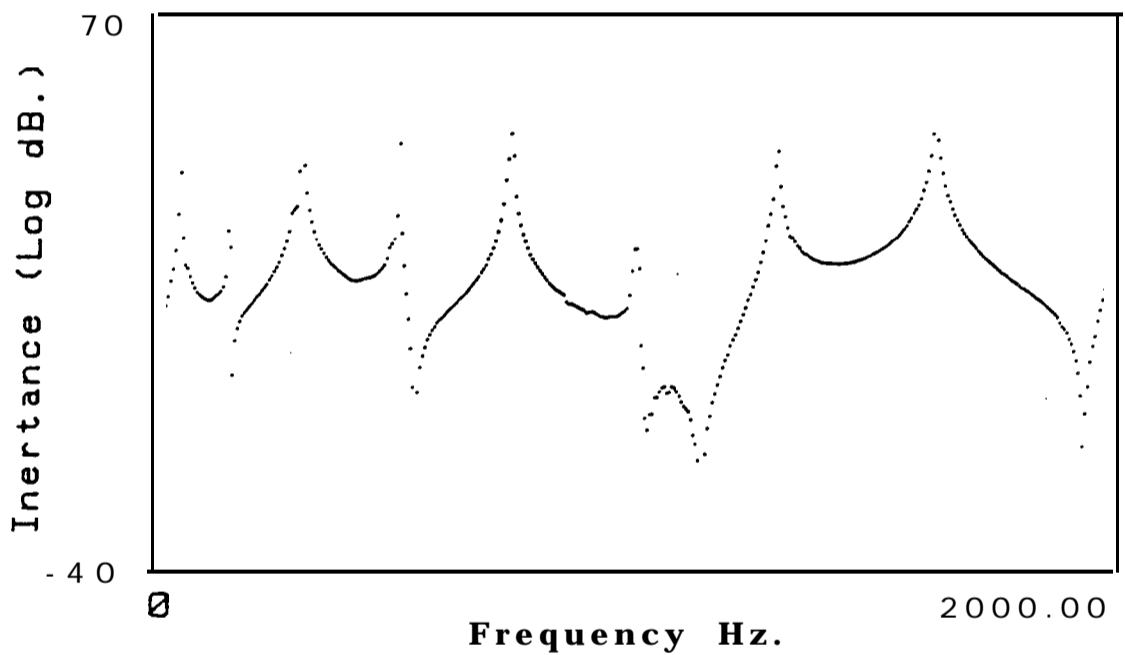
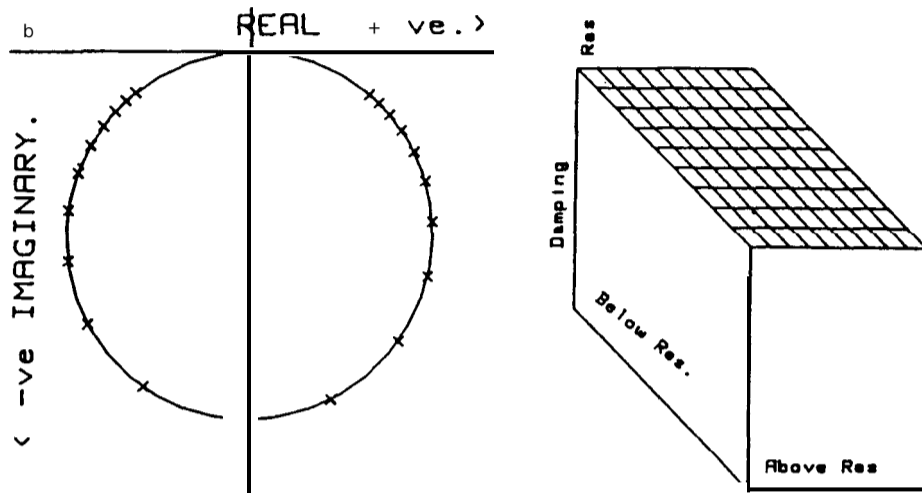
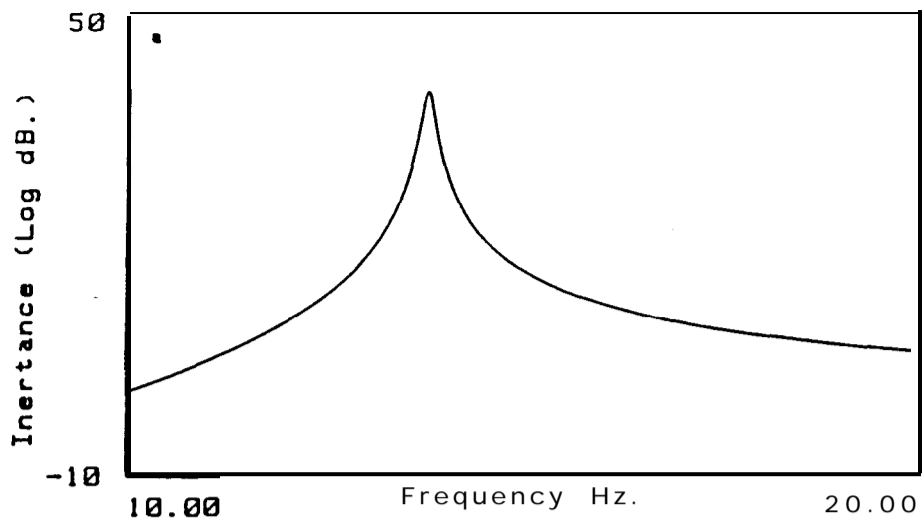


Fig 3.4 Measured FRF from random excitation on a structure, linear frequency spacing over the full frequency range



Resonance Frequency = 13.77 Hz.
 Phase angle = +.5 deg
 Damping Loss Factor = .01044
 Modal Constant = 1.00040E+00 1/kg

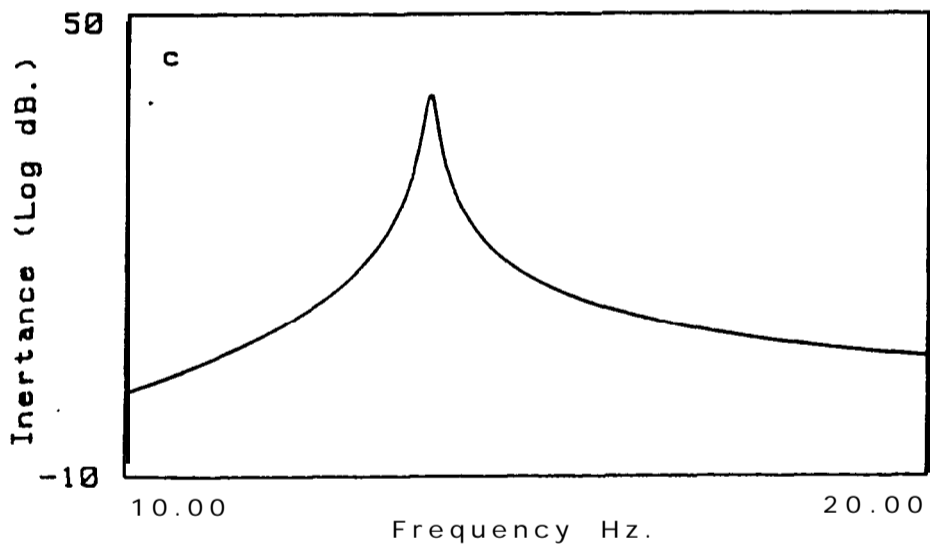


Fig 3.5 Nyquist analysis
a Measured FRF data
b Nyquist circle and 3-D damping plot for Nyquist analysis
c Regeneration of FRF using data from Nyquist analysis

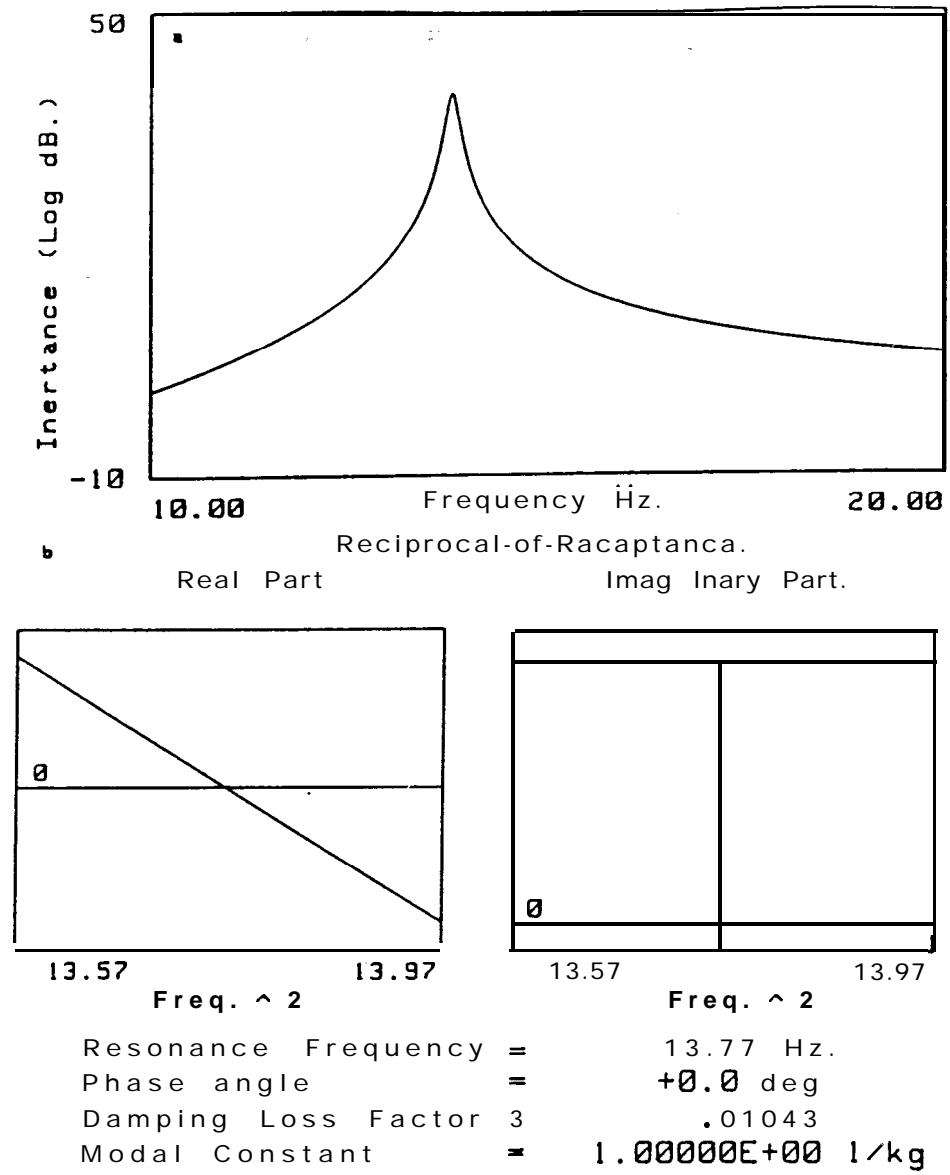
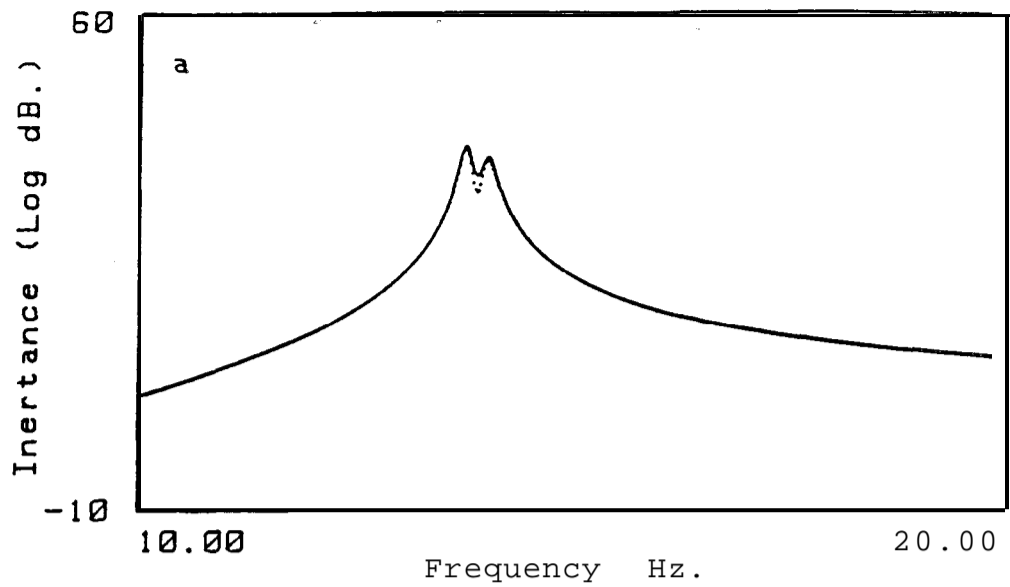
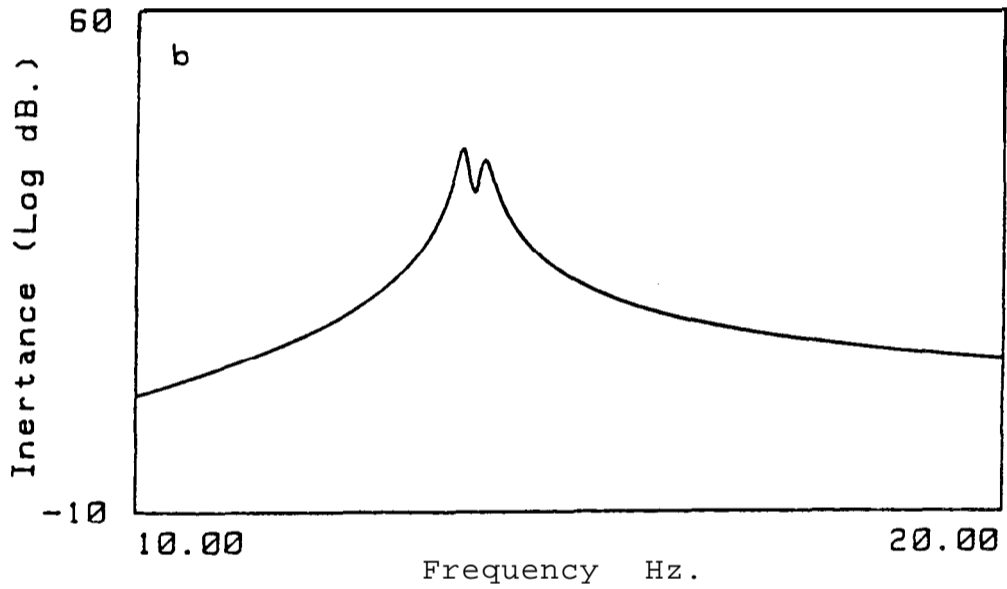


Fig 3.6 Reciprocal-of-receptance analysis
 a Measured FRF data
 b Real and imaginary reciprocal-of-receptance plots and analysis
 c Regeneration of FRF using data from Reciprocal-of-receptance analysis



| Mode No. | Frequency (Hz) | Modal const (1/Kg) | Phase (deg) | Damping loss factor |
|----------|----------------|--------------------|-------------|---------------------|
| 1 | 13.763 | 9.6692E-01 | +13.4 | 0.01060 |
| 2 | 14.015 | 8.0749E-01 | -22.1 | 0.01198 |



| Mode No. | Frequency (Hz) | Modal const (1/Kg) | Phase (deg) | Damping loss factor |
|----------|----------------|--------------------|-------------|---------------------|
| 1 | 13.770 | 9.9732E-01 | +0.5 | 0.01043 |
| 2 | 14.000 | 8.9879E-01 | +1.0 | 0.01199 |

Fig 3.7 Effect of MDOF extension to **SDOF** analysis
 a SDOF analysis of close modes
 b Analysis of close modes using MDOF extension to SDOF methods

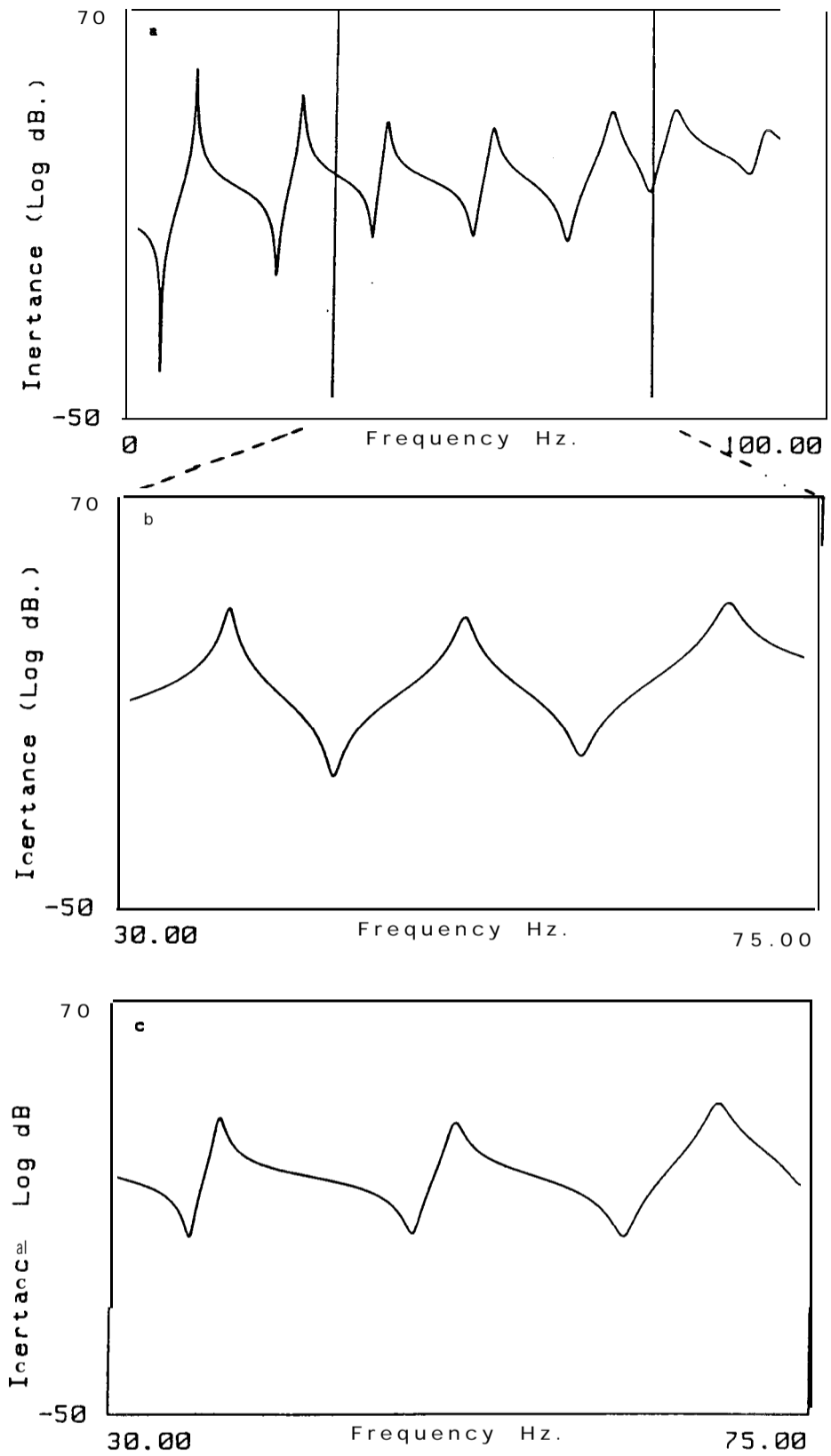


Fig 3.0 Effect of residuals on regenerated **FRF data**
 a FRF of the complete theoretical system
 b Regeneration of the central region without residuals
 c Regeneration of the central region with residual terms

4 REQUIREMENTS FOR TRANSIENT RESPONSE ANALYSIS USING FREQUENCY RESPONSE

4.0 Introduction

The primary objective of this research is to develop a suitable method for transient response prediction of structures using models based on experimental data. As the physical description of a structure cannot be satisfactorily reconstructed from experimental data to enable most of the transient response prediction methods to be used, the frequency response prediction method, discussed in chapter 3, appears to provide the only route for use with experimental data. This method allows for the response to any force input - including transients - to be evaluated in the frequency domain using data from experimental modal tests.

A transient input signal for response prediction is usually specified in the time domain whilst the frequency response method requires the input to be expressed in the frequency domain. There are several techniques available for transforming the working domain, but the most common method used for transfer between the frequency and time domains is the Fourier transform, and it is this technique that will be used to transform the input signal to the frequency domain. The consequent response prediction will be in the frequency domain, and as the transient response of a structure is usually required in a time domain format, to complete the analysis the predicted response is transformed to the time domain using the inverse Fourier transform. This complete procedure will be referred to as the 'Fourier transform method'.

The Fourier transform is strictly defined for continuous bounded signals of infinite length. In experimental analysis measured data are usually discrete and of finite length. Such a signal is accommodated in Fourier transform theory by a version that is known as the discrete Fourier transform (DFT) which uses discrete data, and imposes a periodicity on the signal, defined by the length of the measured sample. This imposed periodicity results in restrictions in the digitisation of measured data to ensure that the transformed data are an accurate description of the original signal. There are several efficient algorithms

available for solving DFTs, the more common of which is known as the fast Fourier transform (FFT). These algorithms reduce the number of computational operations - and therefore the rounding errors - thus providing a more accurate solution than the direct solution of the DFT. As with all numerical techniques, the accuracy of the result from the 'Fourier transform method' depends on the quality of the input data - which in this case includes the experimental modal analysis data. The aim of this chapter is to review the theoretical development of the Fourier transform, to examine the effects that the limitations in the DFT have on the predicted response, and the sensitivity of transient response predictions to the quality of the experimental data used.

4.1 Fourier transform - from theory to practice

This section provides a brief overview of the theory of Fourier analysis, starting with the Fourier series moving through the Fourier integral leading on to the DFT. The theory of Fourier analysis is well covered in extensive literature on the subject, (eg [40] to [45] & [100] to [1 OS]). These references also cover the limitations of Fourier analysis and related theorems, but most of these are of little interest in the application to structural dynamics.

Fourier Series

The basic concept of Fourier analysis is that any periodic function can be broken down into its harmonic components, and conversely, any periodic function can be synthesised by adding together an infinite series of harmonic components. This principle can be written in compact mathematical notation as:

$$x(t) = a_0 + \sum_{k=1}^{\infty} \left(a_k \cos \frac{2\pi kt}{T} + b_k \sin \frac{2\pi kt}{T} \right) \quad \text{Fourier series} \quad (4.1)$$

where T is the period of the signal

and a_0 , a_k and b_k are constant Fourier coefficients given by:-

$$\left. \begin{aligned} a_0 &= \frac{1}{T} \int_{-T/2}^{T/2} x(t) dt \\ a_k &= \frac{2}{T} \int_{-T/2}^{T/2} x(t) \cos \frac{2\pi kt}{T} dt \\ b_k &= \frac{2}{T} \int_{-T/2}^{T/2} x(t) \sin \frac{2\pi kt}{T} dt \end{aligned} \right\} \quad (4.2)$$

There are limitations on the convergence of the Fourier series, including $\int_{-\infty}^{\infty} |x(t)| dt < \infty$ (ie the area under the time signal is finite), but almost every practical vibration problem satisfies these conditions. The main effect worth noting for structural dynamic problems is that the summation of the series at a discontinuity in a signal will give the average $x(t)$ of the two values of response at the discontinuity. This is important in the representation of impulsive excitations in transient response analysis.

The frequency spacing of the harmonic components is $2\pi/T$. As T becomes large the frequency spacing decreases and in the limit, when the signal is effectively no longer periodic ($T \Rightarrow \infty$), the summation can be represented by an integral.

Fourier Integral

Subject to certain conditions the Fourier series (4.1) becomes the Fourier integral (4.3) when the signal is no longer periodic. Also, the individual frequency components of the Fourier series have merged together and the Fourier coefficients (4.2) turn into continuous functions of frequency (4.4) called the Fourier transform (FT). The Fourier integral is also known as the Inverse Fourier transform (IFT). The signals in both domains are now continuous to infinity. This representation of Fourier theory can be written in complex notation as a Fourier transform pair:-

$$x(t) = \int_{-\infty}^{\infty} X(\omega) e^{i\omega t} d\omega \quad \text{Fourier integral or IFT} \quad (4.3)$$

$$X(\omega) = \frac{1}{2\pi} \int_{-\infty}^{\infty} x(t) e^{-i\omega t} dt \quad \text{FT} \quad (4.4)$$

In most practical applications data are sampled, thus providing discrete, not continuous, data. Thus to deal with real data, the requirement is for a transformation using discrete data in both working domains and this is provided by the DFT.

Discrete Fourier Transform (DFT)

The DFT satisfies this requirement by replacing the integrals for the Fourier coefficients in (4.2) by summations. This then provides an approximate formula for calculating the coefficients of the Fourier series. The inverse DFT (IDFT) is similar to the Fourier series but there are now a finite number of frequency components (N) in the series. Using complex notation where X_k is the approximate coefficient of the k^{th} component, and x_r is the r^{th} component of the discrete time series the DFT and IDFT can be written as:-

$$X_k = \frac{1}{N} \sum_{r=0}^{N-1} x_r e^{-i2\pi kr/N} \quad \text{DFT} \quad (4.5)$$

$$x_r = \sum_{k=0}^{N-1} X_k e^{i2\pi kr/N} \quad \text{IDFT} \quad (4.6)$$

Fast Fourier transform

The fast Fourier transform (FFT) is a computer algorithm for calculating the DFT and there is much literature available on this application of the DFT including refs [107] to [109]. The FFT works by partitioning the full sequence $\{x_r\}$ into a number of shorter sequences, and the DFTs of the shorter sequences are then calculated. The FFT then combines the results from the shorter sequences together to form the full DFT of $\{x_r\}$. This full calculation requires less operations than evaluating the transform directly and this means that there are fewer rounding errors in the computation. Overall, this results in a quicker, and more accurate procedure which is widely used in practice.

4.2 Limitations of using the 'Fourier transform method' within the DFT

There are two main sources of error when using the DFT that are discussed in this section: those of frequency aliasing and those of time aliasing. To eliminate frequency aliasing a minimum sample rate - known as the Nyquist frequency - must be applied to the signal. To avoid time aliasing when transforming from the time to the frequency domain, a window can be applied, but it must be noted that this effectively adds damping to the system. Also, when transforming to the time domain, guidelines to the maximum frequency spacing for a given error in a system have been developed to assist in identifying when time aliasing may be a problem.

4.2.1 Frequency aliasing and windowing

Use of the DFT imposes a periodicity on the signal in both the -time and the frequency domains which, in turn, limits the maximum frequency that can be identified in any signal to one half the sample rate of the signal. This is called the Nyquist, or 'folding', frequency. If frequencies above this Nyquist frequency are present in the original signal then the coefficients calculated by the DFT for lower frequencies will be distorted. This problem of errors being introduced when the sample rate is less than twice the maximum frequency component in the signal, is known as frequency aliasing and is a common occurrence with digitising experimental data. The usual solution is to use a low-pass filter on the signal to remove signal component above the Nyquist frequency.

Windowing is a method of truncating time data, such that the signal is reduced to zero outside a specified range. There are several types of window function, their main differences being seen in the frequency domain where the width of the main lobe (ideally a delta function for perfect resolution) is traded against the magnitude of the side lobes. Examples of the more common windows in use, along with their frequency components, are shown in fig (4.1). Frequency components of a signal falling outside the main lobe of the chosen window may also contaminate distant frequencies if the side lobes are large. This phenomenon is called leakage. For good estimates of the frequency components of an experimental signal, a high resolution and low leakage window is required.

This demand on the window - for a narrow main lobe and small amplitude side lobes - has conflicting requirements and, for a given data length, the parameters have to be compromised.

These limitations on the accuracy of the DFT as a result of aliasing are applicable in this study of transient response prediction mainly to transforming the input transient signal to the frequency domain. The nature of a transient input signal is such that it will contain high frequencies but will decay rapidly, which means that the application of a window will not be necessary to reduce the signal to zero, but frequency aliasing may be a problem. The maximum frequency component required from the input signal will probably be dictated by the maximum frequency of the FRF. The transient input should therefore be low-pass filtered at this maximum frequency of the FRF to remove higher components, then sampled at twice this frequency.

4.2.2 **Errors** due to time aliasing

Transforming from the time to the frequency domain it is easy to establish if the time signal has not decayed away within the time length of interest and, if necessary, to apply a window so as to avoid frequency aliasing. Transforming in the other direction - from frequency to time - it is harder to predict if the time signal has decayed away, but a time aliasing effect will result if the time signal has not decayed to zero (ref [110]). For transformation in both directions, a simple relationship between the error in maximum amplitude, the system parameters, and the DFT parameters has been developed for SDOF systems (ref [111]) and also applied to individual modes in MDOF structures. The maximum error in the peak amplitude of the first cycle of a single mode when transforming from frequency to time domain is given by:-

$$\text{Error}(E_m) = \frac{1}{\exp(n\delta)-1} \quad (4.7)$$

where E_m is the largest possible error due to mode m .

δ is the logarithmic decrement (ref [20]) of mode m .

and n is the number of cycles in the calculated response at the natural frequency of mode m .

In terms of frequency spacing (ΔF) and natural frequency (f_o) this can be written as:

$$\frac{\Delta F}{f_o} = \frac{\delta}{\ln((1+E_m)/E_m)}$$

This is the maximum ratio of frequency spacing to natural frequency for a given error.

Time aliasing and the condition that $\int_{-\infty}^{\infty} |x(t)| dt < \infty$ (which is applicable to most decaying systems) have implications for the suspension of a test structure for transient response prediction, and also the type of input signal. Starting with the test conditions of the structure, if the structure is suspended free-free then the displacement time-history will theoretically have a static component that will result in a continually increasing response, and the velocity will finish with a constant value - not necessarily zero. In both these cases the transformed result will not be correct as the convergence criterion is not satisfied. Ideally the structure should be 'grounded' (coupling the structure to ground at specific coordinates) before transforming. If the modal analysis tests are performed on a free-free structure then the rigid body modes should be analysed and included in the modal model to enable the model to be subsequently 'grounded' for transient response prediction.

There are two main types of input signal that may cause problems - those of a step input and step relaxation. Nicolson (ref [112]) has examined the problem of a step input, and replaces the step with a ramp which provides the correct frequency components in the response but not the correct time-history. An alternative approach is to use a long pulse, where the length of the pulse corresponds to the time length of interest in the step response plus a length of time with zero force input that is sufficient to ensure the response has decayed to zero. The predicted response during the time of the pulse is an accurate description of the step response over the same time. The main disadvantage of this method is large extended time period, hence number of samples, required for what may be a short period of interest. Step relaxation, whilst correctly

described as an initial displacement on a structure, could be treated as a step input with the structure starting at zero displacement. The response from the start time to the time when the input returns to zero will represent the response due to step relaxation, but with the displacement origin shifted by the amount of the initial displacement. With careful presentation of the force inputs and interpretation of results, the responses to most transient inputs can be determined using the 'Fourier transform method'.

4.3 Limitations of using the 'Fourier transform method' resulting from errors in experimental data

In generating experimental data for use in the 'Fourier transform method' there are several areas which could cause inaccuracies in the predicted results. These include the choice of linear damping model - viscous or hysteretic - errors in the measured data or calculated modal parameters and also the effect of the out-of-range modes on the predicted response. These topics will now be discussed in detail.

4.3.1 Consequences of linear damping model

In general, the measurement of damping is not a precise procedure, and indeed the mechanism of damping is not fully understood. To permit the analysis of structures in a linear fashion, two main types of damping are used - viscous or hysteretic (structural) - the latter being defined from the former. In many cases the structural damping model is a much better approximation to the actual dissipation mechanism than is the viscous damping model, and for forced vibration and MDOF systems the algebra is much simpler.

In the time domain the responses are calculated using the impulse response function (IRF). In linear theory the IRF is simply the inverse Fourier transform of the frequency response function (FRF). For systems using a viscous damping model the IRF obtained by transforming the FRF is a sine wave at the damped natural frequency (ω_d), multiplied by a decaying exponential.

$$x(t) = \frac{1}{m\omega_d} e^{-\zeta\omega_n t} \sin(\omega_d t)$$

Milne [113] transformed the FRF with hysteretic damping and quantified a resulting non-causal component in the IRF. This predicted movement before the structure sees the pulse is the only difference between the two types of damping for lightly damped structures, but as the damping increases the pre-cursor movement also affects the response after the pulse. Figs (4.2) & (4.3) show examples of the differences in the IRFs when calculated by transforming the FRFs with the two different linear damping models.

For a system to be physically realisable it must have an IRF which is zero for $t < 0$. This implies that the system with a hysteretic damping model, whilst a better description than the viscous damping model in many cases, is not strictly a realisable system. Whilst the differences in the IRF are only minimal for light damping, it is nevertheless recommended that modal models derived for transient response prediction should use the viscous damping model to ensure a linear model for the time domain response. However, as was seen in chapter 3 and Appendix 2, it is usual for the hysteretic damping loss factor to be calculated from modal analysis methods, as this type of damping implies frequency independent modal constants. The relationship between the damping loss factor and the damping ratio (discussed in chapter 3) $\eta = 2\zeta$ (valid only at resonance) should be used to determine the equivalent viscous damping term for each mode in the modal model that is to be used for transient response prediction. It is shown in Appendix 5 that for light damping the relationship $\eta = 2\zeta$ is also applicable for the free decay rate of a system.

4.3.2 Accuracy of experimental data

There are two major sources of error in experimental data - errors in the raw measured data and errors in the modal parameters extracted from the measurements. If experimental data are to be transformed for transient prediction, the measurement errors will effect the prediction. A signal contaminated by random errors (with normal distribution) will result in the transformed signal plus the transform of the errors, which will still ~~be~~ have gaussian distribution (ref [114]).

When using modal parameters, the three variables - natural frequency, (complex) modal constant and damping factor - affect the result in different ways. Errors in the natural frequency affect the timing of events, but not the overall shape of the response of an SDOF element. In MDOF systems, errors in natural frequency will produce largest errors when the contribution from one of the modes shifts a half cycle relative to the others. To demonstrate the errors in this and the next section, a theoretical 12 mode structure is used, the modal parameters of which are given in table (4.1). Fig (4.4) compares the correct

solution to those from a system with 10% error in the location of the first natural frequency, and from a prediction with 10% error in the second natural frequency. All modal analysis techniques are capable of accurately locating natural frequencies from measured data, and errors in this parameter are more likely to be due to the experimental test procedure physically altering the system (eg transducer mass causing a reduction in the natural frequencies). Errors in the modal constant may be of two types: magnitude and phase error. Deviation in the magnitude produces a linear scaling in the time-histories of SDOF elements, but in MDOF systems there may also be an effect on the shape of the response. This is shown in fig (4.5) which is the theoretical structure with 10% error in the magnitude of the modal constants of modes 1 and 3. Incorrect phase alters the 'starting' position of the signal - for instance, if a signal with zero phase starts with maximum velocity, then one with a phase of π , starts with minimum velocity. In most of the analysis methods a phase of 0 or π , is assumed, which is a reasonable approximation for lightly damped structures with uncoupled modes. For structures with very complex modes, errors in the time response can be significant if the phase is not properly accounted for. In this application Nyquist analysis is the method to use for extracting modal parameters as complex modes can be evaluated, but care must be exercised to ensure that the complexity of the mode under examination is not the result of the effects of the other modes. The effect of varying the phase is shown in fig (4.6), where a phase of 10° has been added to modes 1 and 3.

Variation in the damping estimate affects the predicted result more than deviations in either the natural frequency or the modal constant and influences the overall shape of the response. Errors in damping terms evaluated by using the relationship of the half power points or the peak response can be large, but the calculated loss factors are always greater than the true value (ref [115]) and this results in the predicted response showing a quicker decay than applies in the actual system. In some MDOF systems the prediction can be altered quite markedly from the correct solution by erroneous damping factors. This is particularly unfortunate as the damping term is often the least accurate parameter that is calculated from any of the modal analysis methods, frequently being more than a factor of ten greater than the true value. This is

demonstrated in fig (4.7) where the damping is increased by a factor of ten for modes 1 and 3. The most accurate estimate of damping from analysis of FRF data will be obtained by using the Nyquist analysis with sufficient points between the half power points to calculate accurate modal parameters. The damping estimates from the inverse of receptance are usually quite acceptable, but the calculation relies on a line fit between the two damping values above and below resonance, and if either of these are in error then the damping estimate could also have a large error.

4.3.3 Effect of the out-of-range modes

Modes that are outside the frequency range of measured data need to be considered in two separate groups - those below the frequencies of the measured data (low-frequency residuals), and those above (high-frequency residuals). The effect of these residuals on predicted time-histories also depend on the required response - displacement, velocity or acceleration.

The low-frequency modes of a system determine the overall shape of the transient response. Replacing the first few modes, if they were out of the measured frequency range, by a single low frequency residual would not help to correct the response. It is recommended that the experimental testing starts at as low a frequency as practically possible in order to include all the low frequency modes. Figs (4.8) to (4.10) show the displacement, velocity and acceleration predictions of the theoretical 12 mode system, and compares the responses from the complete system to the response with the first three modes omitted, and then to the response with a low-frequency residual included to represent the three low frequency-modes. None of the 'predictions' are an accurate description of the 'true' response, but the acceleration time-histories are a closer representation than either velocity or displacement. When the test structure is suspended 'free-free', then the rigid body modes can be represented as a zero frequency mass residual. However, if the model is to be used for transient response prediction then this zero frequency should be included as a 'mode' to enable the system to be theoretically grounded before attempting to use the 'Fourier transform method'.

With the high-frequency out-of-range modes, the effect on the predicted time-histories is dependent on the type of response. For displacement responses the high-frequency content is very small, and the transient response can often be predicted quite accurately from the first few modes with no residual term included. This is demonstrated with the theoretical structure by first using the lowest six modes, then only the four lowest modes to predict the transient response, and the results are shown in fig (4.11). The effect of the high-frequency modes is more noticeable in the velocity time-histories (fig (4.12)), but for the test system the first six modes still predicts a good representation of the exact response. For acceleration response prediction, the contribution of the high-frequency modes can be almost as significant as the low modes. Omission of these modes can lead to a significantly different shape of response as well as incorrect levels of response as shown in fig (4.13). For an accurate acceleration prediction many modes need to be included in the model.

For all three types of response the first few modes of the structure are very important and need to be well defined. It is suggested that above the low-frequency modes, the FRF in the response parameter of interest is examined, and all modes analysed and included in the model whose response is greater than or within a certain value of the low frequency modes. This model, when used in conjunction with the 'Fourier transform method', should then provide a good estimate to the true transient response of the structure.

4.4 Case study - Transient response analysis of a beam

The 'Fourier transform method' combines modal analysis of the steady state response of a structure and Fourier theory to predict the transient response of the structure from experimental data. There are many routes available in modal analysis - all of which should theoretically result in the same set of modal parameters for a linear system. These modal parameters can be substituted in FRFs and the 'Fourier transform method' used to calculate a transient response of the structure for each set of modal parameters, all of which should correspond to the exact transient response. There is, however, a preferred route using sine excitation and Nyquist analysis to minimise any error possibilities. These routes are summarised in fig (4.14) with the preferred route for linear systems identified.

Several of these techniques have been employed in a study of an aluminium bar to obtain transient response predictions. The experimental setups for the various excitation techniques used are shown in fig (4.15). These experimental testing setups included the measuring of an 'exact' transient response as an acceleration time-history (fig(4.15a)) and the input force signal to be subsequently used in the prediction of the time-histories. The three excitation techniques used were stepped-sine (fig (4.15b)), random excitation (fig(4.15c)) and impulse excitation (fig (4.15d)). In all cases, three accelerometers were in place all the time to avoid any alteration in the structure due to varying the mass distribution which results from the resiting of a single transducer from one point to the next.

Nyquist circle-fit and reciprocal-of-receptance analyses were used on FRF data from the stepped-sine test. Also a technique for lightly damped systems ('IDENT' ref [77]) was used on the same FRF data, and all the evaluated parameters for pt(1,1) (response point, force input point) and pt(3,1) are presented in table (4.2). FRF data from random excitation (up to 2000 Hz) were analysed using reciprocal-of-receptance and 'IDENT' type analyses, and the

two sets of modal parameters for pt(1,1) and pt(3,1) are shown in table (4.3). Impulse excitation resulted in poor quality data, and was only analysable, using an 'IDENT' type technique up to 1000 Hz. The results are also shown in table (4.3).

The measured force signal (fig (4.16)) was then low-pass filtered to ensure that it did not contain frequencies above 2000 Hz. The sample rate chosen for the 'Fourier transform method' was 5000 Hz which would enable a maximum frequency of 2500 Hz to be calculated from the force signal. Examining the first few resonances from the different excitations and analyses indicated that a frequency spacing of 0.2 Hz would result in a maximum of 10% error in the maximum amplitude when transforming to the time domain - this frequency spacing was used, requiring a 25000 point transform. As the beam was suspended free-free an acceleration time-history was predicted for the first 0.04 seconds of the response, with the associated problems of many modes affecting the transient response. The measured acceleration time-history from pt(3,1) (response data the opposite end of the beam to the input) is shown in fig (4.17). where it is immediately clear that high-frequency components are present in the response.

The acceleration time-history was then predicted for pt(3,1) using the six sets of modal parameters in tables (4.2) & (4.3) and the resulting predictions are presented in fig (4.18). In all cases, the predicted time-history generally overestimated the magnitude of the response. In the predictions, there is a response following the input signal, but the measured response indicates only a small response initially followed by a larger response when the input pulse has travelled the length of the structure. This first large acceleration peak in the measured time-history corresponds to the third positive peak in the predicted results (second peak from the impact test). Some of the higher magnitude peaks are identified on the measured time-history (fig (4.17)), and the corresponding peaks located in the predictions (fig (4.18)). The prediction from the impulse test (fig (4.18f)) shows little resemblance to the measured result, but this is to be expected with a predicted acceleration time-history from an FRF lacking in the high-frequency modes. The other five predictions all show some similarity with the measured response despite the large variation in

the calculated modal parameters. Examining the modal parameters from the different modal tests the largest range is seen in the damping estimates, with the modal constants also showing large variations in some cases. Least variation is seen in the damping estimates from the three analyses of data from stepped-sine excitation, where there is sufficient measured data around resonance for an accurate estimate to be made independent of the analysis technique. The variation in the time-histories that these differences in the damping loss factor will cause are more noticeable at longer times, but in this example and for the time length of interest none of the predictions from stepped-sine or random excitation are obviously 'better' than the others despite the large variation in modal parameters.

To make comparison between the different predictions easier to visualise, a shorter time sample was taken and pairs of predictions overlaid. For sufficient data in this expanded region it was necessary to increase the damping on all modes by a factor of 10, or the transform would require upto 250000 points for sufficient data resolution, and to avoid time aliasing. This vast number of points can be a serious problem when attempting to predict the transient response from structures that are so lightly damped, but most engineering structures have greater damping than this single aluminium beam. The comparisons are shown in fig (4.19), where the results from different analyses of the same FRF data and predictions using data analysed with the same technique are compared. From the stepped-sine tests the first major peak is similar from all the analyses (figs (4.19a,b&c)), but the initial response shows a large variation. Fig (4.19d) compares the results from the random tests, and again the two are similar. Comparing the results from the same analysis, clearly the results from the impulse test (fig (4.19g&h)) do not agree with the predictions from the other excitations analysed using an 'IDENT' type analysis, but the results from stepped-sine and random analysed using an 'IDENT' type technique (fig (4.19f)) agree better than when analysed using reciprocal-of-receptance (fig (4.19e)). In theory this aluminium beam should have provided the same result independent of modal test. This has not been shown to be the case for this particular example, where the results are not only dependent on the excitation technique, but also on the analysis method.

4.5 Discussion

In using the discrete Fourier transform (DFT) the main problems are due to aliasing - either frequency or time - which is caused by the periodicity that is imposed on the signal by the DFT in both domains. This problem can be overcome by ensuring that the signal is negligible at either end of the sample (ie that it has decayed away) in the time domain; that the sample rate is at least twice the maximum frequency component in the signal; and that the ratio of frequency spacing to natural frequency gives acceptable errors. With commercially-available FFT routines, there is often a maximum number of points that can be used and this requires a compromise of the other parameters. Another alternative is to apply a window to the function, but the effect of windowing the data introduces other errors as the resulting effect in the frequency domain is to increase the apparent damping - which in turn reduces the amplitude - so causing errors in the maximum amplitude.

If the system data used are not accurate, errors will occur in the predicted transient response. With the hysteretic damping model errors will be generated with high levels of damping due to the non-causal component. It is concluded that for transient response the preferred linear damping model to use is viscous damping, which can be evaluated from the damping loss factor determined from experimental modal analysis. Also in the analysis stage, the preferred method - when the data is to be use for transient response - is the Nyquist circle-fit as this method can estimate reliable damping values and also take account of the phase components. Out-of-range modes also create problems. All the low-frequency modes are required for accurate predictions, and for acceleration responses, many high frequency modes must also be analysed. In displacement, the response can usually be described accurately by using just the first few modes.

Time-aliasing, and the requirement for a response to return to zero places limitations on the support of a structure for transient response prediction, and also on the type of input signal that can be used. Ideally, the structure should be grounded before a transient response analysis is attempted, as a 'free-free' structure will have a large static component and the response will not return to

zero, hence the convergence criterion of Fourier theory will not be satisfied. If the modal model is of a free-free structure, then this model can be theoretically 'grounded' if the rigid body modes of the structure have been included and there is a measurement point at the grounding position. If the input is a step or step relaxation, the DFT will still impose periodicity on the signal with the results being valid for the periodic signals, and not necessarily for the single step. This can be overcome by applying an offset to the step relaxation (so the input appears like a step input) and the input in both situations returned to zero after the time length of interest in the response, with sufficient time at zero for the response to effectively have decayed away.

Using the 'Fourier transform method' with FRF data is an effective method of predicting the transient response of linear structures from experimental data. However, there are several possible sources of error all of which which can be minimised if care is taken over the transformation procedure and the collection and analysis of experimental data.

| Mode | Natural Frequency | Damping ratio | Modal constant |
|------|-------------------|---------------|----------------|
| 1 | 11.5 | 0.00530 | 0.1004 |
| 2 | 15.6 | 0.00680 | 0.0854 |
| 3 | 15.7 | 0.00660 | 0.0845 |
| 4 | 21.9 | 0.01032 | 0.0626 |
| 5 | 23.1 | 0.00689 | 0.0512 |
| 6 | 25.0 | 0.00423 | 0.0998 |
| 7 | 36.2 | 0.00890 | 0.0753 |
| 8 | 47.3 | 0.01010 | 0.0465 |
| 9 | 62.4 | 0.00717 | 0.0886 |
| 10 | 72.8 | 0.00500 | 0.1130 |
| 11 | 81.0 | 0.01230 | 0.0958 |
| 12 | 92.2 | 0.00852 | 0.0658 |

Table 4.1 Modal parameters for theoretical 12 mode structure

STEPPED-SINE EXCITATION: NYQUIST ANALYSIS

| Mode | Natural frequency | Damping ratio | Mode shape pt(1,1) | | Mode shape pt(3,1) | |
|------|-------------------|---------------|--------------------|-------|--------------------|--------|
| | | | Vector | phase | Vector | phase |
| 1 | 56.300 | 1.309E-3 | 2.8043 | + 5.2 | 3.1580 | + 4.7 |
| 2 | 161.397 | 3.988E-4 | 2.212s | + 2.9 | 2.7357 | -175.3 |
| 3 | 312.130 | 8.700E-4 | 1.5873 | - 2.2 | 2.3355 | - 2.3 |
| 4 | 514.000 | 8.700E-4 | 1.391s | - 0.1 | 2.3904 | -160.0 |
| 5 | 750.850 | 1.365E-3 | 0.9193 | - 9.3 | 2.3512 | - 8.0 |
| 6 | 1019.550 | 9.825E-4 | 0.2594 | - 0.3 | 3.1605 | +170.3 |
| 7 | 1304.225 | 1.415E-3 | 0.5183 | - 3.6 | 1.5487 | +177.2 |
| 8 | 1626.412 | 1.501E-3 | 1.0127 | - 1.1 | 1.6017 | + 0.5 |

STEPPED-SINE EXCITATION: RECIPROCAL- OF- RECEPTANCE

| Mode | Natural frequency | Damping ratio | Mode shape pt(1,1) | | Mode shape pt(3,1) | |
|------|-------------------|---------------|--------------------|-------|--------------------|-------|
| | | | Vector | phase | Vector | phase |
| 1 | 58.505 | 1.312E-3 | 2.9918 | 0.0 | 3.3179 | 0.0 |
| 2 | 161.427 | 4.010E-4 | 2.2118 | 0.0 | 2.6473 | 180.0 |
| 3 | 312.112 | 8.750E-4 | 1.5905 | 0.0 | 2.3129 | 0.0 |
| 4 | 514.000 | 8.750E-4 | 1.3913 | 0.0 | 2.3904 | 0.0 |
| 5 | 750.850 | 1.365E-3 | 0.9193 | 0.0 | 2.3512 | 0.0 |
| 6 | 1019.550 | 9.825E-4 | 0.2594 | 0.0 | 3.1605 | 0.0 |
| 7 | 1304.225 | 1.415E-3 | 0.5183 | 0.0 | 1.5487 | 0.0 |
| 8 | 1626.412 | 1.501E-3 | 1.0127 | 0.0 | 1.6017 | 0.0 |

STEPPED-SINE EXCITATION: 'IDENT' TYPE ANALYSIS

STEPPED-SINE EXCITATION: 'IDENT' TYPE ANALYSIS

| Damping ratio | Mode shape pt(1,1) | | Mode shape pt(3,1) | |
|---------------|--------------------|-------|--------------------|-------|
| | Vector | phase | Vector | phase |
| 1.415E-3 | 2.4964 | 0.0 | 2.7007 | 0.0 |
| 4.110E-4 | 1.9894 | 0.0 | 2.8515 | 180.0 |
| 9.700E-4 | 1.6845 | 0.0 | 2.6337 | 0.0 |
| 8.705E-4 | 1.3439 | 0.0 | 2.4978 | 180.0 |
| 1.375E-3 | 0.8971 | 0.0 | 2.5092 | 0.0 |
| 9.855E-4 | 0.2522 | 0.0 | 2.6478 | 180.0 |
| 1.428E-3 | 0.3958 | 0.0 | 1.7041 | 180.0 |
| 1.450E-3 | 0.9951 | 0.0 | 1.6112 | 0.0 |

| Mode | Natural frequency |
|------|-------------------|
| 1 | 58.5 |
| 2 | 161.4 |
| 3 | 312.1 |
| 4 | 514.0 |
| 5 | 750.6 |
| 6 | 1019.7 |
| 7 | 1304.2 |
| 8 | 1626.5 |

Modal parameters from FRF data obtained using stepped-sine excitation

Table 4.2

RANDOM EXCITRTION: RECIPROCL- OF-RECEPTRNCE

| Mode | Natural frequency | Damping ratio | Mode shape pt(1,1) | | Mode shape pt (3,1) | |
|------|-------------------|---------------|--------------------|-------|---------------------|-------|
| | | | vector | phase | vector | phase |
| 1 | 56.422 | 1.395E-3 | 2.4721 | 0.0 | 2.3318 | 0.0 |
| 2 | 161.269 | 1.695E-3 | 1.7145 | 0.0 | 2.7987 | 180.0 |
| 3 | 309.887 | 1.020E-3 | 1.4919 | 0.0 | 2.4921 | 0.0 |
| 4 | 509.769 | 2.055E-3 | 1.6305 | 0.0 | 1.7027 | 180.0 |
| 5 | 741.195 | 1.195E-3 | 0.6824 | 0.0 | 2.0077 | 0.0 |
| 6 | 1284.880 | 2.855E-3 | 0.6860 | 0.0 | 1.4784 | 180.0 |
| 7 | 1617.531 | 2.860E-3 | 8.9909 | 0.0 | 1.7492 | 0.0 |

RANDOM EXCITATION: 'IDENT' TYPE ANALYSIS

| Mode | Natural frequency | Damping ratio | Mode shape pt(1,1) | | Mode shape pt(3,1) | |
|------|-------------------|---------------|--------------------|-------|--------------------|-------|
| | | | Vector | phase | Vector | phase |
| 1 | 60 | 2.672E-2 | 2.3091 | 0.0 | 3.4110 | 0.0 |
| 2 | 160 | 2.280E-3 | 1.9810 | 0.0 | 2.9239 | 180.0 |
| 3 | 310 | 1.440E-3 | 1.5794 | 0.0 | 2.9321 | 0.0 |
| 4 | 510 | 3.060E-3 | 1.1964 | 0.0 | 2.9578 | 180.0 |
| 5 | 740 | 1.930E-3 | 0.6628 | 0.0 | 2.7063 | 0.0 |
| 6 | 1290 | 1.840E-3 | 0.4403 | 0.0 | 2.5668 | 180.0 |
| 7 | 1615 | 2.545E-3 | 0.8797 | 0.0 | 2.1198 | 0.0 |

IMPULSE EXCITATION: 'IDENT' TYPE ANALYSIS

| Mode | Natural frequency | Damping ratio | Mode shape pt(1,1) | | Mode shape pt (3,1) | |
|------|-------------------|---------------|--------------------|-------|---------------------|-------|
| | | | Vector | phase | Vector | phase |
| 1 | 60 | 3.519E-2 | 2.3765 | 0.0 | 3.3663 | 0.0 |
| 2 | 160 | 1.240E-2 | 1.9645 | 0.0 | 3.3016 | 180.0 |
| 3 | 31s | 1.257E-2 | 1.6347 | 0.0 | 3.0771 | 0.0 |
| 4 | 525 | 4.560E-3 | 1.2868 | 0.0 | 3.4318 | 180.0 |
| 5 | 770 | 4.480E-3 | 1.0531 | 0.0 | 12.4818 | 0.0 |

Table 4.3 Modal parameters from FRF data obtained using random and impulse excitations

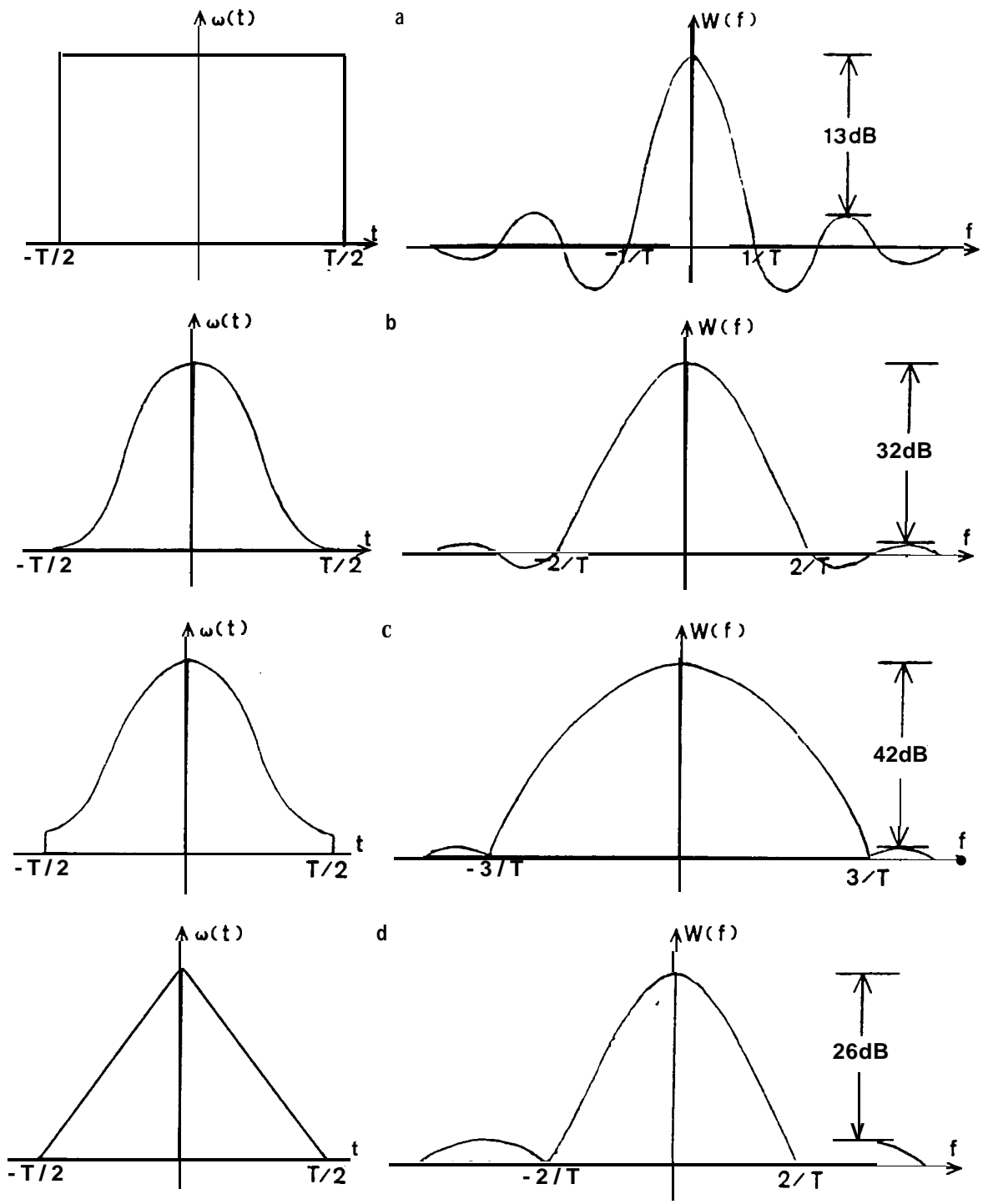


Fig 4.1 Common windows and the i r frequency components
 a Rect angu 1 ar
 b Hanning
 c Hamming
 d Tr i angu 1 ar

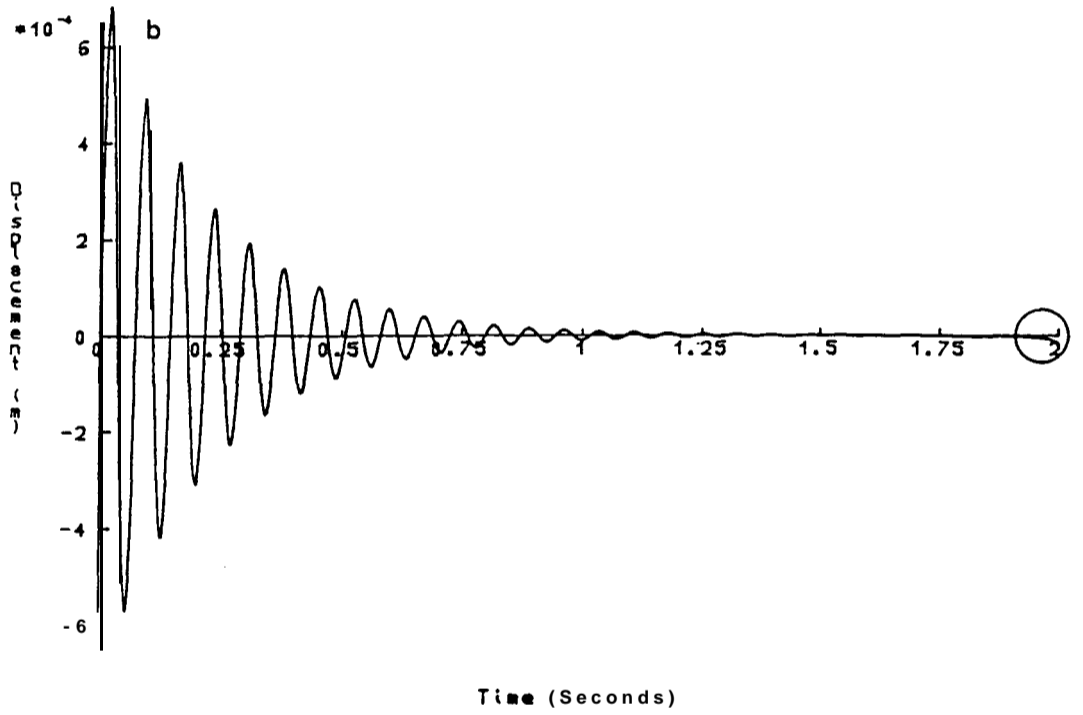
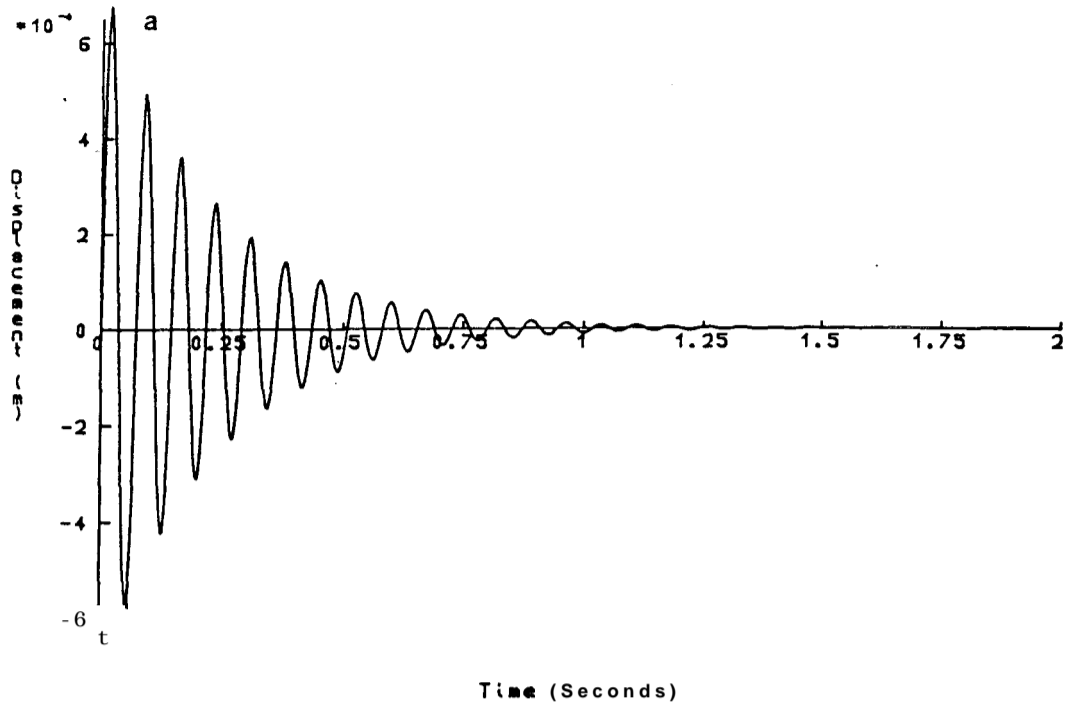


Fig 4.2 Comparison of time-histories transformed from SDOF modal models with equivalent linear damping
 a Viscous damping; $\zeta = 8.05$
 b Hysteretic damping; $\eta = 0.10$

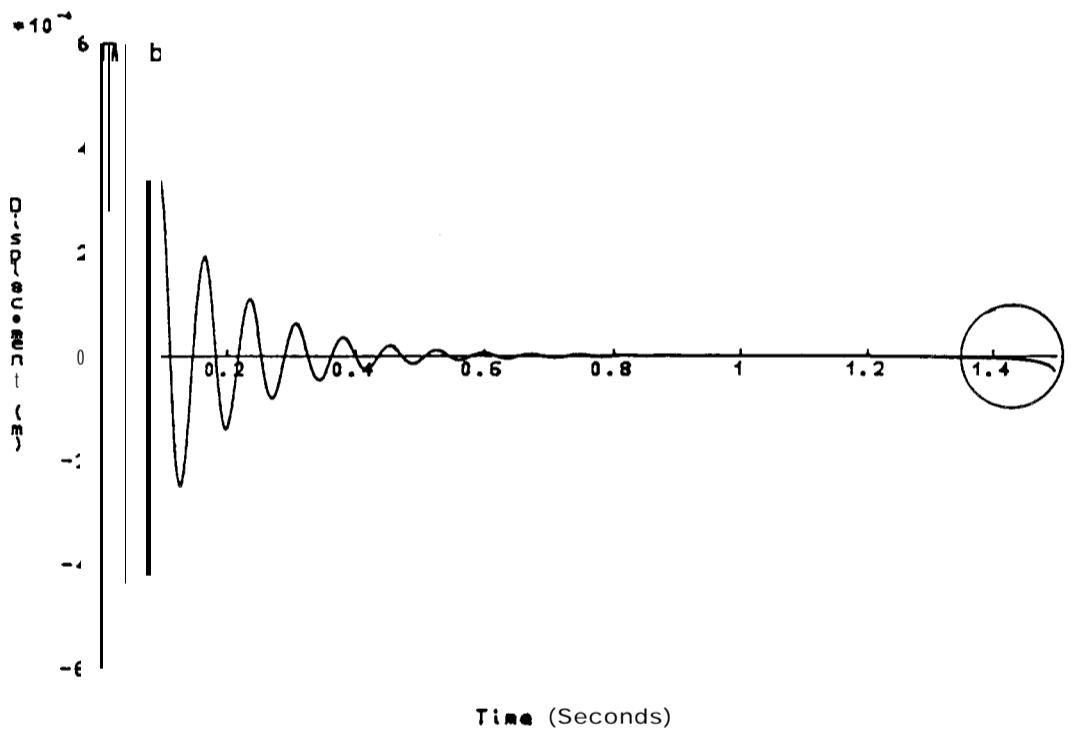
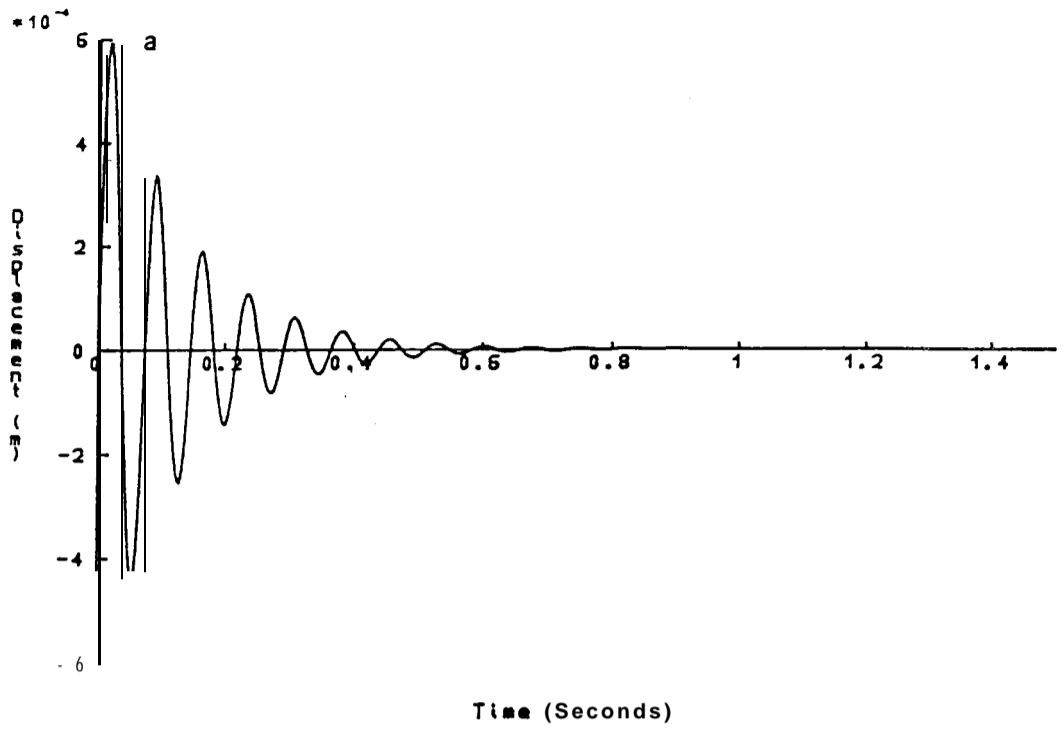


Fig 4.3 Comparison of time-histories transformed from SDOF modal models with equivalent linear damping
 a Viscous damping; $\zeta = 0.09$
 b Hysteretic damping; $\eta = 0.18$

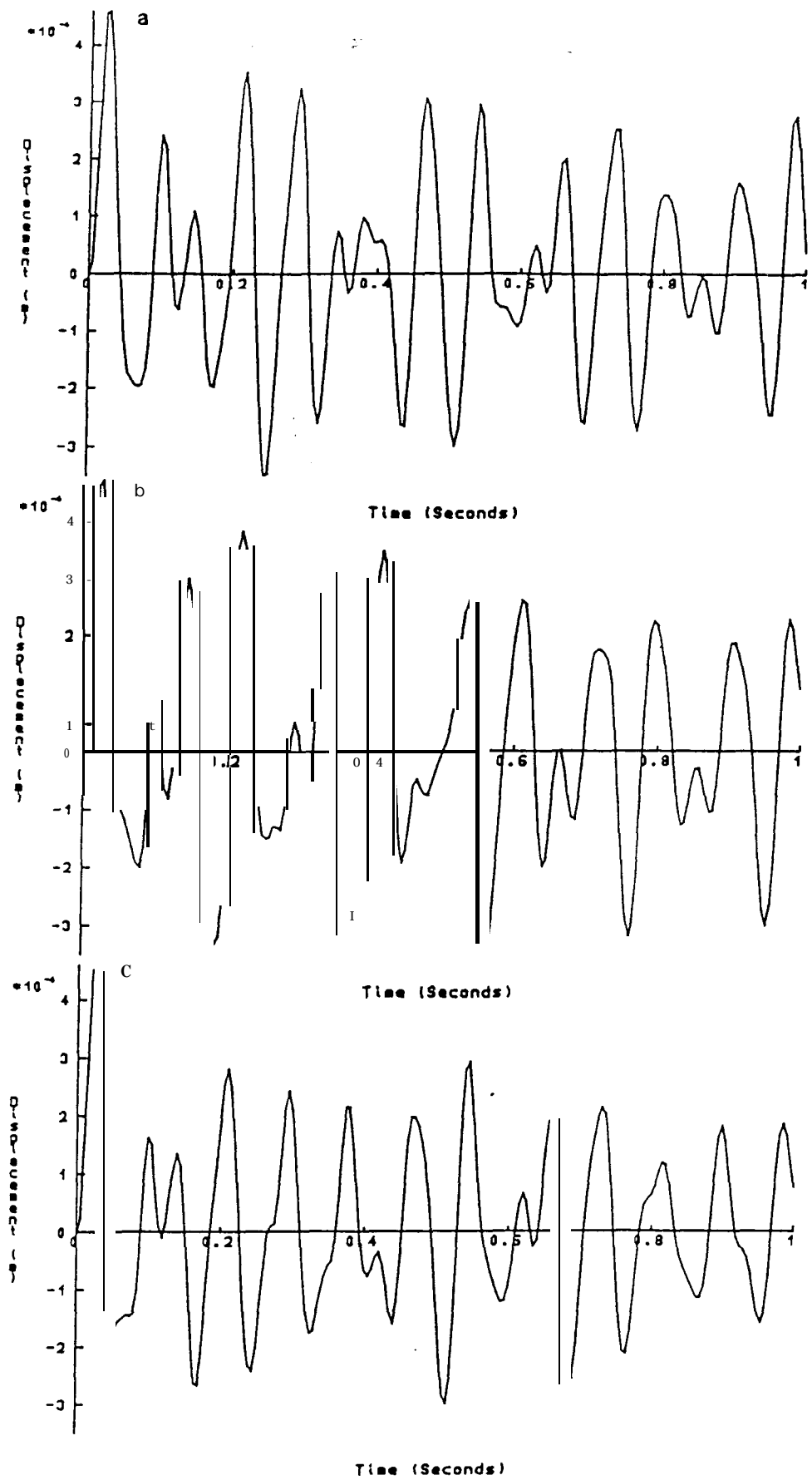


Fig 4.4 Effect of errors in natural frequency on the predicted time-history of a theoretical 12 mode system
 a Correct solution
 b -10% error in the natural frequency of mode 1
 c +10% error in the natural frequency of mode 2

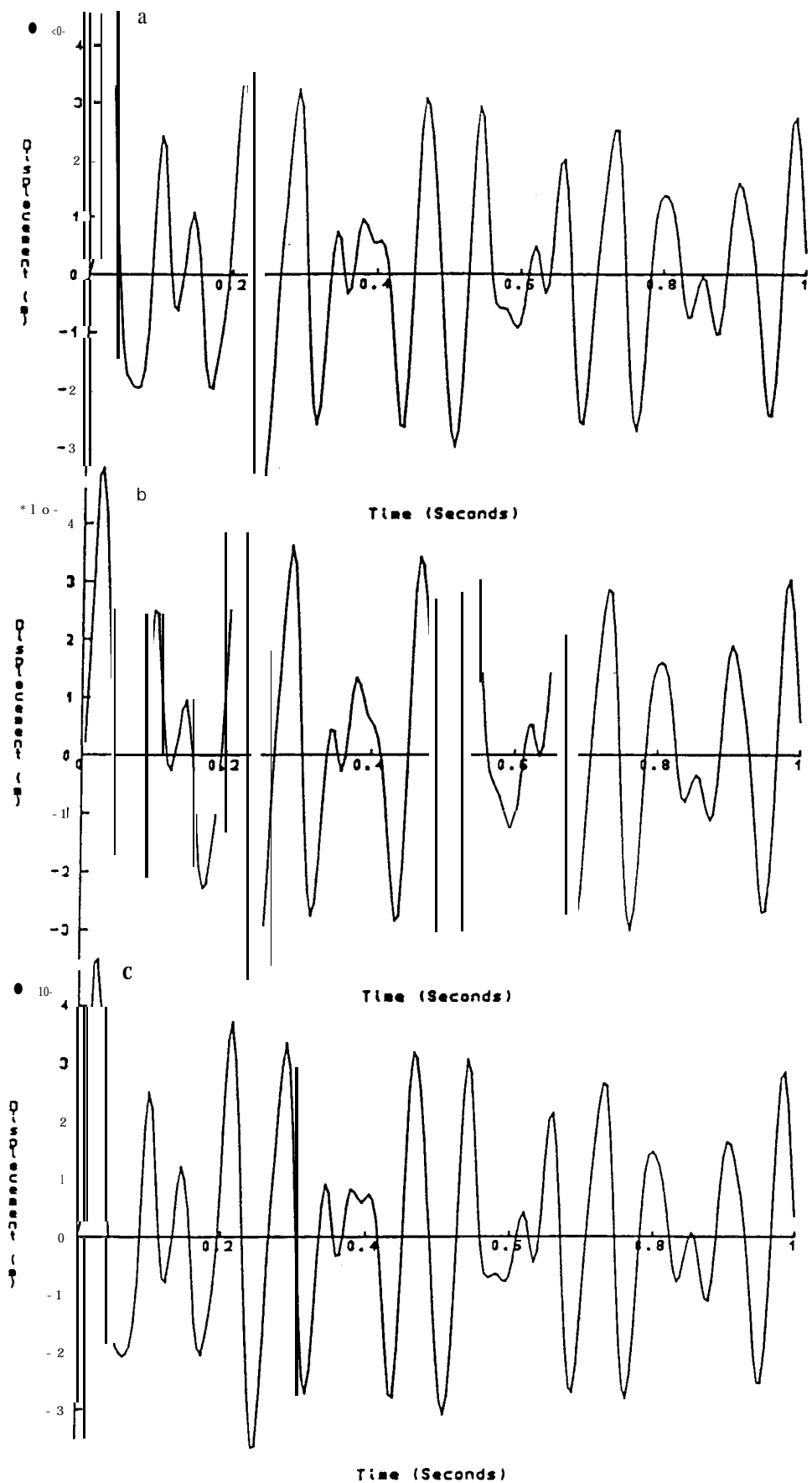


Fig 4.5 Effect of errors in the magnitude of the modal constant on the predicted time-history of a theoretical 12 mode system
 a Correct solution
 b +10% error in the modal constant of mode 1
 c +10% error in the modal constant of mode 3

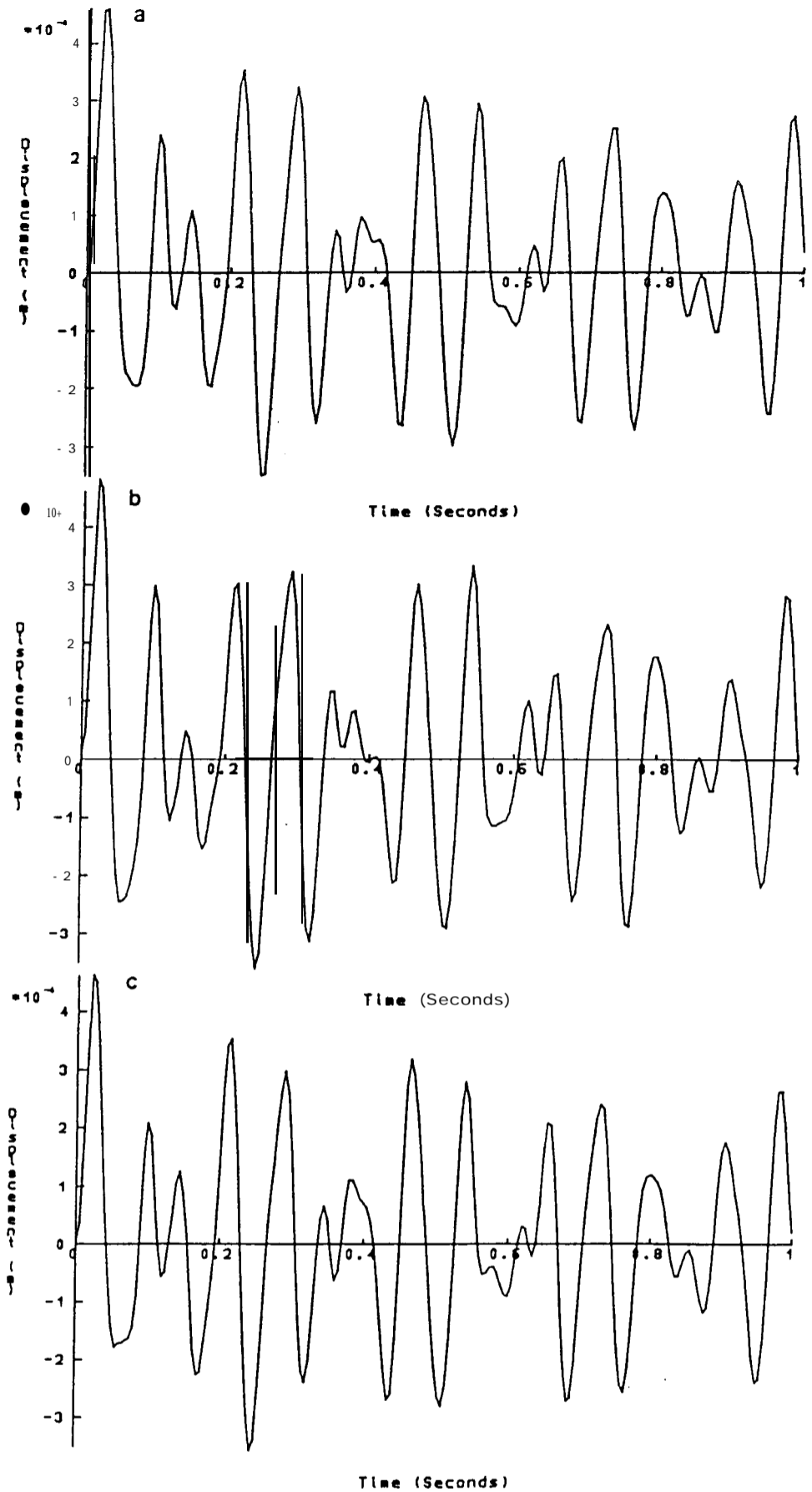


Fig 4.6 Effect of errors in the phase of the modal constant on the predicted time-history of a theoretical 12 mode system

- a Correct solution
- b $+10^0$ on mode 1
- c $+10^0$ on mode 3

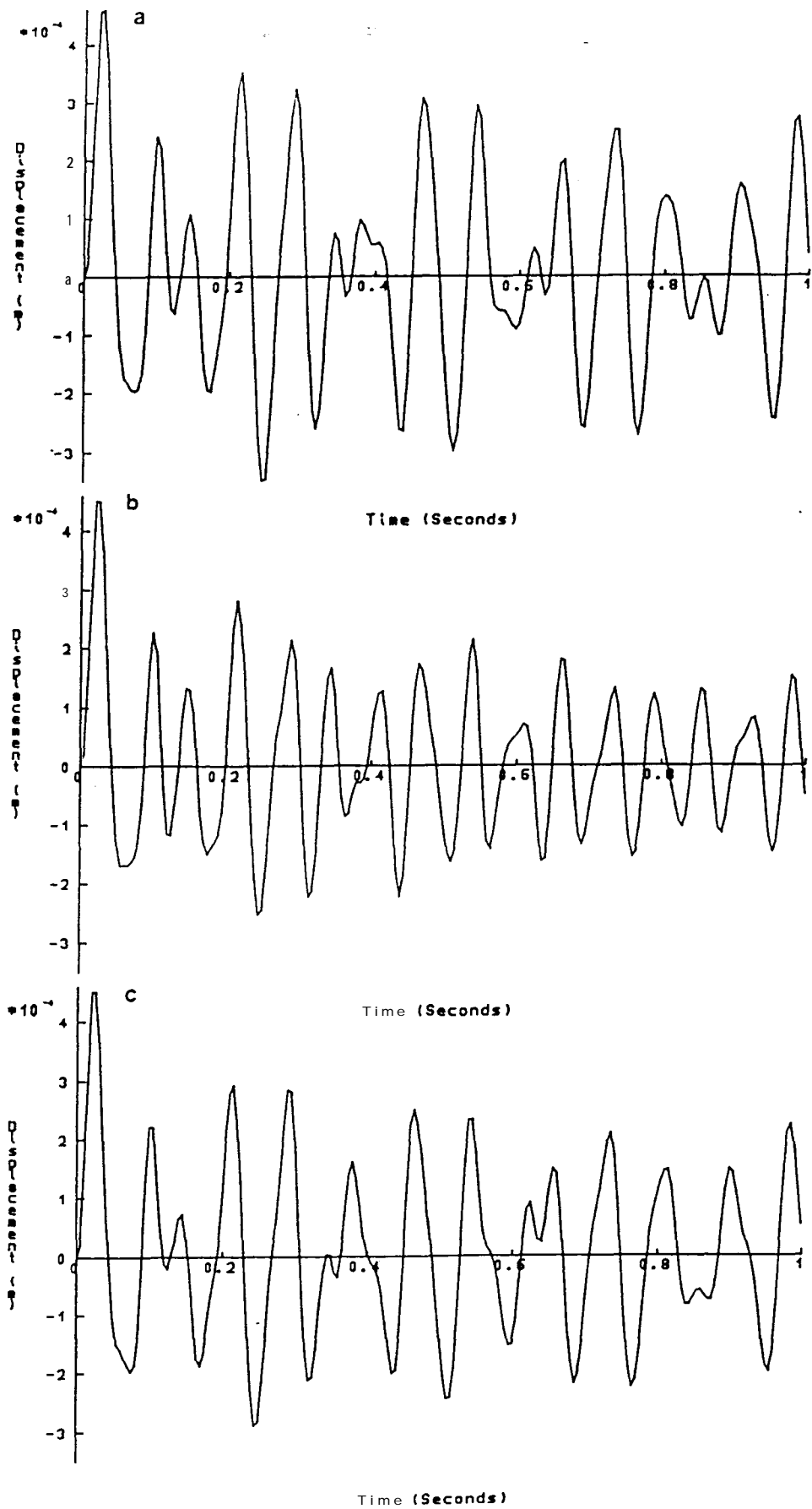


Fig 4.7 Effect of errors in the damping estimate on the predicted time-history of a theoretical 12 mode system

- a Correct solution
- b Damping $\times 10$ on mode 1
- c Damping $\times 10$ on mode 3

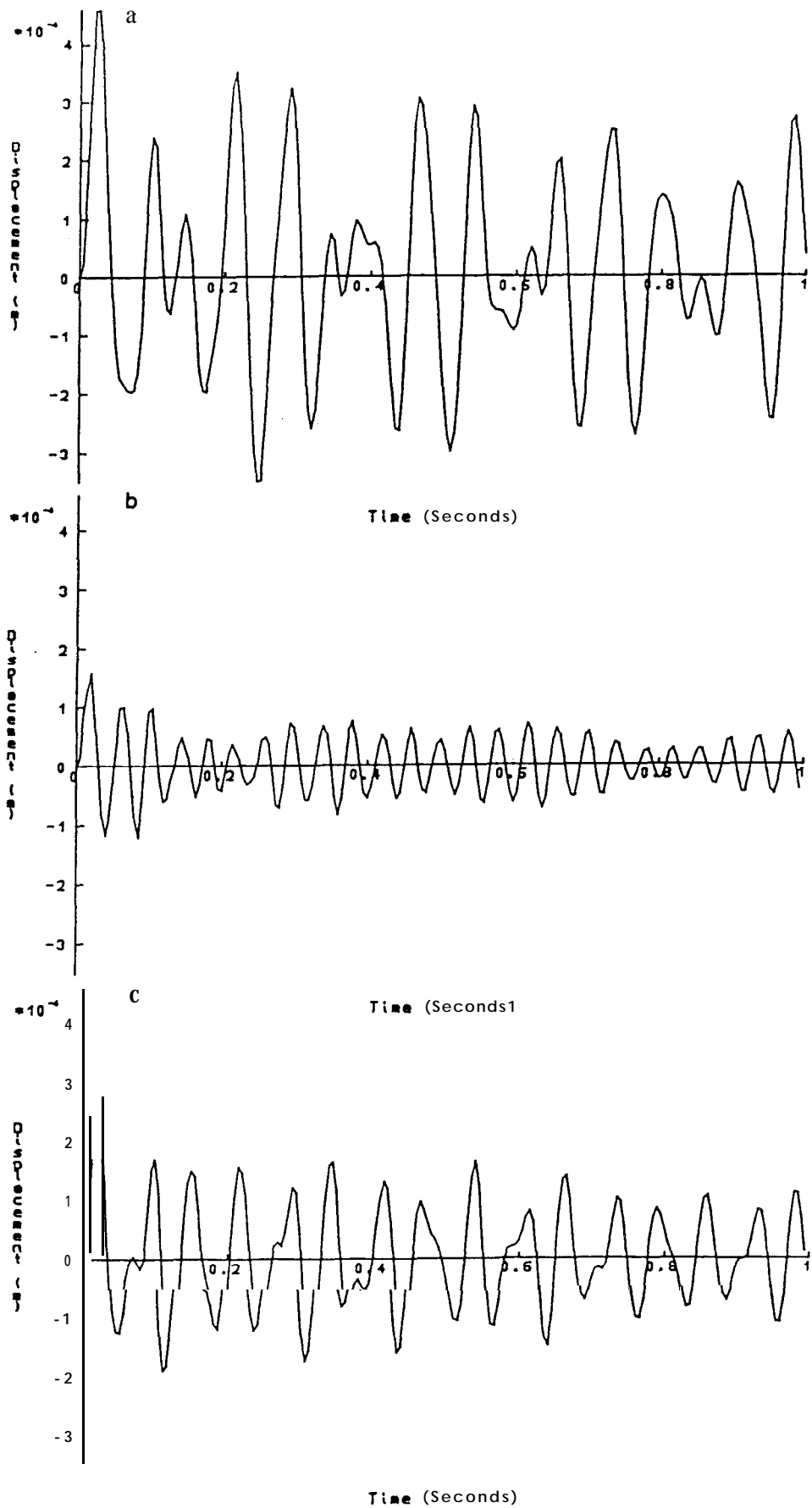


Fig 4.8 Displacement time-histories from a theoretical 12 mode system
 a All modes included
 b Minus the first three modes
 c Residual term replacing the first three modes

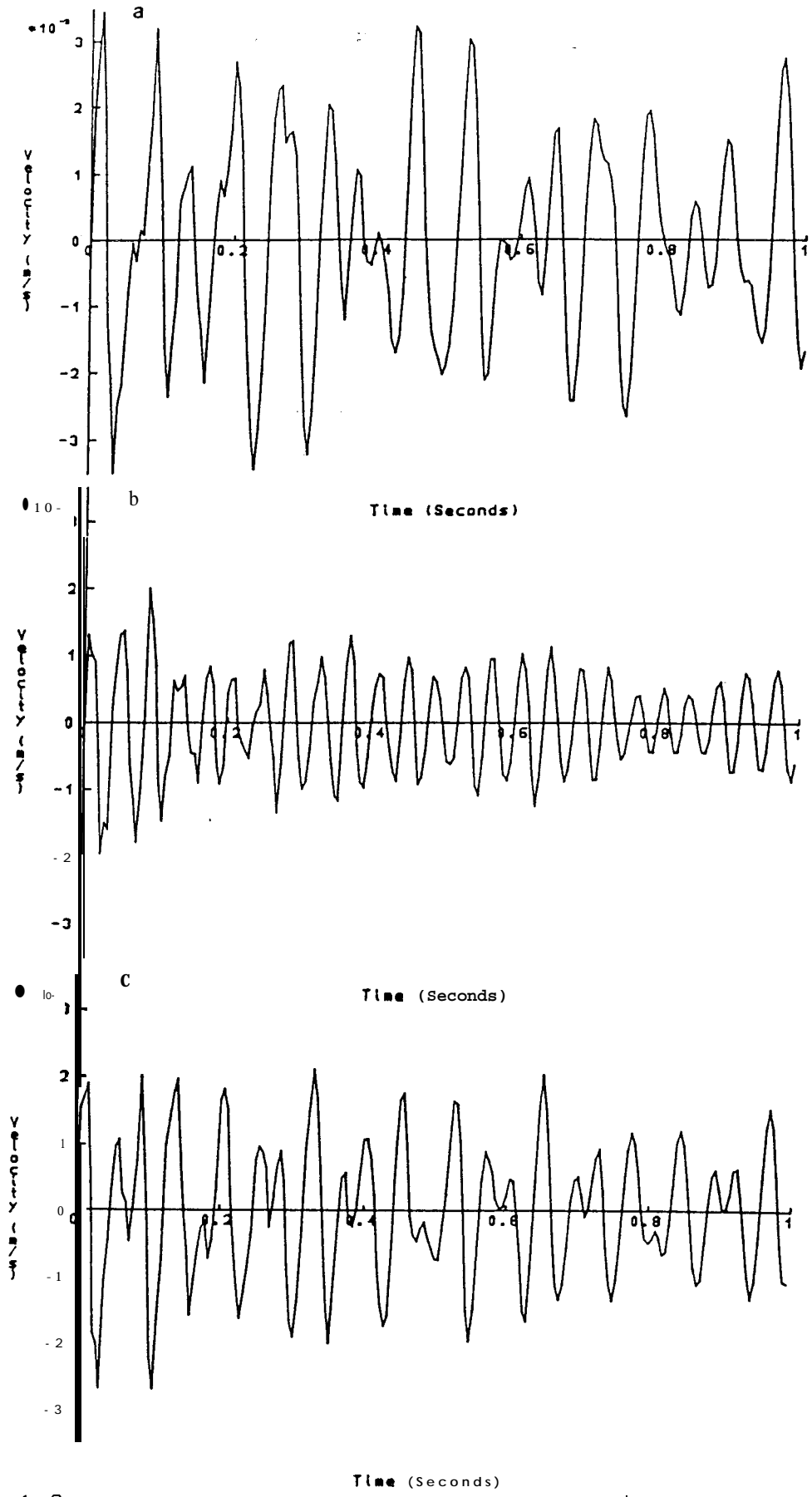


Fig 4.9 Velocity time-histories from a theoretical 12 mode system
 a All modes included
 b Minus the first three modes
 c Residual term replacing the first three modes

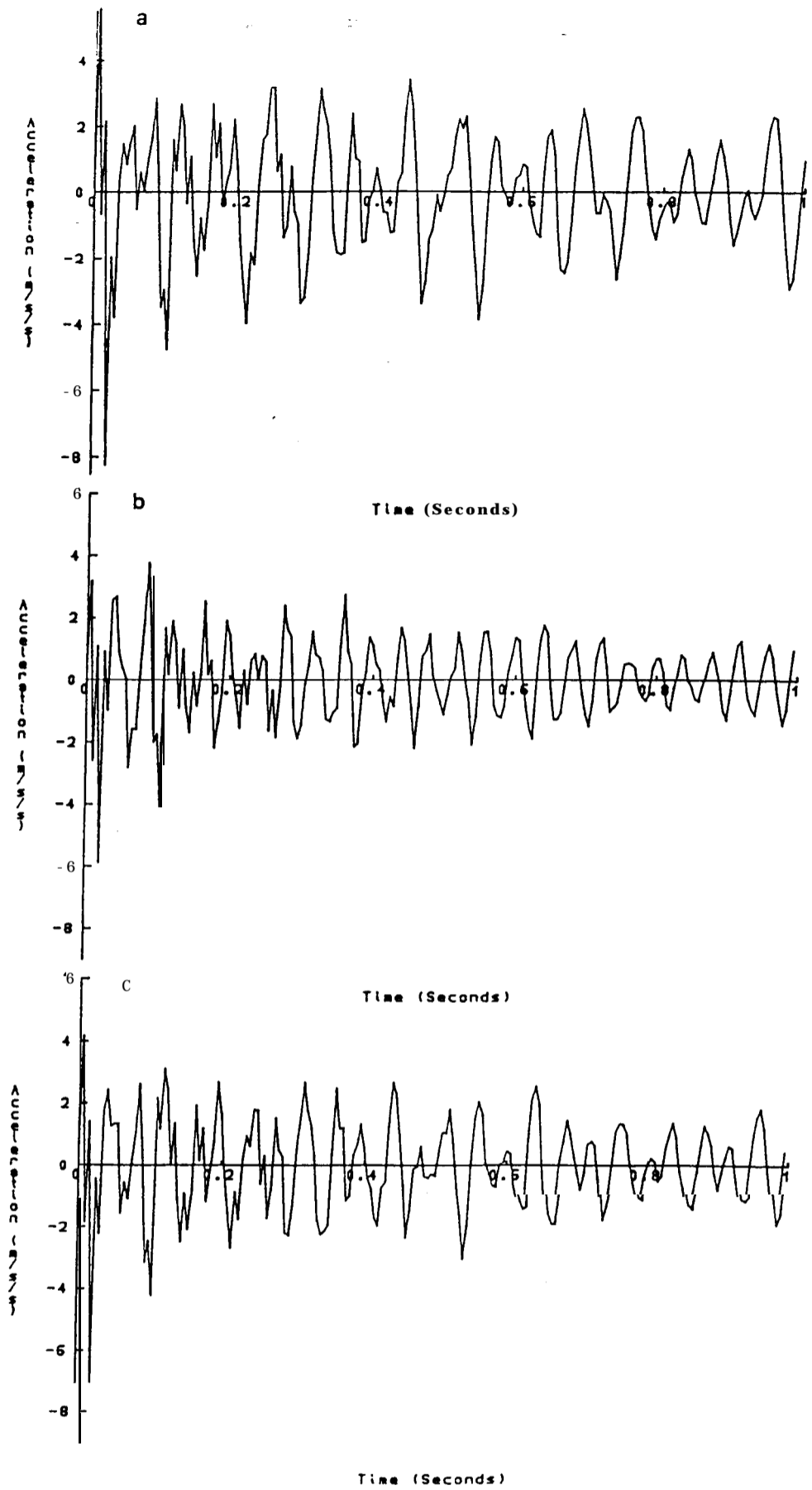


Fig 4.18 Acceleration time-histories from a theoretical 12 mode system
 a All modes included
 b Minus the first three modes
 c Residual term replacing the first three modes

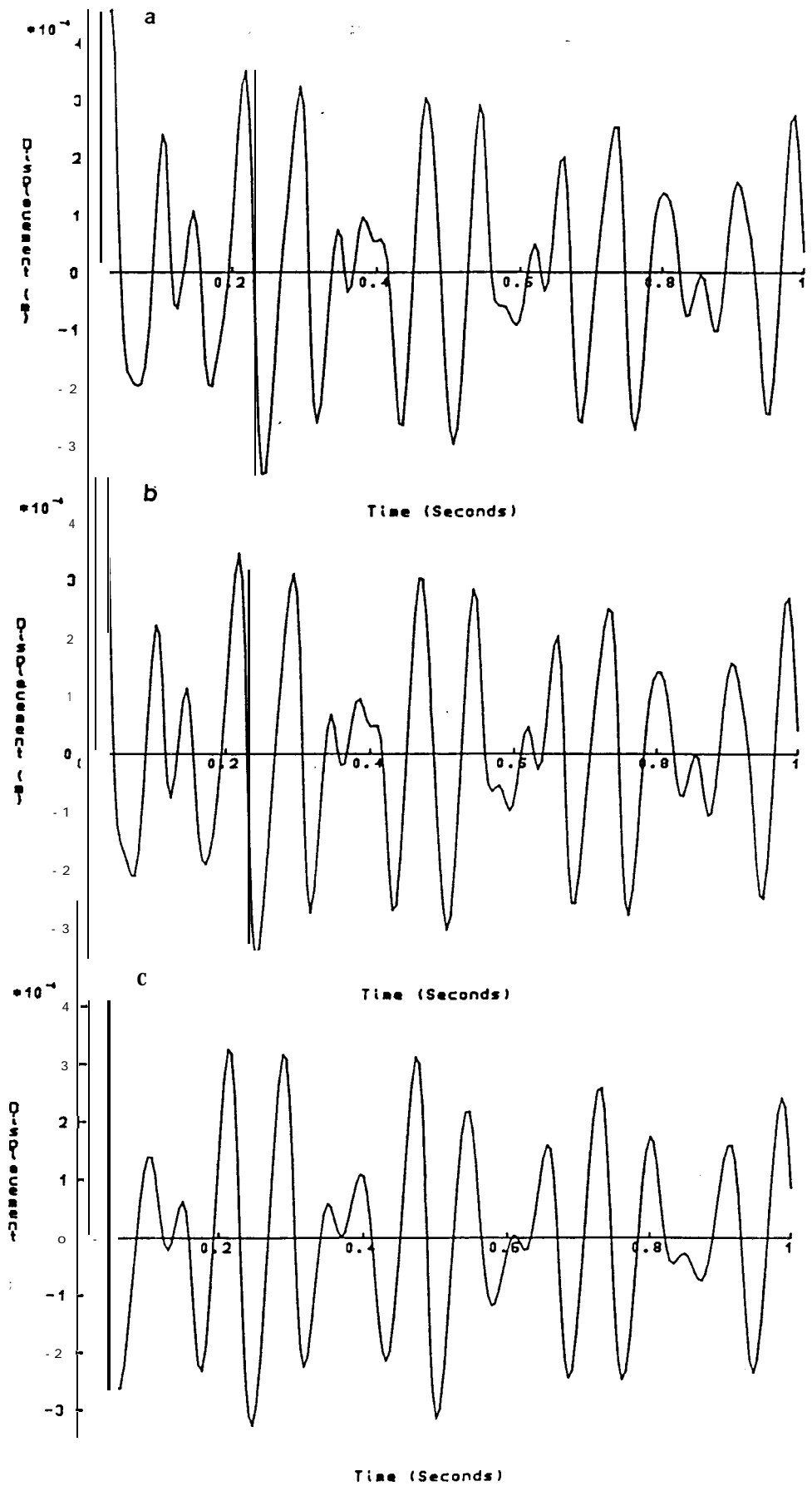


Fig 4.11 Displacement time-histories from a theoretical 12 mode system: effect of high frequency modes
 a All modes included
 b Using the first six modes only
 c Using the first four modes only

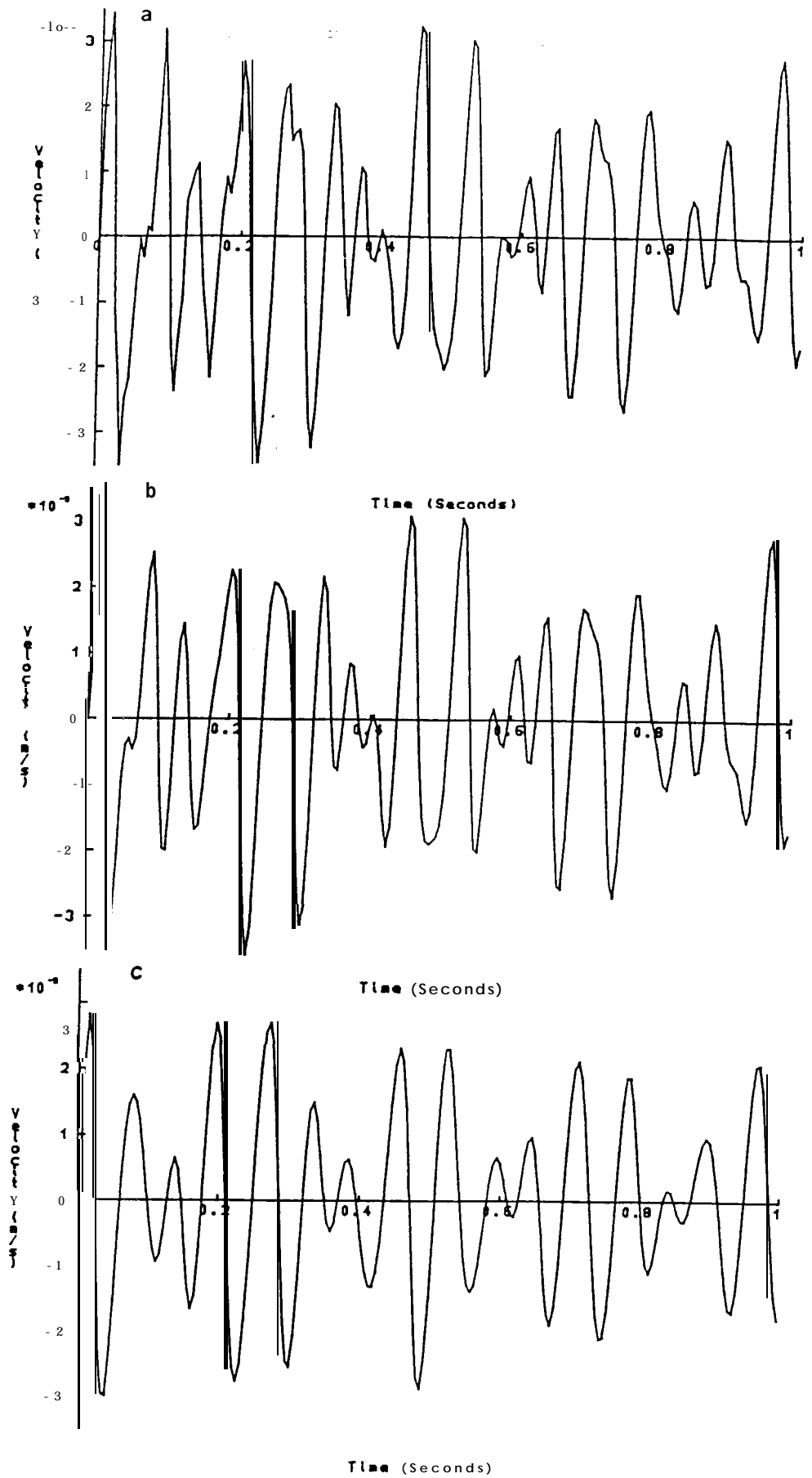


Fig 4.12 Velocity time-histories from a theoretical 12 mode system: effect of high frequency modes
 a All modes included
 b Using the first six modes only
 c Using the first four modes only

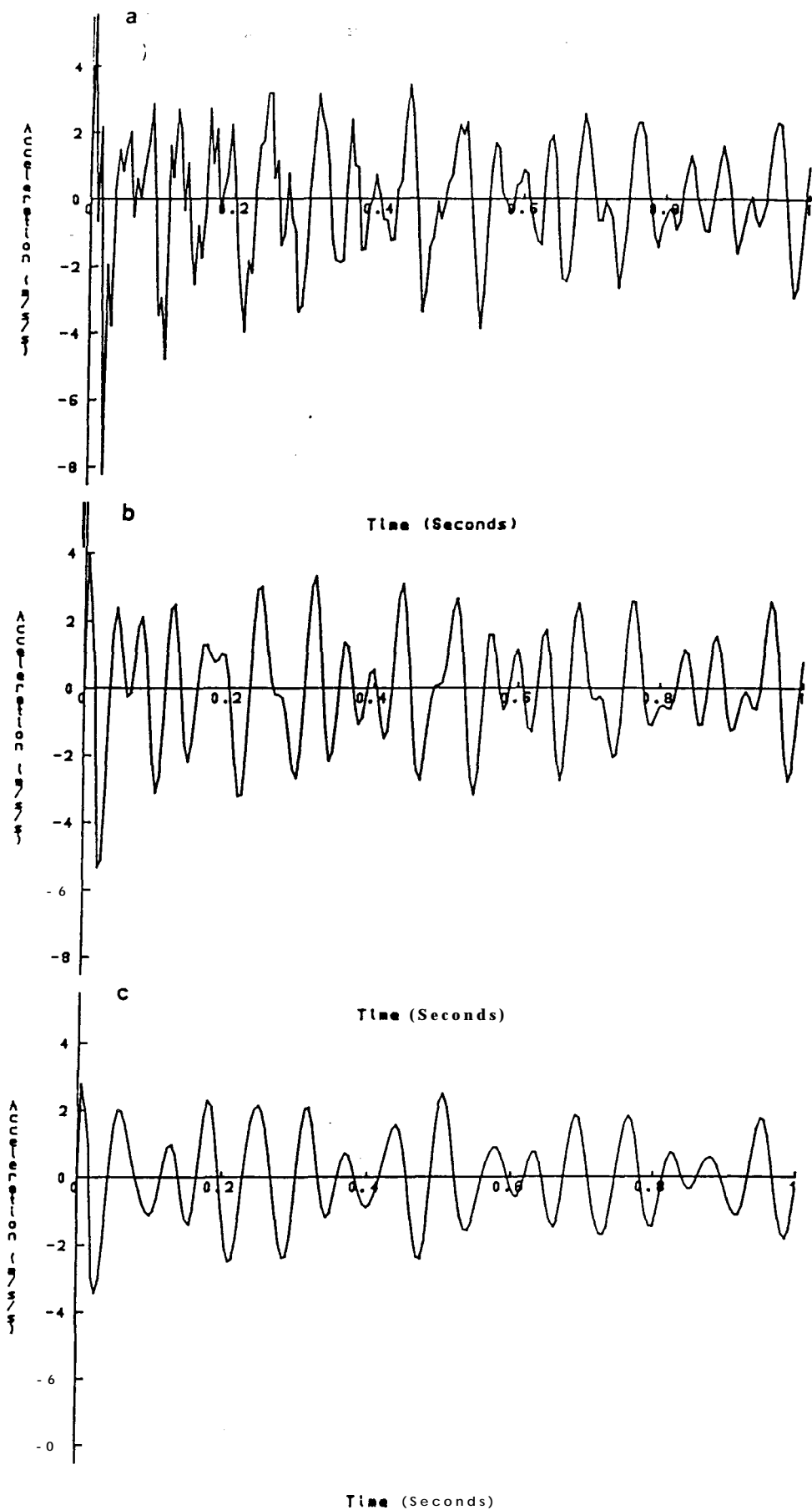


Fig 4 . 1 3 acceleration time-histories from a theoretical 12 mode system: effect of high frequency modes
 a All modes included
 b Using the first six modes only
 c Using the first four modes only

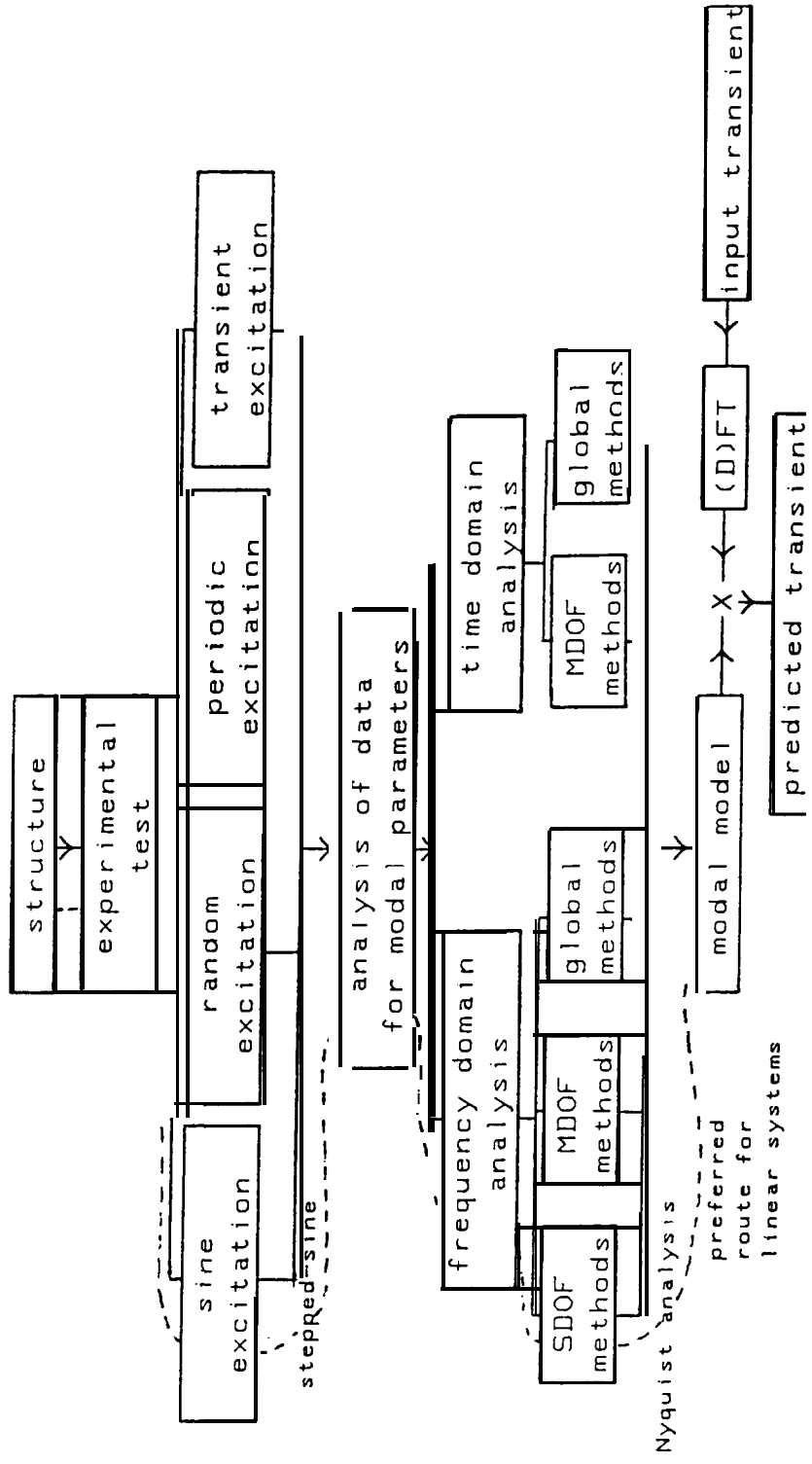


Fig 4.14 Solution routes for the 'Fourier transform method' of transient response prediction

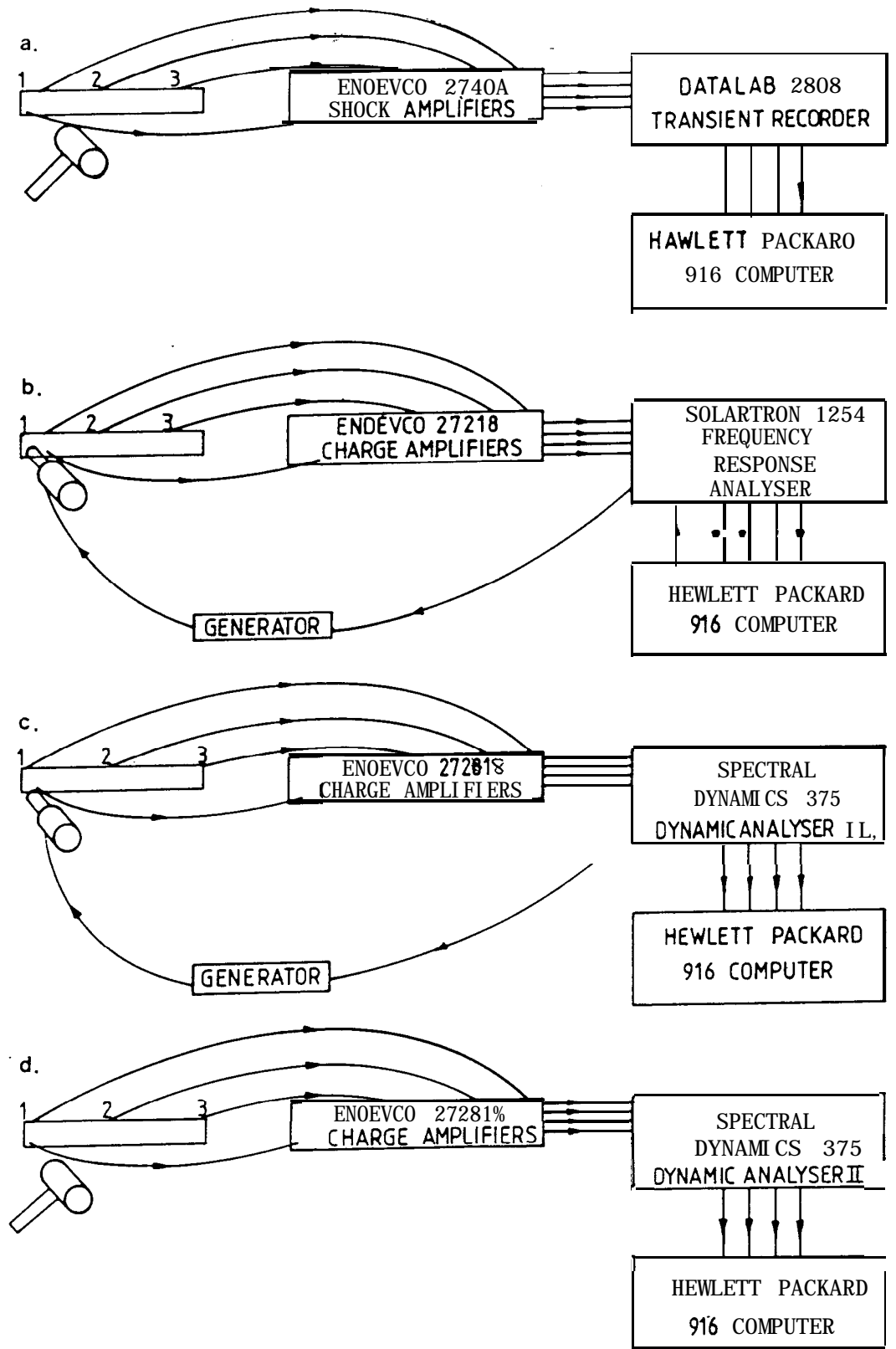


FIG. 4.15 EXPERIMENTAL SETUPS FOR ALUMINIUM BEAM

- a. IMPULSE TESTING FOR AN IRF
- b. STEPPED-SINE EXCITATION FOR AN FRF
- c. RANDOM EXCITATION FOR AN FRF
- d. IMPULSE EXCITATION FOR AN FRF

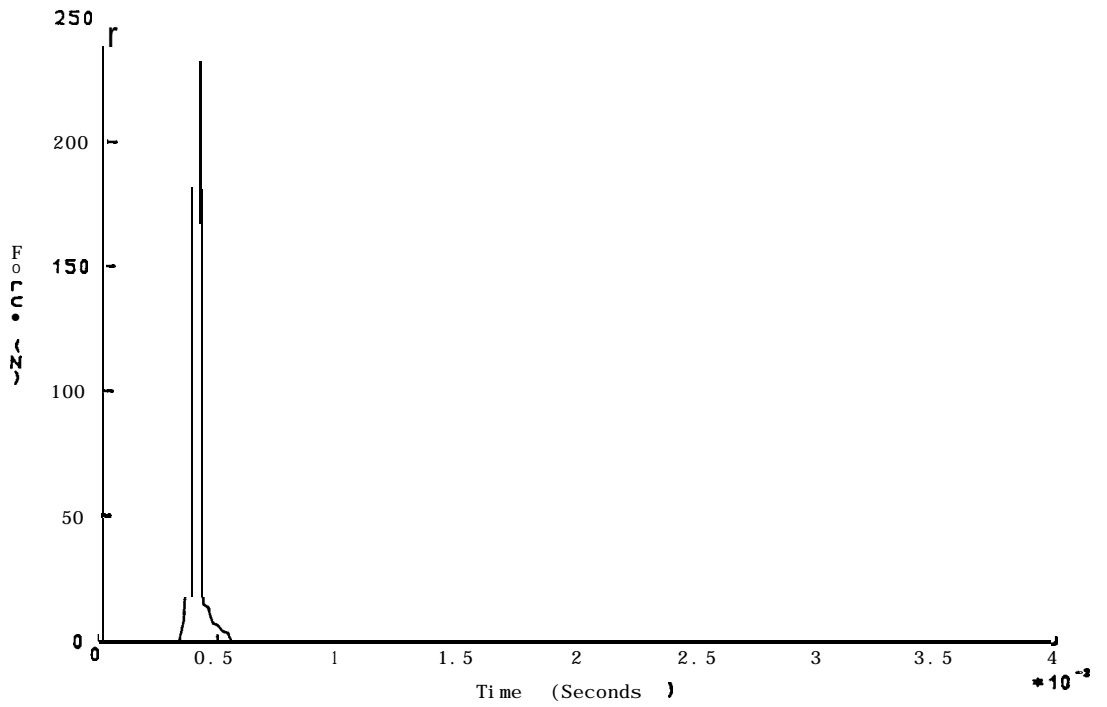


Fig 4.16 Measured input force signal

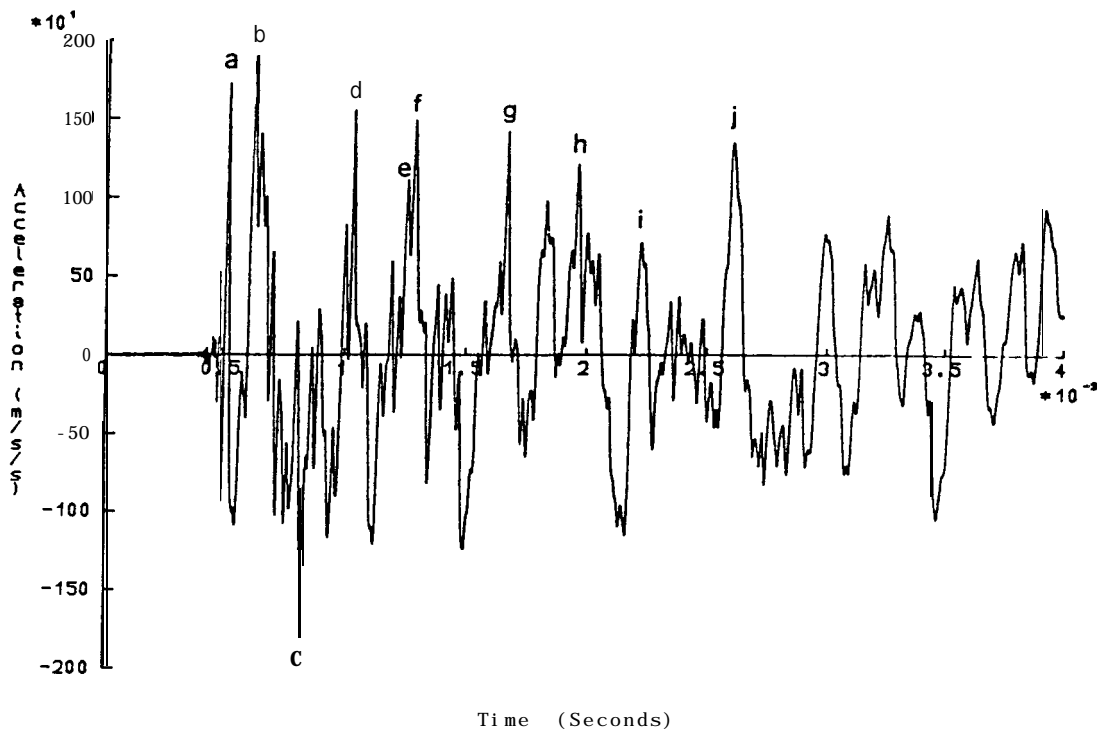


Fig 4.17 Measured acceleration time-history from point (3,1)

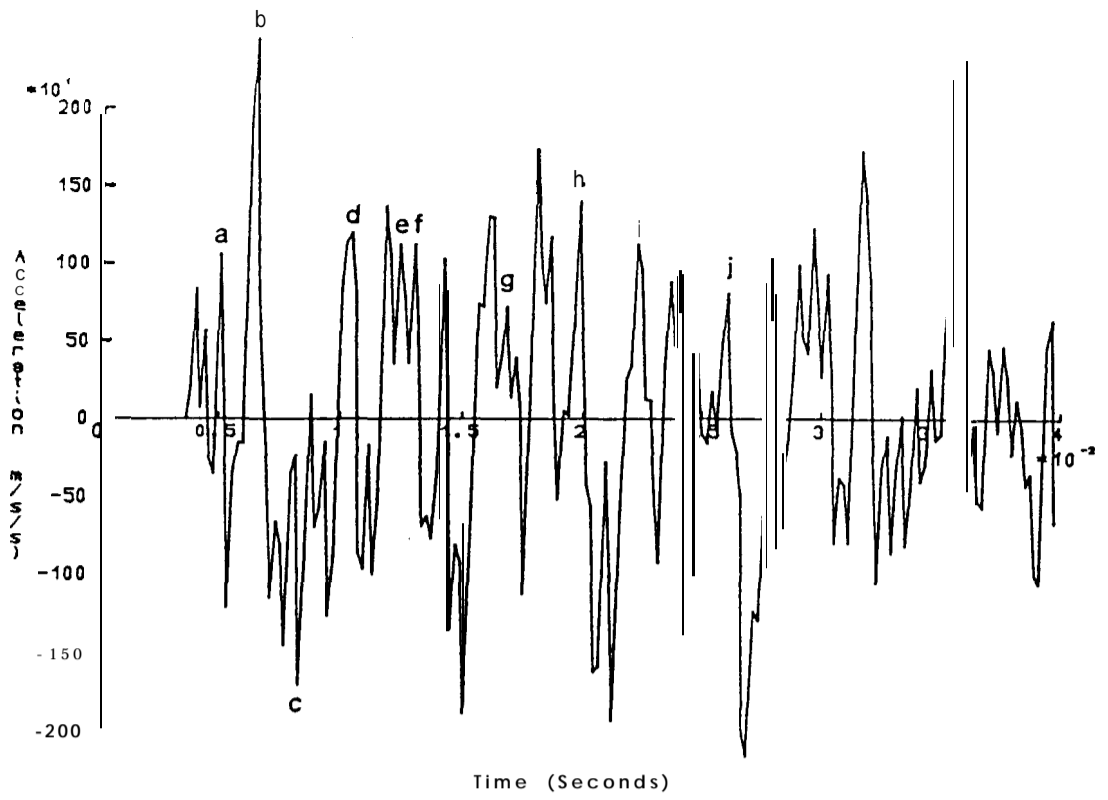


Fig 4.18a Predicted acceleration time-history from point, (3,1); stepped-sine excitation Nyquist analysis

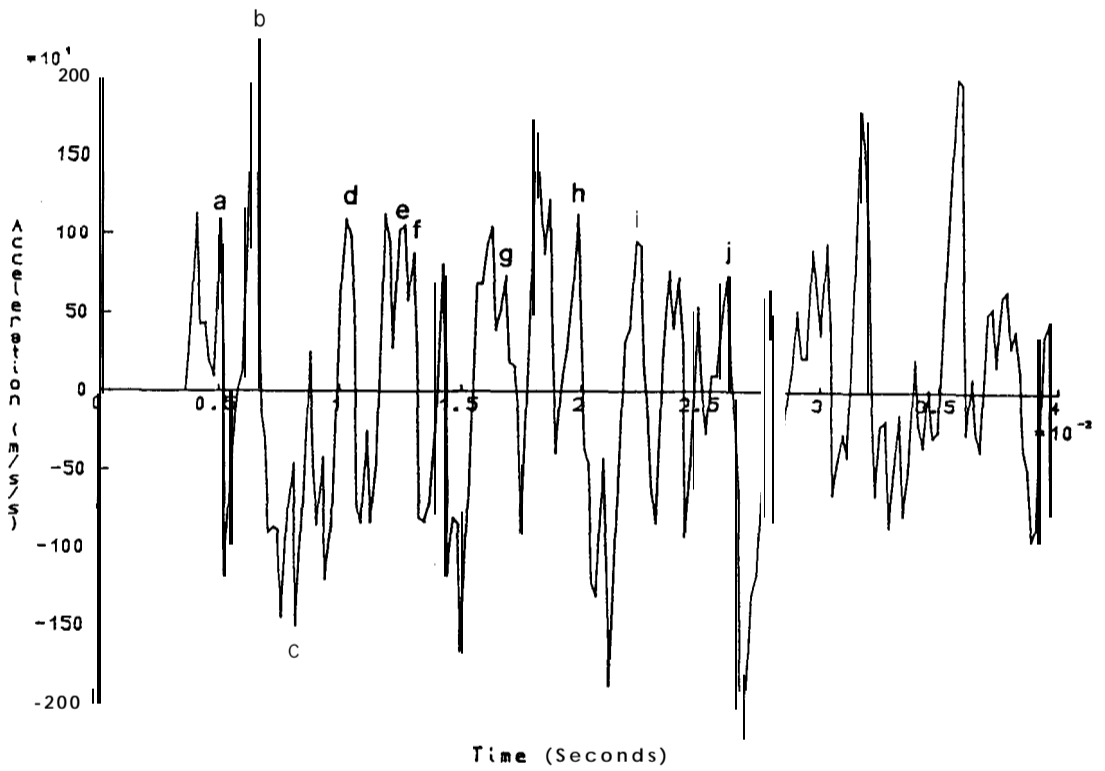


Fig 4.18b Predicted acceleration time-history from point (3,1); stepped-sine excitation; reciprocal-of-receptance analysis

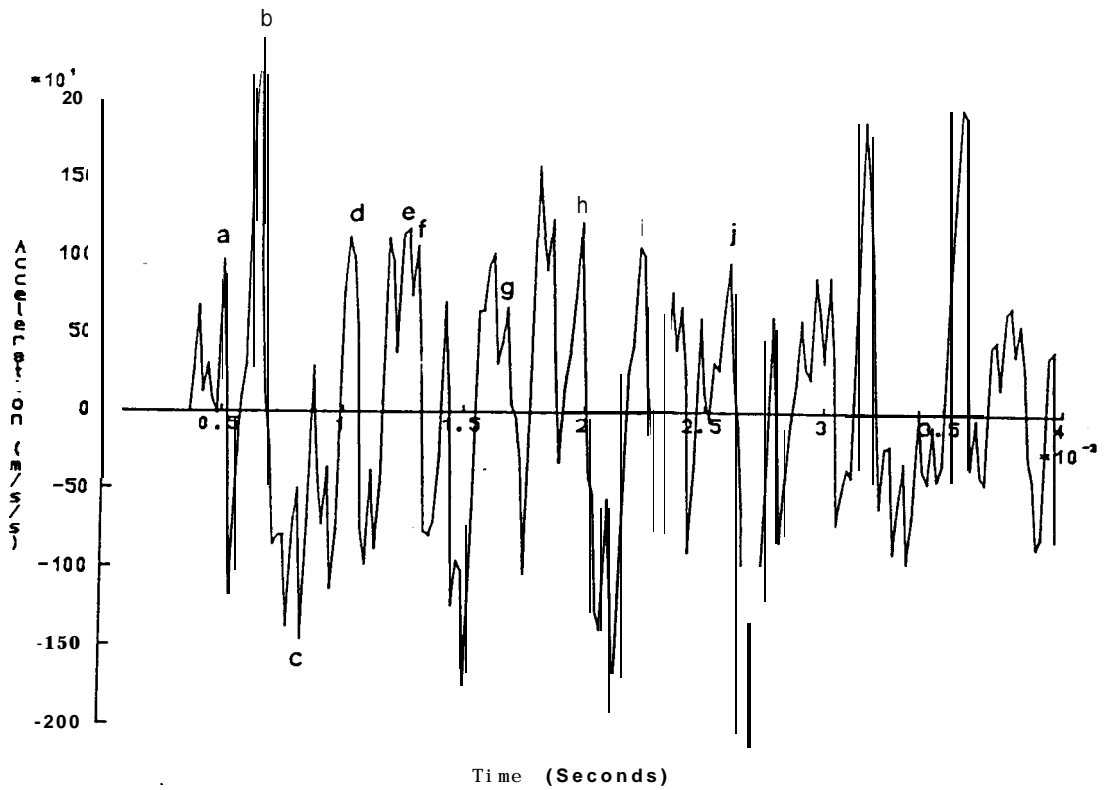


Fig 4.18c Predicted acceleration time-history from point (3,1); stepped-sine excitation; 'IDENT' type analysis

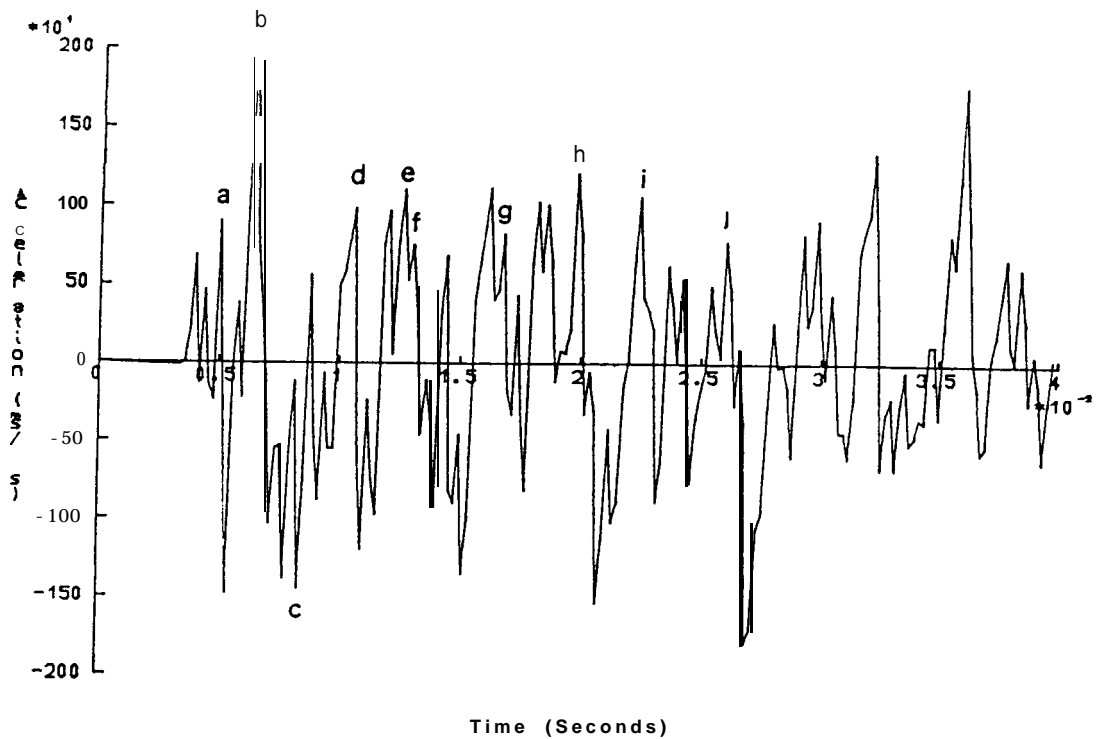


Fig 4.18d Predicted acceleration time-history from point (3,1); random excitation; reciprocal-of-receptance analysis

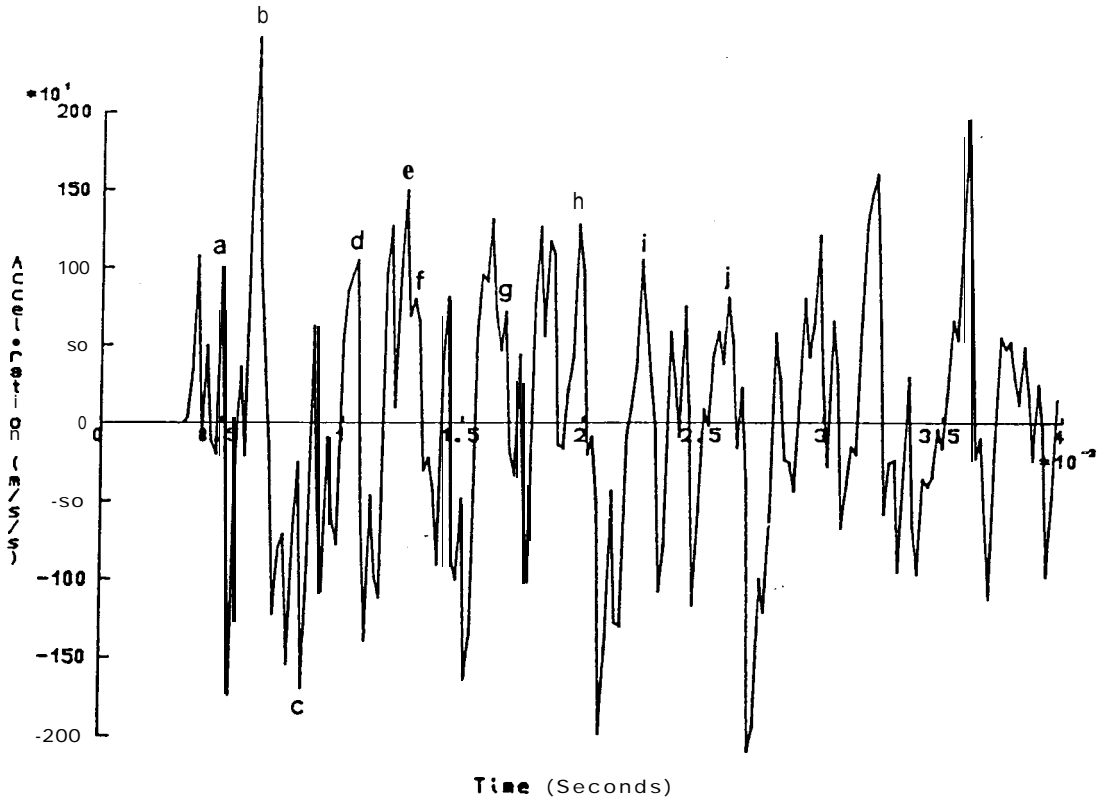


Fig 4.18e Predicted acceleration time-history from point (3,1); random excitation; 'IDENT' type analysis

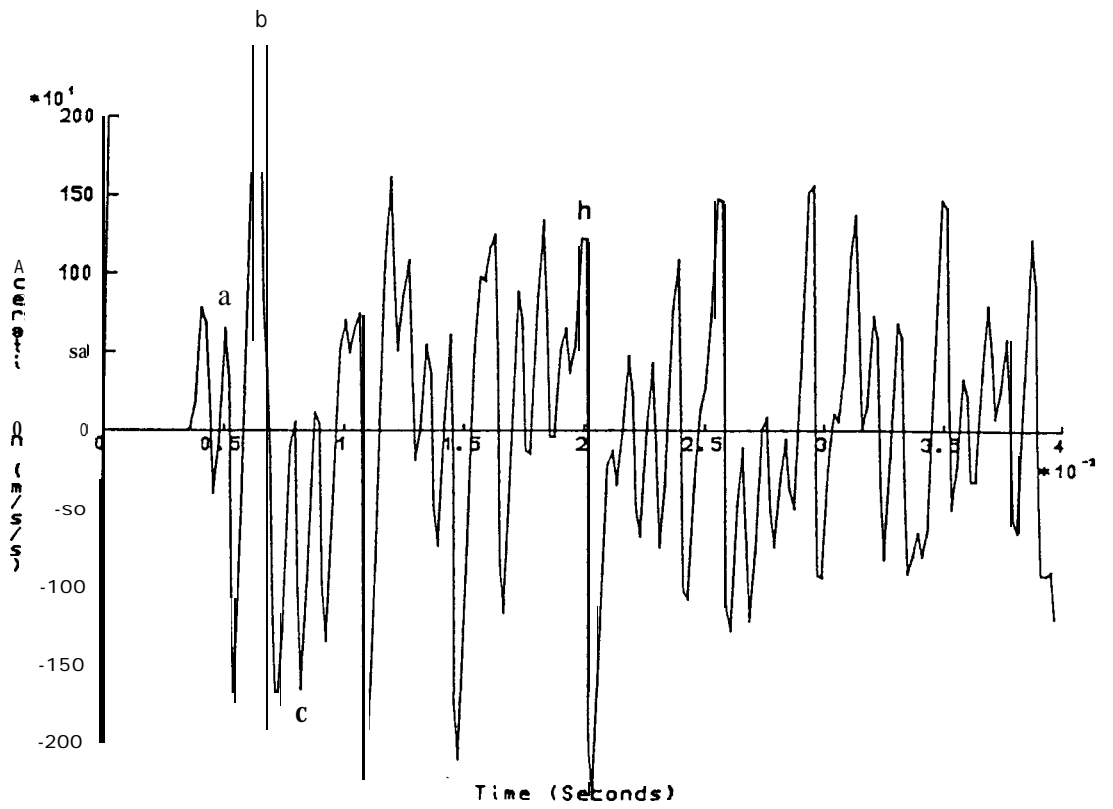


Fig 4 18f Predicted acceleration time-history from point (3,1); impulse excitation; 'IDENT' type analysis

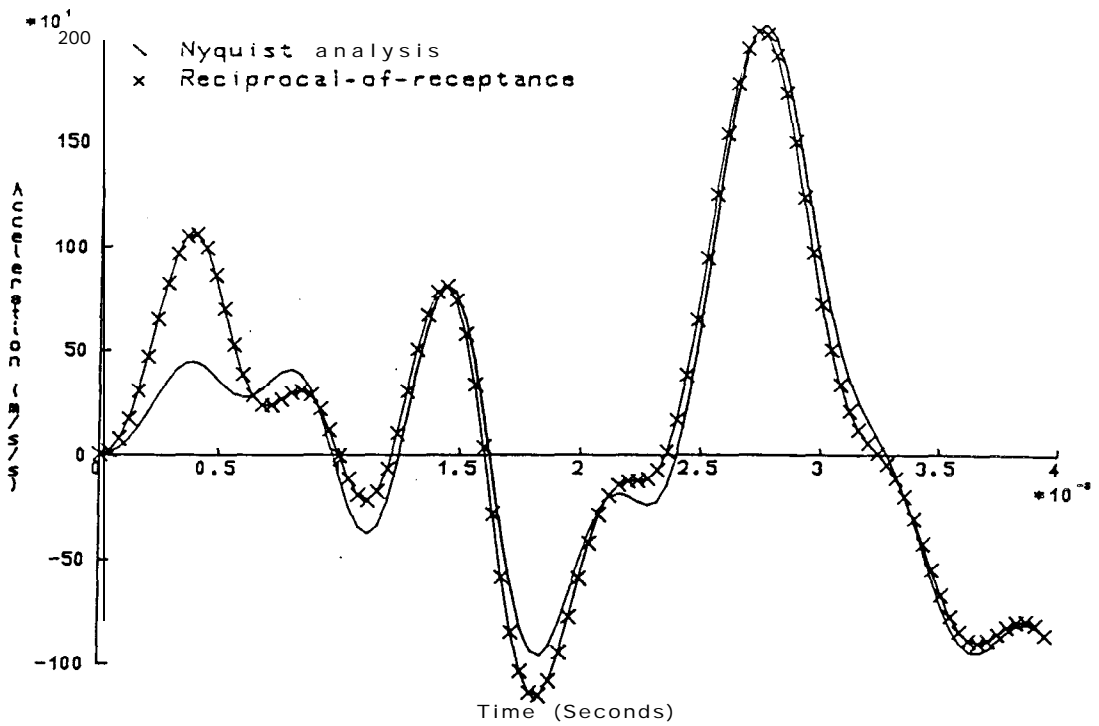


Fig 4.19a Comparison of initial predictions (with extra damping) from point (3,1); stepped-sine excitation; Nyquist and reciprocal-of-receptance analyses

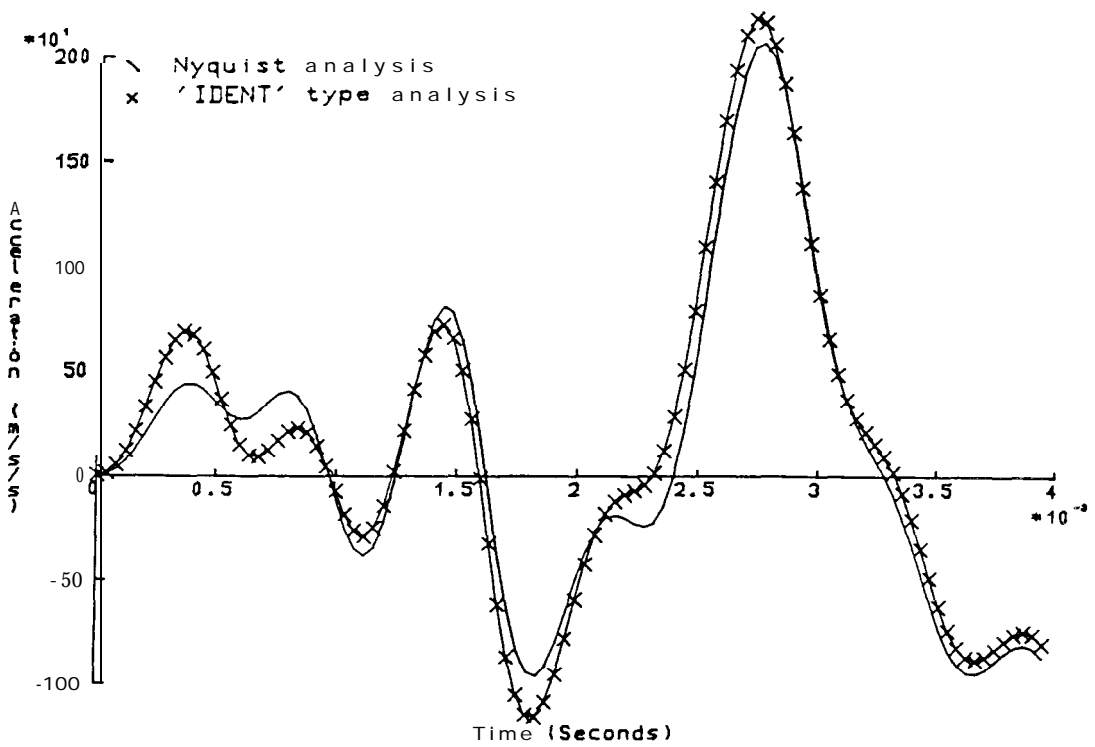


Fig 4.19b Comparison of initial predictions (with extra damping) from point (3,1); stepped-sine excitation; Nyquist and 'IDENT' type analyses

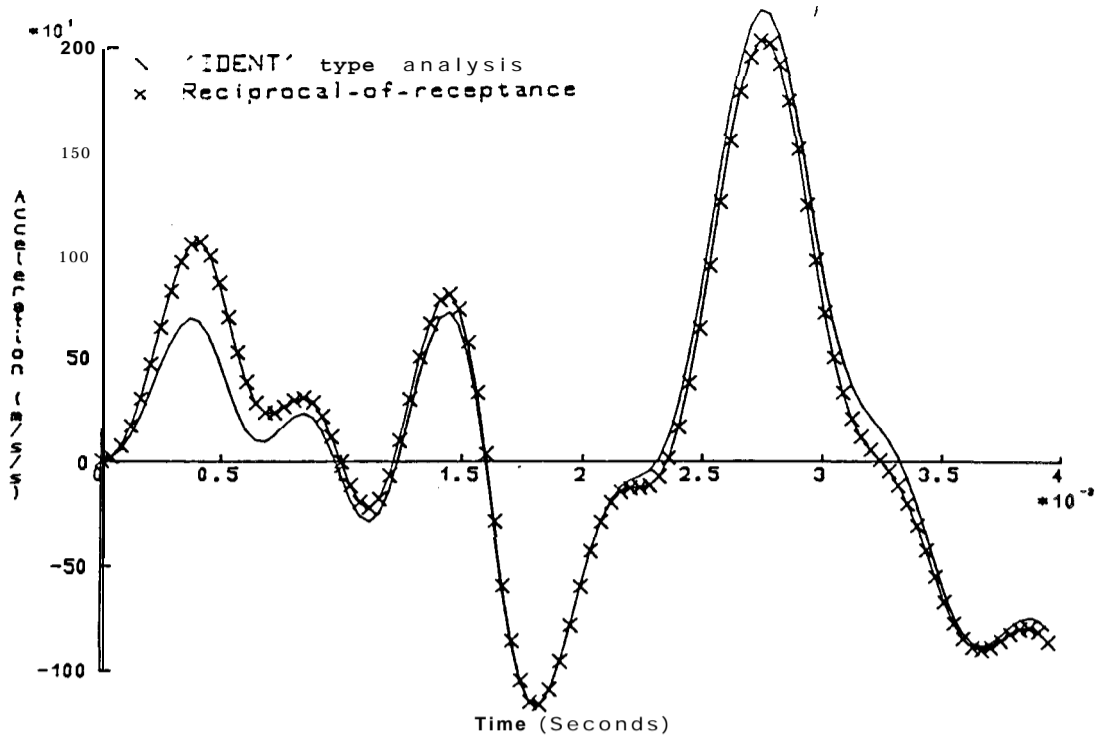


Fig 4.19c Comparison of initial predictions (with extra damping) from point (3,1); stepped-sine excitation; Reciprocal-of-receptance and 'IDENT' type analyses

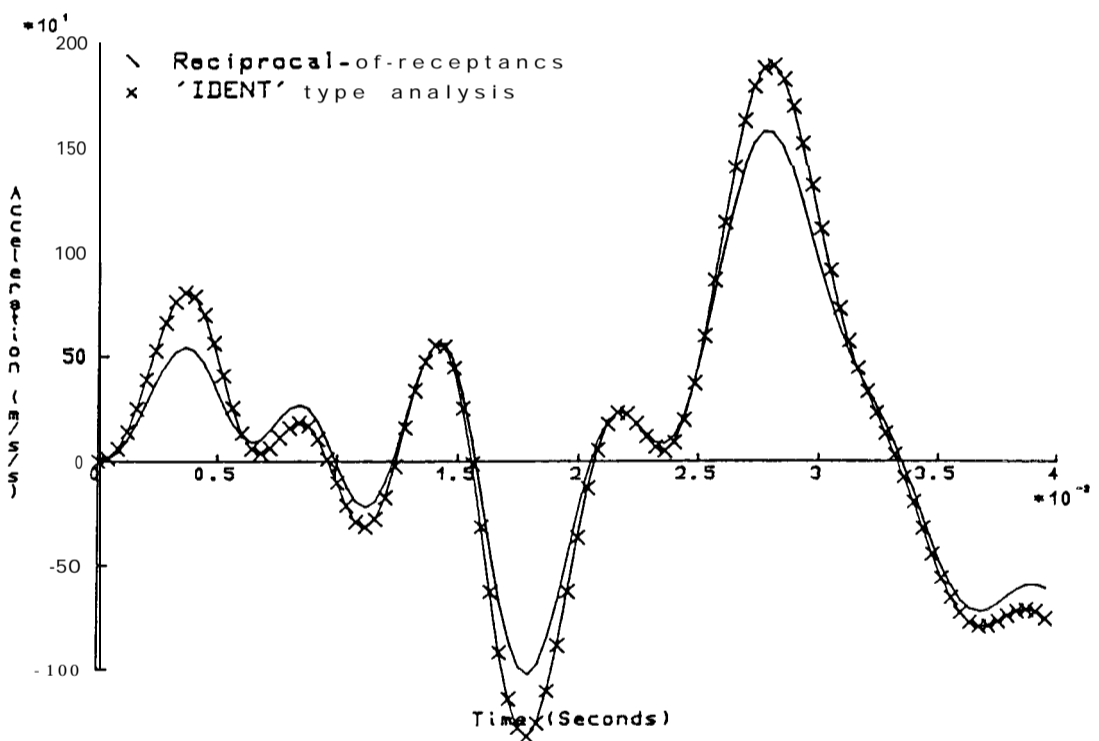


Fig 4.19d Comparison of initial predictions (with extra damping) from point (3,1); random excitation; Reciprocal-of-receptance and 'IDENT' type analyses

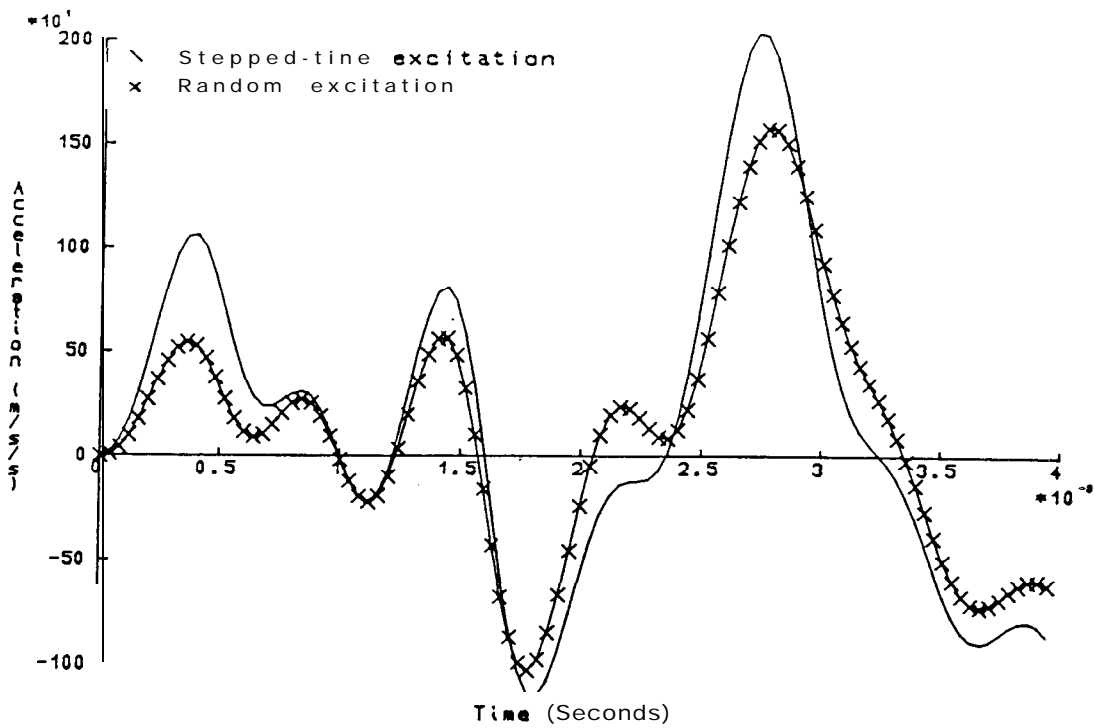


Fig 4. 9e Comparison of initial predictions (with extra damping) from point (3,1); stepped-sine and random excitations; Reciprocal-of-receptance analysis

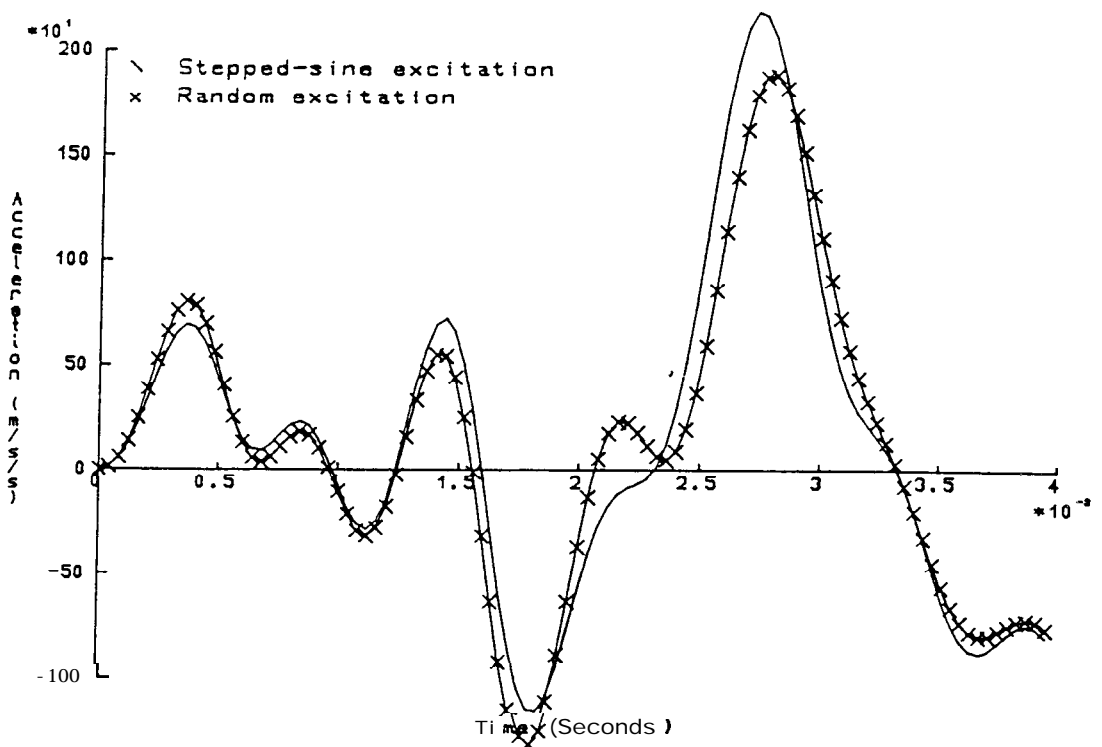


Fig 4. 9f Comparison of initial predictions (with extra damping) from point (3,1); stepped-sine and random excitations; 'IDENT' type analysis

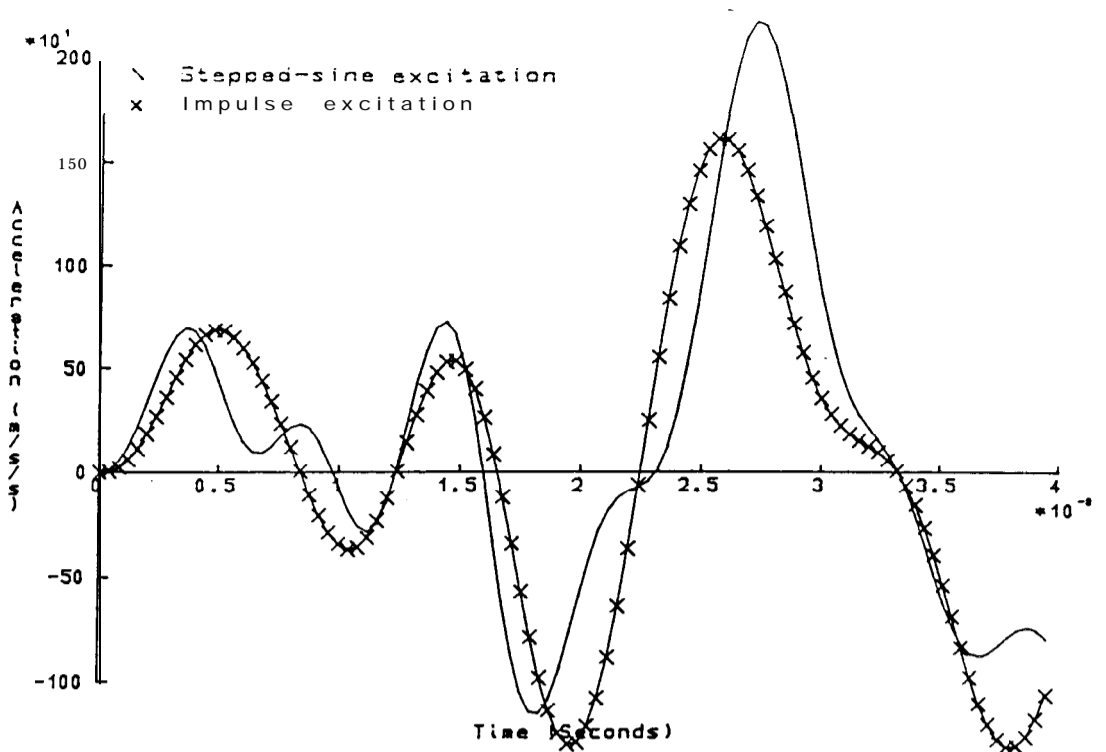


Fig 4. 19g Comparison of initial predictions (with extra damping) from point (3,1); stepped-sine and impulse excitations; 'IDENT' type analysis

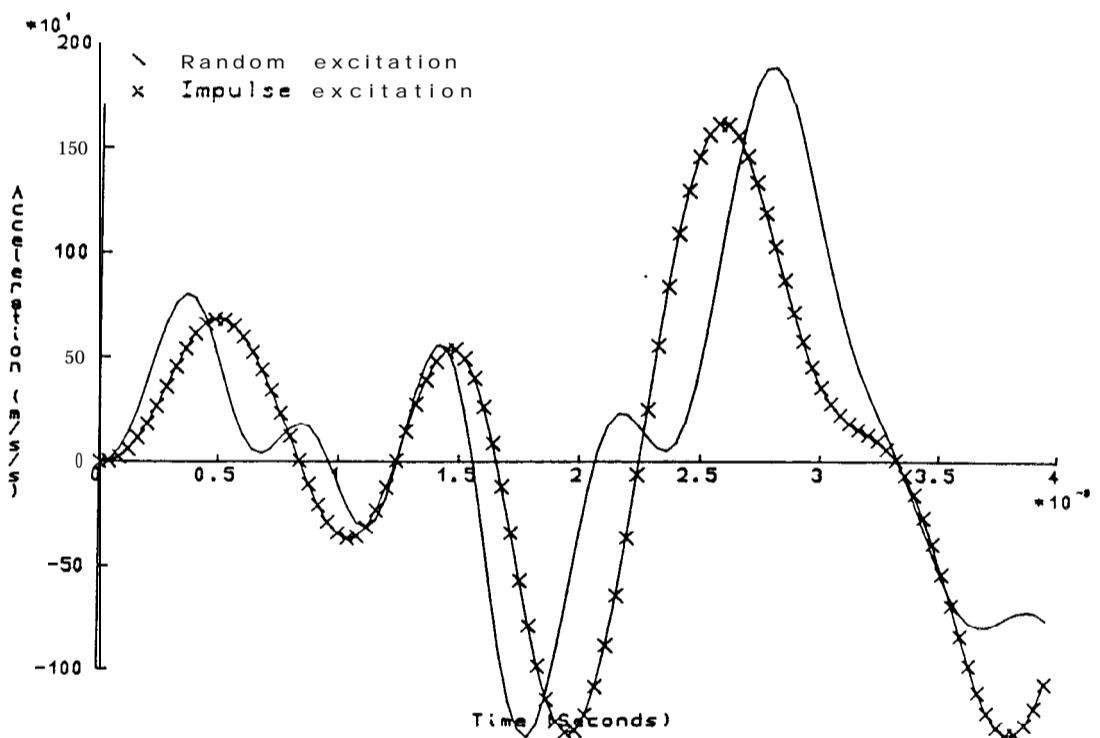


Fig 4 19h Comparison of initial predictions (with extra damping) from point (3,1); random and impulse excitations; 'IDENT' type analysis

5 RESPONSE CHARACTERISTICS OF NON-LINEAR ELEMENTS USING MODAL TESTING TECHNIQUES

5.0 Introduction

All structures are non-linear to some degree, and most non-linearities tend to be concentrated in single elements or components of a structural assembly. Methods discussed previously in this thesis are intended for application to linear structures and this provides a satisfactory approximation for the structures under test for most purposes. However, some structures are sufficiently non-linear that the difference between the measured response and the linear approximation is large. The application of linear modal analysis techniques to such non-linear components needs to be undertaken carefully and the resulting data evaluated in terms of its usefulness in describing some aspects of a non-linear structure. The aim of this chapter is to examine the characteristics of non-linear elements using modal testing methods. The data from two excitation techniques - sine and impulse - are compared in both the frequency and the time domains, and the observed trends are used for classifying the non-linearity.

Generally, a non-linear system does not obey superposition, and for such systems the choice and level of excitation will also determine the response characteristics obtained. The 'modal' parameters obtained by using linear modal analysis methods are no longer a unique description of the system - several different sets of modal parameters may be calculated from the same frequency response function (FRF) using different analysis techniques and criteria to decide which are the 'correct' values. For most non-linearities the results from one test cannot be used with confidence to predict the response to a different excitation, either for a different force level or type of excitation signal, and often the modal-parameters do not regenerate a close match to the FRF from which they were calculated.

This chapter starts with a brief examination of some non-linearities found in practice, followed by a discussion of the measurement of FRFs of non-linear elements. The different non-linearities are then subjected to a simulated constant-force sine excitation, and the results and trends that emerge in data presentation are examined. Next, the non-linearities are analysed using a simulated impulse: first, characteristics in the time-histories are discussed followed by transforming data to the frequency domain where trends in the data are again documented. Transforming measured data from an impulse excitation is the usual procedure for modal analysis, and for linear structures the transformed impulse response function (IRF) is the same as the measured FRF. However, this is not the case for non-linear structures, and the trends in the frequency data obtained by using the two types of excitation - constant-force sine and impulse excitation - are compared. Finally, to complete the cycle, the FRF data are transformed to the time domain (for a linear system the transformed FRF corresponds to the IRF) and the time-histories of the various non-linearities compared from the two excitation methods.

5.1 Some examples of non-linear elements found in practice

Non-linearities in structural dynamics can be broadly split into two types; those that effect the stiffness of the system and those that effect the damping. This can be a useful division in the analysis of non-linear elements, although in practice it is unusual to find only one non-linearity present in a system.

One of the methods of describing identified non-linearities is to use equivalent linearised equations of motion (ref [116] to [118]), these equations being derived assuming a sinusoidal excitation. To form a single linear equation of motion from the non-linear equations, an equivalent natural frequency and damping ratio are calculated. These parameters may be amplitude-dependent but they can be used with the linear FRFs when the input force (or the amplitude of response) is known. There follows in this section a brief description of some non-linear elements, where they are likely to be encountered in structures and, where applicable, the linearised equation of motion is quoted.

5.1 .1 Stiffness type non-linearities

There are many types of stiffness non-linearity of which three will be mentioned here. The schematic representation of the non-linearities and the corresponding relationship between spring force and displacement are shown in fig (5.1) along with the notation definition.

Cubic stiffness

Cubic stiffness (fig (5.1a)) is probably the most researched non-linearity (eg ref [28] & [119] to [121]) and occurs where the stress/strain relationship of the material has a cubic term in addition to the linear term. The equation of motion is the classical Duffing equation:-

$$\ddot{x} + 2\zeta\omega_0\dot{x} + \omega_0^2(x + \beta x^3) = f_t$$

Where β can be positive or negative for hardening or softening cubic stiffness respectively, and $f_t = (F_o/m)\sin \omega t$. The equivalent linearised equation of motion for forced harmonic vibration is:-

$$\ddot{x} + 2\zeta\omega_o\dot{x} + \omega_o^2(1 + 3\beta a^2/4)x = f_t$$

where a is the amplitude of response.

Examining the linearised equation of motion shows that the damping is not affected by the non-linearity, but that the equivalent natural frequency does change with amplitude of response. The additional term in the equivalent natural frequency is $3\beta a^2/4$ where a is a positive displacement and β is the non-linearity. If β is positive, ie a hardening cubic stiffness, then the natural frequency will tend to increase in value in comparison with the linear system when the non-linearity or the response level is increased. If β is negative, representing a softening cubic stiffness, then the natural frequency will decrease for the same conditions. This type of non-linearity is one specific example from a family of power laws on displacement (βx^n), each of which have their own characteristics.

Backlash

This non-linearity (fig (5.1 b)) is often found at loose-fitting joints where there is a small gap between contacts in positive and negative displacements. The equations of motion are:-

$$\begin{array}{ll} \ddot{x} + 2\zeta\omega_o\dot{x} + \omega_o^2(x - x_o) = f_t & |x| > x_o \\ \ddot{x} & = f_t & |x| < x_o \end{array}$$

Other versions of this type of non-linearity have a secondary spring in the gap which is much softer than the main spring. Also, the equilibrium position may be displaced from the centre of the gap either by pre-loading or self weight.

Bi-linear stiffness

Bi-linear stiffness (fig (5.1c)) is often found in bolted joints where the stiffness of the bolt in tension is different to that when the bolt is in compression. For this case, bi-linear stiffness is defined as a spring whose stiffness takes one of two different values depending upon whether the displacement is positive or negative. The equations of motion are:-

$$\begin{aligned}\ddot{x} + 2(\zeta\omega_o)\dot{x} + \omega_1^2x &= f_t & x < 0 \\ \ddot{x} + 2(\zeta\omega_o)\dot{x} + \omega_2^2x &= f_t & x \geq 0\end{aligned}$$

and the equivalent linearised equation of motion is:-

$$\ddot{x} + 2(\zeta\omega_o)\dot{x} + \left(\frac{k_1 + k_2}{2m}\right)x = f_t$$

Whilst this is a non-linear element, the equivalent linearised equation shows the equivalent damping and natural frequency to be independent of amplitude or force. This implies that a given system with bi-linear stiffness would exhibit superposition and appear to be linear for any excitation level in the frequency domain, but clearly any time-history will be dominated by the two different stiffnesses and as such this non-linearity is important.

5.1.2 Damping type non-linearities

There are many types of damping non-linearity of which two will be mentioned here. The schematic diagrams and the relationship between the damping force and the response are shown in fig (5.2) with the notation definition.

Friction

Friction (fig (5.2a)) is the more familiar of the damping type non-linearities and has a force characteristic that is positive if the velocity is negative, and negative if the velocity is positive. Friction usually occurs when two moving surfaces are in contact, eg the surfaces at joints and is also known as coulomb damping. The equation of motion for friction is:-

$$\ddot{x} + 2\zeta\omega_o\dot{x} + \omega_o^2x + R \frac{\dot{x}}{|\dot{x}|} = f_t$$

and the equivalent linearised equation of motion is:-

$$\ddot{x} + \left(2\zeta\omega_o + \frac{4R}{\pi a\omega_o} \right) \dot{x} + \omega_o^2 x = f_t$$

Inspection of the linearised equation of motion indicates that the natural frequency will not change with the introduction of this type of non-linearity.

The damping, however, will be increased by $4R/\pi a\omega_o$ showing that for decreasing response amplitudes or increasing friction force the effective damping is increased. These equations all assume that the friction force remains constant: in reality, a slipping friction force is less than the corresponding sticking friction force, neither of which is necessarily a constant value. No attempt has been made here to simulate that more complex condition due, largely, to an absence of reliable data.

Quadratic viscous damping

This form of non-linearity (fig (5.2b)) is one from the family of power laws on velocity to provide a non-linear damping term of the form $(d\dot{x}^n)$. In this case the equation of motion is:-

$$\ddot{x} + 2\zeta\omega_o \dot{x} + q \frac{\dot{x}^3}{|\dot{x}|} + \omega_o^2 x = f_t$$

and the equivalent linearised equation of motion is:-

$$\ddot{x} + \left(2\zeta\omega_o + \frac{q 8a\omega_o}{3\pi} \right) \dot{x} + \omega_o^2 x = f_t$$

From this equation it is clear that there is no change in the resonance frequency of the system with varying amplitude, but that the effective damping increases with non-linearity or response level. Quadratic viscous damping often arises from the displacement of fluids, eg air flow over a panel.

5.2 Frequency response measurement of non-linear elements

Unlike the linear case, where the FRF is independent of the excitation technique, non-linear elements respond in a different manner to different types of excitation and to various levels of a given excitation type. This section examines the response of some non-linear elements to some of the 'standard' excitation methods available (see chapter 3) and the techniques that can be used either to linearise the response or to enhance the non-linearity so as to assist in the identification of non-linear behaviour in a structure.

Sine excitation

Using the stepped-sine excitation technique (ref [122]), where the output voltage from the generator is kept constant, the input force to the structure is allowed to vary and this results in a rapid decrease in the force to the structure around resonance. The resulting FRFs from non-linear structures may appear to be linear, double peaked, or simply very noisy. As can be seen from the equivalent linearised equations, the response of a non-linear element is usually amplitude-dependent. If the response of the structure is kept constant over the frequency range of interest, then the structural behaviour has effectively been linearised and this is one technique of dealing with non-linear systems. To enhance the effect of a non-linearity in the FRF a wide range of amplitudes is required and this can be obtained by providing a constant-force input to the structure which will ensure a large range of response amplitudes around resonance. If non-linearity is suspected, a suitable test is sinusoidal excitation using force control on the input to the structure. If the results from two tests at different force levels show a change in the characteristics of the response then, assuming that the excitation equipment - generator, amplifiers and shaker - has not been driven into a non-linear regime, the structure is behaving in a non-linear fashion and care must be exercised when analysing that region of data. Examples of different FRFs obtained by using two different force levels are shown in fig (5.3). These results were calculated from the linearised equations of motion of two nonlinearities with the input force amplitude kept constant for each FRF.

Random excitation

Because of the nature of the various random excitation methods, these procedures tend to 'average' out any non-linearities - resulting in an optimum linearised model for the given excitation (ref [123]). By using several levels of random excitation, different FRFs can be obtained indicating the presence of non-linearities, but analysis of any one of the FRF plots would suggest the system to be linear. The parameters that are obtained from this type of test can be used in vibration analysis, but are not generally suitable for transient response analysis. There is one other parameter that provides an indication that the system is non-linear - the coherence. The coherence for measurements on a non-linear system is less than for a corresponding linear system with the same quality signals. There may also be coherence drops at harmonic frequencies (ref [124]) which could be used to assist in identifying a system as being non-linear.

Impulse excitation

Very little work has been performed on impact testing with non-linearities (ref [120] to [123]), probably for several reasons. The main reason is that impact testing usually requires many averages to obtain a noise-free result and, unless the impacts are monitored and are identical for non-linear systems, the results are then of no use as the non-linearities are 'averaged' out, in the same manner as for random excitation. The results from an impact test depend on the free decay of the system which means that the range of response amplitudes is large, so there is potential for non-linear classification using impact testing. In non-linear systems the relationship between the IRF and the FRF is no longer through the Fourier transform, thus bringing into question the validity of using impact testing to find the FRF. However, the interest in this thesis is in predicting the transient response so the relationship between the FRFs from sine testing and impact testing needs to be examined further.

5.3 Frequency response characteristics from sine tests

Having discussed the various non-linearities and the application of excitation techniques, the frequency domain results - Bode, Nyquist, 3-D damping and reciprocal-of-receptance plots - from constant-force sine excitation of the non-linearities are now examined for identifiable trends. Also in this section the term 'effective non-linearity' is introduced, which has meaning only when discussing altering the non-linear effect in a system. The term, apart from the value of the non-linearity, includes the effect of changing the amplitude of the input force: increasing the force may have the same effect as either increasing or decreasing the non-linearity.

Non-linear frequency domain characteristics are clear from measurements using constant-force stepped-sine excitation, and many of the characteristics are well documented (eg [117] & [125]) and are summarised below. Using constant-response amplitude sine tests produces a linear FRF therefore there are no trends in the individual plots with which to identify non-linearities other than the fact that different response amplitudes result in different (linear) characteristics. This type of test can be used for producing a linear model, and a change in response level will generate a different linear model. Conventional sine tests, where the input force level is allowed to vary, have the same amplitude-dependent characteristics as the constant-force sine tests, but any trends are not as immediately evident. A new method has been developed [126] to extract the characteristics from these tests.

The following results for constant-force sine tests were produced in three ways:-

- (i) using an analogue computer to simulate the non-linearity;
- (ii) computing the response characteristics by using the equivalent linearised equations of motion; and

(iii) direct time-marching solution of the non-linear equations of motion for sinusoidal forcing functions over a specified range of frequencies. The magnitude of the response at the forcing frequency is then calculated along with the phase relationship between the input and response. This technique is similar to that used by frequency response analysers (FRA) and will be referred to as the 'simulated FRA' method.

5.3.1 Characteristics of the measured Bode plot

A frequency response plot from a linear structure is expected to be a smooth and continuous curve. If the plot is not continuous, or the resonance appears to lean uncharacteristically, then there is a strong possibility of non-linearities being effective in that region. It has been shown (eg refs [119],[120],[127] & [128]) that the type of distortion in the Bode diagram, or the trend with changing force level (or changing non-linearity), can be used to classify the type of non-linearity. These trends for individual non-linearities are now reviewed.

Cubic stiffness

The main characteristic of cubic stiffness is a change in the frequency of the peak response with varying force level or non-linearity and also sweep direction. **Mayman** and Richfield [121] explored the use of the frequency and magnitude at maximum amplitude to calculate the non-linearity in the system. Results for cubic stiffness were generated during this study from the analogue computer and from the equivalent linearised equation of motion. The Bode plot characteristics for hardening cubic stiffness are shown in fig (5.4), displaying a distortion around resonance that increases with increasing non-linearity. For softening cubic stiffness the trends are just the opposite. For these systems, increasing non-linear effect is increasing the β parameter or increasing the input force level.

Backlash

The Bode plots for a system with backlash lean forward, with the resonance frequency decreasing with increasing gap or decreasing force. The FRF before resonance is increased relative to the linear system, and decreased after resonance. Data for this non-linearity were calculated using the 'simulated FRA' method and the trends in these FRFs are shown in fig (5.5). For a system with backlash, increasing the non-linear effect is achieved by increasing the gap or by decreasing the input force level.

Bi-linear stiffness

According to the equivalent linearised equation of motion, the FRF for a system with bi-linear stiffness should appear linear with a resonance frequency related to the average of the stiffnesses. Using the 'simulated FRA' solution route, the results did appear linear, but the main resonance is not at the predicted frequency. Also, there are several other 'resonances' that occur at frequencies which are multiples of the main resonance frequency, none of which distort or alter in the Bode plot with changing force level (fig (5.6)). With this non-linearity, changing the force level did not alter the FRF, as seen in fig (5.6a).

Friction

The equivalent linearised equation of motion is used to generate data for this example and examining the equation indicates that the resonance frequency is not altered by the non-linearity; only the effective damping levels vary. Examples of Bode plots for this type of non-linearity are shown in fig (5.7), where it can be seen that as the level of friction in the system increases the inertance FRF decreases. Decreasing the input force has the same effect as increasing friction and is increasing the effective non-linearity.

Quadratic viscous damping

These solutions were obtained from the equivalent linearised equation of motion and, as in the case of friction, the resonance frequency is found not to change; only the effective damping alters with changing non-linearity or response level. The inertance decreases with increasing quadratic viscous damping or increasing force, which is also increasing the effective non-linearity. Details of the variation in the resonance region of the Bode plot for quadratic viscous damping are shown in fig (5.8).

5.3.2 Modal parameters obtained from SDOF modal analysis

Examination of the two frequency domain modal analysis methods - Nyquist analysis and the inverse of receptance (discussed in chapter three) - yields that there are several forms of data presentation which can provide indications of the type of non-linearity. The Nyquist locus is fairly sensitive to the presence of non-linearities as is the associated 3-D damping plot. It was found that plots of the inverse of receptance can also be used to classify the non-linearity and to differentiate between stiffness and damping type non-linearities. There is an increasing amount of literature on the subject of trends in data caused by non-linearities (eg refs [69], [116], [119], [120] & [128]) and the characteristics shown from these plots and from the Bode plots are summarised in table (5.1).

Cubic **stiffness**

For a system with hardening cubic stiffness, the Nyquist plot loses its symmetry - as shown in fig (5.9a)- the amount of distortion increasing with effective non-linearity. For systems with small effective non-linearity the loss factor increases as the upper frequency point is raised, and decreases as the lower frequency point moves down (fig (5.9b1)). Locating the 'natural' frequency using the position of greatest sweep rate for systems with large effective non-linearity will result in similar 3-D damping plots as obtained above, but if the criterion used for locating the resonance frequency is that of least damping variation, then the loss factor - for both hardening and softening cubic stiffness - increases as either frequency point used in the calculation is further from the 'natural' frequency (fig (5.9b2)). Using Nyquist analysis,

“ different parameters are obtained depending on the criterion used - eg maximum sweep rate, least variation on the 3-D damping plot or closest to zero phase.

With reciprocal-of-receptance, the real part shows a decrease in the slope approaching the resonance frequency, after which it returns to the original slope (fig (5.9c)). The slope of the real part away from resonance corresponds to the linear system; this is important as it enables the parameters of the underlying linear system to be determined - not just a set of linearised parameters. The imaginary part of the reciprocal-of-receptance is not affected by this non-linearity, so the correct damping value can be taken from this plot. Table (5.2) provides some idea to the range of parameters that can be calculated from a single FRF of a system with hardening cubic stiffness.

Backlash

The Nyquist plot for a system with backlash shows a similar distortion as for the hardening cubic stiffness case (fig (5.10a)), and with large non-linear effects the jump phenomenon. The loss factor increases as the higher frequency point is increased, and decreases as the lower frequency point moves down, as shown in the 3-D damping plot in fig (5.10b). The real part of the inverse of receptance plot (fig (5.10c)) has a smaller slope than a linear system before resonance and greater slope after resonance, but plots for different levels of effective non-linearity all cross the axis at about the same point. The change in slope near the resonance frequency in the real part is also reflected in the imaginary part. This change in the imaginary part is to be expected as the model used assumes no damping over the centre section so the effective damping will alter with the change in relative time spent in the free zone to time in contact with the spring. A summary of some results from a single measurement of a system with backlash is given in table (5.3).

Bi-linear stiffness

With bi-linearity there is no indication from either of the analysis methods of the presence of a non-linearity. Examples of plots from the fundamental resonance and from the first harmonic are shown in figs (5.11) & (5.12) where the Nyquist plots are circular, 3-D damping plots are flat and level, and the plots of the reciprocal-of-receptance appear 'linear'. The imaginary part for both plots is not quite as flat or as smooth as might be expected from a linear system, but there is insufficient deviation from a linear system to enable this to be used to identify and to categorise bi-linear stiffness.

Friction

For a system with coulomb friction damping subjected to constant-force stepped-sine excitation, the Nyquist plot is almost circular when the effective non-linearity is low. However, the distortion of the plot increases with increasing effective non-linearity and at high levels of non-linearity the Nyquist plot becomes egg-shaped (fig (5.13a)). The 3-D damping plot decreases away from the resonance point both above and below (fig (5.13b)). Using reciprocal-of-receptance the real part is not affected, but the imaginary part shows a marked deviation from its usual straight line, with a turning point coinciding with the frequency at which the real part crosses the axis (fig (5.13c)). The values of coulomb damping and viscous damping can be calculated separately using the imaginary part of the reciprocal-of-receptance and is shown in Appendix 6. The results from using different analyses on these data are shown in table (5.4).

Quadratic viscous damping

For this case, the Nyquist plot takes on the opposite shape to friction - a squashed circle (fig (5.14a)). The 3-D damping plot is flat for most cases, and no particular trends were observed (fig (5.14b)). There is no change in the real part of reciprocal-of-receptance, whilst the imaginary part deviates from the usual straight line as shown in fig (5.14c). It is possible to calculate the values of viscous and quadratic viscous damping from the imaginary part of reciprocal-of-receptance in a similar manner to that described for friction. Table (5.5) shows the range of values obtained from different analyses.

5.3.3 Hilbert transform

The application of the Hilbert transform in non-linear structural vibrations is a fairly recent development. The theory of the Hilbert transform has been developed for the identification of non-linearities refs [118], [123], & [129] to [134]. If a system is linear, the Hilbert transforms of any form of its FRF data (eg magnitude and phase, real and imaginary, or Nyquist) will overlay the original data. However, if the Hilbert transforms do not overlay, it may be because of errors in the transform, eg truncation errors, or due to the presence of non-linearities. This method has the potential of showing the presence and the type of non-linearity by comparison of the transform with the original data from a single measurement. In general, the trends in the Hilbert transformed data are opposite to the trends in the measured data, and any of the displays - Bode, reciprocal-of-receptance, Nyquist or real and imaginary - can be used to compare results. Hilbert transform descriptors have also been defined in the form of energy ratios. The way that these descriptors change with applied force and their relative magnitudes can be used to classify different types of non-linearity (refs [118] & [123])

5.3.4 Characteristics using 'standard' sine excitation

Using 'standard' sine excitation - where there is no control on the input force to the structure or on the response amplitude - the trends that have been seen in the constant-force tests can still be identified if the amplitudes of response or the input force levels to the system are known at each frequency measurement point. It is the variation in response amplitude that causes the trends in the results from non-linear structures, and so long as the response amplitude is not constant (in which case a linearised response is measured) then these effects are present and can be used to classify the type of non-linearity. He [126] has developed a technique to enhance and exploit these trends in data from 'standard' sine excitation with some success in quantifying the non-linearity.

5.3.3 Hilbert transform

The application of the Hilbert transform in non-linear structural vibrations is a fairly recent development. The theory of the Hilbert transform has been developed for the identification of non-linearities refs [118],[123], & [129] to [134]. If a system is linear, the Hilbert transforms of any form of its FRF data (eg magnitude and phase, real and imaginary, or Nyquist) will overlay the original data. However, if the Hilbert transforms do not overlay, it may be because of errors in the transform, eg truncation errors, or due to the presence of non-linearities. This method has the potential of showing the presence and the type of non-linearity by comparison of the transform with the original data from a single measurement. In general, the trends in the Hilbert transformed data are opposite to the trends in the measured data, and any of the displays - Bode, reciprocal-of-receptance, Nyquist or real and imaginary - can be used to compare results. Hilbert transform descriptors have also been defined in the form of energy ratios. The way that these descriptors change with applied force and their relative magnitudes can be used to classify different types of non-linearity (refs [118] & [123])

5.3.4 Characteristics using 'standard' sine excitation

Using 'standard' sine excitation - where there is no control on the input force to the structure or on the response amplitude - the trends that have been seen in the constant-force tests can still be identified if the amplitudes of response or the input force levels to the system are known at each frequency measurement point. It is the variation in response amplitude that causes the trends in the results from non-linear structures, and so long as the response amplitude is not constant (in which case a linearised response is measured) then these effects are present and can be used to classify the type of non-linearity. He [126] has developed a technique to enhance and exploit these trends in data from 'standard' sine excitation with some success in quantifying the non-linearity.

5.4 Response characteristics from impulse tests

Trends that exist in data from non-linear elements, when excited using constant-force sine input, have been assessed for their suitability in classifying and quantifying the non-linearity for the five types listed at the beginning of the chapter. Attention is now focused on testing non-linearities with impulse excitation and the subsequent information that is available from the measured data. The measured time-histories are first compared with a 'reference' linear time-history; then the impulse responses are transformed to the frequency domain and the presentations - Bode, Nyquist, 3-D damping and reciprocal-of-receptance - are examined for identifiable trends.

Using impulse testing the primary information sought and obtained is the impulse response function (IRF). This IRF is often immediately transformed to the frequency domain in commercially-available analysers to provide an FRF and the initial measurement of the IRF is generally not displayed. Non-linear systems can produce IRFs that are distinctly different from the exponentially decaying sine waves of a linear system. If these non-linear IRFs are then transformed to the frequency domain the characteristics are often quite dissimilar to those obtained from FRFs measured directly using sine excitation. Both measured and transformed IRFs are now examined and the trends discussed. In the examples below, the IRFs were generated by direct solution of the equations of motion with the initial conditions set up with an initial velocity to simulate an impulse. The displacement, velocity and acceleration time-histories from the reference linear system are shown in fig (5.15).

5.4.1 Characteristics of the time-histories

Cubic stiffness

With this non-linearity there is little variation from the linear case; only a slight shift in the major frequency component which slowly returns to the linear period as the response amplitude decreases. Examples of IRFs from systems with hardening cubic stiffness are shown in fig (5.16). The most significant difference is seen in the acceleration trace (fig (5.16d)) where, as well as a frequency shift, the response level is higher than for the linear example but by less than 10%.

Backlash

For a system with backlash the acceleration trace indicates the presence of non-linearity more clearly than do the velocity or displacement traces. As there is no spring in the centre of the element (fig (5.1b)) there is no force on the mass whilst it is in this region. This implies that, so long as there is no external force on the mass, the acceleration in the middle is zero - and therefore constant velocity and linearly increasing displacement. The acceleration trace is shown in fig (5.17d) where the zero acceleration is clear. The corresponding velocity plot has flat-topped sine waves (fig (5.17c)), while the displacement plot - although not clearly non-linear from the enlarged view (fig (5.17b)) - does not decay as fast as the linear case when a longer time period is examined (fig (5.17a)). Also the response period varies throughout the decay.

Bi-linear stiffness

The IRF generated for the bi-linear stiffness element is as expected - a different period whilst the displacement is positive to that whilst the displacement is negative. An example is shown in figs (5.18a and b). The velocity trace is a leaning sine wave (fig (5.18c)), and the acceleration time-history in this example has a shorter period and larger magnitude when the acceleration is positive (corresponding to the time when the displacement is negative) than when the acceleration is negative (fig (5.18d)).

Friction

The IRF of a system with friction as the only form of damping is the classical linearly-decaying 'sine' wave (fig (5.19a)). With viscous damping also present in the system, there is still the 'dead zone' and the decay rate is a combination of a linear decay due to friction and the exponential decay from the viscous damping (fig (5.19b)). Returning to the system with only coulomb damping, the velocity trace appears similar to the displacement trace (fig (5.19c)), and the discontinuities in the acceleration at the extremes of motion are evident in the corresponding plot (fig (5.19d)).

Quadratic viscous damping

The IRF for a system with quadratic viscous damping has the opposite characteristics to the IRF for a system with friction. The initial decay in this case is more rapid than for the linear system (fig (5.20b)), but the response continues at a small amplitude for a long time (fig (5.20a)). The corresponding velocity and acceleration traces are shown in fig (5.20c & d) where the feature of interest in this example is the high initial acceleration response and the apparent discontinuity where the displacement reaches its first maximum; for low effective non-linearities the acceleration time-history does not exhibit this high initial response.

5.4.2 Data trends in the frequency domain from impulse excitation

After deriving the IRF, data are then transformed to the frequency domain in order to obtain an FRF for modal analysis. This transformation has been performed for the non-linearities under consideration and the frequency domain presentations are examined for trends. These results are summarised in table (5.6) and are discussed below.

Cubic stiffness

The Bode plot of the FRF obtained by Fourier transforming the IRF (which will be referred to as the impulse response FRF - or IRFRF) from a system with hardening cubic stiffness subjected to impulse excitation still exhibits the 'jump' phenomenon with large non-linear effects, but now the 'jump' is on the low frequency side of resonance (fig (5.21a)) and, in addition, 'harmonic resonances' (apparent modes at frequencies that are multiples of the fundamental resonance) also become evident. The frequency of maximum response increases with effective non-linearity. There is a corresponding shift clockwise in the distortion of the Nyquist plot as shown in fig (5.21 b), and the 3-D damping plot now decreases away from resonance in both directions (fig (5.21~)). The plot of real part of the reciprocal-of-receptance (fig (5.21d)) has a similar slope to the linear system, but lies parallel and crosses the axis at a higher frequency with increasing effective non-linearity. There is also a slight distortion just before resonance where there is a 'dip' in the line. The imaginary part is also affected in this case with a drop in the value just before

resonance and tending to a greater value after the dip for systems with higher non-linear effects (fig (5.21d)). The results obtained from different analyses of the same impulse data are shown in table (5.7). The 'harmonic resonances' (starting with the second harmonic frequency) that begin to show in the Bode plot with increasing effective non-linearity possess similar trends to the fundamental resonance when analysed, but the Nyquist plot is translated from the origin (fig (5.22)).

Backlash

The IRFRF for this type non-linearity appears to be very 'noisy' (fig (5.23a)) with the noise content increasing with the effective non-linearity. A 'harmonic resonance' also begins to show through the noise within the frequency range of the FRF. Around resonance there is a 'jump' on the low frequency side of resonance for higher levels of non-linearity and, as the non-linear effect increases, the frequency of maximum response decreases. The points on the Nyquist plot are distorted clockwise, and there is a bulge out of the circle on the low frequency side of resonance as shown in fig (5.23b). The 3-D damping plots are not smooth, nor are the perturbations of a random nature, but clear trends are not easily identified (fig (5.23-)). The reciprocal-of-receptance plot (fig (5.23d)) shows a large variation below resonance in both parts, but above resonance the real part becomes parallel lines crossing the axis at lower frequency with increasing non-linearity while the imaginary part converges to the linear line. Results from some analyses are shown in table (5.8) and a plot from analysis of the harmonic resonance is shown in fig (5.24).

Bilinear stiffness

For a single grounded element, the IRFRF plots appeared to come from a multi-mode system (fig (5.25)). Data analysed around any of the 'modes' appear linear (although from a MDOF system), with evenly-spaced highly complex Nyquist circles, and flat 3-D damping plots. The reciprocal-of-receptance plots are also as expected from a linear MDOF system: however, in the development of the analysis method based on this form of presentation all modes are assumed to be real and so the approach is not really valid for such highly complex 'modes'. The analysis plots for the 'modes' shown in the Bode plot are presented in fig (5.26), and the results from analysing the 'modes' are in table (5.9).

Friction

The IRFRF plot for a system with just coulomb damping appears initially to have many heavily damped 'modes' and harmonic resonances that are distinguishable (fig (5.27a)). As the ratio of viscous damping to coulomb damping increases, these perturbations near resonance in the IRFRF smooth out into the familiar Bode plot plus an harmonic resonance showing through. The amplitude of the fundamental resonance decreases with increasing non-linearity and is displayed in fig (5.27a). The Nyquist plot maps these extra 'modes' (fig (5.27b)) and the trend is for the 'circle' to become squashed with increasing non-linear effect. The 3-D damping plots decrease away from resonance in either direction (fig (5.27~)). The reciprocal-of-receptance shows a distinctive characteristic in the imaginary part (ref [135]) as shown in fig (5.27d). There are large variations in this plot which can be enveloped with the lower limit relating to the amount of viscous damping in the system and the angle between the upper and lower envelopes to the amount of coulomb damping present. The real part averages to a straight line of the same slope as the linear system and the plots all cross the axis at the natural frequency. Fig (5.28) present the reciprocal-of-receptance displays for increasing viscous damping or increasing coulomb damping, and the results from various analyses of a single FRF measurement are presented in table (5.10).

Quadratic **viscous damping**

In this case, each individual IRFRF plot appears to be linear with only a small distortion evident around the second harmonic frequency, but the magnitude of the response at resonance decreases with increasing non-linear effect (fig (5.29a)). The Nyquist plots are smaller than the linear system and become elongated along the imaginary axis (fig (5.29b)) whilst the 3-D damping plots increase away from resonance in both directions (fig (5.29c)). Plots of reciprocal-of-receptance are shown in fig (5.29d) where the real part is displaced in slope around resonance but always crosses at the same frequency, and the imaginary part is also distorted. Results from analyses on different non-linearities are given in table (5.11).

5.5 Comparison of response characteristics in the time domain

Distinct response characteristics, that depend not only on the non-linearity but also on the excitation technique used, have emerged for non-linear systems. These differences have been discussed in the previous section for frequency domain presentations, and in this section the focus is on the variations in the time domain presentation. To examine the differences in the time domain responses, frequency response data from constant-force sine tests were transformed to the time domain using the inverse discrete Fourier transform (which will be referred to as the frequency response IRF- or FRIRF) and compared with the IRF. One effect to note is that in this transformed data there is an apparently non-causal component from some of the non-linear components. As this non-causal component is due to the non-linearities in the system, removal of this part of the response would bring the total response closer to the linear ideal. A method for calculating this 'linearised' response involves averaging the non-causal time function and the time domain representation of its Hilbert transform (refs [118],[123],[130] & [131]). The result is a causal response, which is a partially linearised function representing the original system. Using data from any analysis to regenerate curves would produce an exponentially decaying sine wave (which is not shown), but the linear example in fig (5.30) can be used to identify differences between the exact time-histories from the non-linearities and a linear response. The differences between the IRF & FRIRF are now briefly discussed for each non-linearity.

Cubic stiffness

The comments made here are for hardening cubic stiffness elements: trends are opposite for the softening cubic stiffness cases. In the time-history (fig (5.31)) the results from an impulse are similar to the linear example (fig (5.30)) with a slight change in period at the start. The transformed constant-force sine test data, however, decay away rapidly at the start and the large non-causal component effects the end of the data and also the magnitude at the beginning of the record. The IRF & FRIRF results for cubic stiffness are very dissimilar in appearance.

Backlash

The time-histories for backlash non-linearity can be very different due to the varying time that the mass spends in the gap and for the example shown in fig (5.32) the IRF decay is very similar to the linear system until the displacement is less than the gap when there is no more decay. The FRIRF has a large non-causal component which will affect the magnitude at the beginning, but the general trend is a rapid initial decay which becomes less than the linear example after a short time.

Bi-linear stiffness

For bi-linear stiffness the IRF and the FRIRF, unlike the FRF and the IRFRF, can be very different (fig (5.33)) if there is much variation between the two spring stiffnesses when the ratio of the two periods spent in positive or negative displacement is large. Also, the amplitude of response is different for positive or negative displacements. This is because in this example the damper is assumed to be the same for both springs, which means that the damping ratio ($\zeta=c/2\sqrt{km}$), hence the maximum amplitude and decay rate, differs for each spring stiffness. These variations in the IRF and FRIRF are important when predicting the transient response for this non-linear element.

Friction

The FRIRF of a system with friction (fig (5.34)) appears similar to a linear system, but with a little more damping. There is an indication of the non-linearity by the small non-causal component at the end. The IRF however, decays to within the dead zone of the friction element well within the decay time of the FRIRF and so the actual decay rate is much greater than the FRIRF would indicate.

Quadratic viscous damping

In the time-histories of a system with quadratic viscous damping (fig (5.35)) the FRIRF has a small non-causal component the amplitude at the start is larger than in the IRF, and the response finishes in less time than the response from the impulse test. In both cases (IRF and FRIRF) the response is less than the linear example which is to be expected as the quadratic viscous damping increases the total damping of the system.

5.6 Discussion

In this chapter conventional modal analysis techniques have been applied to non-linear elements to establish characteristics that can be used in classifying and quantifying non-linearities. Of the excitation techniques used to measure the frequency response function (FRF), random excitation and constant-response amplitude sine tests produce linearised models that represent the non-linear element for that particular excitation condition and have not been considered in detail. FRFs from constant-force sine tests and from impulse tests exhibit distinct trends, and furthermore, the FRFs from these two types of excitation do not usually agree for non-linear elements. Trends exist in data from sine tests where the input force is allowed to vary, but manipulation is required on the data to enable the trends to be highlighted. Of particular importance to this research are the characteristics of the response from impulse tests, as these need to be fully understood in order to be able to predict accurately the impulse response function (IRF) of a non-linear element from modal tests.

Trends of plots from constant-force sine tests in the Bode, Nyquist and 3-D damping formats are well documented (eg refs [69],[116],[119],[120][128] and section 5.3 of this thesis), and it is also shown that the reciprocal-of-receptance plots can be used to identify and quantify some aspects of non-linearity. Similar displays are also examined for data from impulse tests where the trends are not usually the same for a given non-linearity as from a constant-force sine test, but may correspond to a different non-linearity subjected to a constant-force sine test. It is therefore important to know what excitation technique was used to measure an FRF so that trends in the data can be attributed to the correct non-linearity.

The different trends exhibited for the same non-linearity subjected to an impulse or constant-force stepped-sine test, are mainly due to the mechanism of excitation and the amplitude dependence of non-linearities. The constant-force stepped-sine test will result in a steady-state response - not necessarily a sine-wave, but the amplitude of the input frequency component of the response will be constant. Varying the amplitude of the input will change the level of the response, and hence the system characteristics. The impulse

5.6 Discussion

In this chapter conventional modal analysis techniques have been applied to non-linear elements to establish characteristics that can be used in classifying and quantifying non-linearities. Of the excitation techniques used to measure the frequency response function (FRF), random excitation and constant-response amplitude sine tests produce linearised models that represent the non-linear element for that particular excitation condition and have not been considered in detail. FRFs from constant-force sine tests and from impulse tests exhibit distinct trends, and furthermore, the FRFs from these two types of excitation do not usually agree for non-linear elements. Trends exist in data from sine tests where the input force is allowed to vary, but manipulation is required on the data to enable the trends to be highlighted. Of particular importance to this research are the characteristics of the response from impulse tests, as these need to be fully understood in order to be able to predict accurately the impulse response function (IRF) of a non-linear element from modal tests.

Trends of plots from constant-force sine tests in the Bode, Nyquist and 3-D damping formats are well documented (eg refs [69],[116],[119],[120][128] and section 5.3 of this thesis), and it is also shown that the reciprocal-of-receptance plots can be used to identify and quantify some aspects of non-linearity. Similar displays are also examined for data from impulse tests where the trends are not usually the same for a given non-linearity as from a constant-force sine test, but may correspond to a different non-linearity subjected to a constant-force sine test. It is therefore important to know what excitation technique was used to measure an FRF so that trends in the data can be attributed to the correct non-linearity.

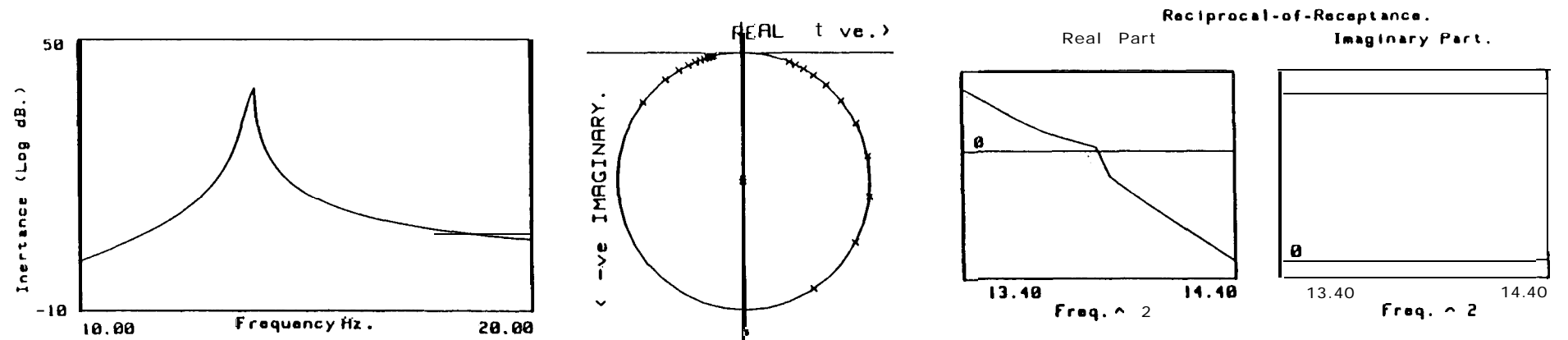
The different trends exhibited for the same non-linearity subjected to an impulse or constant-force stepped-sine test, are mainly due to the mechanism of excitation and the amplitude dependence of non-linearities. The constant-force stepped-sine test will result in a steady-state response - not necessarily a sine-wave, but the amplitude of the input frequency component of the response will be constant. Varying the amplitude of the input will change the level of the response, and hence the system characteristics. The impulse

test however, relies on an average value of response from the initial pulse down to zero response. Stiffness-type non-linearities generally cause the natural frequency of a system to change with response amplitude, and so the alteration may be visible in the IRF as the amplitude decays: the IRFRF will therefore have a resonance that is an average as the response decays to zero. However, any change in the natural frequency of the IRFRF from that of the linear system will still be in the same direction as for the FRF. Using friction as an example of damping-type non-linearity, the non-linear effect decreases with increasing amplitude. For the constant-force test, the response around resonance is largest and so the system is most linear at that point. This is seen in the Nyquist plot where the points close to resonance are closer to the linear system than the points away from resonance. With the impulse test however, the response decays away much more quickly than for a linear system, hence the average amplitude around resonance is low and the IRFRF is most non-linear around resonance. This is again seen in the Nyquist plot where the points close to resonance are now furthest away from those of the linear plot. The opposite is the case for quadratic viscous damping, where small response amplitudes imply a more linear response. In general, if the non-linear effect is reduced with decreasing response amplitude, then the response from an impulse test will probably appear more linear than the response from a constant-force stepped-sine test, as the response at resonance from the latter test will be large even with small input amplitudes.

As a first attempt at predicting the IRF of a non-linear element, the FRF data measured from a constant-force sine test were transformed to the time domain. For most of the non-linearities this is clearly an unacceptable prediction, and therefore different approaches need to be examined for predicting the IRF of non-linear systems using data from experimental modal analysis.

| Non- Linearity / Display | Bode Plot | Nyquist | 3-O Damping | Reciprocal-of- Receptance- Real | Reciprocal-of - Receptance - Imaginary |
|-----------------------------------|--|--|--|---|---|
| (Hardening) CUBIC STIFFNESS | Leans forward. Frequency increases with increasing non-linearity | Remains circular - same diameter, but points move anti-clockwise, leaving gap at jump frequency. | Increases moving above resonance and below for light non-linearity or using position of maximum sweep. Otherwise increases in both directions. | Linear away from resonance. Slope decreases approaching resonance then jumps down. | Not affected. |
| BACKLASH | Leans forward. Frequency decreases with increasing non-linearity. Response greater before resonance, less after. | Remains circular. and points distort anti-clockwise. | Increases moving above resonance and decreases moving away below. | Slope remains straight but less below resonance and greater slope above resonance. All cross at same point. | Increase in slope before resonance and decrease after. About same value near resonance. |
| BI-LINEAR | Appears linear. but multi-moded. | Circular and evenly spaced. | Flat | Straight line | Same approximate slope but not a smooth line. No particular trend. |
| FRICTION | Response amplitude decreases with increasing non-linearity. | Become smaller and elongated down imaginary axis. | Decrease moving away from resonance in both directions | Straight line as linear. | Becomes 'V' shaped with minimum value near resonance |
| QUADRATIC VISCIOUS DAMPING | Response amplitude decreases with increasing non-linearity. | Become smaller and squashed down imaginary axis. | Appears fairly flat, no apparent trends. | Straight line as linear. | Becomes bumped with maximum value near resonance. |

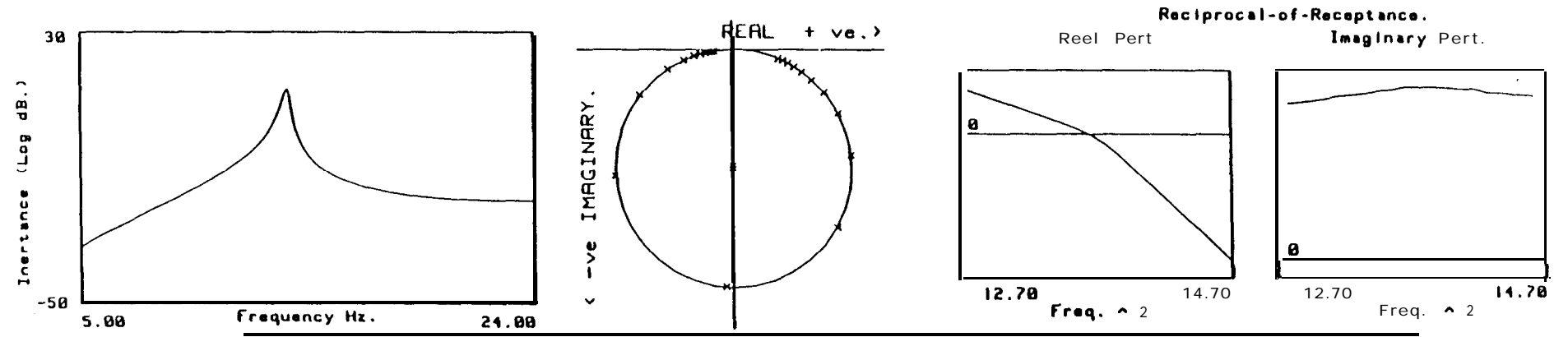
Table 5.1 Trends in Frequency domain displays from non-linear systems subjected to sine testing.



126

| System and Criterion used | Natural Frequency (Hz) | Radius (Error) m/R (X) | Modal Constant | Damping Loss Factor (Variation %) | Phase (Deg) |
|---------------------------------|------------------------|------------------------|----------------|-----------------------------------|-------------|
| LINEAR | 13.77 | 6.398E-3(0.0) | 1.000 | 0.01044(0.7) | 0.0 |
| CUBIC STIFFNESS NYQUIST | | | | | |
| Greatest sweep rate | 13.92 | 6.340E-3(0.1) | 0.988 | 0.01018(61) | -39.7 |
| Least damping variation | 13.91 | 6.340E-3(0.1) | 1.013 | 0.01045(16.3) | -5.7 |
| Closest to real mode | 13.91 | 6.340E-3(0.1) | 0.083 | 0.00856(18.3) | 2.45 |
| RECIPROCAL-OF-RECEPTANCE | | | | | |
| Pts well above resonance | 0.79 | | 0.0965 | 0.01005 | 0.0 |
| Pts well below resonance | 13.83 | | 1.1798 | 0.01226 | 0.0 |
| Pts immediately below resonance | 13.95 | | 2.2881 | 0.02154 | 0.0 |
| Slope of line crossing axis | 13.91 | | 0.2951 | 0.00305 | 0.0 |
| All data | 13.81 | - | 0.9660 | 0.01007 | 0.0 |

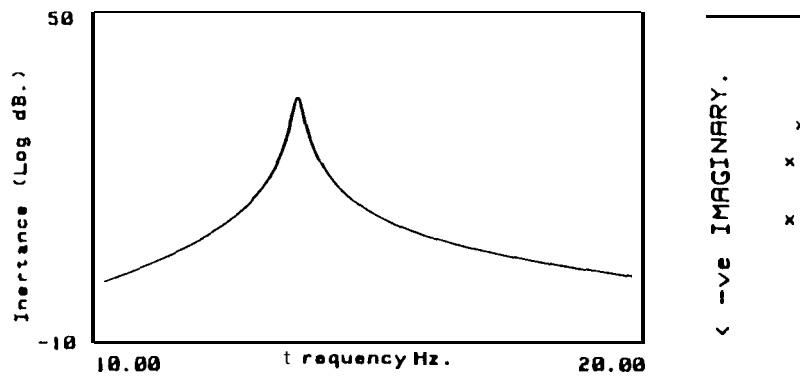
Table 5.2 Various parameters evaluated from a single constant-force stepped-sine test of a system with cubic stiffness (Response of system shown at the top)



127

| System and Criterion used | Natural Frequency (Hz) | Radius (Error) m/N (%) | Modal Constant | Damping Loss Factor (Variation %) | Phase (Deg) |
|---------------------------------|------------------------|------------------------|----------------|-----------------------------------|-------------|
| LINEAR | 13.77 | 3.1731E-4 (.1) | 0.6100 | 0.02088 | 0.0 |
| BACKLASH NYQUIST | | | | | |
| Greatest sweep rate | 13.73 | 3.2594E-4 (.3) | 0.0083 | 0.01701 (64.4) | -25.24 |
| Least damping variation | 13.71 | 3.2594E-4 (.3) | 0.0097 | 0.02013 (7.5) | -8.32 |
| Closest to real mode | 13.70 | 3.2594E-4 (.3) | 0.0093 | 0.01920 (20.0) | -0.42 |
| RECIPROCAL-OF-RECEPTANCE | | | | | |
| Points below | 13.75 | | 0.0147 | 0.03039 | 0.0 |
| Points above | 13.75 | | 0.0053 | 0.01098 | 0.0 |
| Points close to resonance | 13.68 | | 0.0092 | 0.01914 | 0.0 |
| All 20 points | 13.52 | | 0.6079 | 0.01671 | 0.0 |

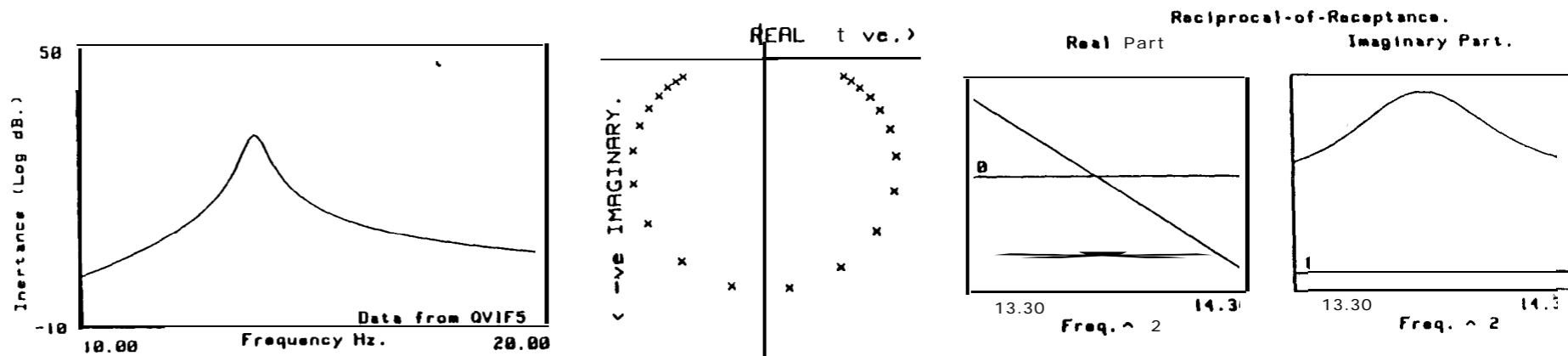
Table 5.3 Various parameters evaluated from a single constant-force stepped-sine test of a system with backlash (Response of system shown at the top)



128

| System # d Criterion used | Natural Frequency (Hz) |
|---|---------------------------|
| LINEAR | 13.17 |
| FRICION - RECIPROCAL- OF- RECEPTANCE | 13.77 |
| NYQUIST | |
| 20 pts. cloeet to real mode, and least damping variation | 13.77 |
| Fastest sweep rate | 13.77 |
| Using only 6 pta around resonance | 13.77 |

Table 5.4 Various parameters evalu:
(Response of system shown

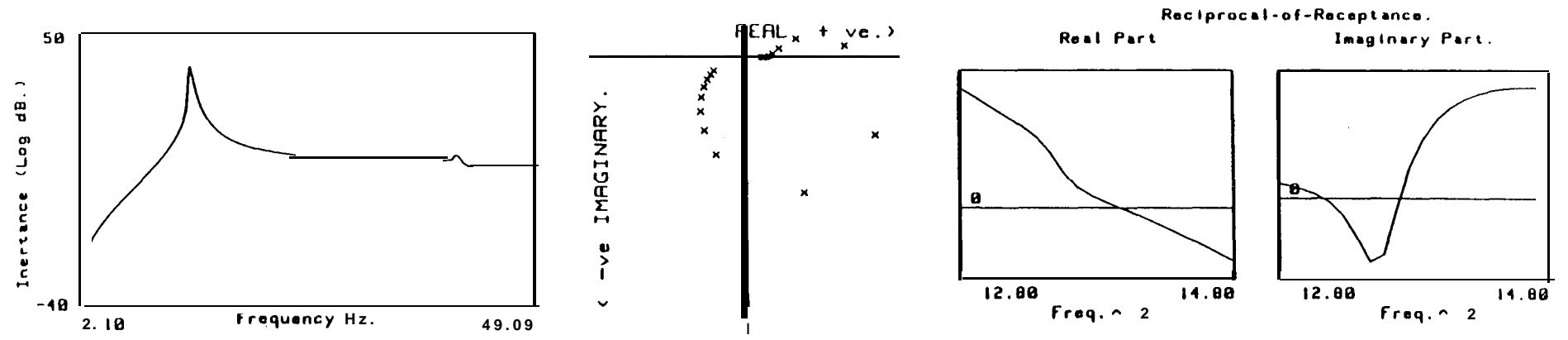


| System and Criterion used | Natural Frequency (Hz) | Radius (Error) m/N (%) | Modal Constant | Damping Loss Factor (Variation %) | Phase (Deg) |
|--|------------------------|------------------------|----------------|-----------------------------------|-------------|
| LINEAR | 13.77 | 6.398E-3(0.0) | 1.0000 | 0.01044(0.7) | 0.0 |
| QUADRATIC VISCOUS DAMPING | | | | | |
| Reciprocal-of-Receptance | 13.77 | | 1.0000 | 0.02836 | 0.0 |
| NYQUIST | | | | | |
| All 20 pts | 13.77 | 2.6179E-3(3.2) | 1.15921 | 0.02958(.7) | 0.6 |
| pts around resonance - greatest sweep rate and least damping variation | 13.71 | 2.7889E-3(.4) | 1.3872 | 0.03322(.6) | 0.1 |
| Closest to real mode | 13.77 | 2.7889E-3(.4) | 1.3881 | 0.03323(.7) | -0.6 |

Table 5.5 Various parameters evaluated from a single constant-force stepped-sine test of a system with quadratic viscous damping
(Response of system shown at the top)

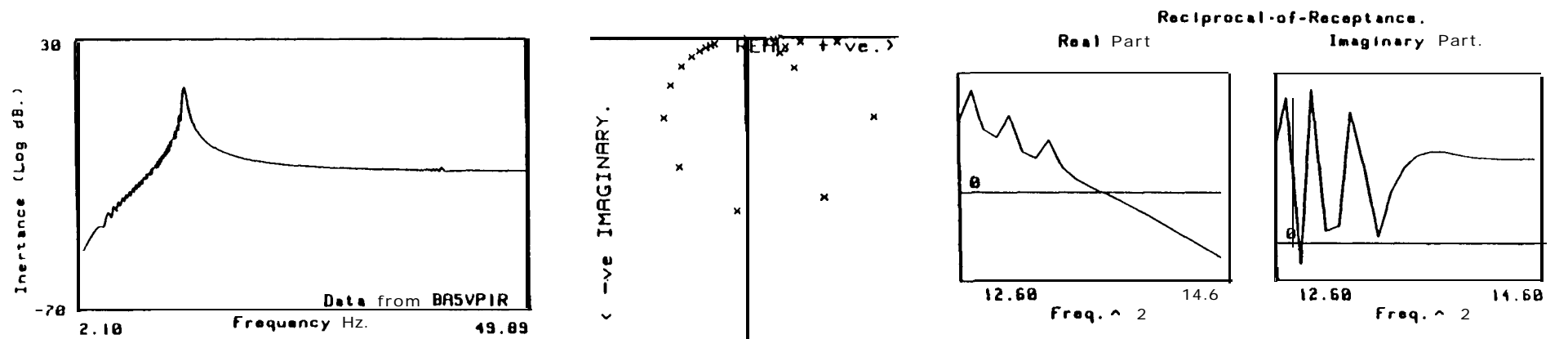
| Display on-nearity | Bode | Nyquist | 3-D Damping | Reciprocal-of-Receptance - Real | Receiprocal-of-Receptance - Imaginary |
|---------------------------------|--|--|--|---|---|
| Hardening) UBIC TIFFNESS | Jump on low frequency side of resonance. Harmonics present, Resonance frequency increases with effective non-linearity | Distortion on low frequency side and plot centre also pulled round to low frequency side. | Decreases in both directions moving from resonance. | Slope remains the same, but crosses axis higher with increasing non-linearity. Distortion around resonance. | Drops away sharply around resonance. |
| JACKLASH | Increasing non-linearity decreases magnitude and frequency of resonance. Appears 'noisy'. Harmonics present. | Distortion on low frequency side. Noise modes' showing through on plot. | No identifying trends noted. | After resonance all take parallel straight lines - decreasing crossing point with increasing non-linearity. | After resonance all converge to same line. |
| BI-LINEAR | Many harmonics including zero Hz for grounded structure. | All appear linear, but highly complex. | All appear linear | Appear to come from multimode system, with change of slope just before resonance. | Appear to come from multimode system. (Not a suitable analysis for complex modes). |
| FRICION | Appears stepped in construction - decreasing as viscous content increases. Harmonics present. | Becomes squashed but steps in Bode plot are evident in Nyquist as small circles near origin. | Decreases in both directions moving away from resonance. | The stepped response shows here as a wavy line about the linear equivalent. Straight just as it crosses axis, always at same point. | Can be enveloped by a bottom line indicating amount of viscous damping and angle between that and the top line depicts amount of coulomb damping. |
| QUADRATIC VISCOUS DAMPING | Flattened peak - distortion at harmonic. Amplitude decreases with increasing non-linearity. | Elongated. | Increases moving away from resonance in both directions. | '\ ' shaped, becoming more pronounced with increasing non-linearity. Always crosses axis at same point. | 'V' shaped, moving away from origin with increasing non-linearity. |

Table 5.6 Trends in frequency domain displays from non-linear systems subjected to impulses.



| System and Criterion used | Natural Frequency (Hz) | Radius (Error) σ/N (%) | Modal Constant | Damping Loss Factor (Variation %) | Phase (Deg) |
|---------------------------------|------------------------|-------------------------------|----------------|-----------------------------------|-------------|
| LINEAR | 13.77 | $6.3984(0.0)$ | 2.0000 | 0.02088(1.0) | 0.0 |
| CUBIC - NYQUIST | | | | | |
| Fastest sweep rate | 13.84 | $6.0526E-3(12.1)$ | 1.5685 | 0.01714(64.4) | 51.99 |
| Least damping variation | 13.64 | $6.0526E-3(12.1)$ | 1.9582 | 0.02131(9.3) | 36.4 |
| Closest to real mode | 13.93 | $6.0526E-3(12.1)$ | 1.9202 | 0.02072(68.6) | .9 |
| RECIPROCAL-OF-RECEPTANCE | | | | | |
| Pts above | 14.013 | | 2.5333 | 0.03760 | 0.0 |
| Pts below | 14.255 | | 1.9932 | 0.03461 | 0.0 |
| Pt. just below | 13.77 | | 0.06127 | 0.00164 | 0.0 |
| Pts crossing | 13.99 | | 2.9923 | 0.03636 | 0.0 |
| Harmonic using Nyquist | 41.93 | $7.0531E-6(1.9)$ | 0.0271 | 0.02762 | -132.9 |

Table 3.7 Various parameters required from single impulse test of a system with cubic stiffness (Response of system shown at the top)



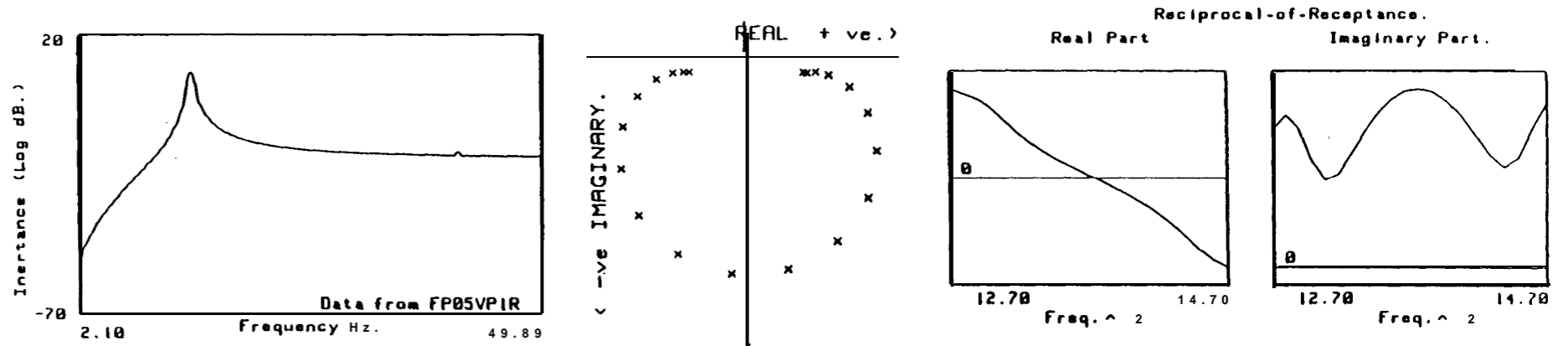
132

| System and Criterion used | Natural Frequency (Hz) | Radius (Error) m/N (%) | Modal Constant | Damping Loss Factor (Variation %) | Phase (Deg) |
|---------------------------|------------------------|------------------------|----------------|-----------------------------------|-------------|
| LINEAR | 13.77 | 3.1992E-4(0.) | 0.10000 | 0.02088(1.0) | 0.0 |
| BACKLASH - NYQUIST | | | | | |
| Greatest sweep rate | 13.58 | 3.3495E-4(2.5) | 0.10513 | 0.02157(31.3) | 47.5 |
| Closest to real mode | 13.66 | 3.3495E-4(2.5) | 0.14018 | 0.02840(21.6) | .9 |
| Least damping variation | 13.62 | 3.3495E-4(2.5) | 0.13079 | 0.02665(9.1) | 22.5 |
| RECIPROCAL-OF-RECEPTANCE | 13.71 | | 0.10335 | 0.02543 | 0.0 |
| Harmonic - Nyquist | 40.83 | 2.1045E-7(2.9) | 1.7881E-4 | 0.00646(28.4) | -79.1 |

Table 5.8 Various parameters evaluated from a system with backlash subjected to an impulse. (Response of system shown at the top).

| Mode' No | Resonance Frequency (Hz) | Circle Radius (Error) m/N (%) | Modal Constant | Damping Loss Factor (Variation %) | Phase (Deg) |
|----------|-----------------------------|----------------------------------|----------------|--------------------------------------|----------------|
| 1 | 9.183 | 4.715E-4(.1) | 0.09802 | 0.03122(3.4) | 29.6 |
| 2 | 18.361 | 4.2851E-5(.1) | 0.01787 | 0.01566 | -29.9 |
| 3 | 27.539 | 9.0487E-6(0) | 0.00559 | 0.01031 | -89.0 |
| 4 | 36.723 | 1.2141E-6(.8) | 9.866E-4 | 0.00763(3.6) | -151.96 |
| 5 | 45.896 | 4.6098E-7(1.4) | 4.7045E-4 | 0.00614(3.1) | -29.65 |

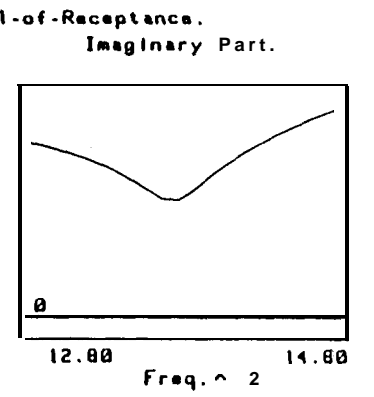
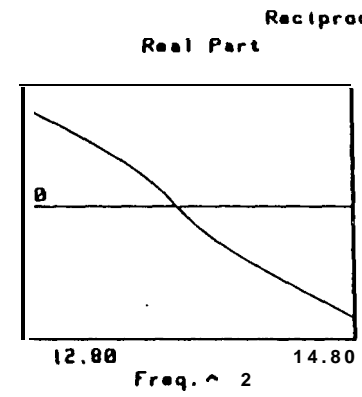
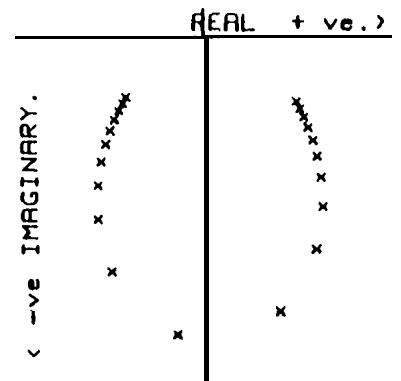
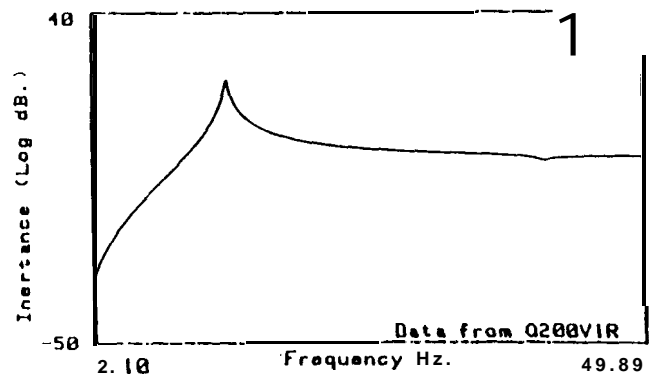
Table 5.9 Parameters from the 'modes' of a bi-linear system subjected to a single impulse



134

| System and Criterion used | Natural Frequency (Hz) | Radius (Error) m/M (I) | Modal Constant | Damping Loss Factor (Variation %) | Phase (Deg) |
|---|------------------------|------------------------|----------------|-----------------------------------|-------------|
| LINEAR | 13.71 | 3.1992E-4(0.0) | 0.1000 | 0.02088(1.0) | 0.0 |
| FRICION RECIPROCAL-OF- RECEPTANCE | 13.77 | | 0.1020 | 0.04027 | 0.0 |
| NYQUIST - ALL PTS Fast sweep rate and least damping variation | 13.77 | 1.8726E-4(7.1) | 0.1222 | 0.0436(10.1) | .99 |
| Closest to real mode | 13.77 | 1.8726E-4(7.1) | 0.1215 | 0.04331(10.2) | -54 |
| NYQUIST - PTS AROUND RESONANCE Fastest sweep rate and least damping variation | 13.76 | 2.0129E-4(1.2) | 0.1727 | 0.05737(5.2) | 2.16 |
| Closest to real mode | 13.77 | 2.0129E-4(1.2) | 0.1678 | 0.05566(10.4) | -51 |
| Harmonic | 41.24 | 1.9237E-7(2.0) | 3.284E-4 | 0.01271(11.1) | -58.68 |

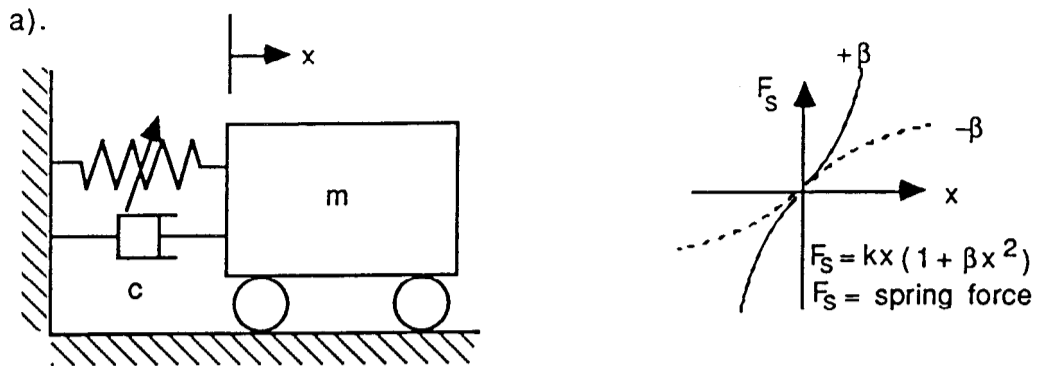
Table 5.10 Various parameters evaluated from a system with friction subjected to an impulse (Response of system shown at the top)



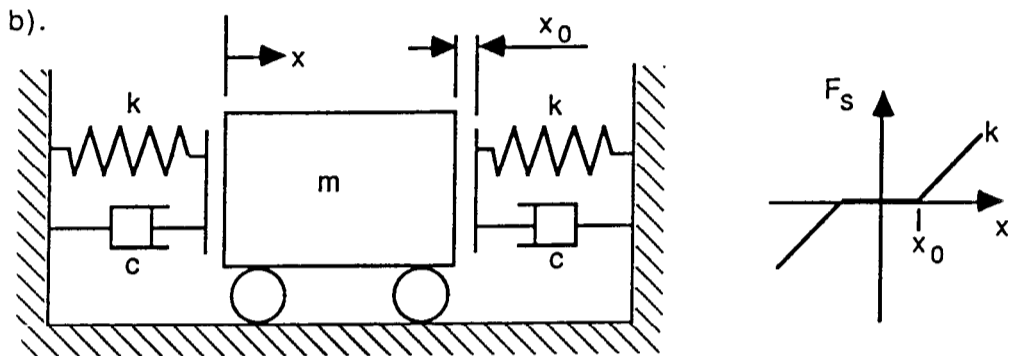
135

| System and Criterion used | Natural Frequency (Hz) | Radius (Error) m/M (%) | Modal Constant | Damping Loss Factor (Variation %) | Phase (Deg) |
|--|------------------------|--------------------------|----------------|-----------------------------------|-------------|
| LINEAR | 13.77 | 3.1992E-3(0.0) | 1.0000 | 0.02088(1.0) | 0.0 |
| QUADRATIC VISCOUS DAMPING | | | | | |
| NYQUIST - ALL POINTS | | | | | |
| Greatest sweep rate | 13.77 | 6.5476E-4(5.4) | 0.46293 | 0.04724(8.8) | 1.96 |
| Least damping variation and closest to real mode | 13.77 | 6.5476E-4(5.4) | 0.46286 | 0.04720(8.7) | -1.42 |
| NYQUIST - PTS CLOSE TO RESONANCE | | | | | |
| Greatest sweep rate | 13.77 | 6.0091E-4(1.4) | 0.28525 | 0.03172(4.9) | 2.25 |
| Least damping variation and closest to real mode | 13.77 | 6.0091E-4(1.4) | 0.28428 | 0.03159(4.5) | -1.59 |
| RECIPROCAL-OF-RECEPTANCE | | | | | |
| Pts above resonance | 13.58 | - | 0.90080 | 0.08920 | 0.0 |
| Pts below resonance | 13.93 | - | 0.87471 | 0.08284 | 0.0 |
| Pts crossing axis | 13.77 | - | 0.47810 | 0.04068 | 0.0 |
| All pts shown on plot | 13.77 | - | 0.70000 | 0.05954 | 0.0 |
| Pts shown on Nyquist plot | 13.77 | - | 0.27737 | 0.03073 | 0.0 |

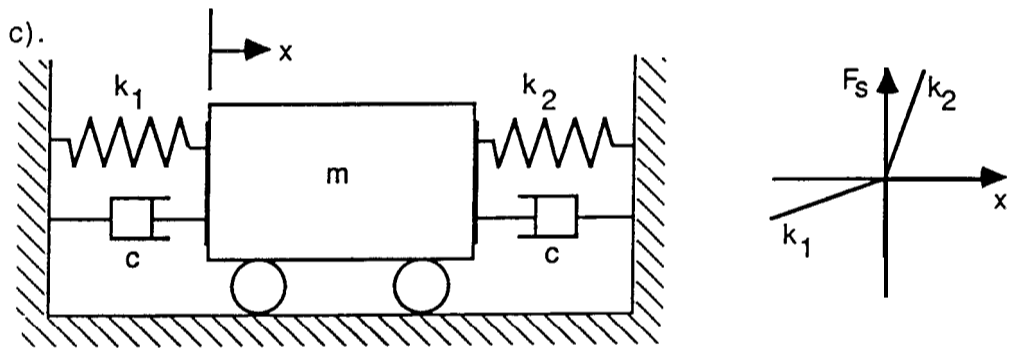
Table 5.11 Various parameters evaluated from a system with quadratic viscous damping subjected to an impulse. (Response of system shown at the top)



$\zeta = \frac{c}{2\sqrt{km}}$; $\omega_0^2 = \frac{k}{m}$; $f_t = \frac{F_0}{m} \sin \omega t$; F_0 is amplitude of forcing signal



$\zeta = \frac{c}{2\sqrt{km}}$; $\omega_0^2 = \frac{k}{m}$; $f_t = \frac{F_0}{m} \sin \omega t$; F_0 is amplitude of forcing signal

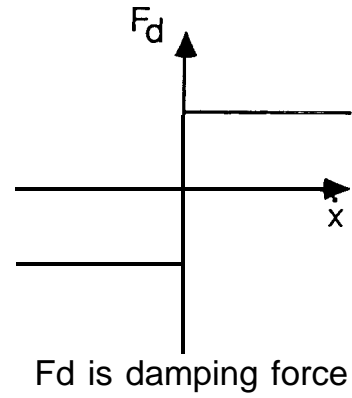
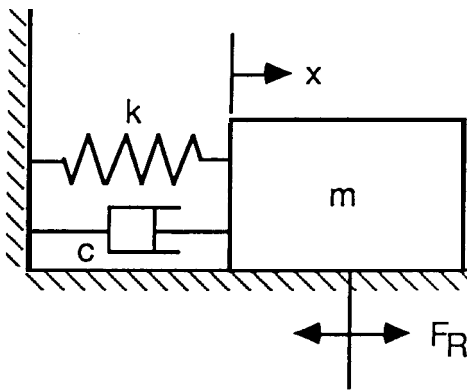


$\omega_{01}^2 = \frac{k_1}{m}$; $\omega_{02}^2 = \frac{k_2}{m}$; $\zeta\omega_0 = \frac{c}{2m}$; $f_t = \frac{F_0}{m} \sin \omega t$; F_0 is amplitude of forcing signal

Fig 5.1 Stiffness-type non linearities.

- a). Cubic stiffness
- b). Backlash.
- c). Bi-linear stiffness.

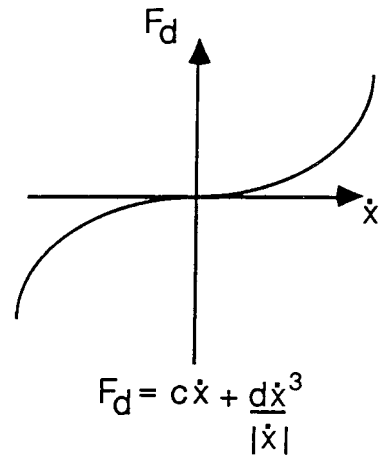
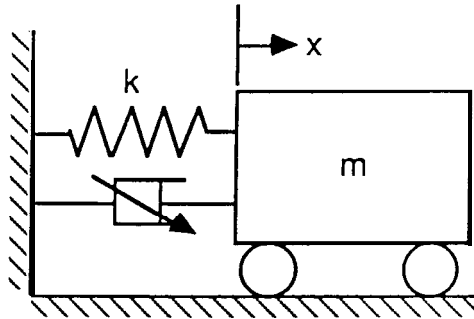
a).



$$R = \frac{F_R}{m} ; \quad \zeta = \frac{c}{2\sqrt{km}} ; \quad \omega_0^2 = \frac{k}{m} ;$$

$$f(t) = \frac{F_0}{m} \sin \omega t \quad \text{where } F_0 \text{ is the amplitude of forcing signal}$$

b).



$$q = \frac{d}{m} ; \quad \zeta = \frac{c}{2\sqrt{km}} ; \quad \omega_0^2 = \frac{k}{m} ;$$

$$f(t) = \frac{F_0}{m} \sin \omega t \quad \text{where } F_0 \text{ is the amplitude of forcing signal}$$

Fig 5.2 Damping-type non-linearities

- a). Friction
- b). Quadratic viscous damping

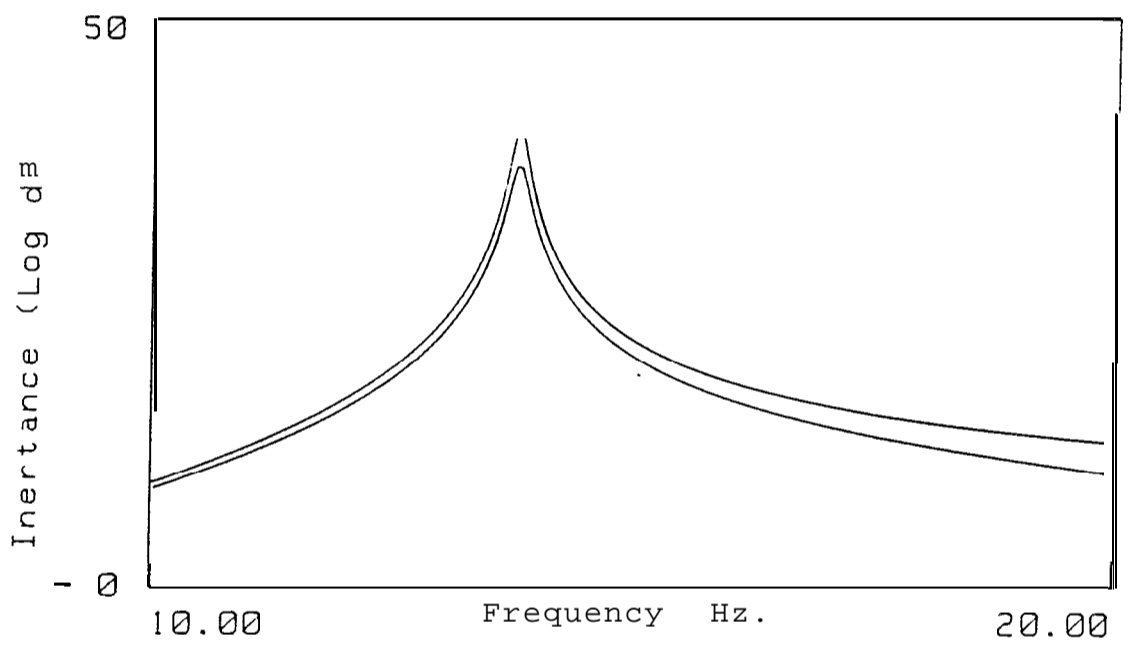
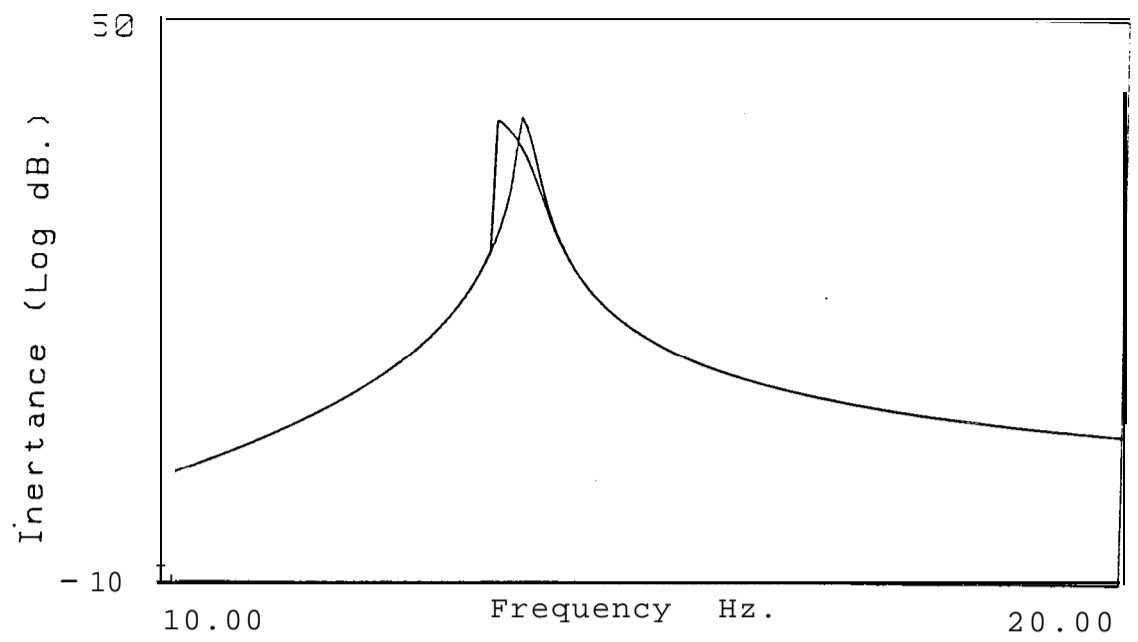


Fig 5.3 Examples of the differences in Bode plots due to changing input force level

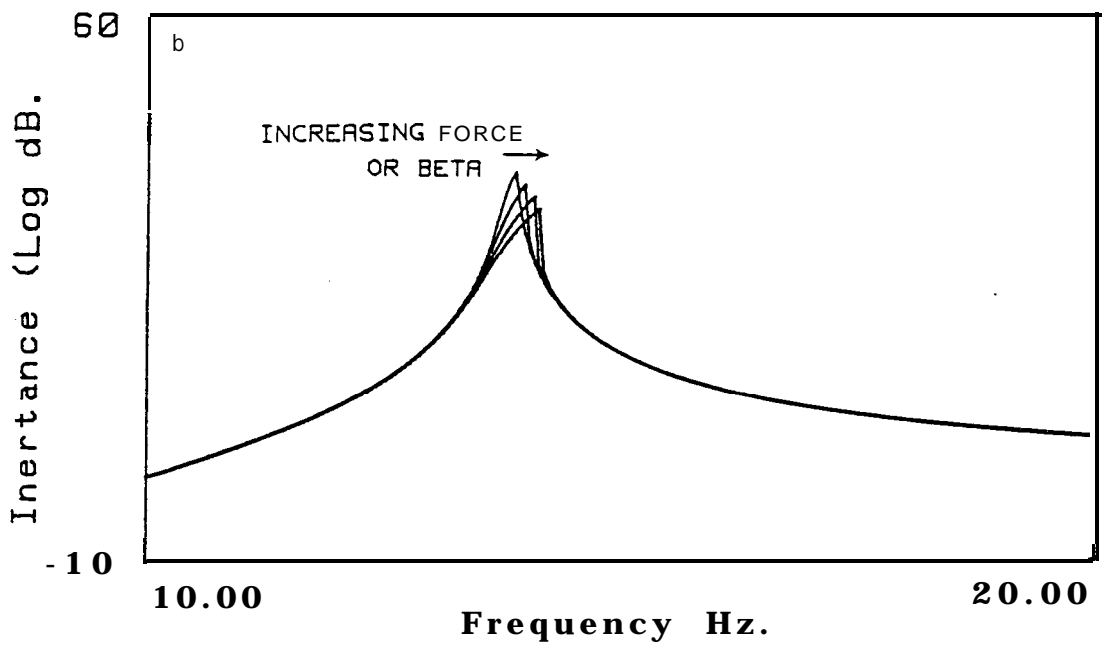
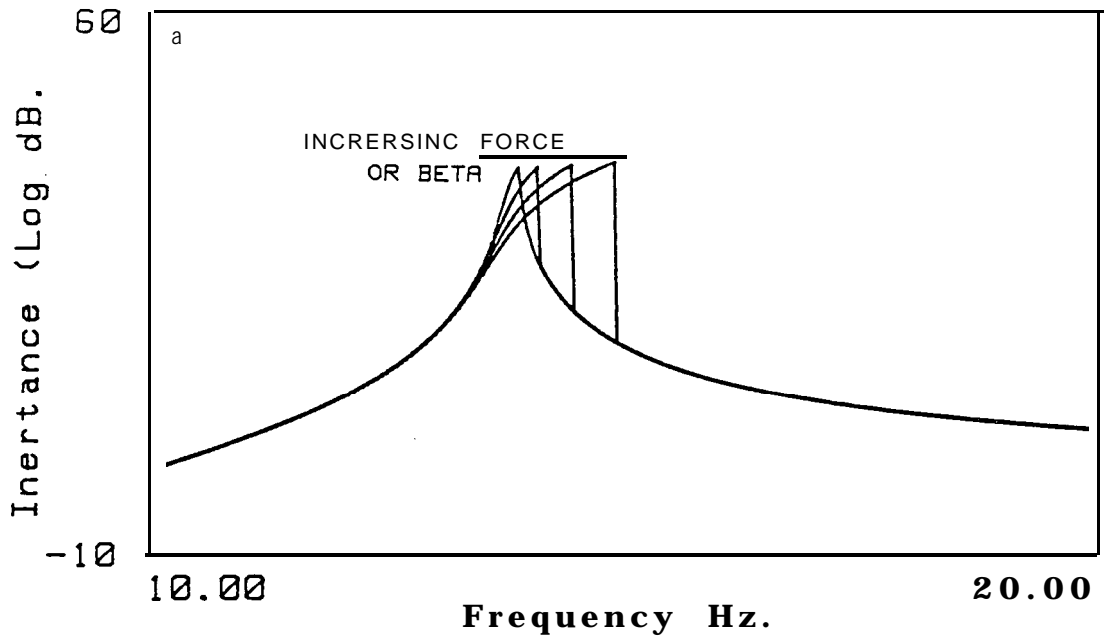


Fig 5.4 Trends in Bode plots from a system with **hardening cubic stiffness**
 a Stepped-sine excitation sweeping up
 b Stepped-sine excitation sweeping down

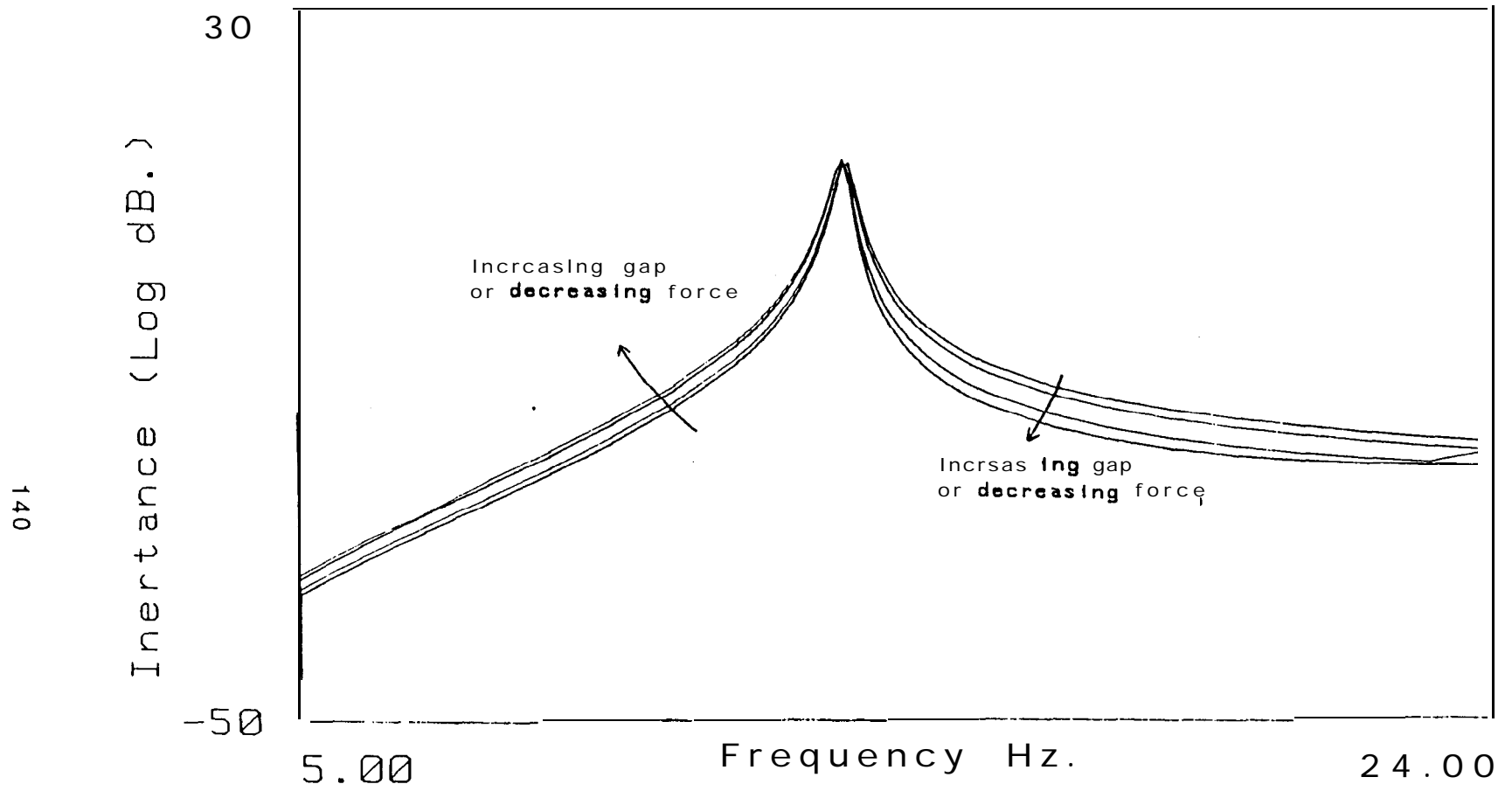


Fig 5.5 Trends in **Bode plots** from systems with backlash

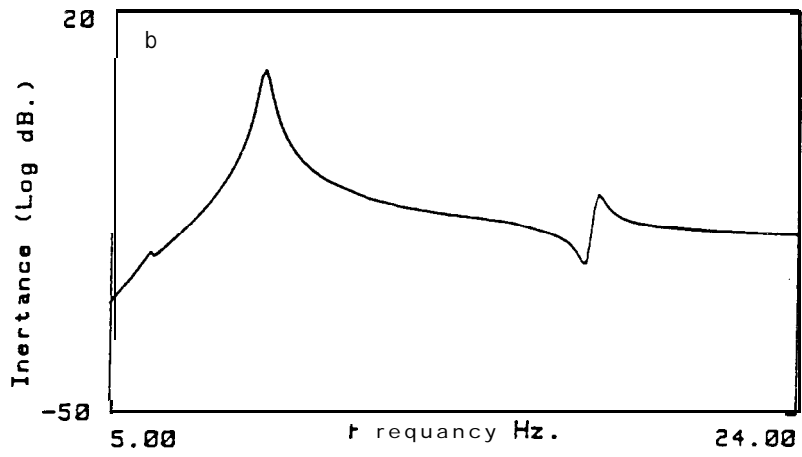
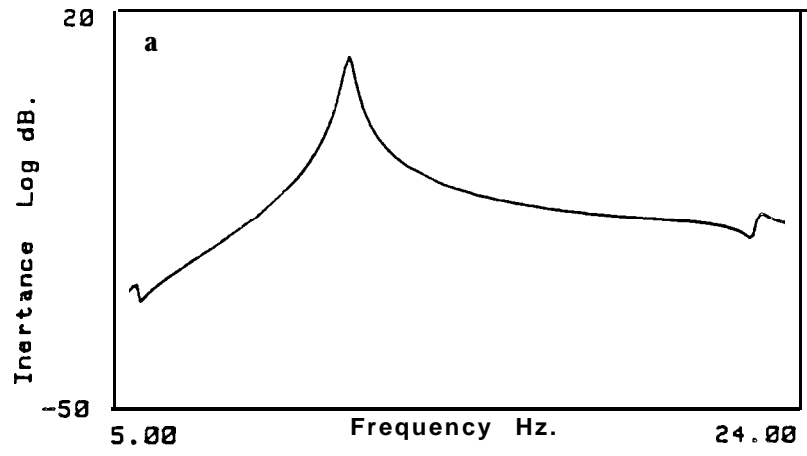


Fig 5.6 Trends in Bode plots from systems with bi-linear stiffness
 a Bode plots from two different force levels
 b One Bode plot from a system with a spring stiffness ratio of twice that in Fig 5.6a

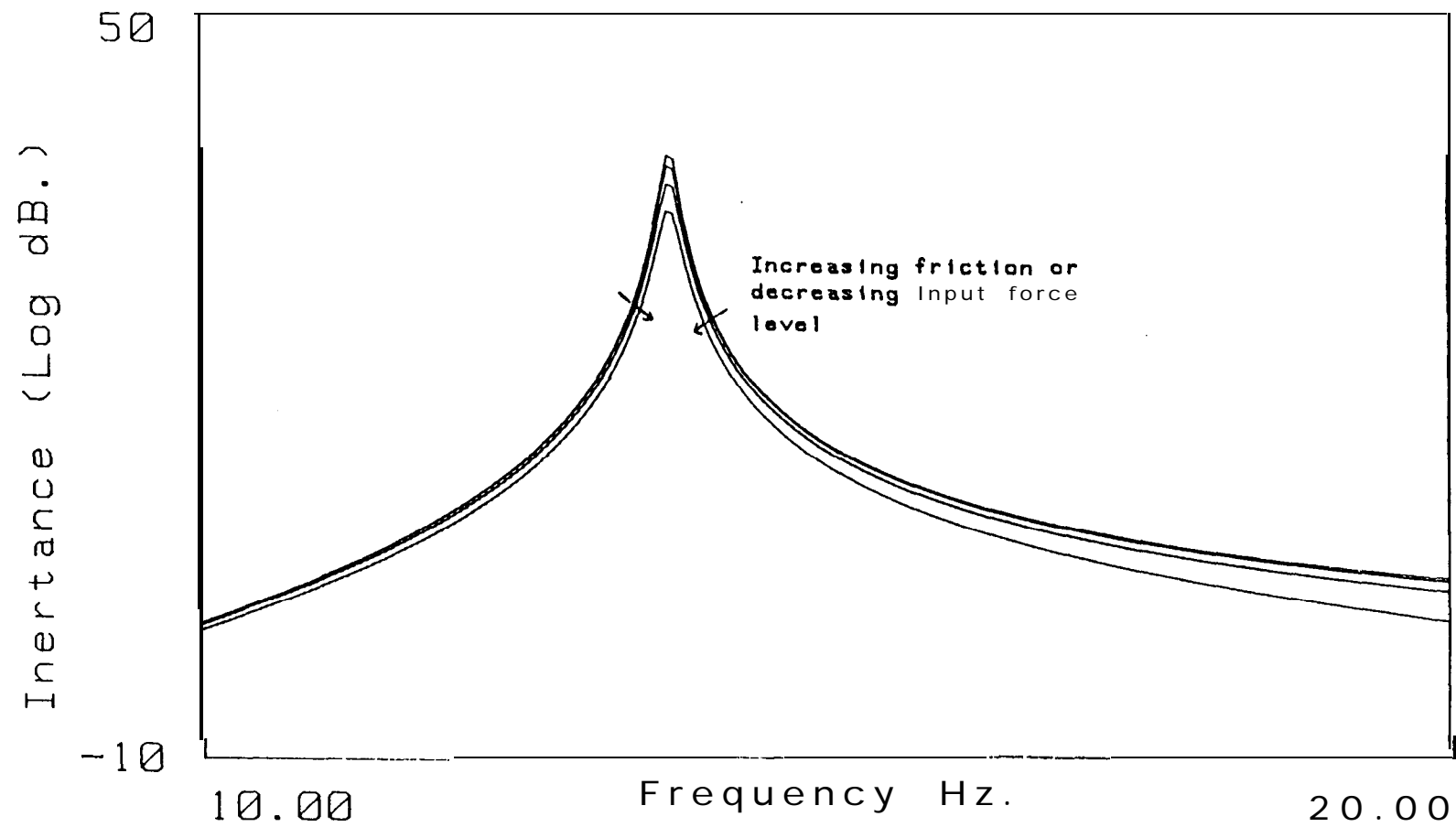


Fig 5.7 Trends in Bode plots from systems with friction

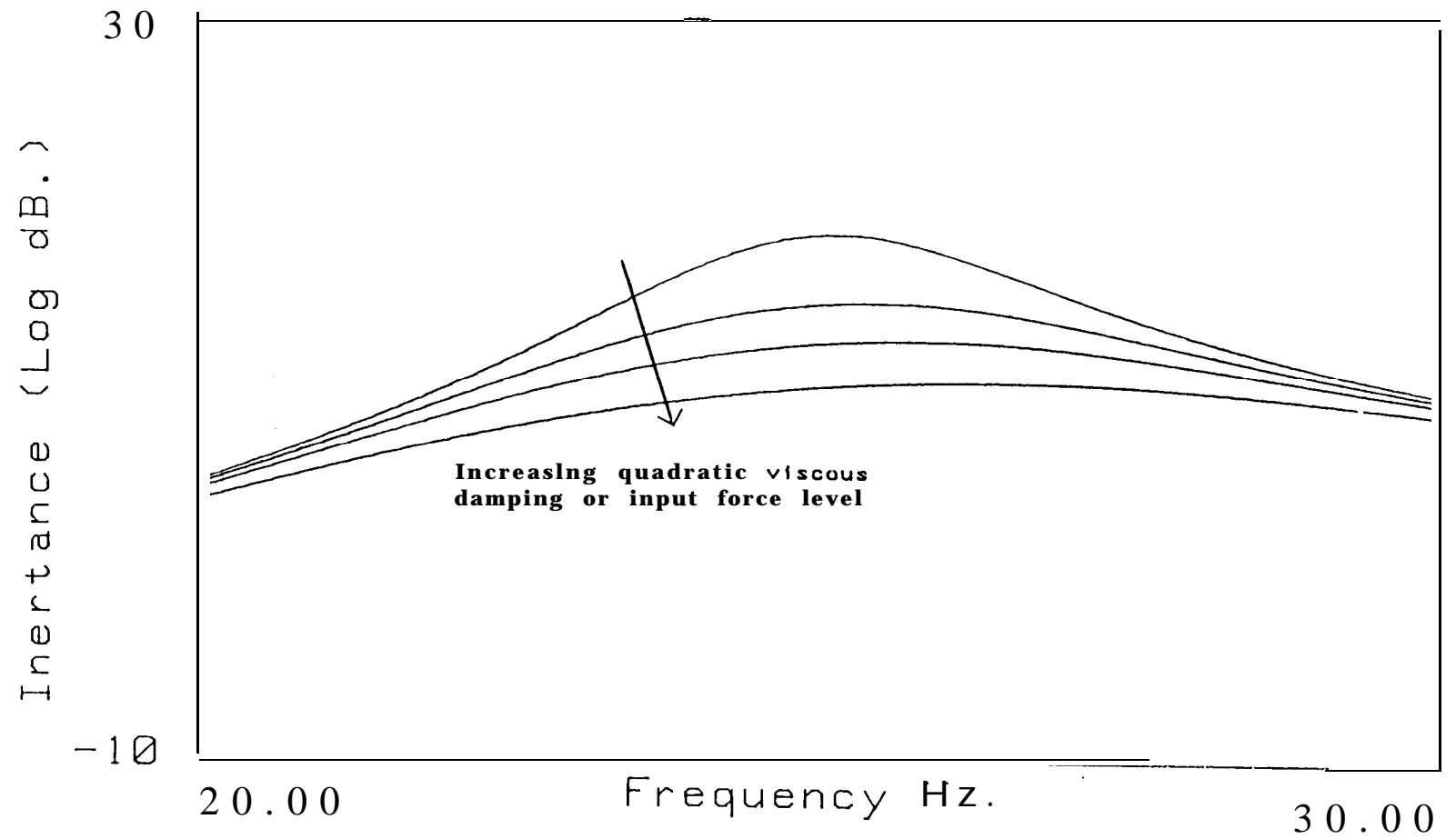


Fig 5.8 Detail 1 of trends near resonance in Bode plots from systems with quadratic viscous damping

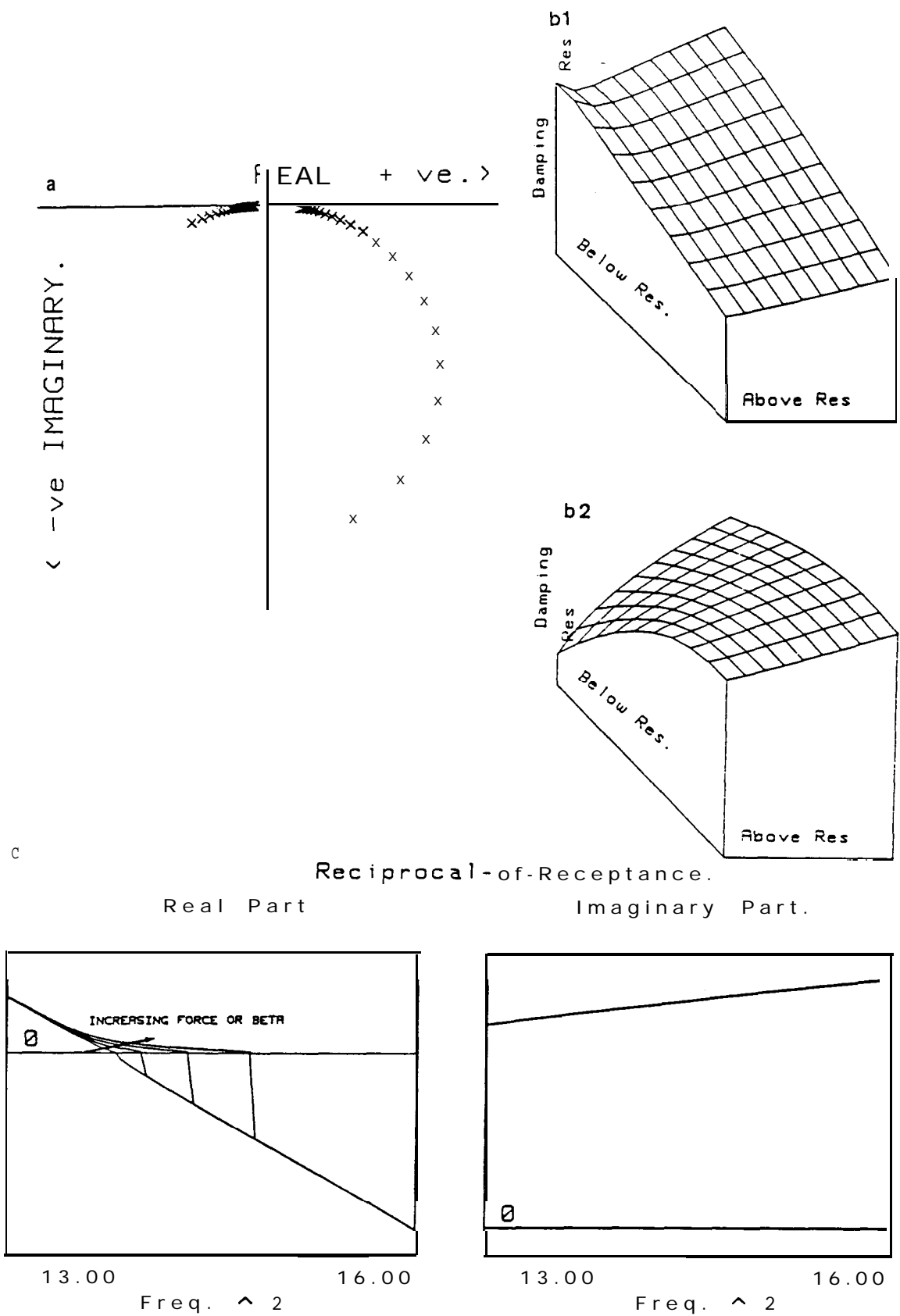


Fig 5.9 Trends in the frequency domain from a system with hardening cubic stiffness
 a Nyquist plot
 b1 3-D damping plot
 b2 3-D damping plot; high non-linearity and least damping variation
 c Reciprocal-of-receptance plots

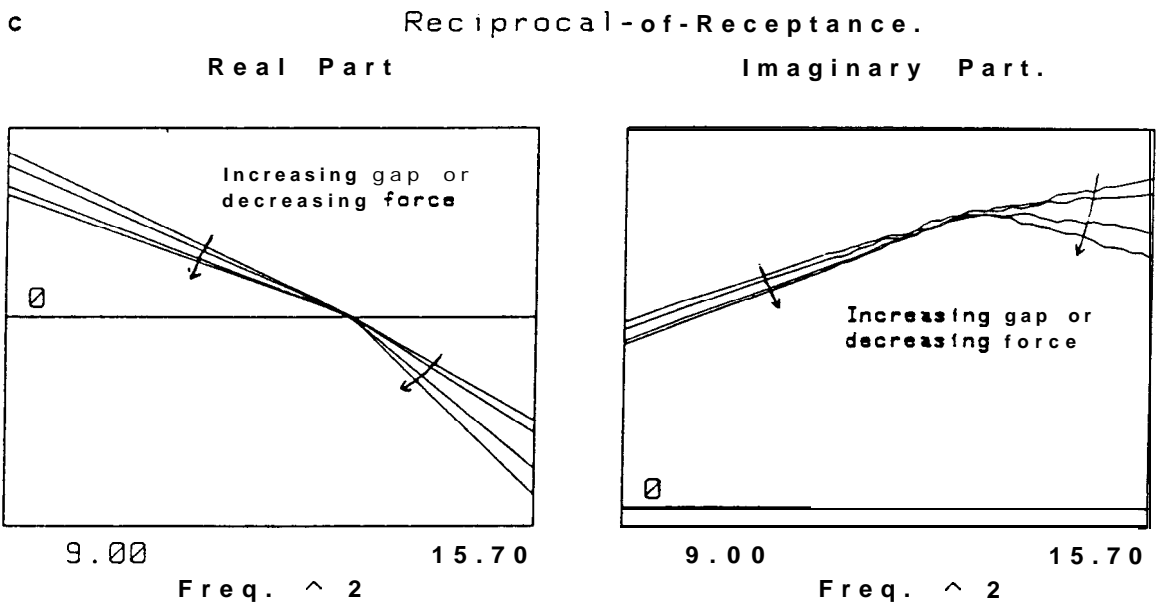
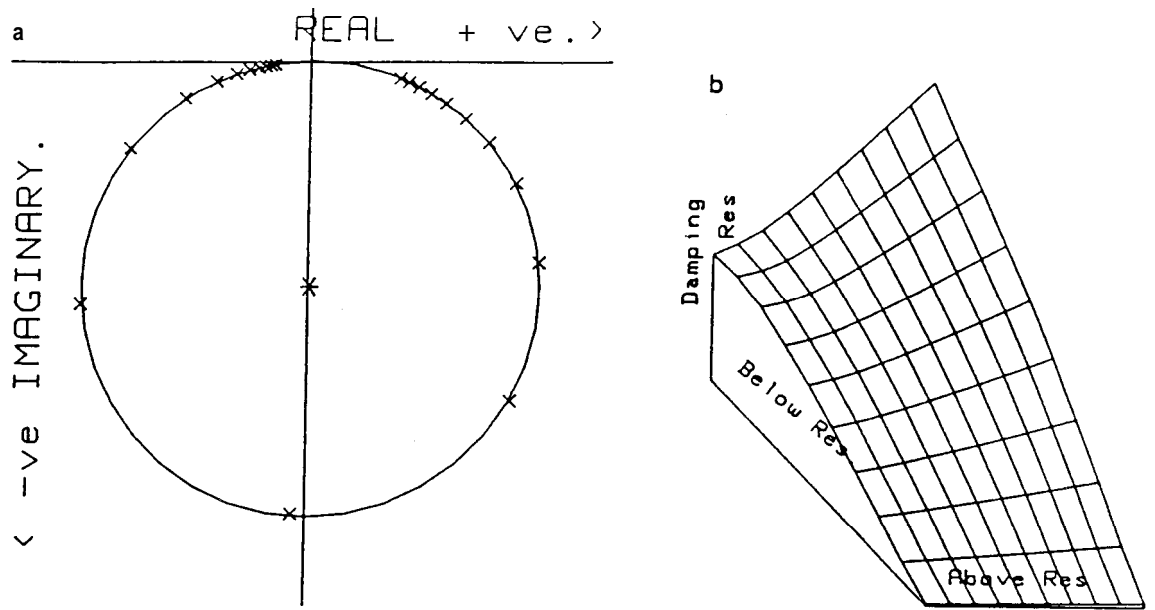


Fig5.18 Trends in the frequency domain from a system with backlash
 a Nyquist plot
 b 3-D damping plot
 c Reciprocal-of-receptance plots

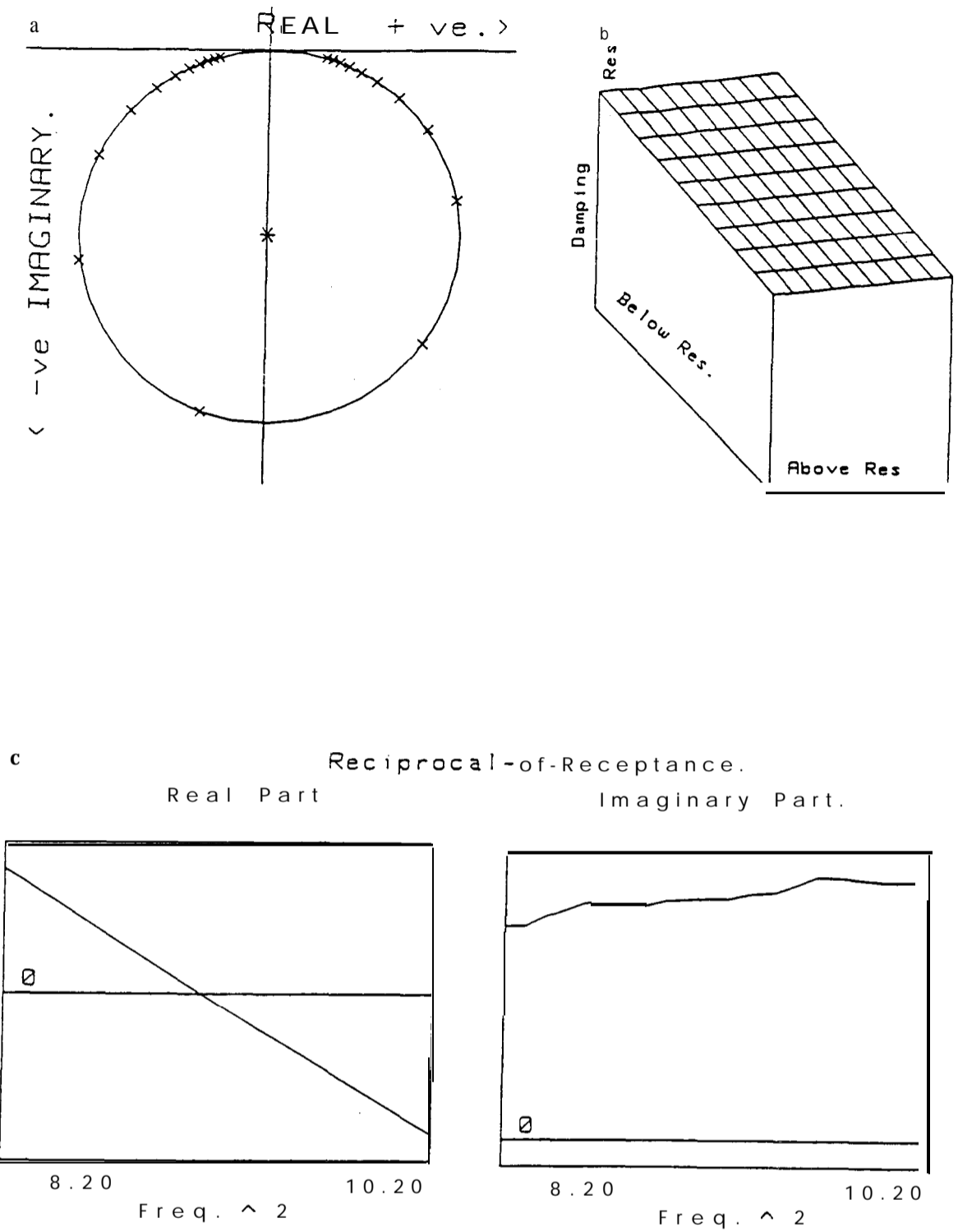


Fig 5.11 Trends in the frequency domain from a system with bi-linear stiffness

- a Nyquist plot
- b 3-D damping plot
- c Reciprocal-of-receptance plots

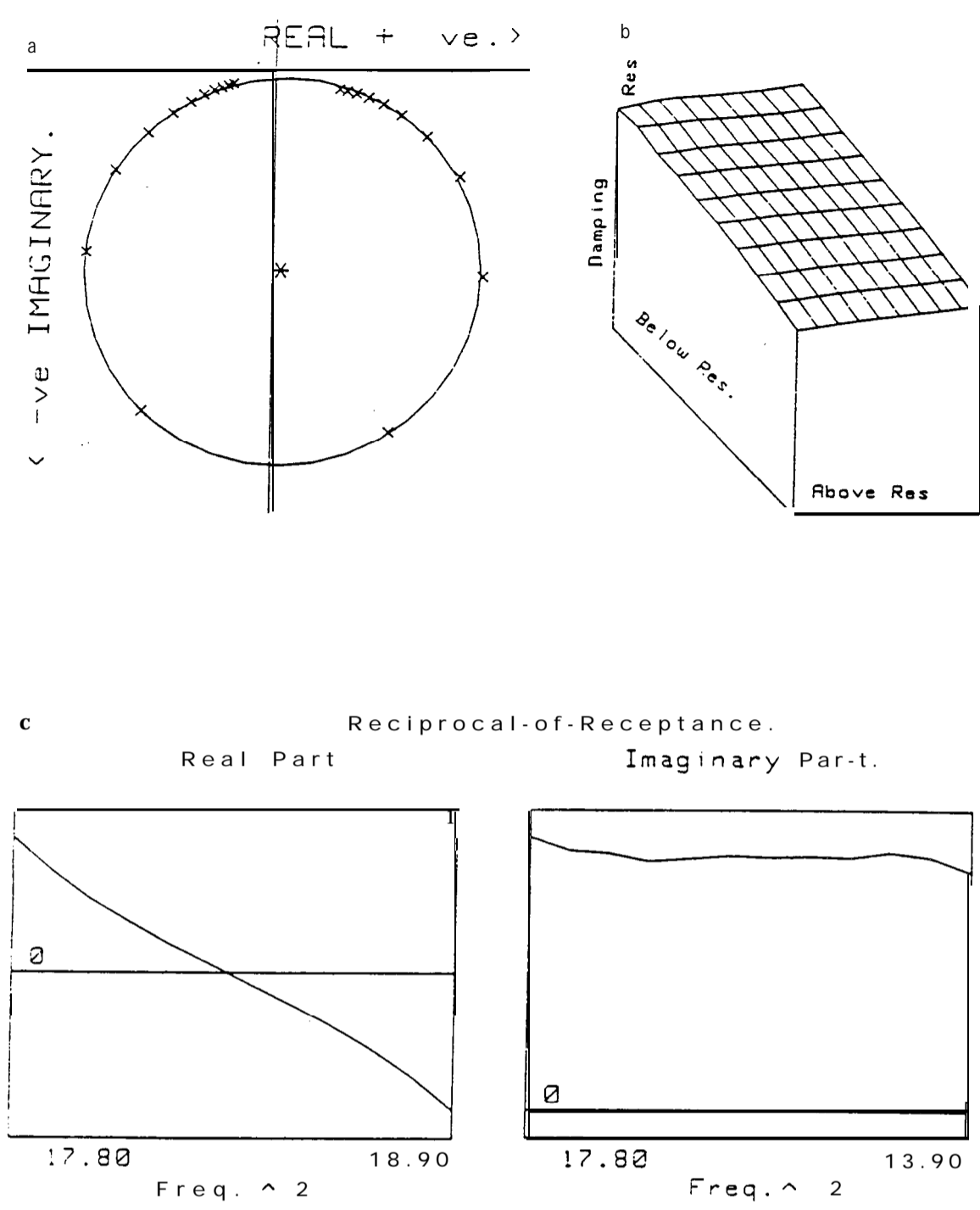
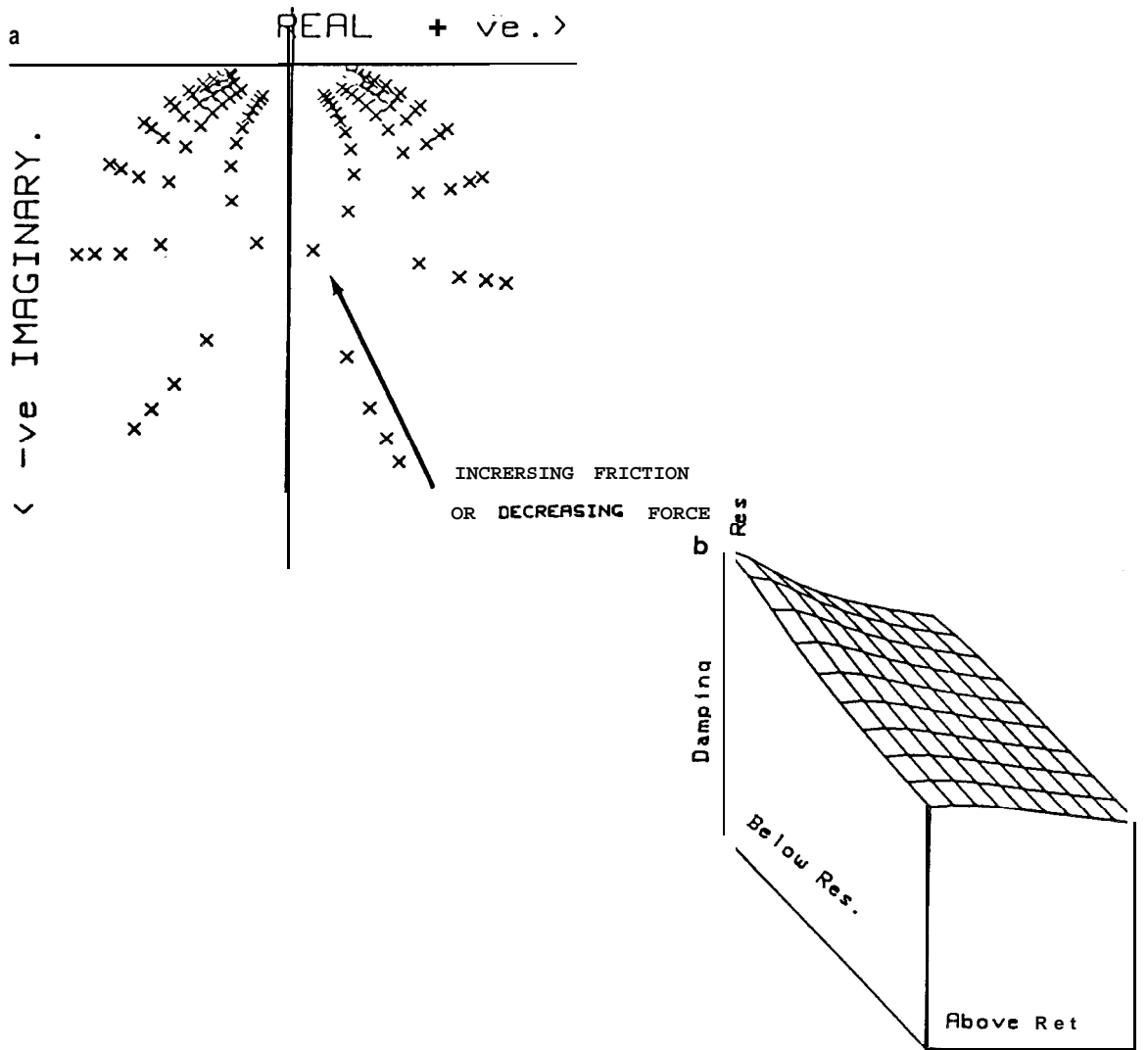


Fig 5.12 Trends in the frequency domain from the first harmonic of a system with bi-linear stiffness
 a Nyquist plot
 b 3-D damping plot
 c Reciprocal-of-receptance plots



c **Reciprocal-of-Receptance.**
Real Part **Imaginary Part.**

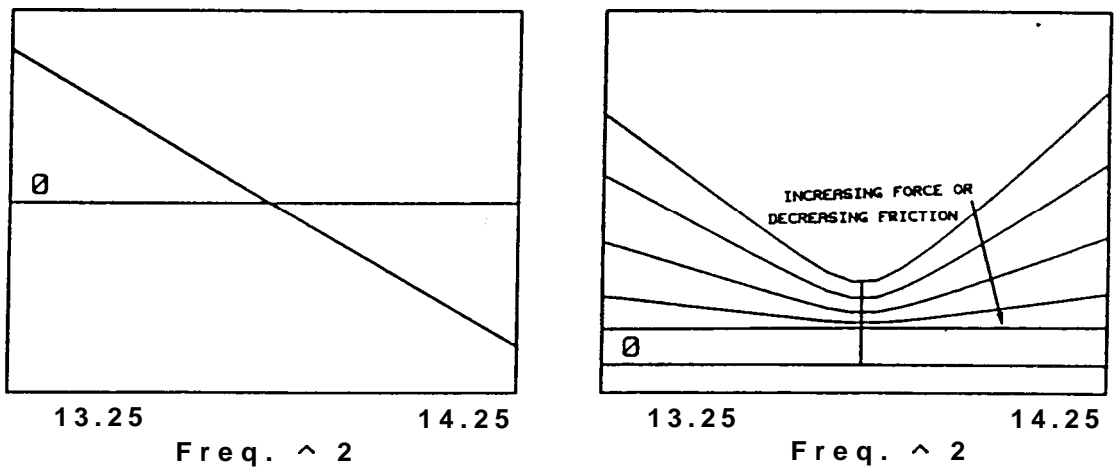


Fig 5.13 Trends in the frequency domain from a system with friction
 a Nyquist plot
 b 3-D damping plot
 c Reciprocal-of-receptance plots

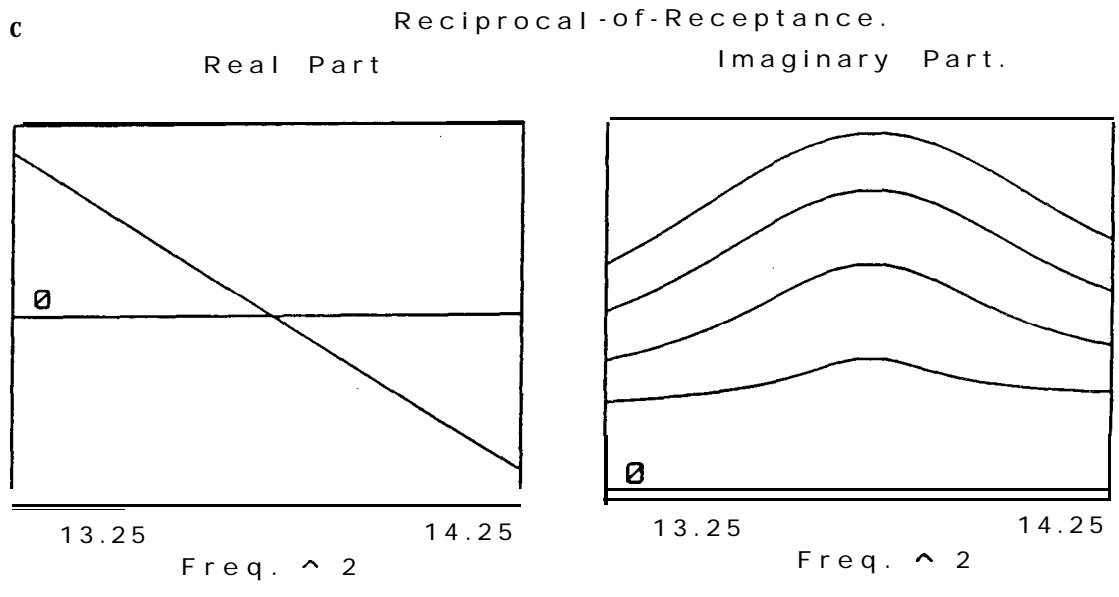
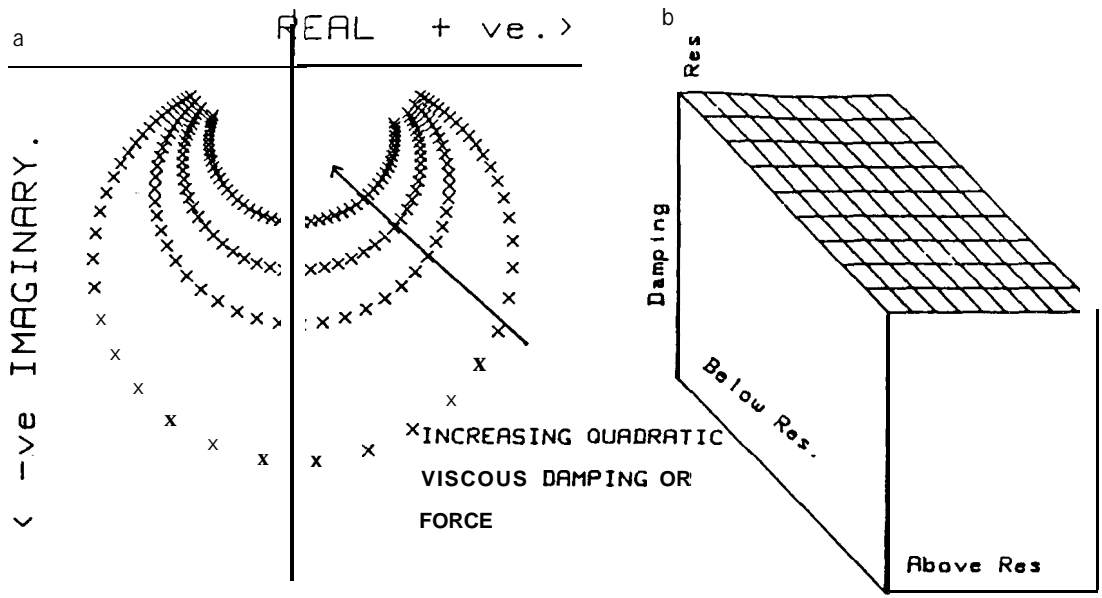


Fig 5.14 Trends in the frequency domain from a system with quadratic viscous damping
 a Nyquist plot
 b 3-D damping plot
 c Reciprocal-of-receptance plots



Fig 5.15a Displacement time-history from a linear system

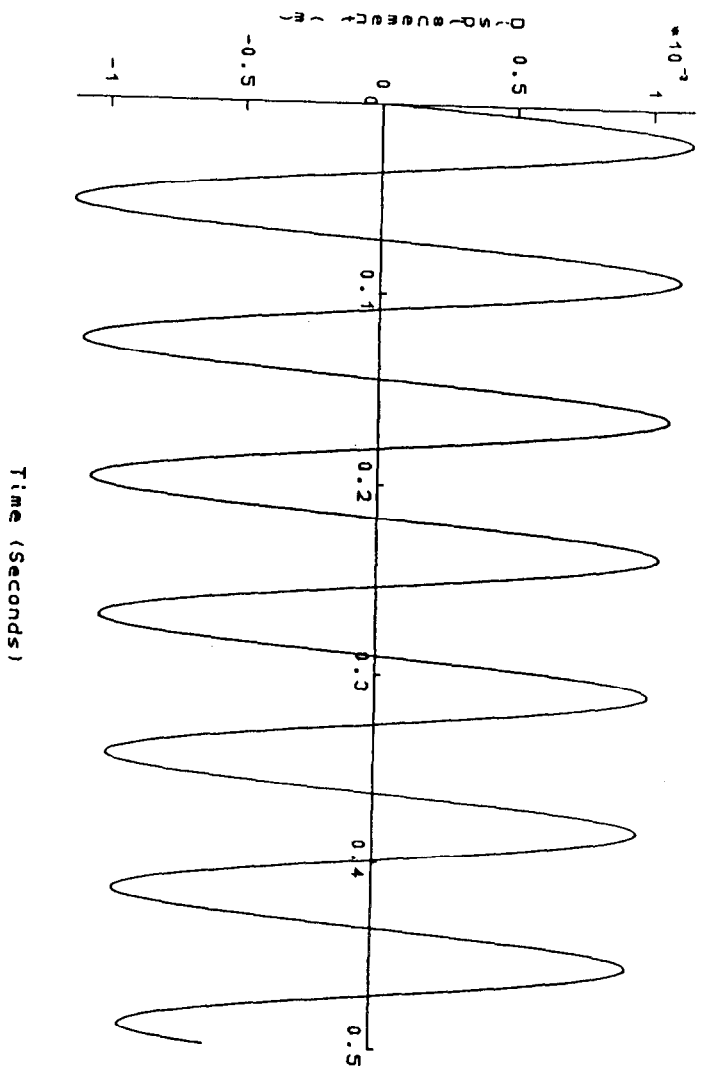


Fig 5.15b Expanded view of the displacement time-history of a linear system

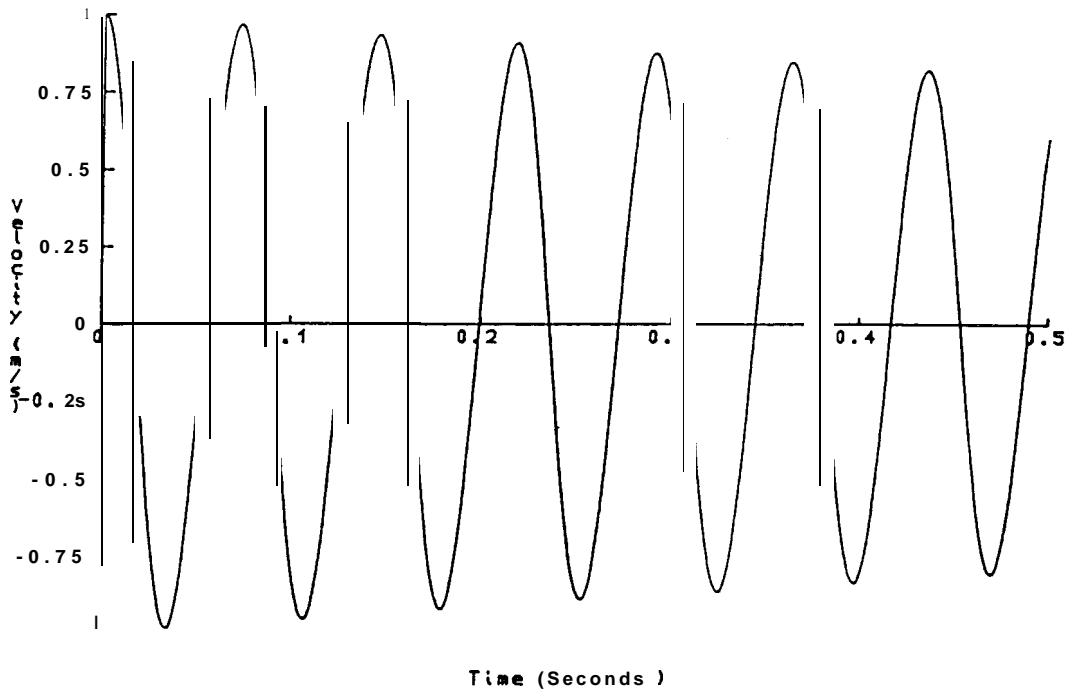


Fig 5.15c Expanded view of the velocity **time-history** of a **linear** system

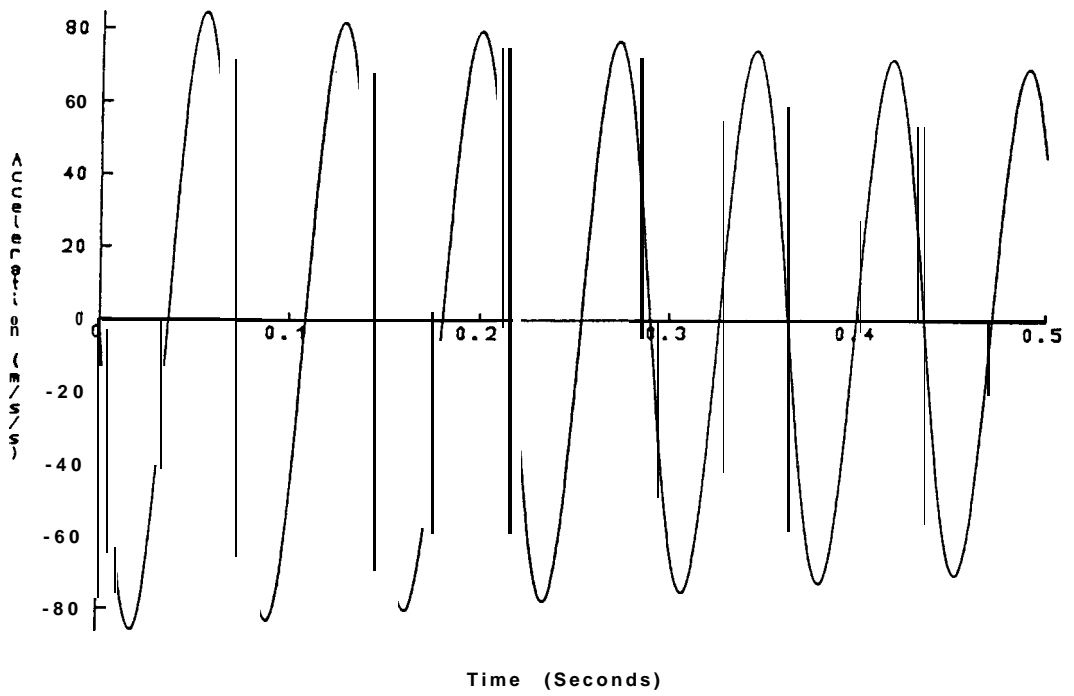


Fig 5.15d Expanded view of the acceleration time-history of a linear system

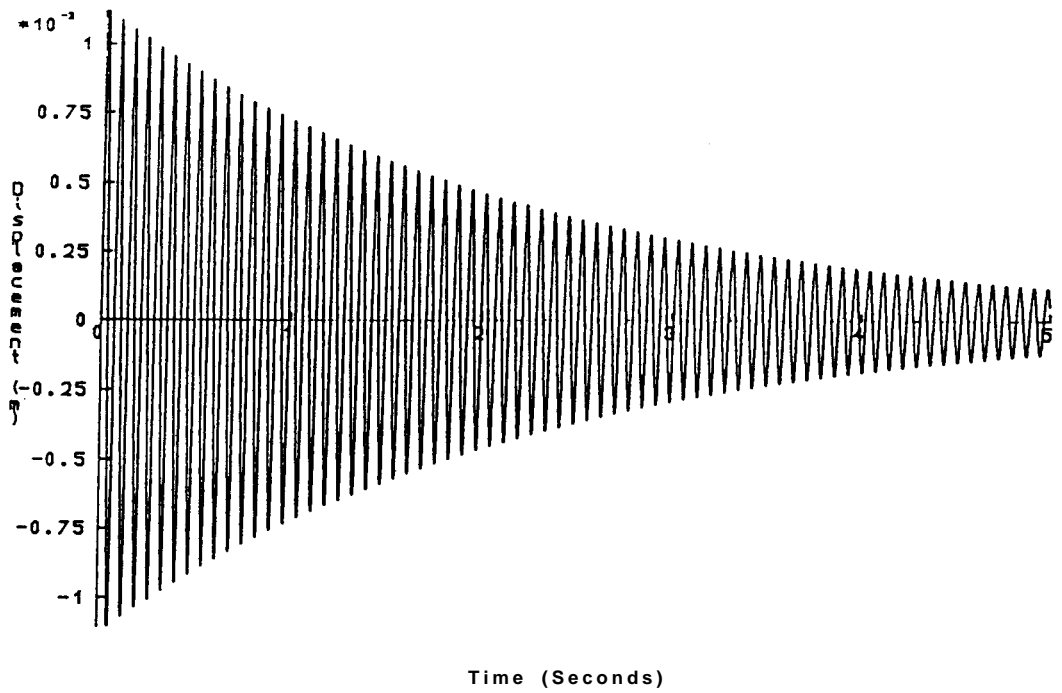


Fig 5.16a Displacement time-history from a system with cubic stiffness

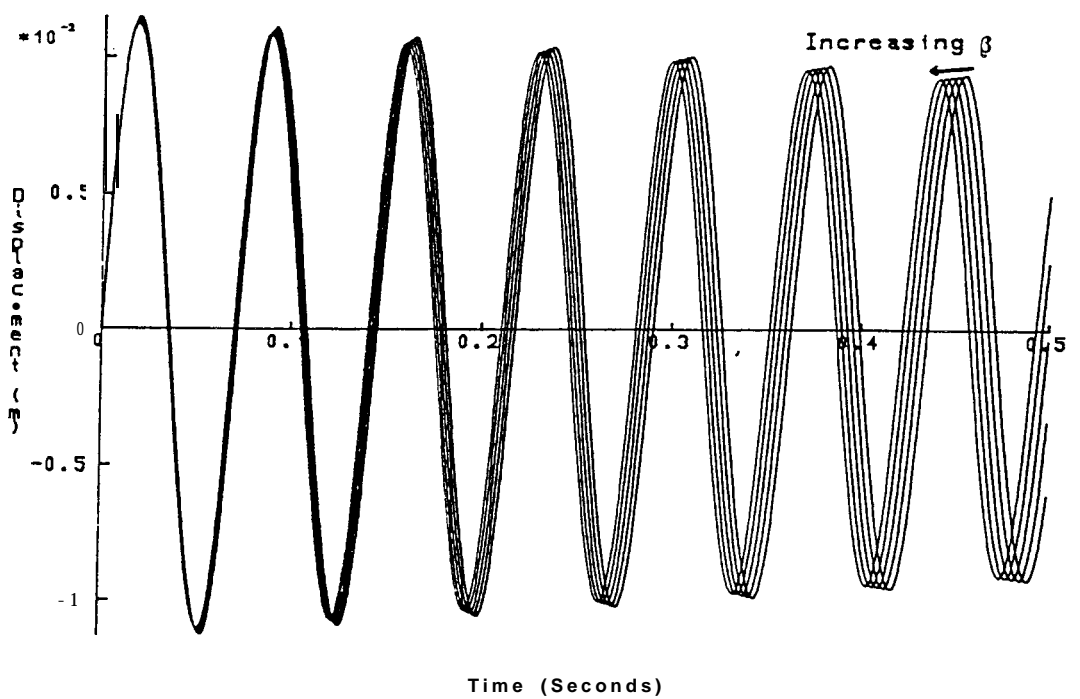


Fig 5.16b Expanded views of the displacement time-histories of systems with cubic stiffness

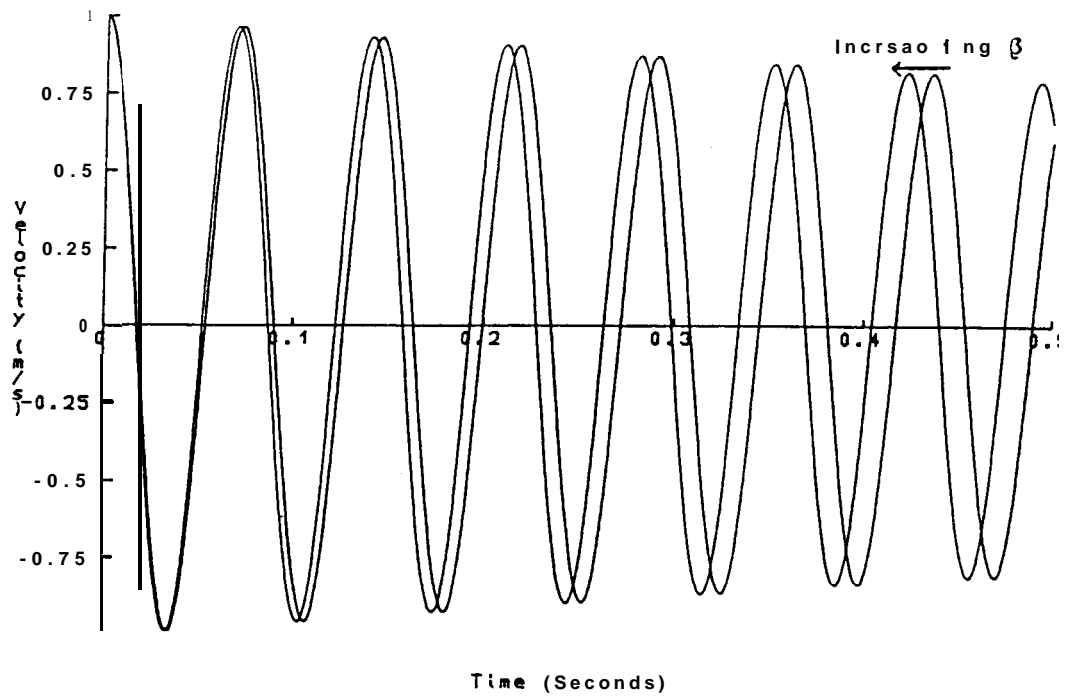


Fig 5.16c Expanded views of the velocity time-histories of systems with cubic stiffness

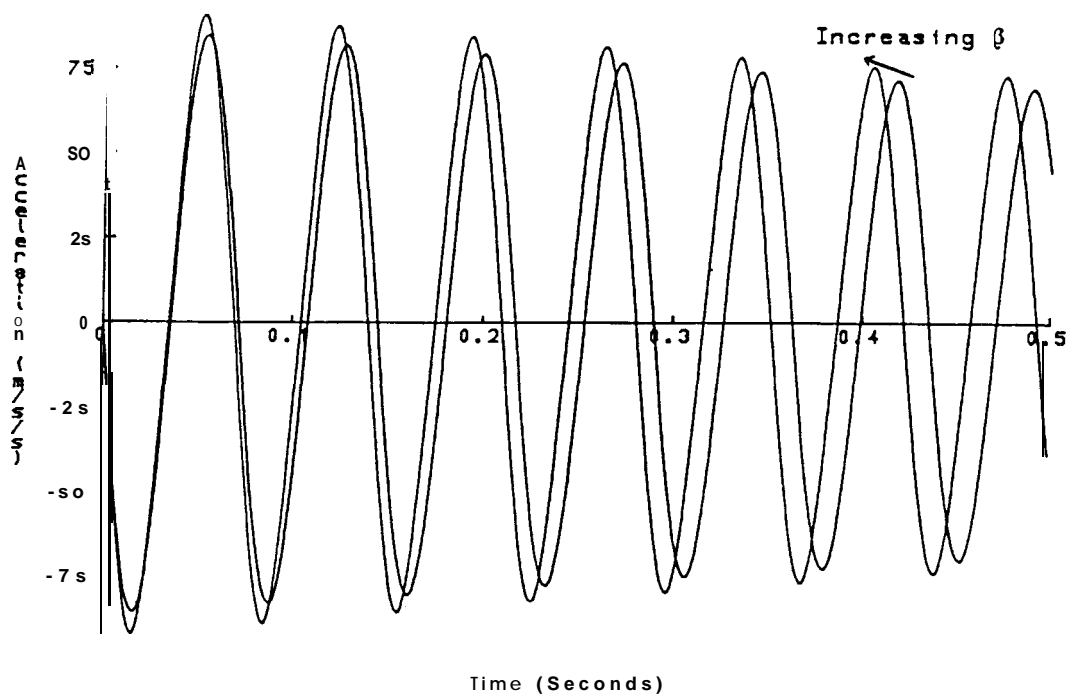


Fig 5.16d Expanded views of the acceleration time-histories of systems with cubic stiffness

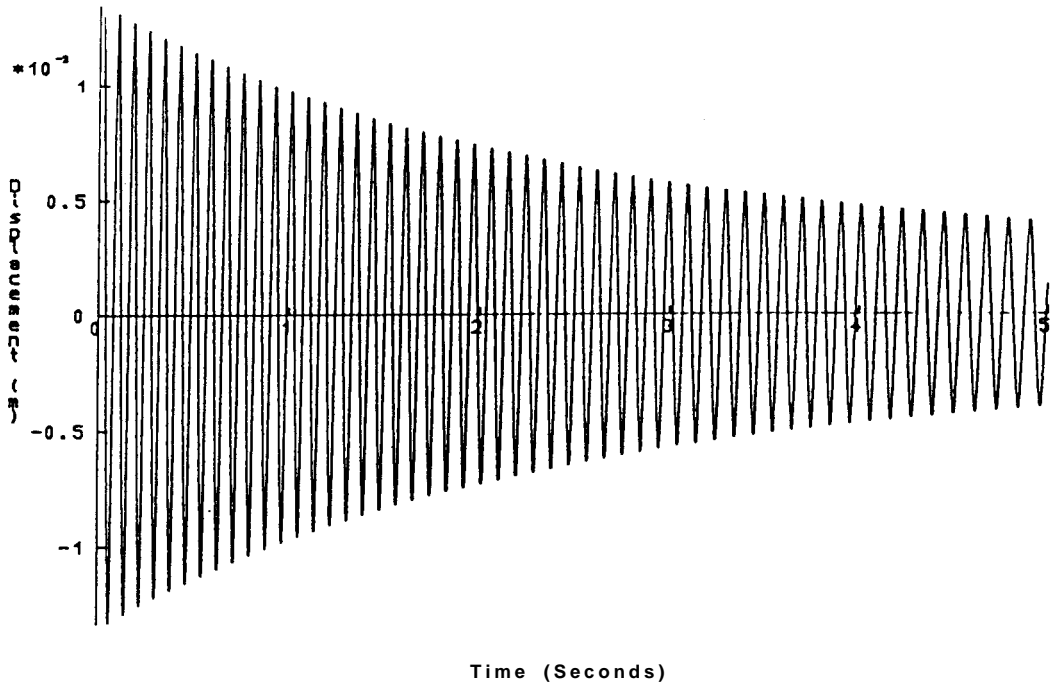


Fig 5.17a Displacement time-history from a system with backlash

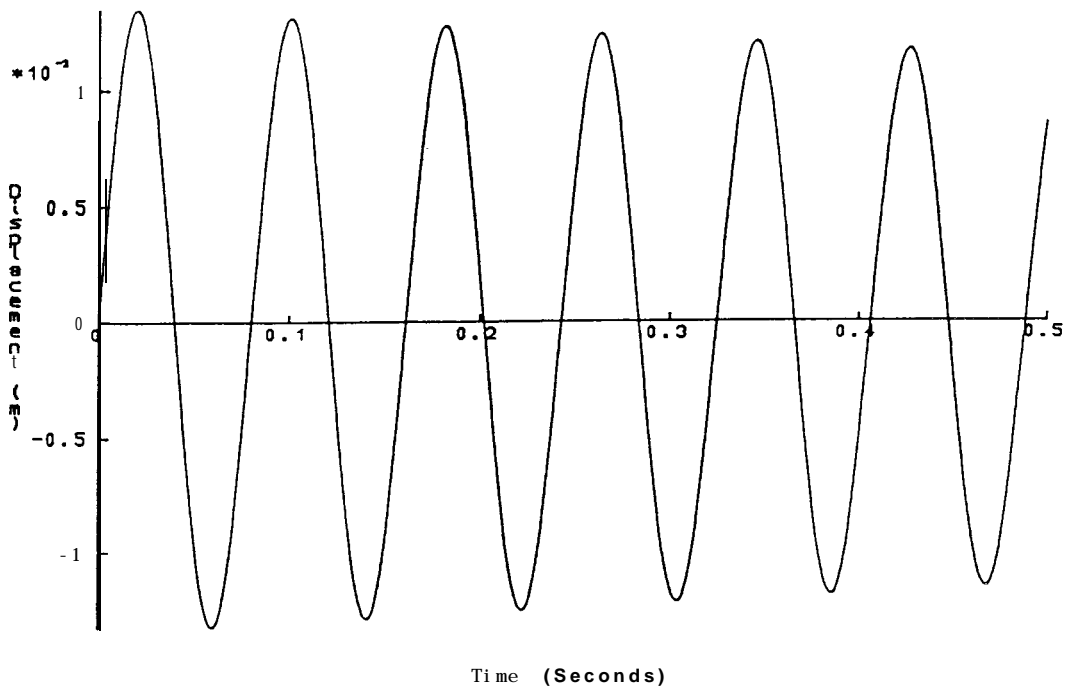


Fig 5.17b Expanded view of the displacement time-history of a system with backlash

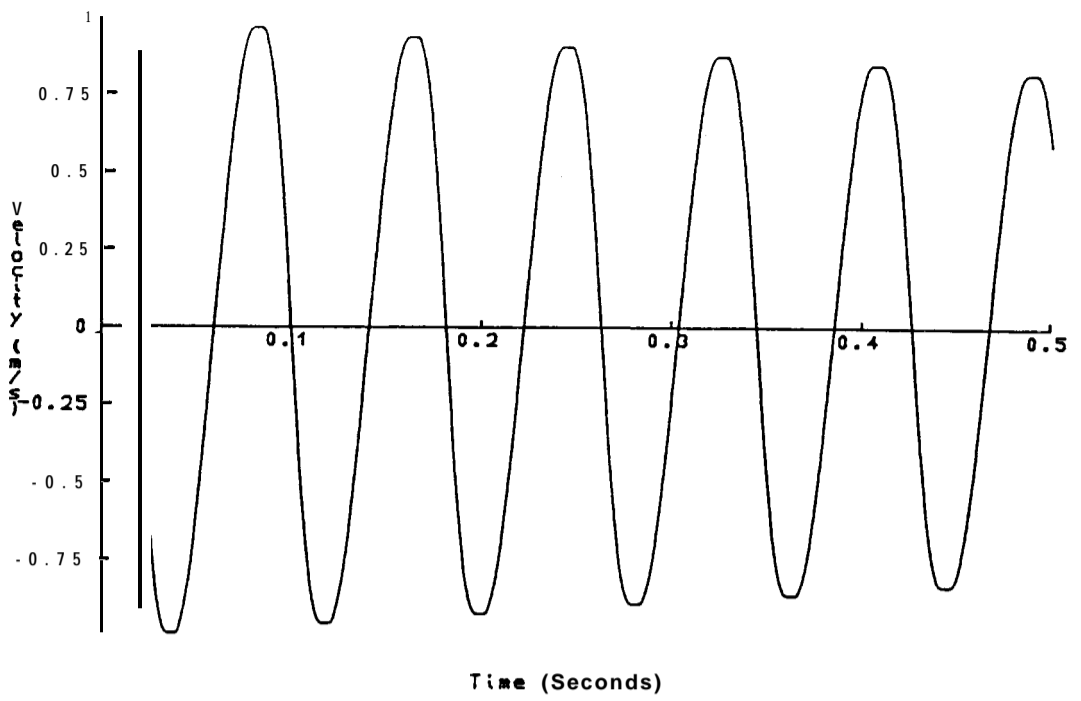


Fig 5.17c Expanded view of the velocity time-history of a system with back1 ash

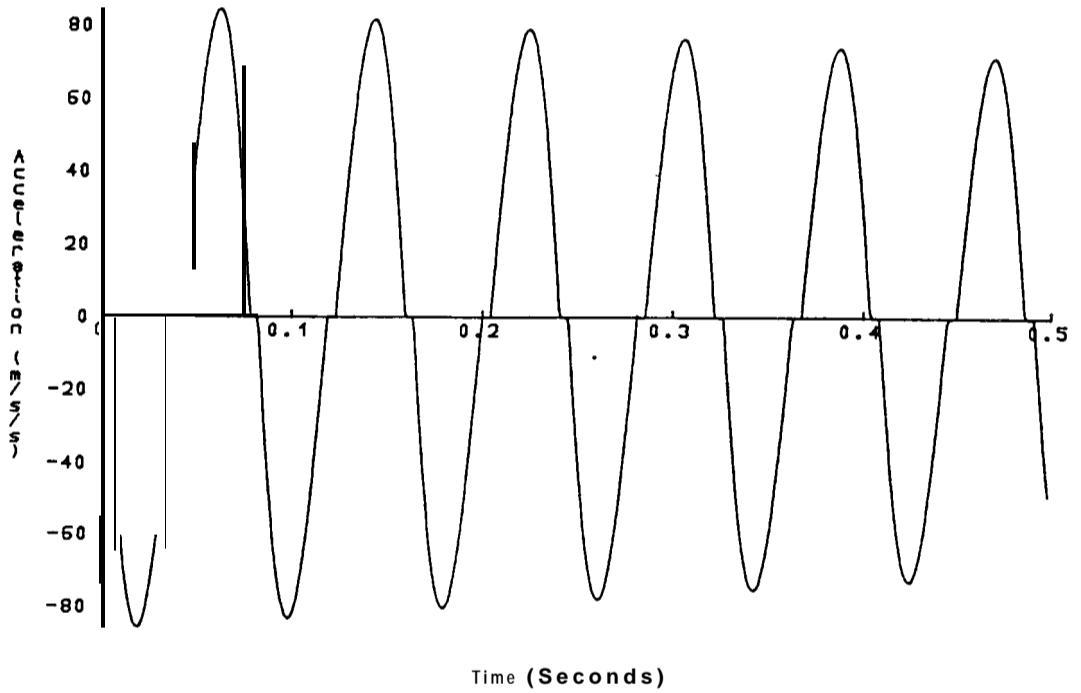


Fig 5.17d Expanded view of the acceleration time-history of a system with back1 ash

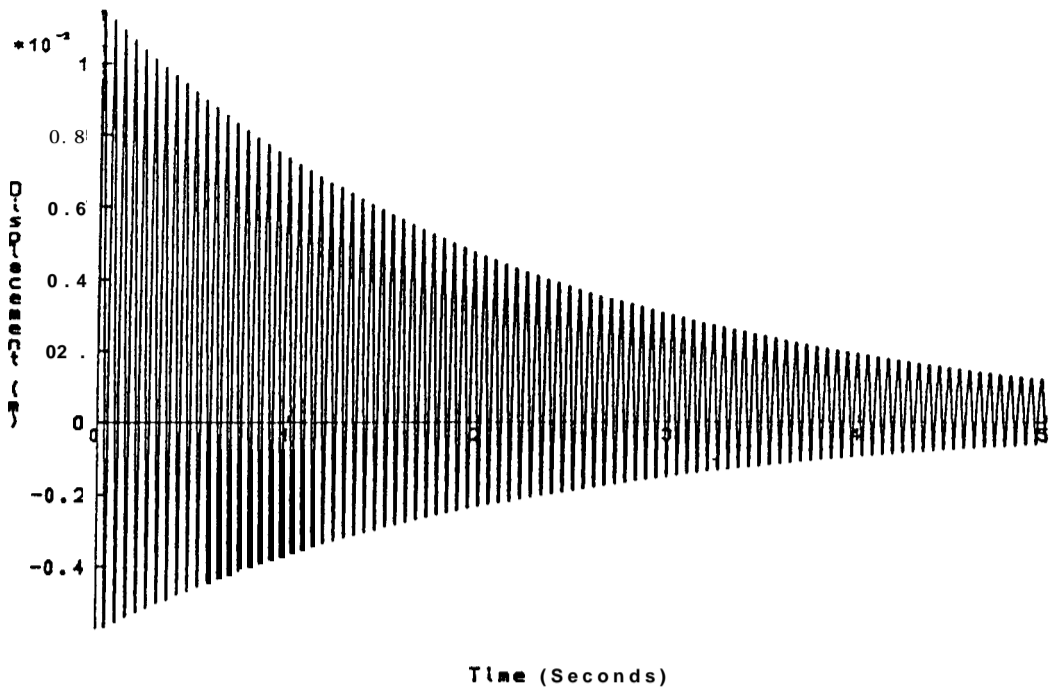


Fig 5.18a Displacement time-history from a system with bi-linear stiffness

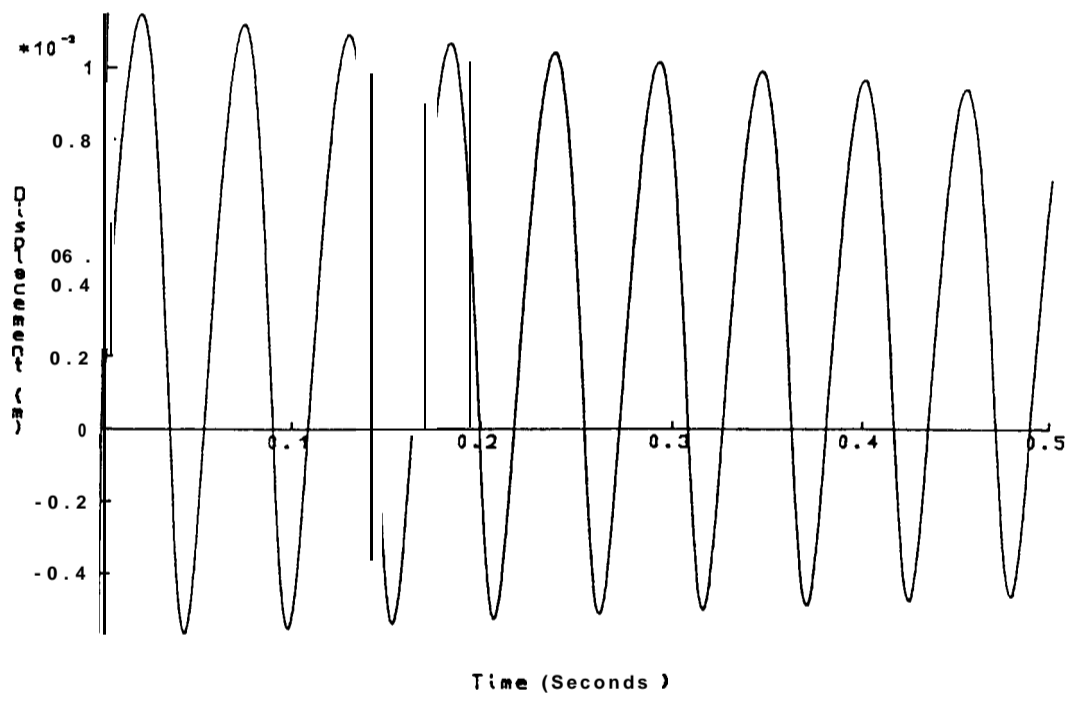


Fig 5.18b Expanded view of the displacement time-history of a system with bi-linear stiffness

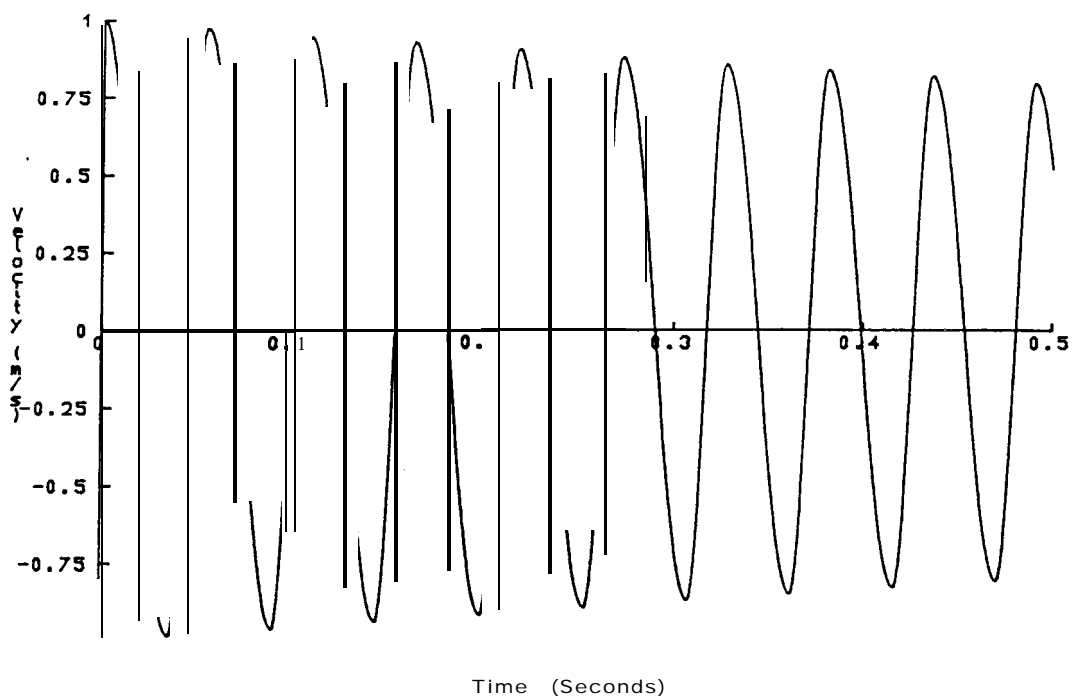


Fig 5.18c Expanded view of the velocity time-history of a system with bi-linear stiffness

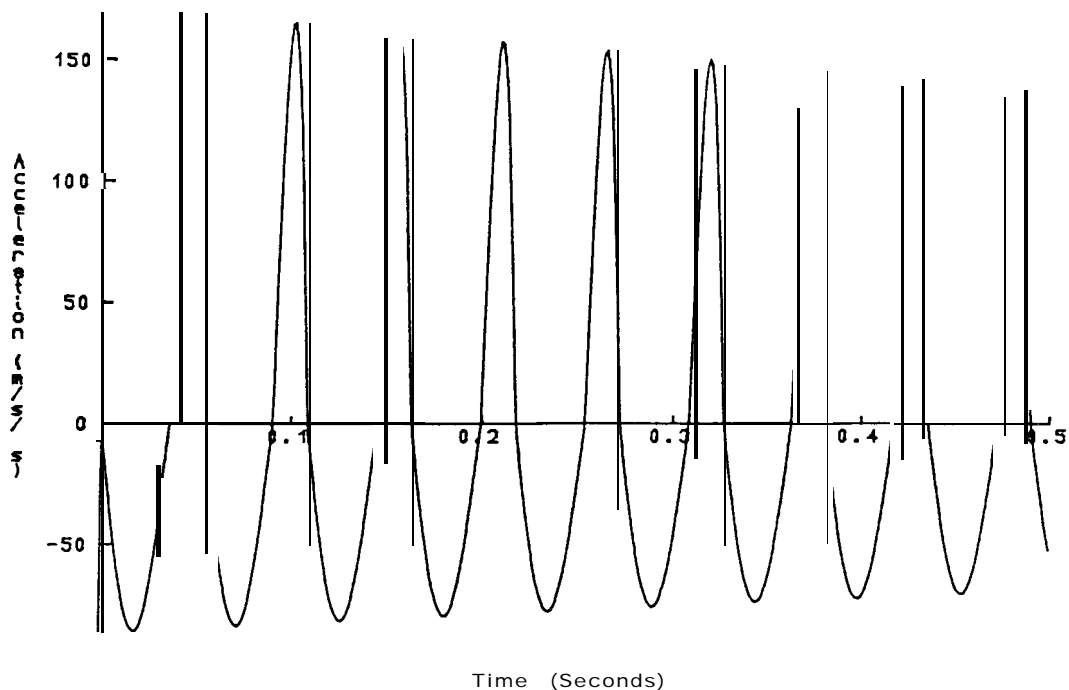


Fig 5.18d Expanded view of the acceleration time-history of a system with bi-linear stiffness

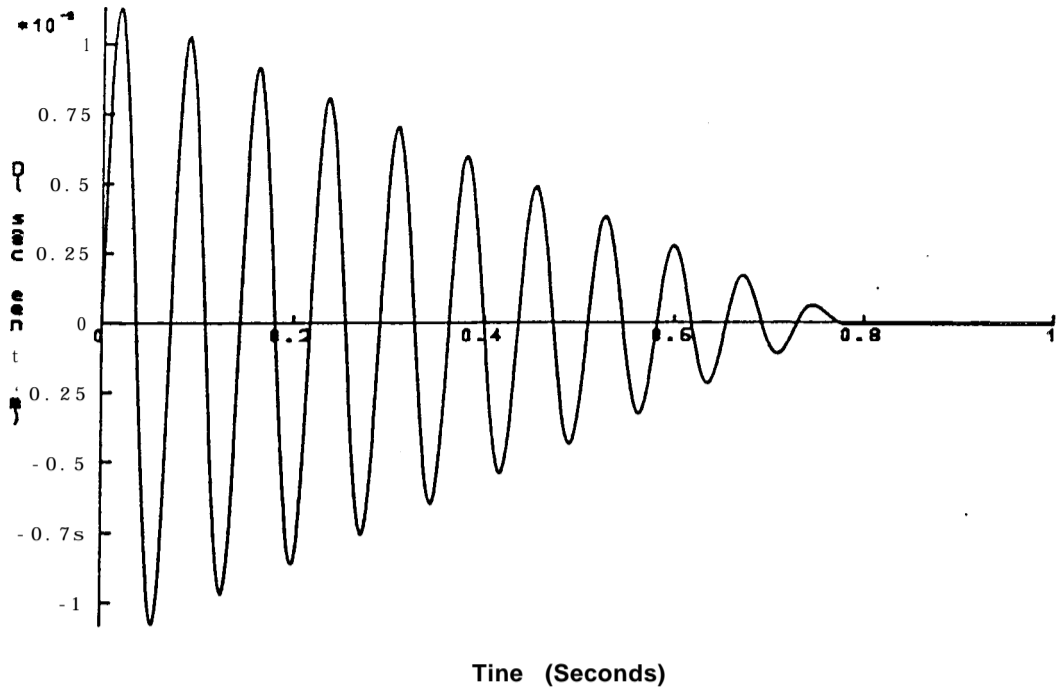


Fig 5.19a Displacement time-history from a system with friction damping only

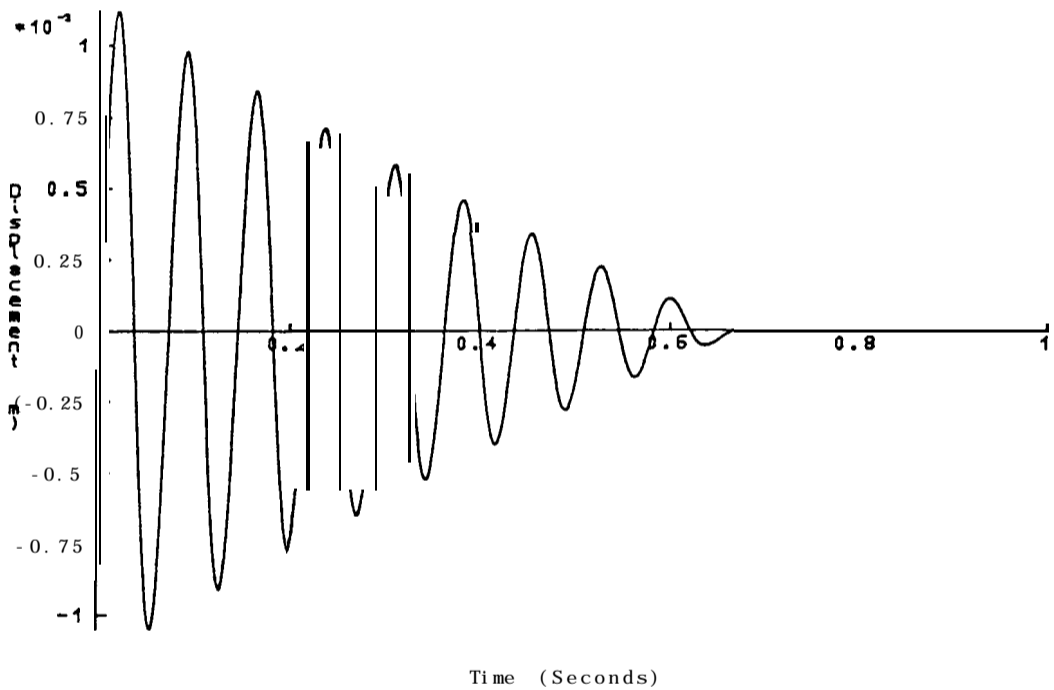


Fig 5.19b Displacement time-history from a system with friction and viscous damping

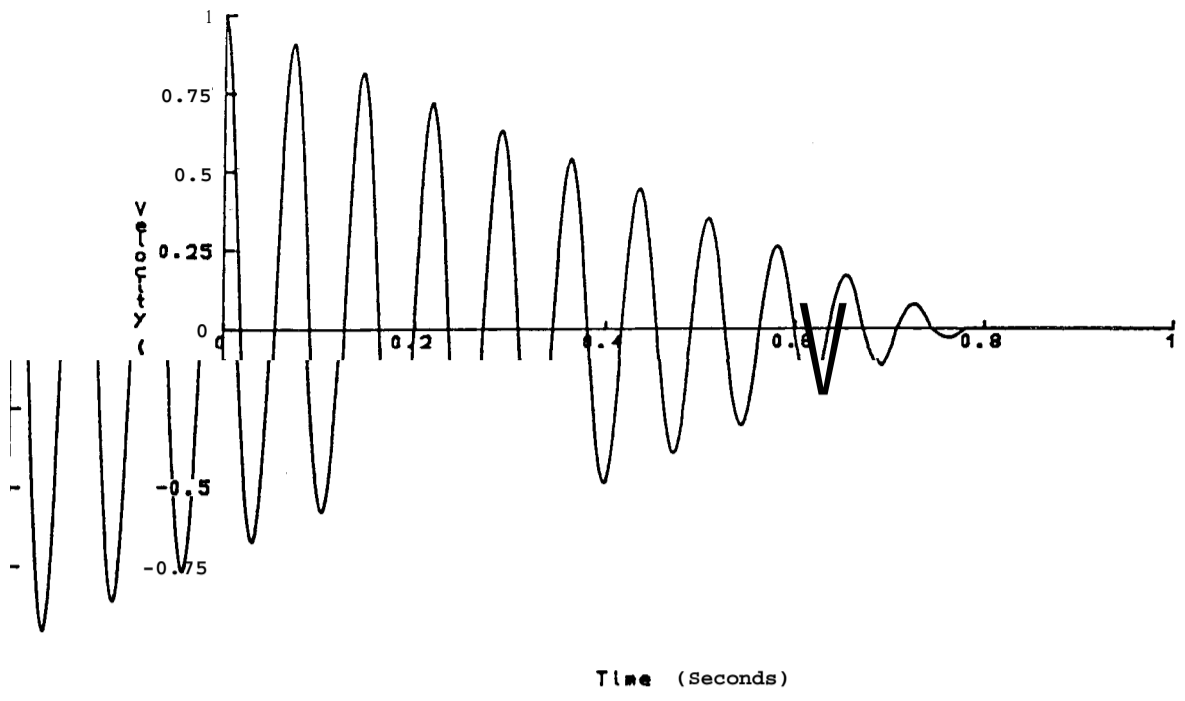


Fig 5.19c Velocity time-history from a system with friction damping only

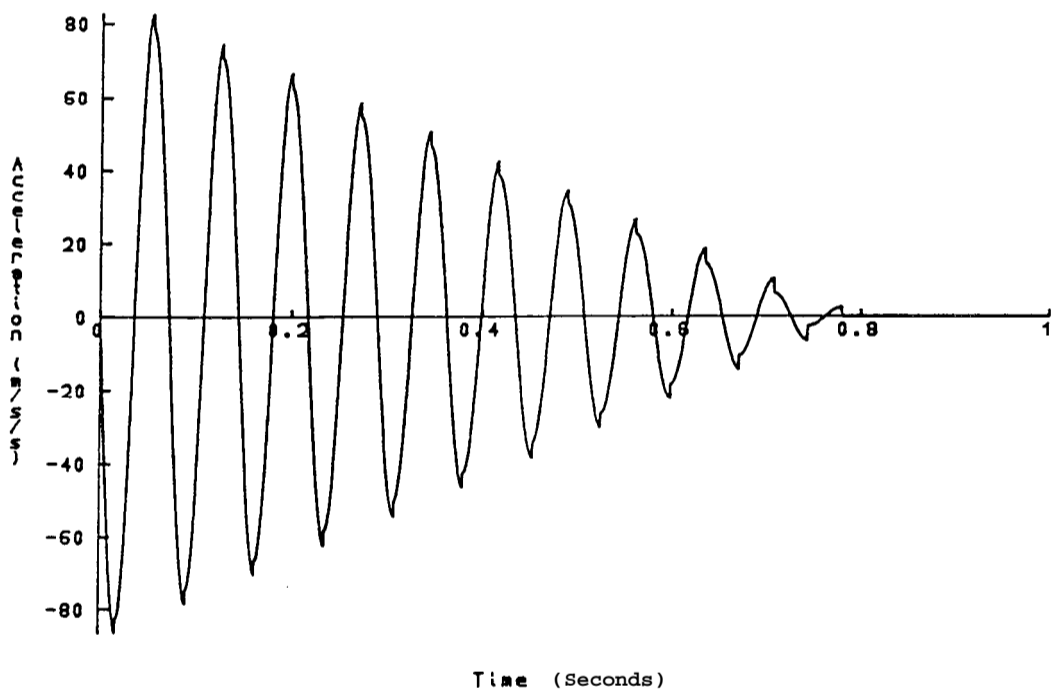


Fig 5.19d Acceleration time-history from a system with friction damping only

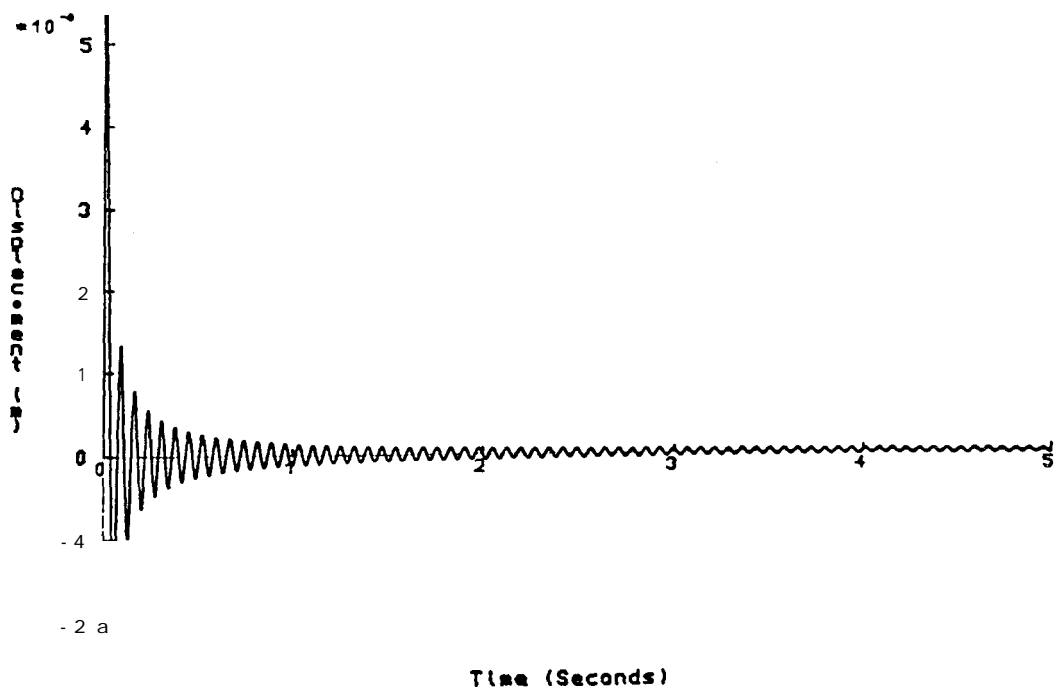


Fig 5.20a Displacement time-history from a system with quadratic viscous damping

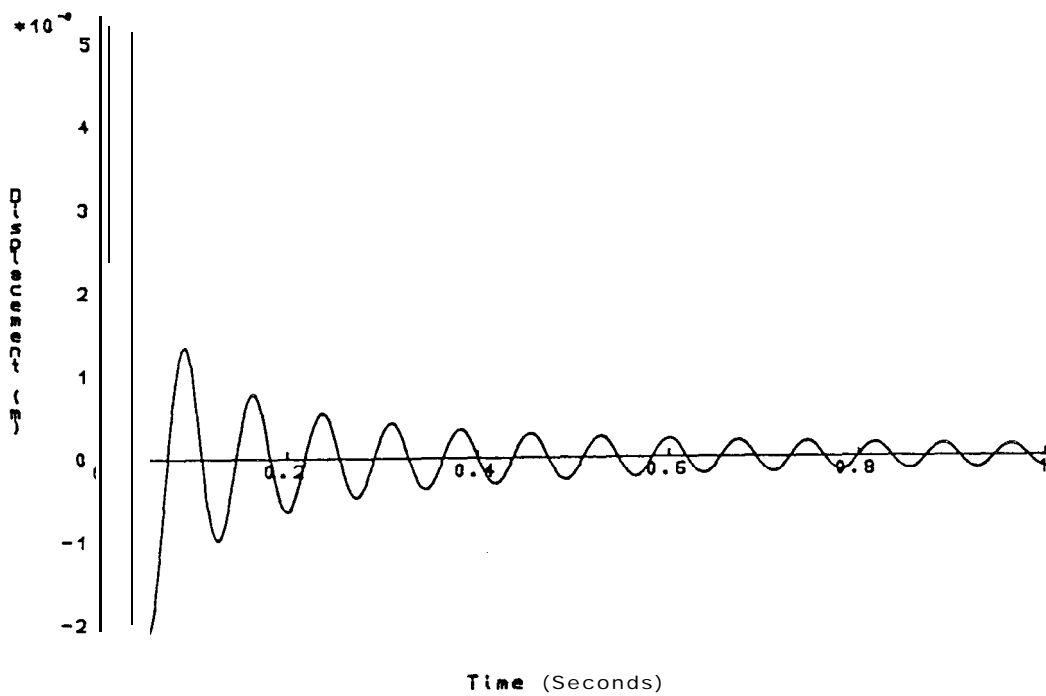


Fig 5.20b Expanded view of the displacement time-history of a system with quadratic viscous damping

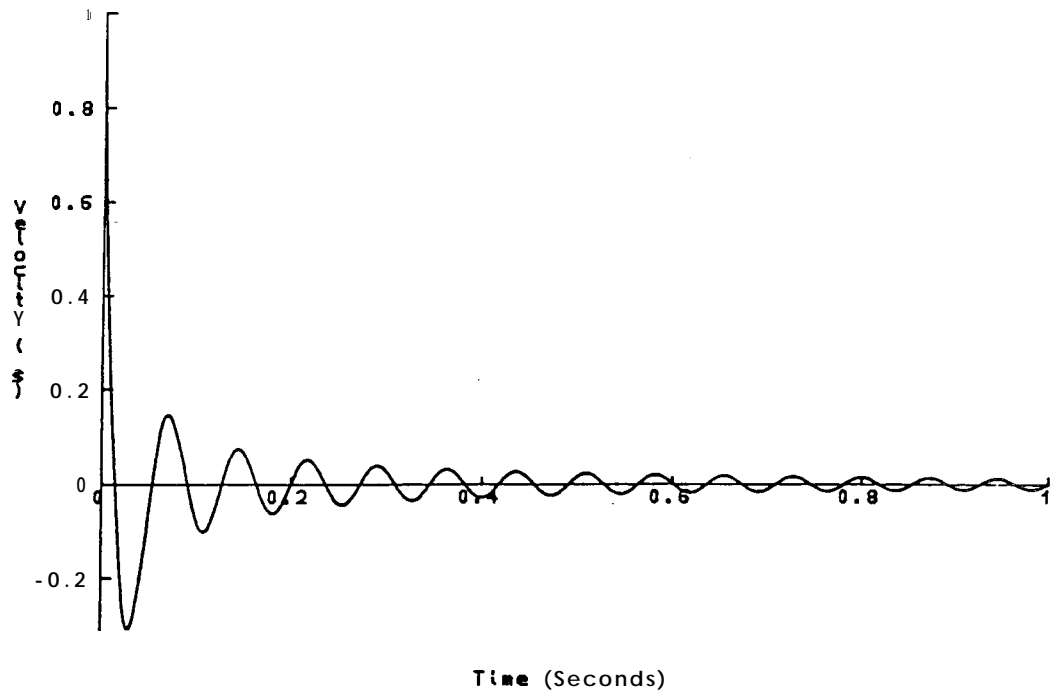


Fig 5.20c Expanded view of the velocity time-history of a system with quadratic viscous damping

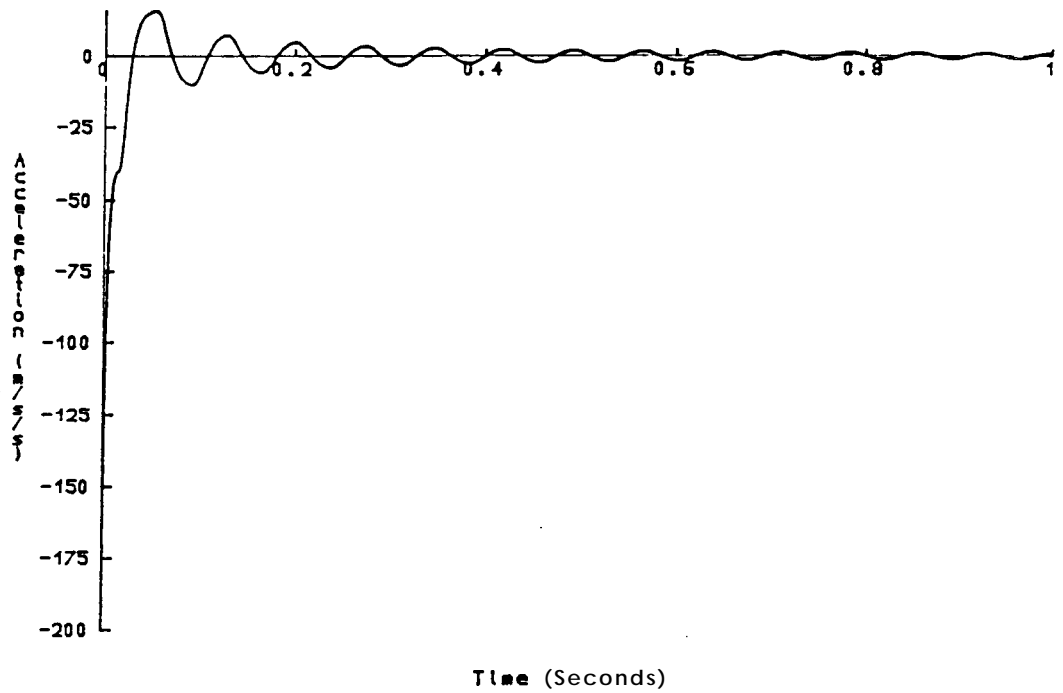


Fig 5.20d Expanded view of the acceleration time-history of a system with quadratic viscous damping

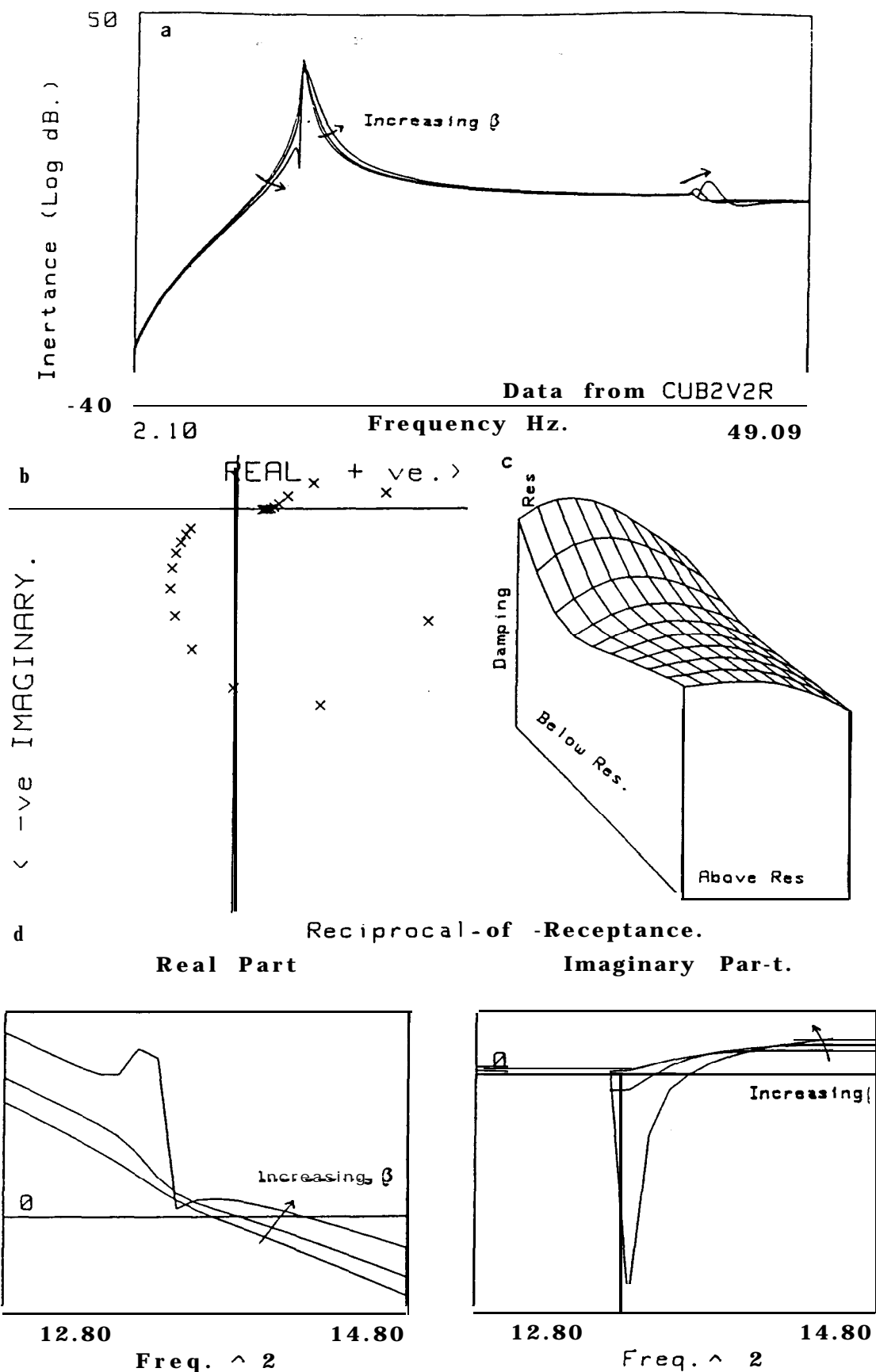


Fig 5.21 Trends in the frequency domain from systems with cubic stiffness subjected to impulse excitation
 a Bode plots
 b Nyquist plot
 c 3-D damping plot
 d Reciprocal-of-receptance plots

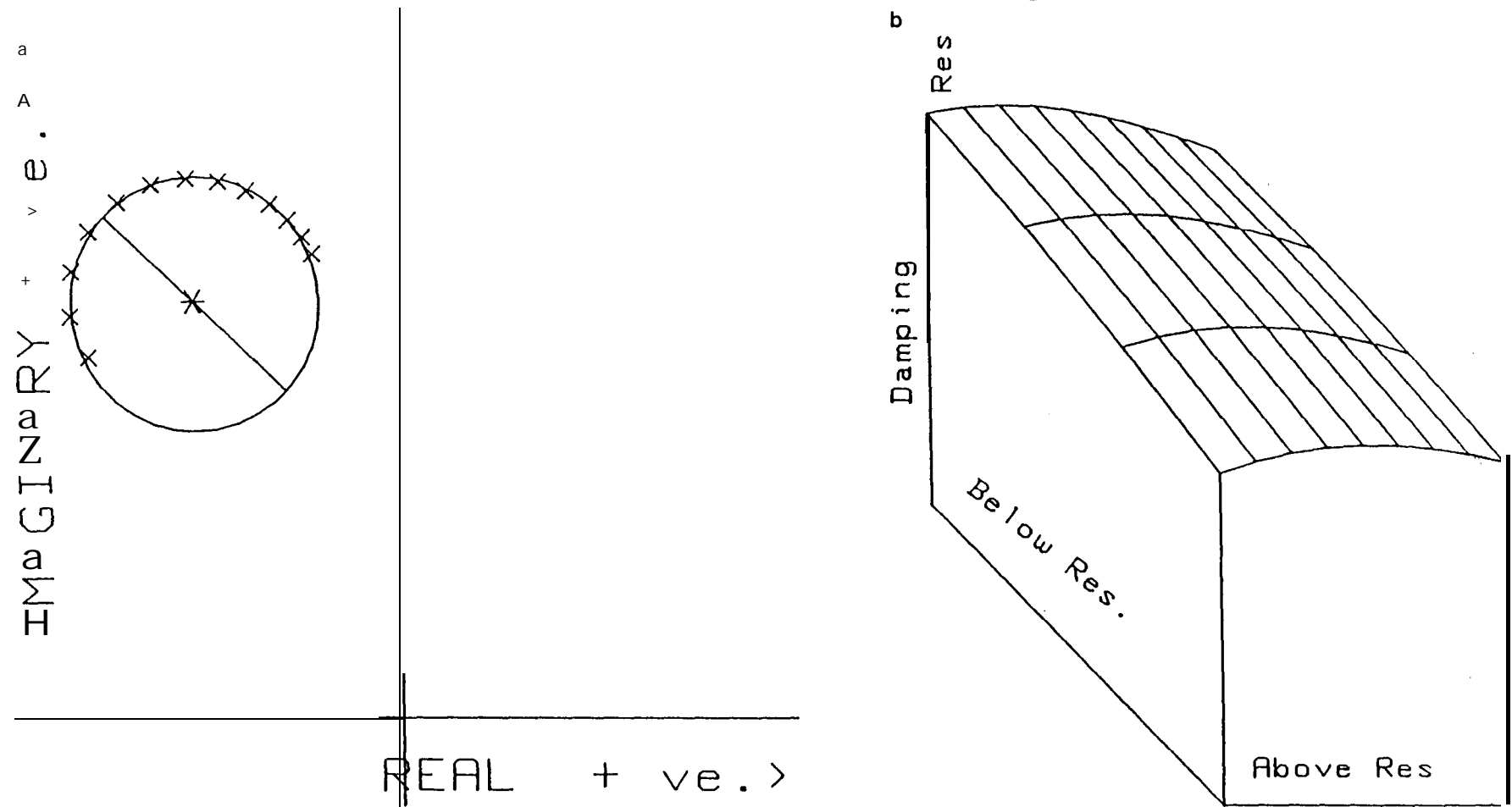


Fig 5.22 Trends in the frequency domain from the first harmonic resonance of fig(5.21a)
 a Nyquist plot
 b 3-D damping plot

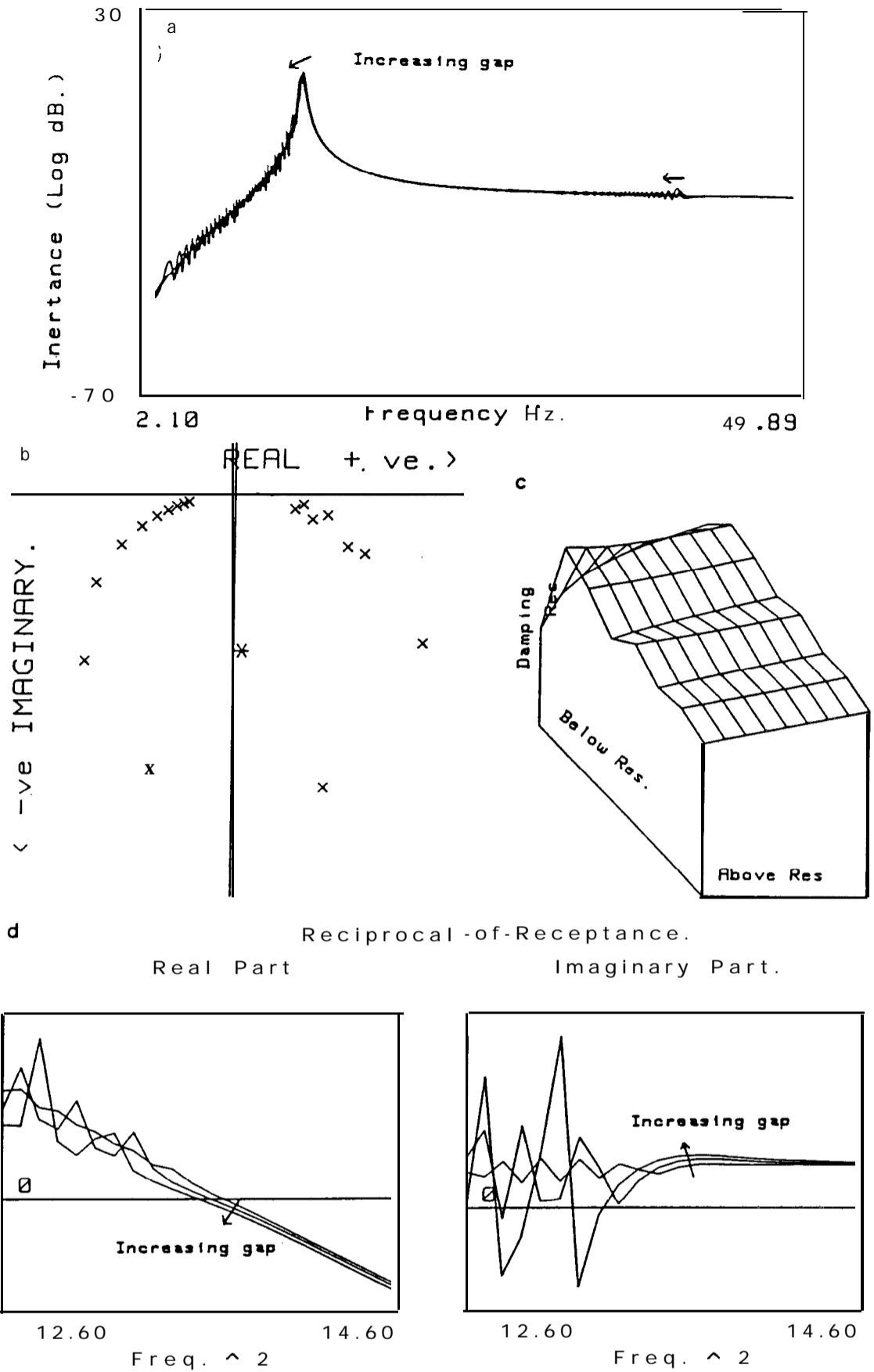


Fig 5.23 Trends in the frequency domain from systems with backlash subjected to impulse excitation

- a Bode plots
- b Nyquist plot
- c 3-D damping plot
- d Reciprocal-of-receptance plots

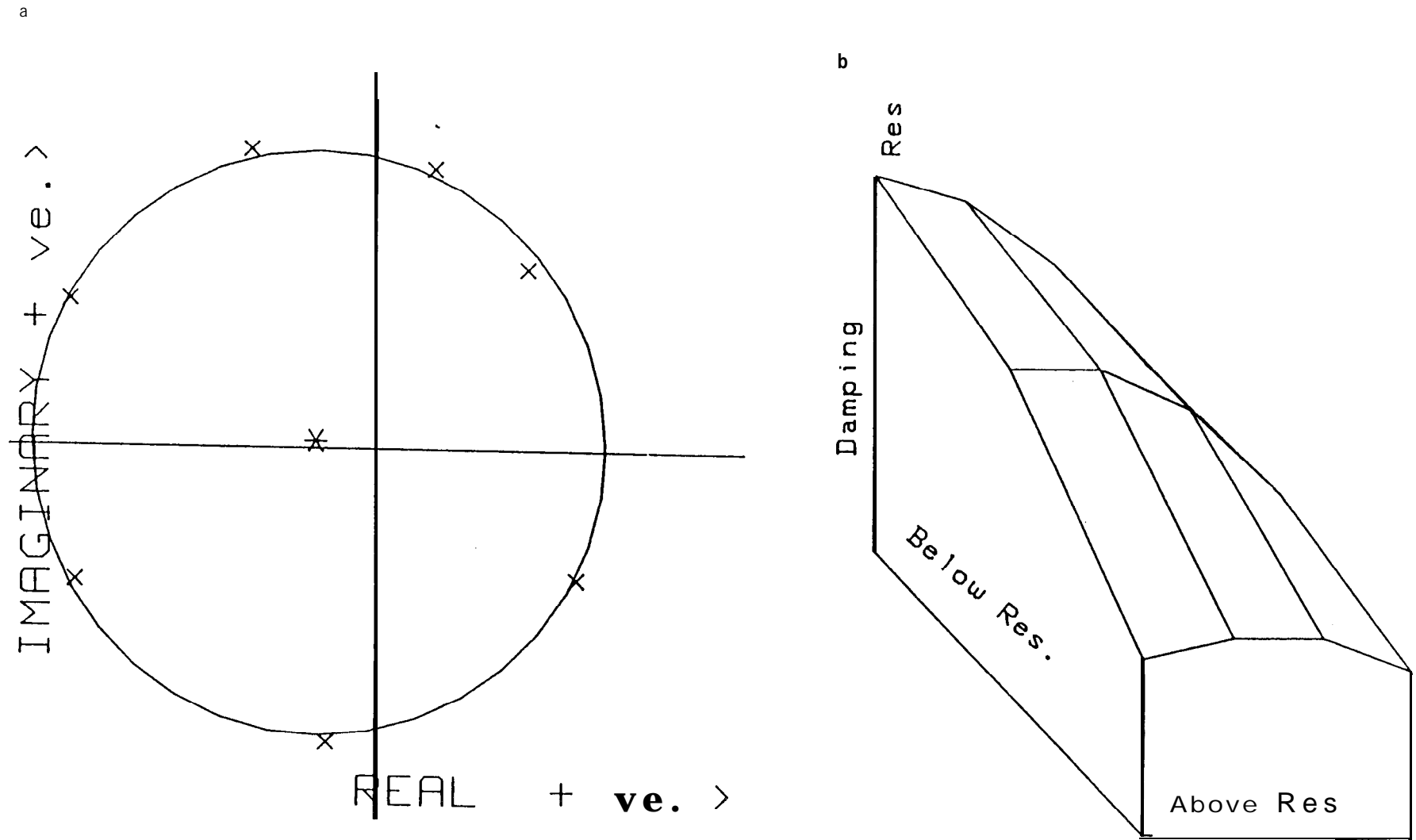


Fig 5.24 Trondr in the frequency domain from the harmonic resonance of fig (5.23a)
 a Nyquist plot
 b 3-D damping plot

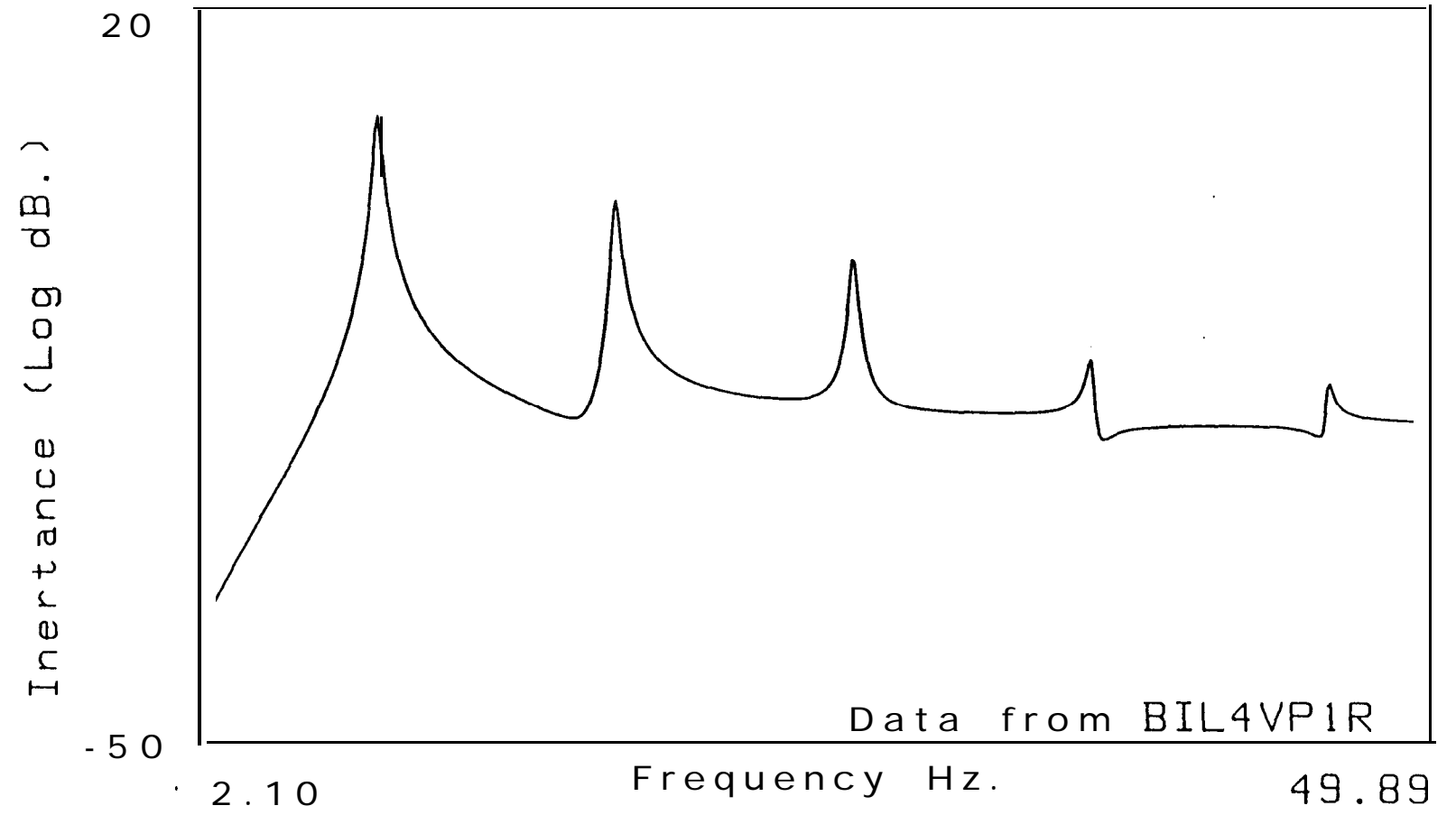
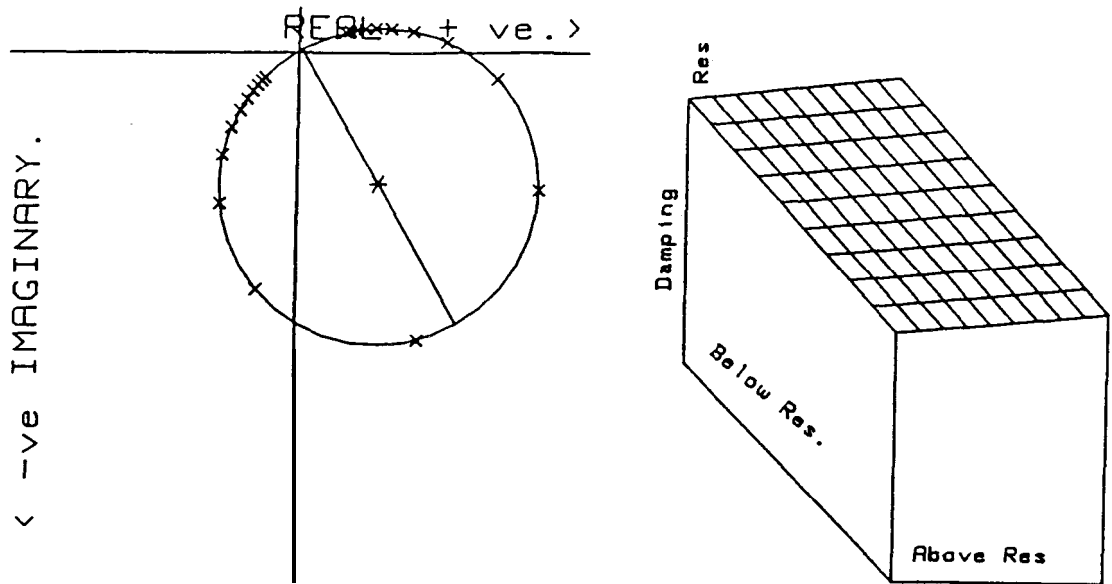


fig 5.25 Bode plot from a system with bi-linear stiffness (ratio 4:1) subjected to an impulse



Reciprocal-of-Receptance.

Real Part

Imaginary Part.

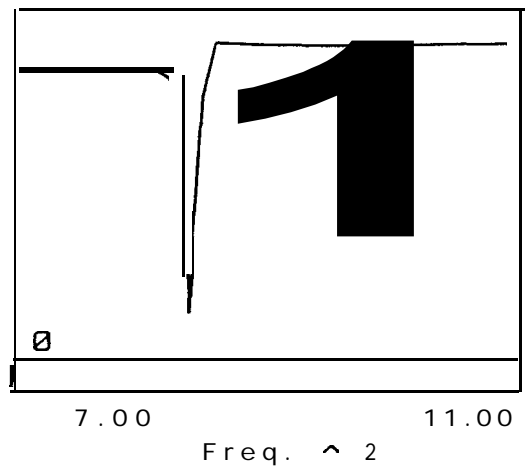
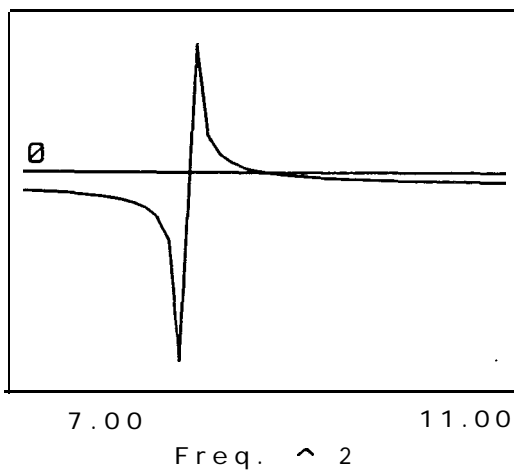
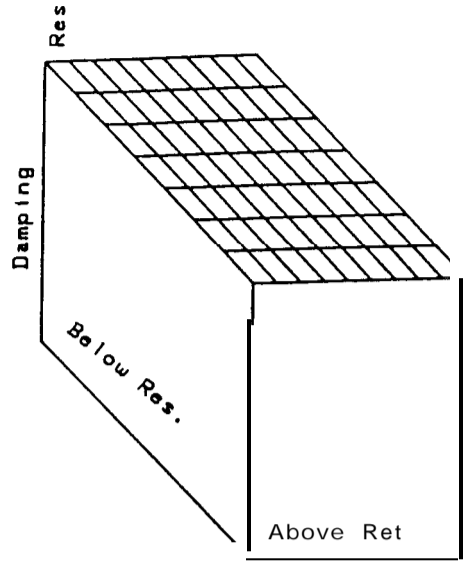
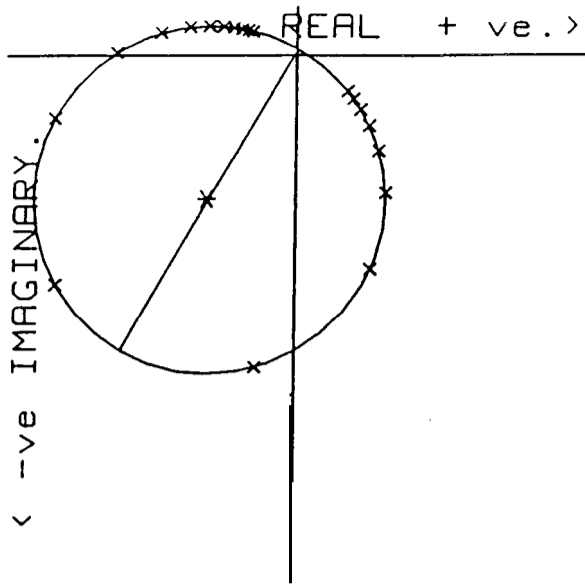


Fig 5.26a Nyquist, 3-D damping and reciprocal-of-receptance plots of the fundamental resonance in fig (5.25)



Reciprocal-of-Receptance.

Real Part

Imaginary Part.

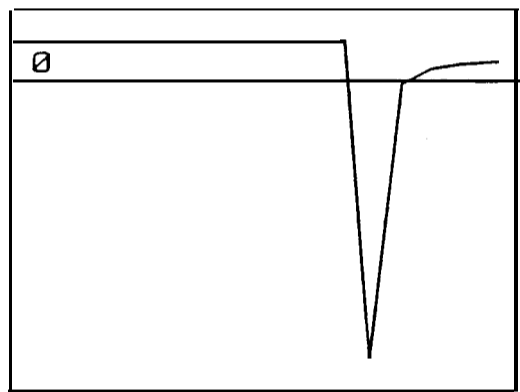
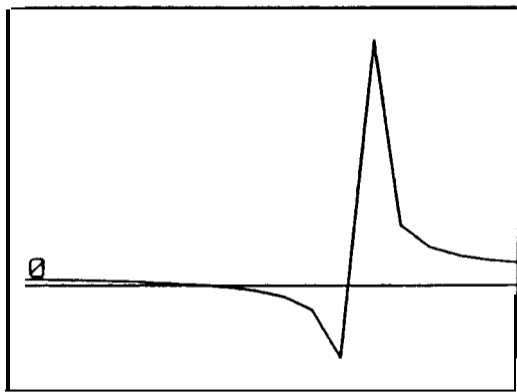
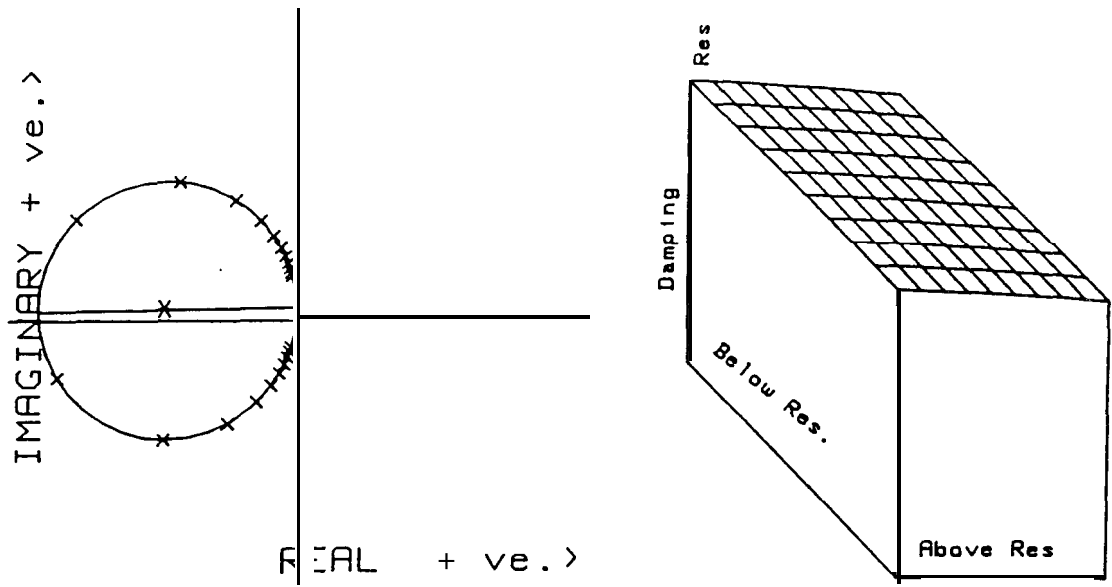


Fig 5.26b Nyquist, 3-D **damping** and reciprocal-of-receptance plots of the first harmonic resonance in fig (5.25)



Reciprocal-of-Receptance.

Real Part

Imaginary Part.

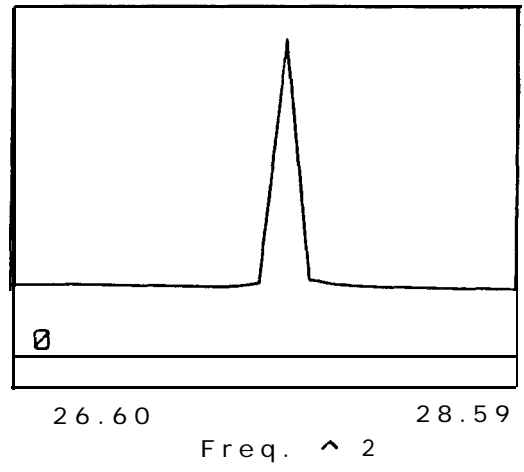
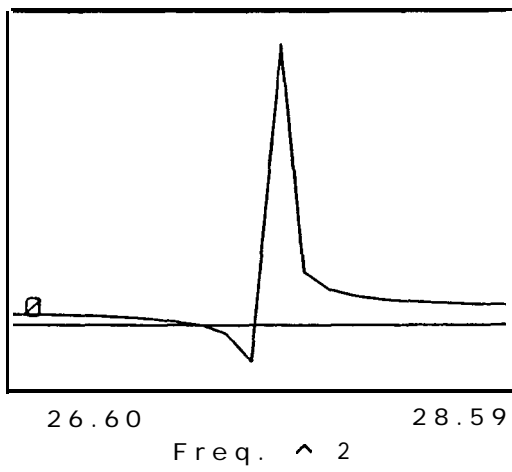
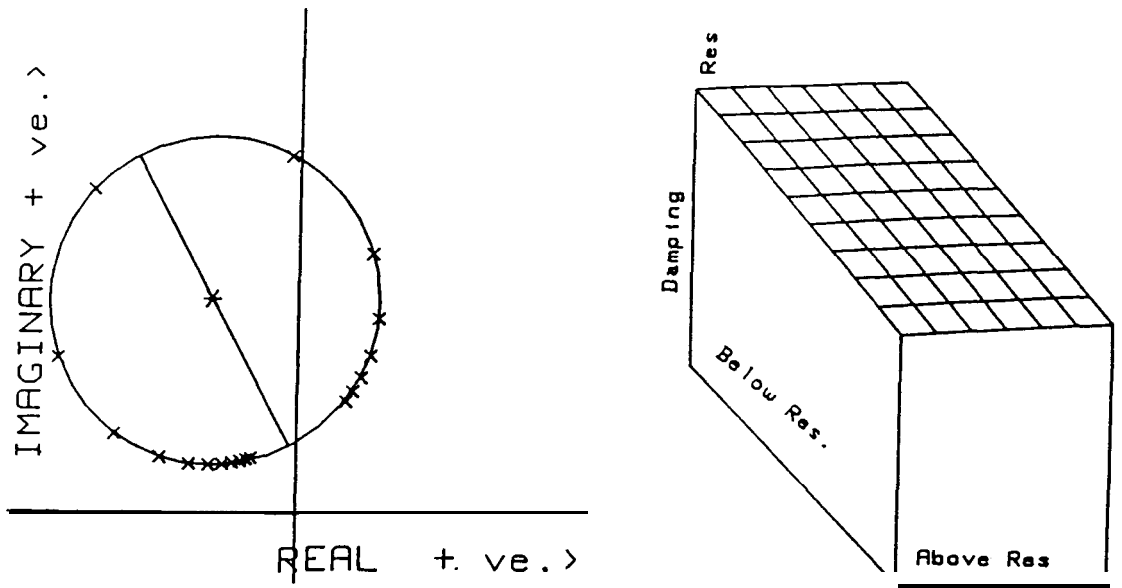


Fig 5.26c Nyquist, 3-D damping and reciprocal -of -receptance plots of the second harmonic resonance in fig (5.25)



Reciprocal-of-Receptance.

Real Part

Imaginary Part.

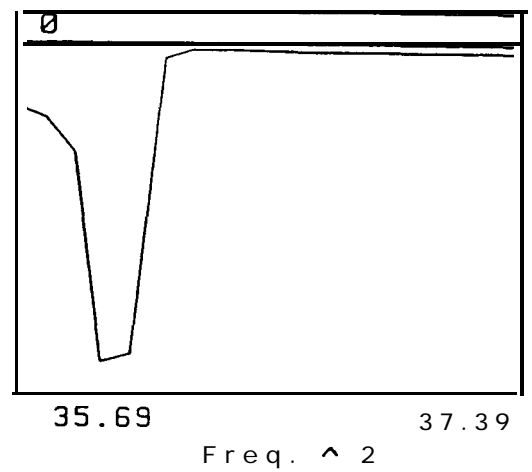
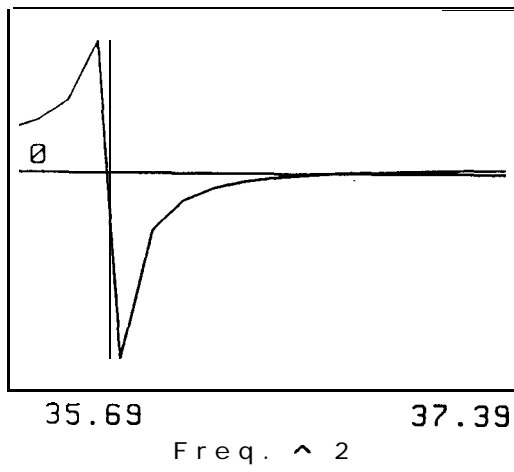
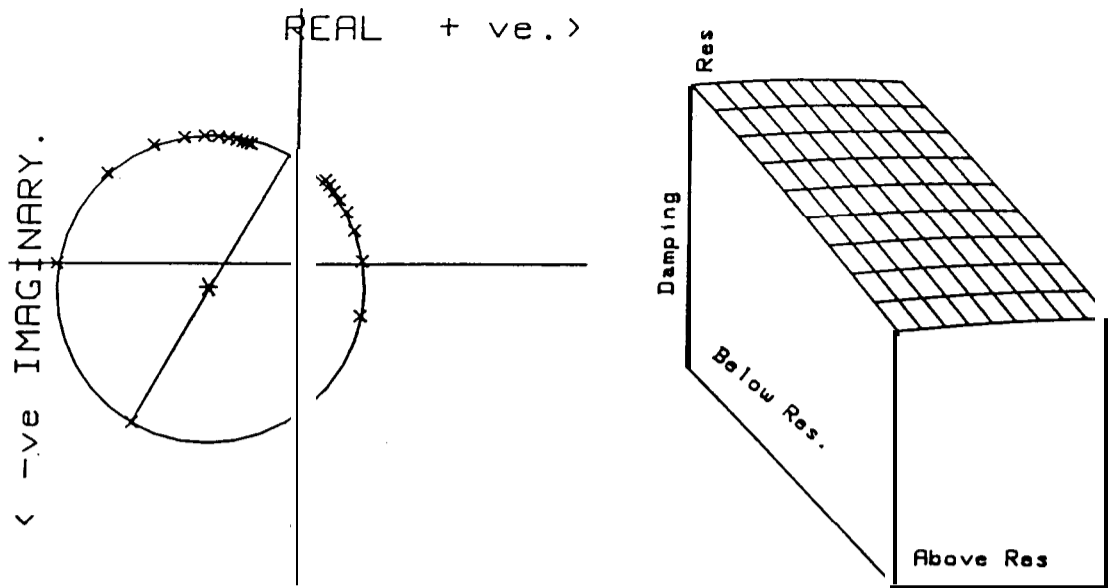


Fig 5.26d Nyquist, 3-D damping and reciprocal-of-receptance plots of the third harmonic resonance in fig(5.25)



Reciprocal-of -Receptance.

Real Part

Imaginary Part.

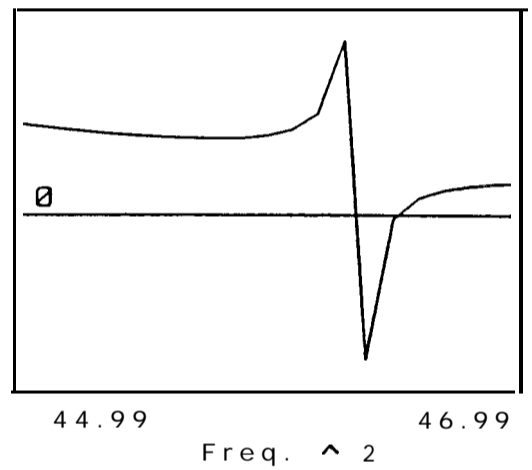
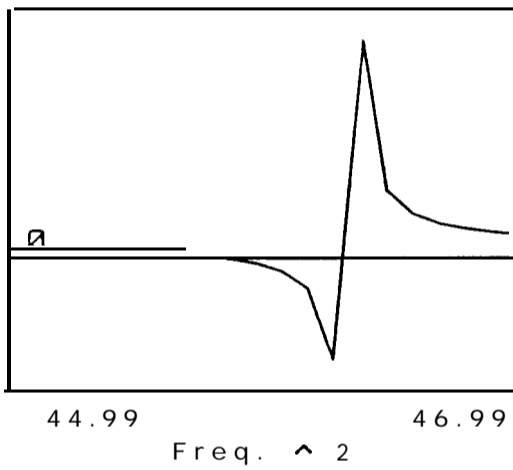


Fig 5.26e Nyquist, 3-D damping and reciprocal-of-recsptance plots of the fourth harmonic resonance in fig (5.259

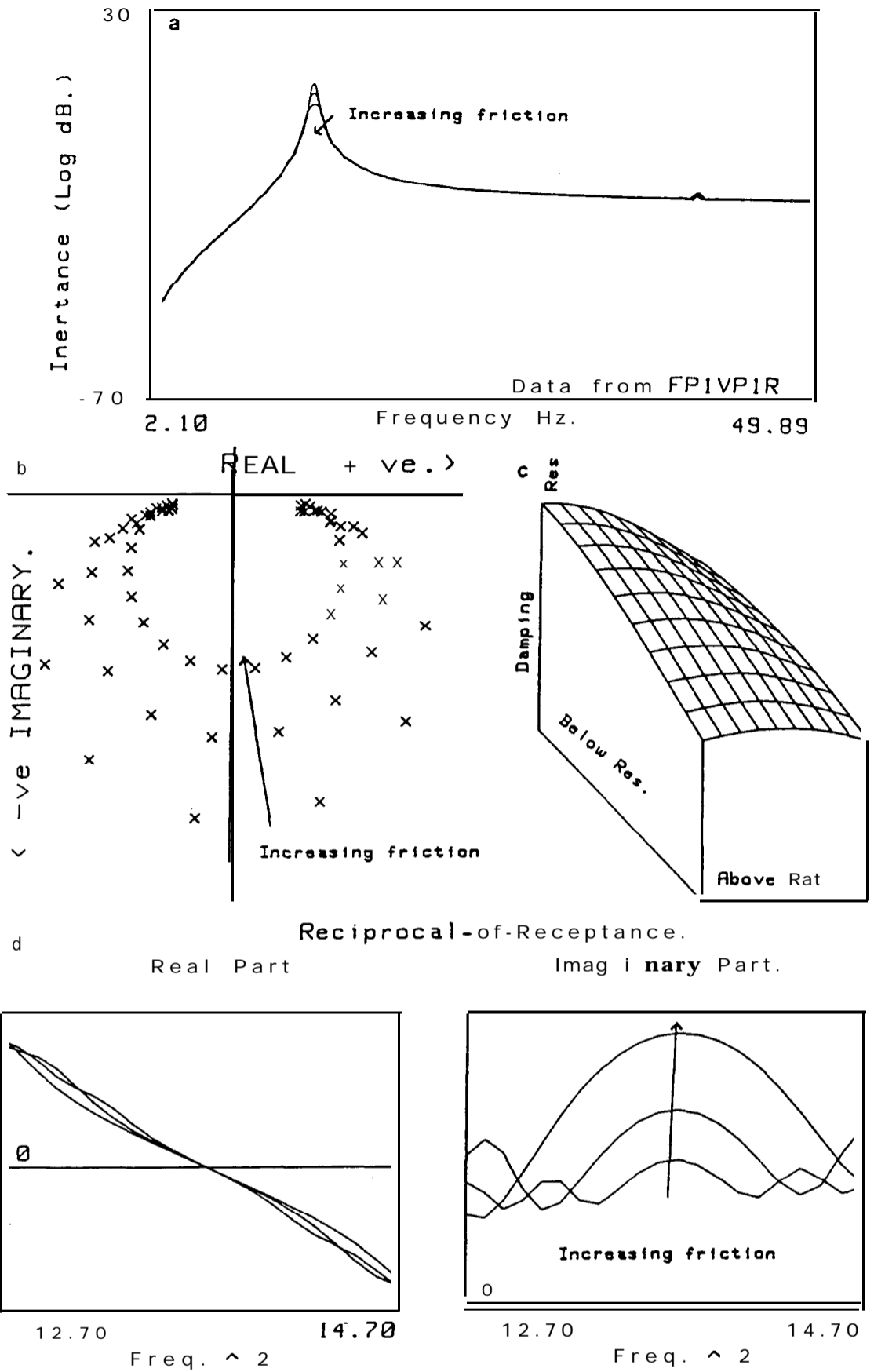


Fig 5.27 Trends in the frequency domain from systems with friction subjected to impulse excitation

- a Bode plots
- b Nyquist plots
- c 3-D damping plot

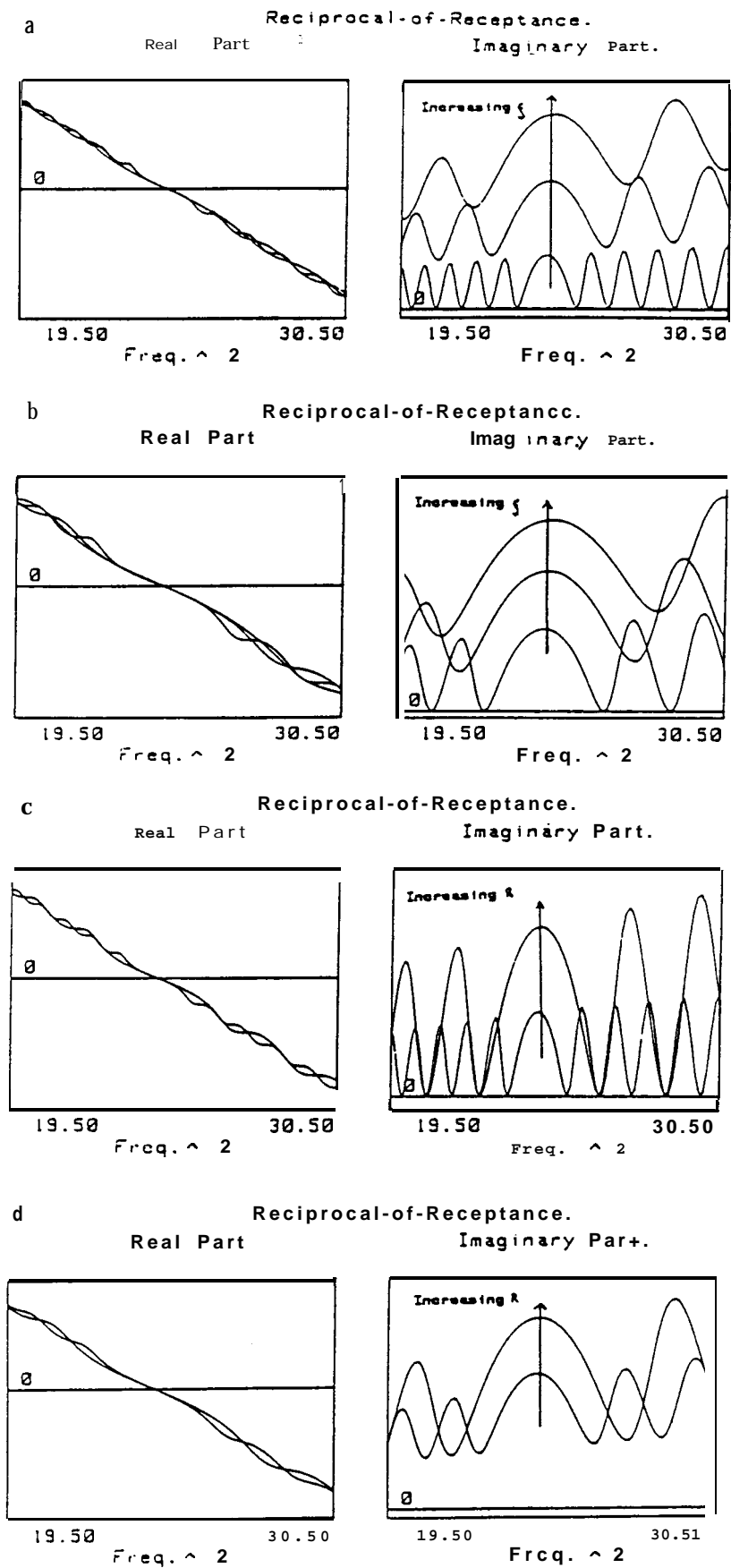


Fig 5.28 Trends in reciprocal-of-receptance plots from systems with friction subjected to impulse excitation
 a Friction $R=0.1571$; $(-0.0 \zeta=0.015 \zeta=0.02938$
 b Friction $R=0.3142$; $\zeta=0.0 \zeta=0.015 \zeta=0.02938$
 c Viscous damping $c=0.0$; $R=0.1571$ $R=0.3142$
 d Viscous damping $c=0.02338$; $R=0.1571$ $R=0.3142$

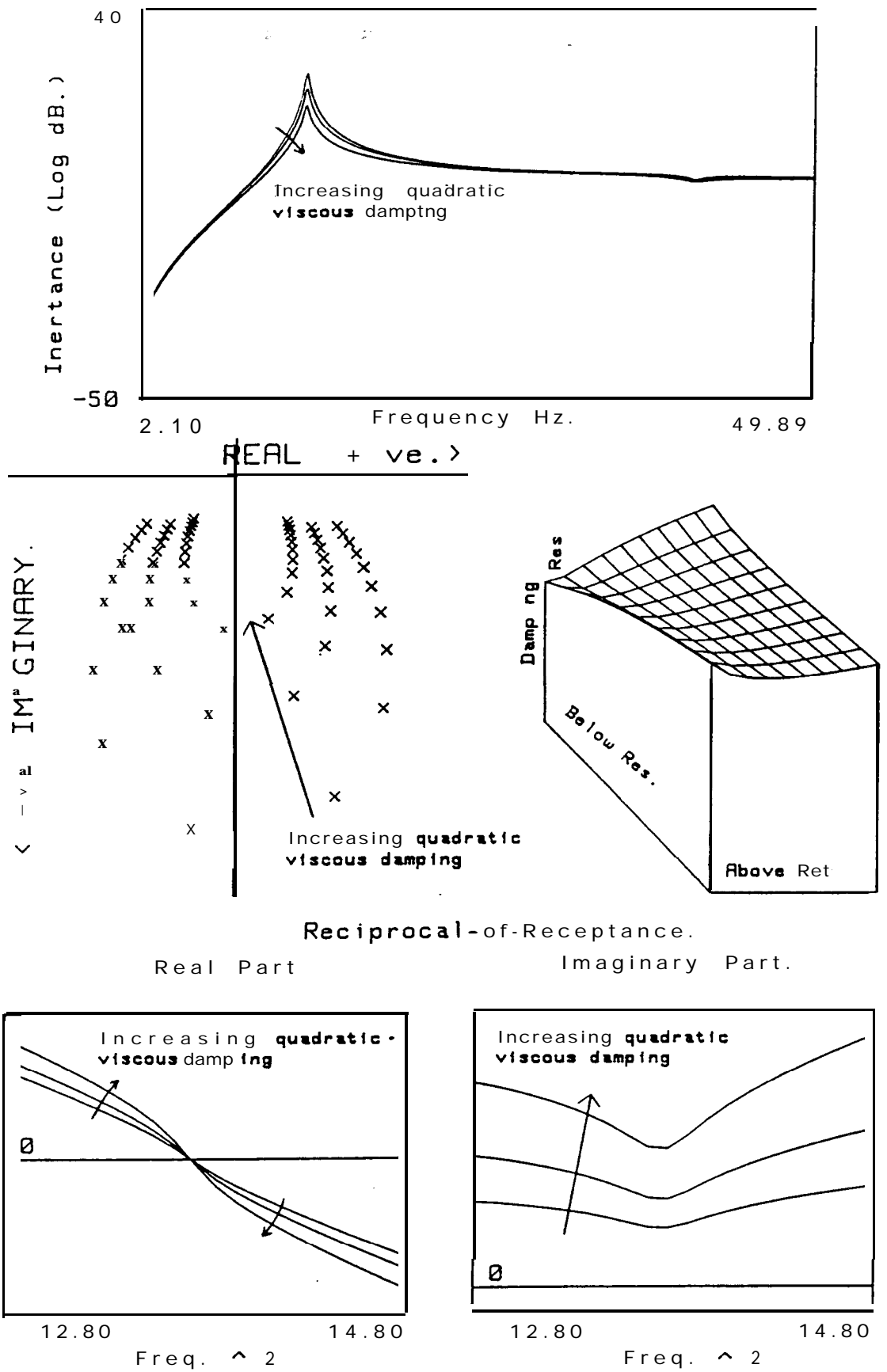


Fig 5.29 Trends in the frequency domain from systems with quadratic viscous damping subjected to impulse excitation

- a Bode plots
- b Nyquist plots
- c 3-D damping plot
- d Reciprocal-of-receptance plots

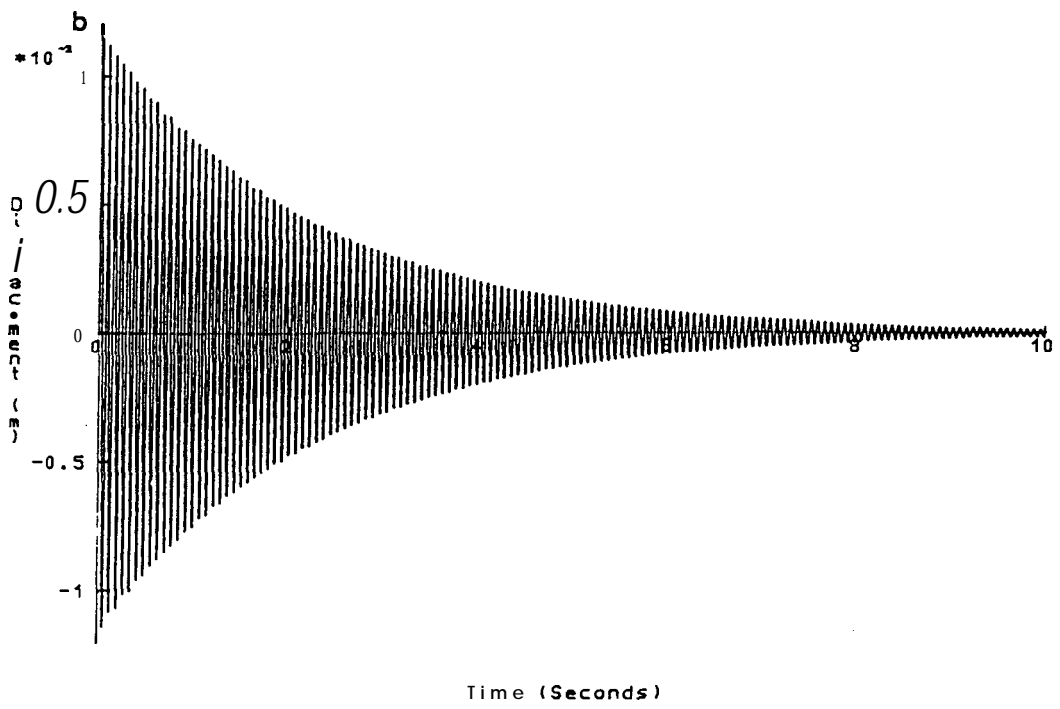
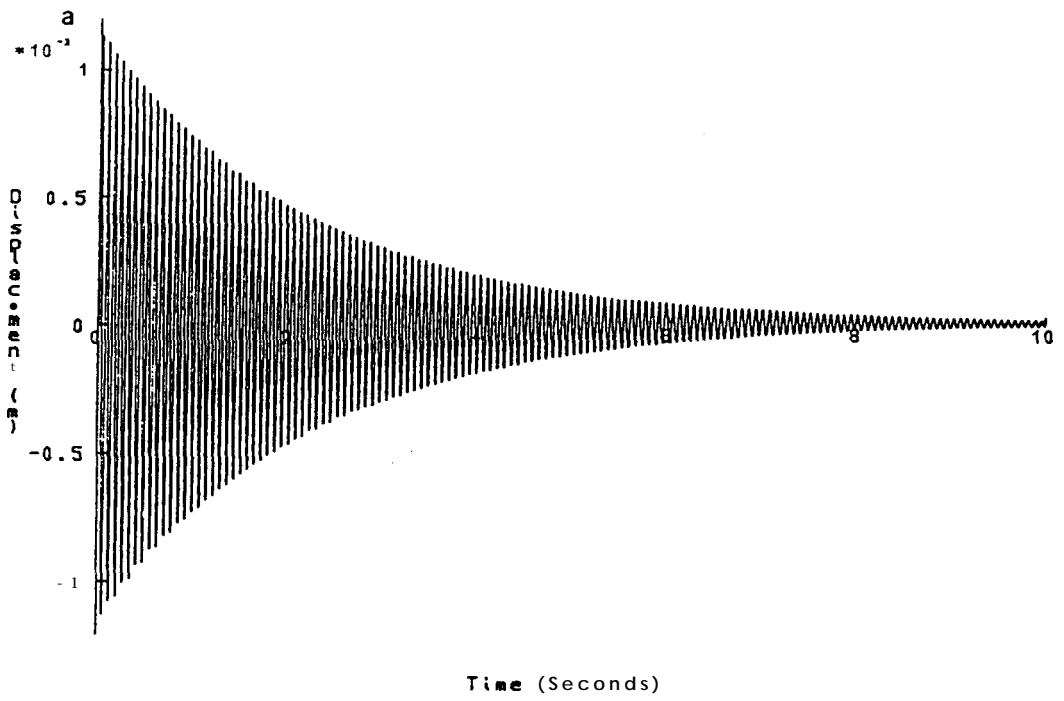


Fig 5.30 Comparison of **time-histories** from a linear system using data from:-
 a Impulse test
 b Transformed sine test

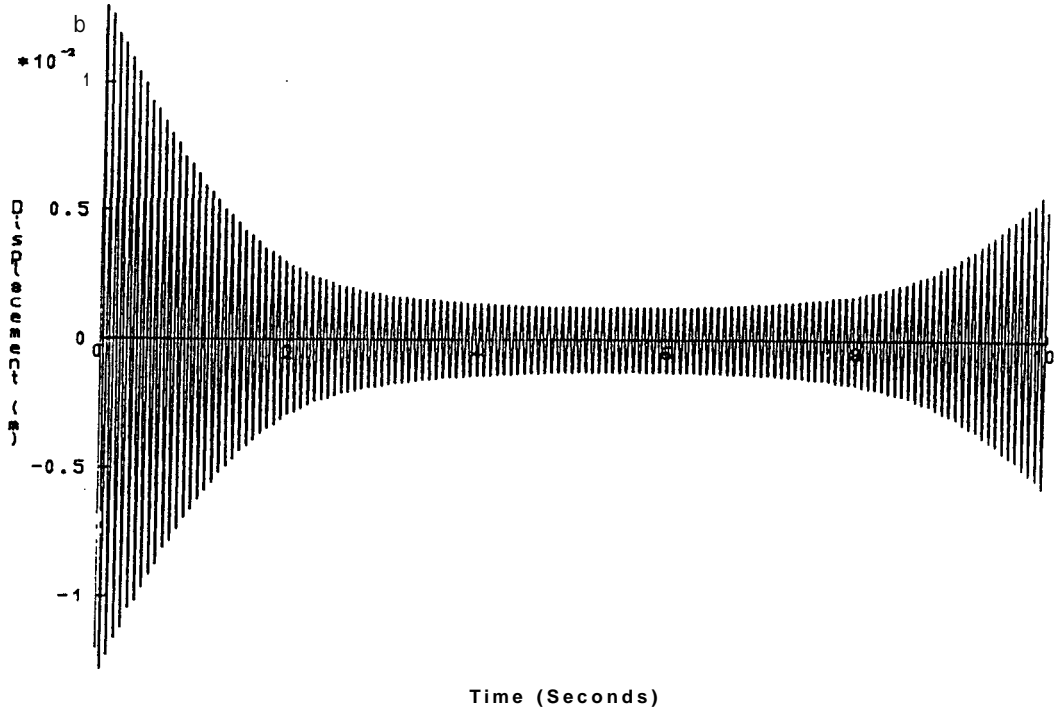
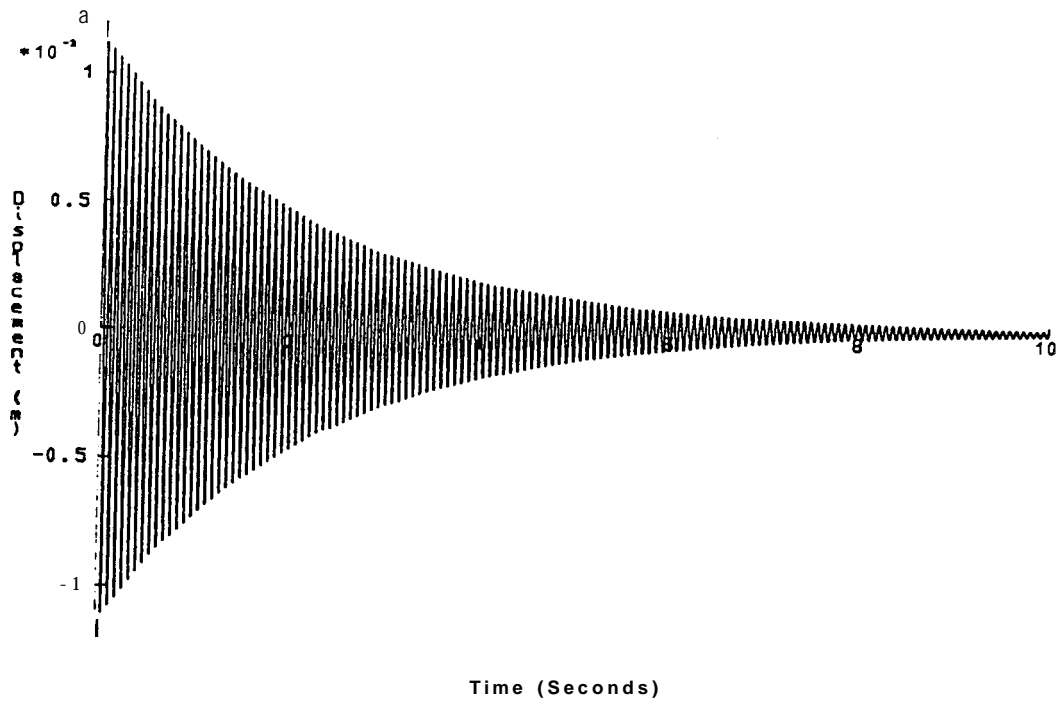


Fig 5.31 Comparison of time-histories from a system with cubic stiffness using data from:-
 a Impulse test
 b Transformed sine test

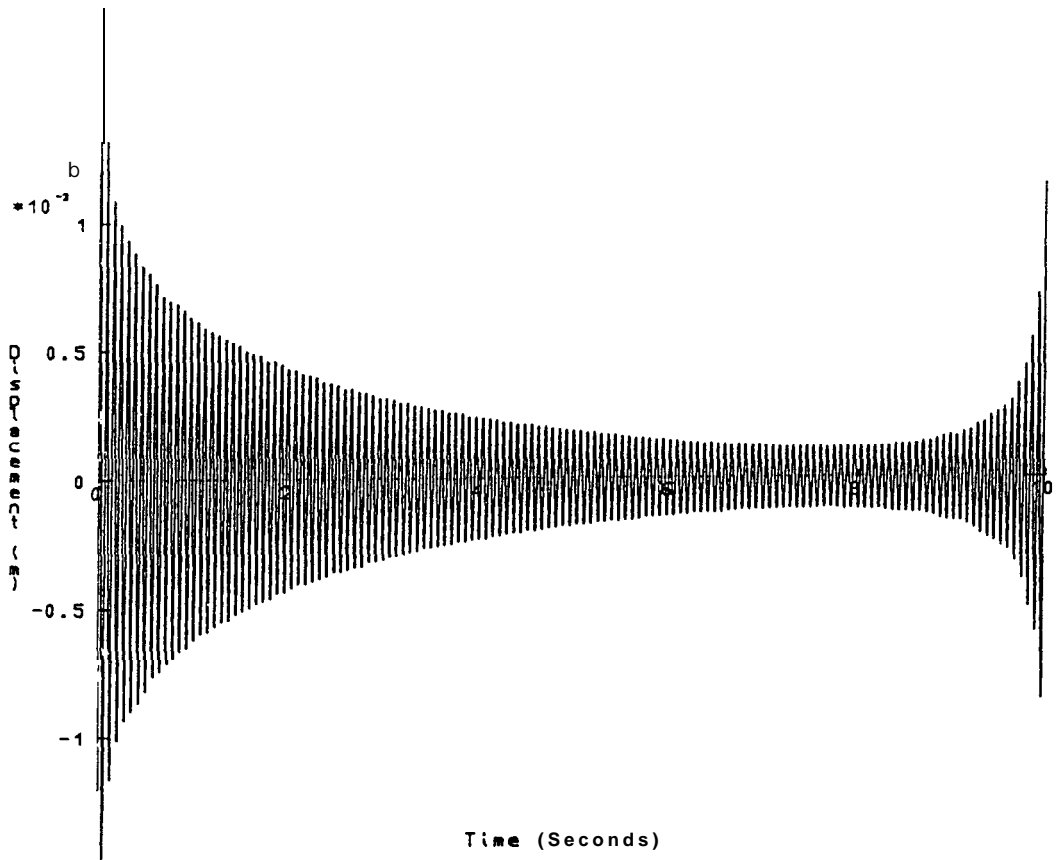
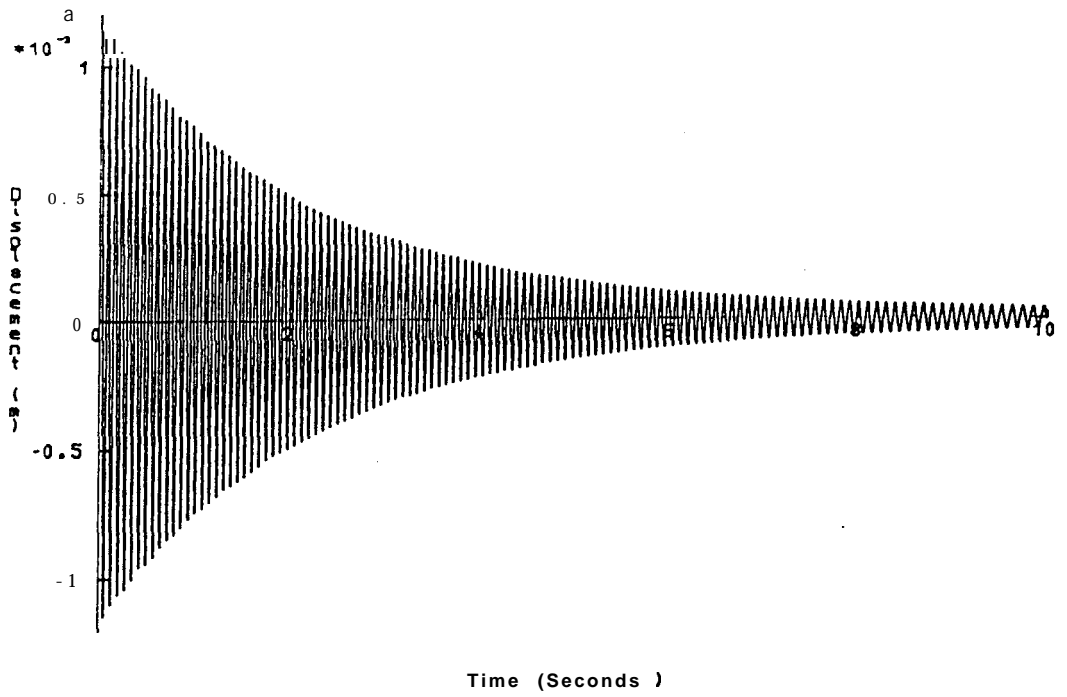


Fig 5.32 Comparison of time-histories from a system with backlash using data from:-
 a Impulse test
 b Transformed sine test

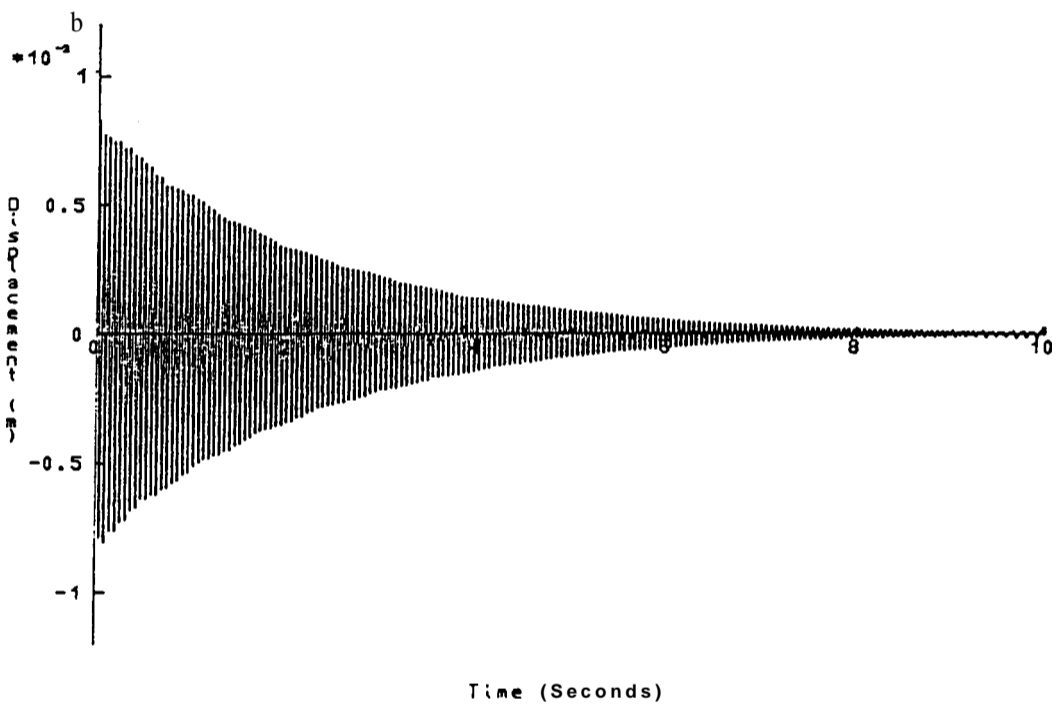
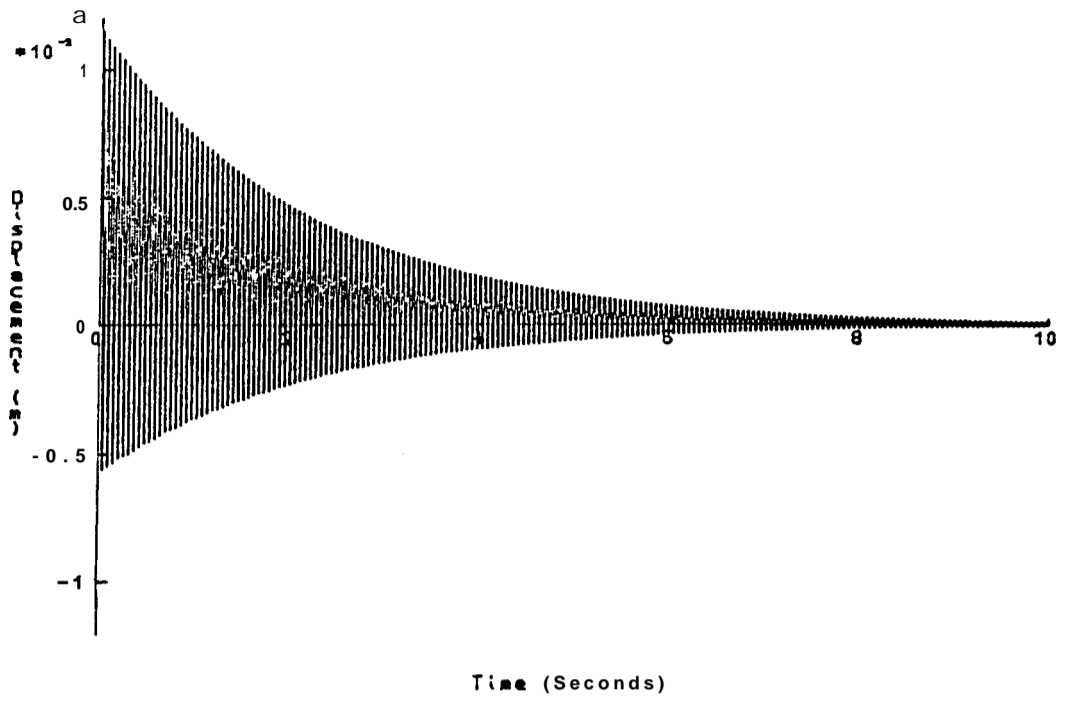


Fig 5.33 Comparison of **time-histories** from a system with **bi-linear** stiffness using data from:-
a Impulse test
b Transformed sine test

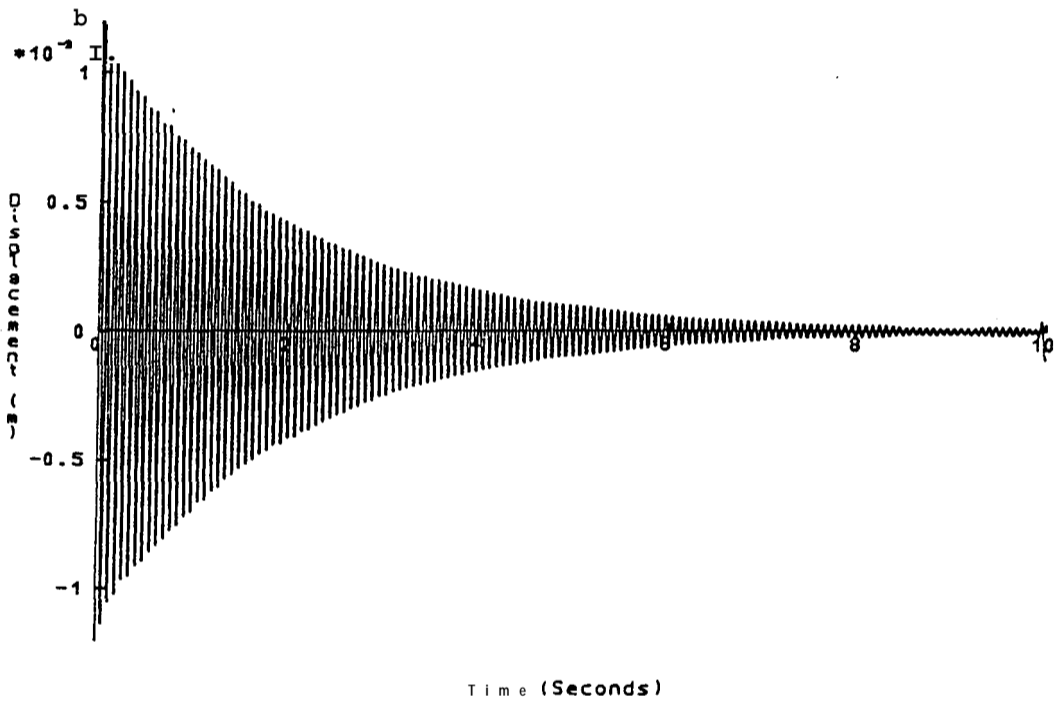
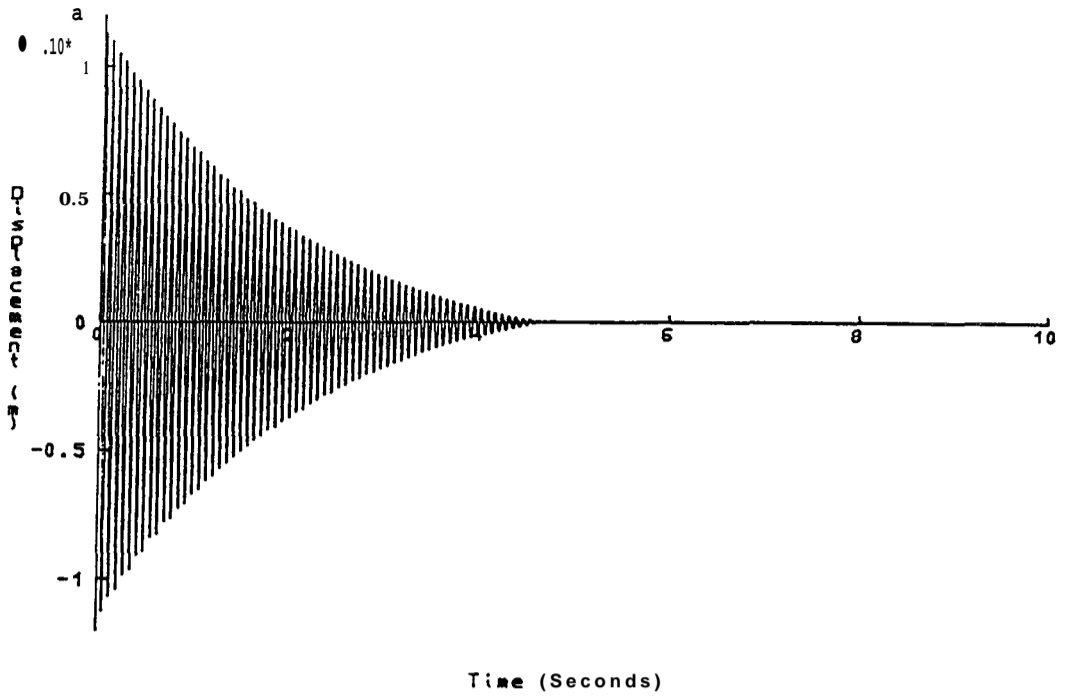


Fig 5.34 Comparison of time-hysteresis from a system with friction using data from:-
 a Impulse test
 b Transformed sine test

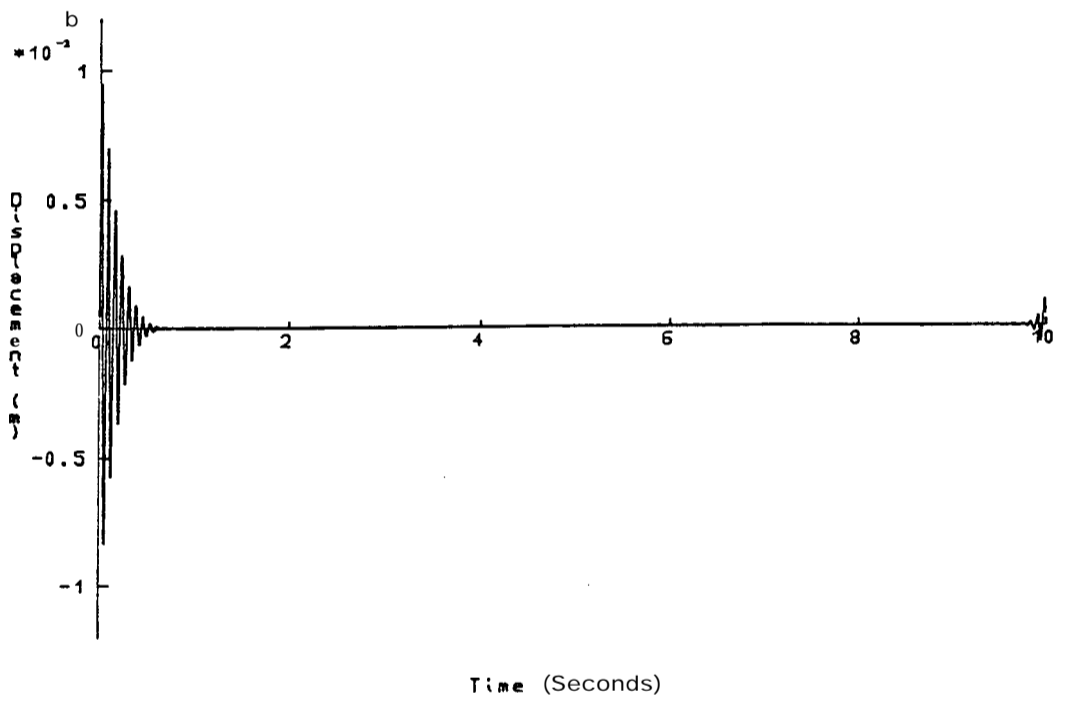
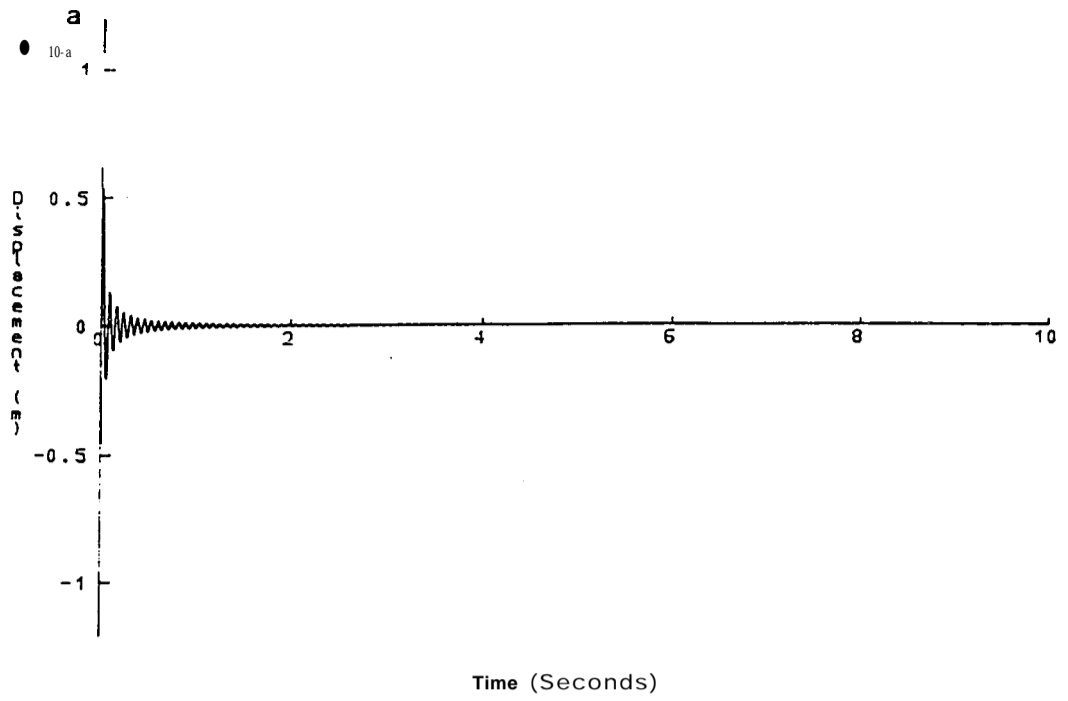


Fig 5.35 Comparison of time-histories from a system with quadratic viscous damping using data from:-
 a Impulse test
 b Transformed sine test

6 TRANSIENT, RESPONSE PREDICTION OF NON-LINEAR ELEMENTS USING DATA FROM MODAL TESTS

6.0 Introduction

The previous chapter explored the application of modal testing procedures to non-linear structural elements. It was found that the results in both the time and frequency domains depend on the type of test performed and the excitation level of the test, and many of the graphical presentations exhibit characteristic trends with changes in the non-linear effect. The application of transient response prediction methods for non-linear elements, using experimental data that are obtained from modal tests and modal analysis, is now examined.

There are three main types of input where the transient response of a system (linear or non-linear) may be required as a time-history: the response between two different steady-state conditions; the response to an impulse-like excitation, and the response to a non-steady forcing function. Often, this latter type of excitation is found in working machinery and the level and form of excitation can be measured - the tests in these cases can also be performed in situ with the correct excitation. The transient response is short between steady-state conditions, unless the system is very lightly damped. In these short transients the effect of the non-linearity is likely to be small, so a linear model can be used if this response is required. The response to an impulse-like excitation is mainly free decay and it is this response - the impulse response - that is now examined in more detail with the intention of calculating a satisfactory approximation to the impulse response function (IRF).

There are several approaches to impulse response prediction, all of which will provide an answer. In the case of a linear system, all such answers must be the same, but in the non-linear situation the results from different methods can show marked differences. It is the aim of this chapter to examine the alternative solutions for various non-linear elements and to establish the feasibility and accuracy of the results in providing transient response prediction for non-linear elements. The different solution routes are shown on fig (6.1), and are summarised below.

6.1 Summary of routes for transient response prediction

The first route (A) shown in fig (6.1) is by direct solution of the equations of motion. This requires the system to be described analytically which, as explained previously, is not usually possible in practical cases. However, solutions for theoretical systems with well defined non-linear elements were calculated using this procedure with the computer program 'NONLIN' ref [136] and the results are used as the basis for comparison of the accuracy of the other prediction methods.

The initial step in experimental modal analysis is to measure the frequency response function (FRF) properties. Depending on the choice of excitation method and the level of excitation, this can result in one of several alternative FRFs for each non-linear system. These data can be transformed to the time domain to provide corresponding transient response predictions. As was seen in figs (5.31) to (5.35), when comparing these results with the impulse response functions (IRFs) this technique does not always generate time-histories that resemble the exact solution, and also often have a non-causal component.

The alternative FRFs can all be analysed using available modal analysis routines and, combined with criteria used for selecting the data points for analysis, several sets of modal parameters can be calculated from the same experimental data. These sets of modal parameters from all the FRFs of the same non-linearity can be used in the (linear) formulae to regenerate FRFs which can then be inverse Fourier transformed to provide corresponding estimates for the transient response prediction of the non-linear element. For some non-linearities in limited applications, one of these solutions may provide an acceptable approximation to the IRF.

Alternatively, models could be developed to account for the non-linearities in a system. These 'non-linear models' may be described in either the frequency or the time domain, but whether the predicted transient response is transformed from a non-linear frequency domain model, or generated using a time-domain

model, the resulting prediction will be a closer approximation to the true time-history than a linear approximation. Non-linear models have to be developed individually for each non-linearity and the information required from modal analysis may include the underlying linear system parameters and the non-linear parameters of the system. For some non-linearities, these parameters are relatively straightforward to evaluate, but others need examining in more detail to determine how to separate the linear parameters from the non-linearities, and how to calculate the non-linear parameters. The non-linear model will usually be dependent on the initial conditions of the free decay, so these will also need to^{be} calculated for the impulse or at the start of the free decay of a system.

6.2 Transient response prediction for a cubic stiffness element

With cubic stiffness, the presence of non-linearity is evident from all displays from either constant-force sine test or impulse tests. It is least obvious from the exact IRF where the only indications are found in cases with high effective non-linearity when phase shifts may be observed in the initial part of the response. From examination of the exact IRF of an element with cubic stiffness (either theoretically generated or from an analogue computer) it is clear that the response of a cubic stiffness element in free decay resembles the response of the underlying linear system closer than the large distortions in the FRFs obtained from the constant-force sine tests would imply.

For this type of non-linearity it is found that using the underlying linear parameters will provide an adequate impulse response prediction and, once these parameters have been obtained, the implication is that a linear model can be used in any future analysis where the primary interest is in the transient response. Clearly, this model would not provide good FRF predictions if the requirement was the steady state response of the structure as the large resonance frequency changes due to the increasing response amplitudes at resonance would not be exhibited.

Linear models can be obtained from analysis of the data produced by any of the excitation methods, but the most reliable model is evaluated from a constant-force sine test. Here, included in the range of modal parameters that can be calculated from a single FRF, is a set that are very close to the underlying linear parameters. This set can be calculated using reciprocal-of-receptance analysis on data points above resonance (or below resonance for softening cubic stiffness). There is very little variation in this parameter set with excitation force level.

Random testing conveniently, in this case, produces a linear model from which a set of linear parameters can be estimated. The variation in response with different force levels is not as great as in sine testing techniques and the calculated modal parameters can be used as a first approximation to the linear

system. These parameters would probably be slightly different if the test was performed with a second random signal, but will generate adequate transient response predictions - provided the conditions on random testing for transient response prediction are satisfied; that is, there must be sufficient data points around resonance to determine the damping accurately.

Once cubic stiffness is identified in the system, the recommended procedure is to calculate the underlying linear parameters using reciprocal-of-receptance analysis on data from a sine test. The parameters thus produced can then be used in a linear model for transient response prediction using the 'Fourier transform method' (as discussed in chapter 4). This corresponds to route β in fig (6.1), with the reciprocal-of-receptance analysis method used so that the underlying linear parameters can be evaluated.

Examples of transient response prediction for a system with hardening cubic stiffness using the recommended procedure are shown in figs (6.2) & (6.3). The system has the following properties:-

$$\omega_o = 13.77 \text{ Hz}$$

$$\beta = 200 \text{ 1/m}^2$$

$$\zeta = 0.00522$$

$$\text{Modal constant} = 1.0 \text{ l/Kg}$$

From reciprocal-of-receptance analysis on data from a sine test, using data points above resonance, the calculated parameters are (from table (5.2)):-

$$\omega_o = 13.79 \text{ Hz}$$

$$\zeta = 0.005025$$

$$\text{Modal constant} = 0.965 \text{ l/Kg}$$

These parameters are then used in a linear FRF model and transformed to the time domain to provide a prediction of the IRF, calculated for four initial conditions:-

- i) $\dot{x}(0) = 1.0 \text{ m/s}$
- ii) $x(0) = 2.0 \text{ m/s}$
- iii) $\dot{x}(0) = 5.0 \text{ m/s}$
- iv) $\dot{x}(0) = 10.0 \text{ m/s}$

In the first example (fig (6.2a)) no difference is evident between the exact and the predicted response from the full comparison, but the expanded view (fig (6.2b)) highlights the slight change in the period of oscillation that is present. The results were similar for $\dot{x}(0)=2.0 \text{ m/s}$. For $\dot{x}(0)=5.0 \text{ m/s}$ and $x(0)=10.0 \text{ m/s}$ cases the discrepancies between the exact and the predicted responses increase, with the initial predicted amplitude now being larger than the exact (fig (6.3)). However, the decay rate of the 'exact' solution is not constant, and the response amplitudes converge as the damping in the 'exact' response converges with the underlying linear damping parameter. This apparently non-linear damping effect in the IRF was indicated in the imaginary part of the reciprocal-of-receptance plots of a system subjected to an impulse (fig (5.21)).

In a system with softening cubic stiffness, and with large initial displacement, the true transient response will be greater than the predicted response using a linear model. Although the decay rate will initially be greater than exponential, the two amplitudes will converge at about the same stage as for the hardening cubic stiffness. This means that for most of the response the predicted amplitude would be lower than the exact response.

Using the recommended route (β from fig (6.1)) the predictions are quite good for low effective non-linearities with variations between exact and predicted responses increasing with non-linear effect. Initially, it is just the frequency that changes as the amplitude decreases, but with the higher responses, the amplitudes differ also. For this example the predicted response is greater than the exact response, but for a system with softening cubic stiffness the predicted response may be less than the exact response and the initial conditions should be examined to ensure a valid prediction.

6.3 Transient response prediction for a system with backlash

With a backlash characteristic, the presence of a stiffness-type non-linearity is evident from both impulse tests and from constant force sine tests, viewed in the frequency domain plots or the time domain plots. Some of the characteristics from both tests are similar to those from a system with cubic stiffness but there are sufficient differences to be able to differentiate the two types of non-linearity if not from a single plot then from the trends exhibited from comparing tests with different force conditions.

There are three categories of the transient response:-

- (i) where the response is similar to the system without a gap (fig (6.4)).
- (ii) where the response is greater than the linear system (fig (6.5a)).
- (iii) a region between the two where part of the response approximates to the linear system and the tail end of the response is greater than that for the linear system (fig (6.6)).

The actual category of the response is determined by the ratio of the initial displacement amplitude to the gap dimension and for any response parameter - displacement velocity or acceleration - the traces fall into the same category. If the gap is less than about 1% of the maximum displacement, then using the linear parameters from the system would provide a good approximation to the transient response. If the gap is greater than about 10% of the maximum displacement, then using the linear parameters would grossly underestimate the response.

The problem with this type of non-linearity is in evaluating the linear parameters. As the non-linear effect is reduced at high amplitudes, using a sine test with as high a force level as possible could approximate to the linear system, and if data points close to resonance are used for the analysis then good approximations will be obtained to the linear parameters. It is interesting to note that from a constant-force sine test the average modal constant and damping loss factor from two separate reciprocal-of-receptance analyses are very close to the linear system as shown in table (6.1). These parameters are evaluated

by first using data points above resonance, then data points below. The two sets of modal parameters produced are then averaged, and this has been performed using varying force levels and systems with different gap dimensions.

Transient response predictions using the average values from this table were calculated and compared with the exact solution when the initial response is over one hundred times the gap dimension. In all cases the prediction was good for the maximum amplitudes, and for the first few cycles the responses overlaid. As the response level decreases, there is a slight change in the period of oscillation. Fig (6.4) shows an example of these transient response predictions using route β from fig (6.1) with the following properties calculated from the average of the two reciprocal-of-receptance analyses (system 1 from table (6.1)).

$$\omega_o = 13.7595 \text{ Hz}$$

$$\zeta = 0.01047$$

$$\text{Modal constant} = 0.10013 \text{ l/Kg}$$

For gap dimensions greater than about 10% of the maximum displacement, the true responses are larger than those predicted by the linear system throughout the full time-history, as shown in fig (6.5a). This is for system 1 from table (6.1) with an initial displacement of about 10 times the gap dimension. In this case, the linear model does not provide a good estimation and a non-linear model (route (BDE2) from fig (6.1)) must be recommended. The reason for the high response of this system is because of the zero damping in the gap, so the effective damping of the system is reduced as the ratio of time spent in the gap to time spent in contact with the spring increases. One possible approach to developing a model (MI) to provide a reasonable approximation to the transient response of a system with backlash is to find a relationship between an apparent damping of the system and the system parameters and excitation conditions. This could then be used in a linear model for a transient response prediction. The example in fig (6.5a) is calculated a second time using an apparent viscous damping factor of 0.007 and the result is shown in fig (6.5b). Whilst the maximum responses are still not predicted accurately, the general response

prediction is better than using the linear system parameters. The alternative is to develop a full non-linear model (M2) that includes a type of 'dead zone' where the mass continues to oscillate but with an increasing period. Either of these models (M1 or M2) require knowledge of the system parameters including the gap size which can be calculated using known offsets on the system. It is interesting to note that it is the resulting damping non-linearity in this particular backlash element (no damping within the gap) that causes most of the errors in the transient response prediction.

Response predictions when the displacement-to-gap ratio is greater than 1% and less than 10% could take either route - using the underlying linear system parameters (route β from fig (6.1)) or a non-linear model (route (BDE2)) - depending on the requirements of the results. In general, for responses in this category, the maximum amplitude of the first peak is estimated quite well using the linear parameters obtained from averaging the results from two reciprocal-of-receptance analyses. Examples using system 1 from table (6.1) are shown in fig (6.6) where the gap dimension is about 5% of the initial displacement. In this example the prediction is good for the first four cycles. The larger the initial response of the system, the more cycles of oscillation are predicted accurately using the linear model: if only the peak response is of interest the linear model will provide a good estimation. However, depending on the time length of interest in the signal, a non-linear model may have to be used. In all cases the extended vibration in the gap will be of interest if it is significant in comparison with the maximum amplitudes and fatigue is of interest.

For this backlash non-linearity two different routes are recommended, depending on the application and the amplitude of response. In all cases, the non-linearity first needs to be identified and a suitable test performed to classify it as backlash. When the response is large in comparison with the gap, or initial values only are of interest, then, if the linear system parameters can be evaluated, a linear model can be used with those parameters (route β from fig (6.1)). In the other cases all the system parameters need to be calculated including the gap, and a non-linear model developed (route (BDE2)) that will also be dependent on the initial amplitude of response.

6.4 Transient response prediction for a system with bi-linear stiffness

This non-linearity is most distinct in the exact IRF where the two different frequencies and amplitudes are clearly evident (fig (6.7)). However, from the frequency domain displays there are no indications of non-linearity present in the system as all displays and analyses indicate the system to be linear. There is a suggestion of bi-linear stiffness in the FRFs as all of the 'modes' are found at harmonics of the fundamental frequency, and if the FRF from a sine test is transformed, then the resulting IRF will have a small non-causal component (fig (5.33)). Applying an offset to the system and repeating the modal test will alter the resonance frequencies and, if the offset is known, the change in frequencies can be used to identify the ratio of the stiffnesses. Observing the response signal from a sine test would indicate the presence of this type of non-linearity as the response will be different above and below the equilibrium position. It may be necessary to identify the origin before the start of the test as the response may resemble a displaced sine wave. The ratio of the two stiffnesses can also be evaluated from inspection of the IRF, but such an identification of the two stiffness parameters by examining the time response - either the time history or the response signal - may not be possible for a multi-degree-of-freedom system as the response could be too complex to identify any asymmetry about the time axis.

If the two stiffnesses are known, it is fairly easy to set up the time domain model to predict the transient response of the bi-linear system as shown in fig (6.7). However, a frequency domain model that predicts a non-symmetric time-history is not available, and the transformed IRF would need to be examined in detail to determine if this non-linear model can be developed.

This type of non-linearity is quite common, and although the steady-state model is effectively linear in behaviour, the impulse response is dominated by the difference in the two spring stiffnesses. It is recommended that in this case the non-linearity should first be identified (which may be the hardest part), then the ratio of the two springs evaluated by inspecting the free decay from the

element or the response signal from a sine test. A non-linear time domain model should then be used, although the model consists of a pair of linear equations for this particular element. If it is not possible to identify the spring ratio, a conservative solution would be provided by using the value of the softer spring, since that produces the largest response in a linear model.

6.5 Transient response prediction for a system with friction

The damping-type non-linearity provided by coulomb friction is easily identified from almost all the displays of either impulse tests or sine tests. The Bode plot from a sine test is the hardest to interpret correctly, as a single plot may be classified as a heavily damped linear mode. From constant-force sine tests it is possible to evaluate the values of viscous and coulomb damping using reciprocal-of-receptance analysis by recording two values of the imaginary part and using a simple relationship derived from the linearised equation of motion. The FRF response derived from an impulse test also appears to have potential to predict the two values of damping, again from the reciprocal-of-receptance plot. There are clear trends in the imaginary part of the reciprocal-of-receptance that depend on the amount of viscous and coulomb damping present in the system.

When the force level in a constant-force sine test is high in comparison with the friction force, the results may indicate a linear behaviour, and analysis can be performed on the data to obtain a set of linear parameters with a single damping value. In this case, the linear parameters thus determined would have a damping value that is higher than the underlying system but which combines the effect of the coulomb damping with the linear viscous damping. Also, reciprocal-of-receptance analysis on data from a sine test will yield parameters close to those of the linear system, with a single damping factor combining the viscous damping and the effective coulomb damping for that test. If the initial velocity of the transient is of the same order as the velocity around resonance of the sine test, then this linear model (route α from fig (6.1)) can be used with the 'Fourier transform method' and a result obtained in this way is shown in fig (6.8). This calculation relates to the system in table (5.4) using the parameters from the reciprocal-of-receptance analysis. However, if the initial velocity of the transient is much higher than the response velocity in the vicinity of resonance in the sine test, then the effective damping is correspondingly lower so that the predicted curve decays away too quickly, as is shown in fig (6.9a) where the initial velocity is twice that in fig (6.8). If the initial velocity is less than the velocity around resonance in the sine test, then

the opposite occurs as shown in fig (6.9b) but in this case the prediction is a conservative estimate. In the extreme, using only the viscous damping in the system for the model would always provide a conservative estimate to the transient response.

The alternative approach is to develop a non-linear model that takes account of both the viscous and the coulomb damping elements and the initial conditions. A non-linear model has been developed for friction (assuming a constant slipping friction force) by examining the time histories of several systems under different impulse conditions (ref [135]), and the results are summarised in Appendix 7. This non-linear model requires the modal constant, the resonant frequency (which does not change with friction), the viscous damping component and the coulomb damping component of the system, all of which can be calculated using an adapted version of the reciprocal-of-receptance analysis on constant-force sine test data (Appendix 6). Also required is the response level at the start of the free decay, and this whole procedure corresponds to route γ in fig (6.1). This non-linear frequency domain model does not represent the steady-state solution, and is only suited for transforming to the time-domain for transient response prediction. Examples using the non-linear model are shown in fig (6.10) and correspond to the same initial conditions as in fig (6.9). The predictions are clearly an improvement over those using the linear parameters evaluated with standard analysis techniques.

For this non-linearity it is recommended that after identifying friction in the system, the amount of viscous and coulomb damping present then be calculated using reciprocal-of-receptance FRF plots. Then, the non-linear model (route γ) needs to be used for transient response prediction as the limitations on the validity of using a linear model are such that it eliminates most applications for the simpler prediction method (route (BD2E1)), although a conservative prediction can always be obtained by using the underlying linear system parameters with the 'Fourier transform method' (route β).

6.6 Transient response prediction for an element with quadratic viscous damping

For most displays in the frequency domain or the time domain from either the constant-force sine test or an impulse test, the trends for quadratic viscous damping are opposite to those for friction: the difference being that the non-linearity increases with increasing force for systems with quadratic viscous damping. It is possible to distinguish between the viscous damping and the quadratic viscous damping terms using a similar technique to that used for friction on the reciprocal-of- receptance data.

For this non-linearity the initial free decay is more rapid than for the linear system, and so using a linear model with only the viscous damping in the system will always overestimate the maximum response in the displacement time-history as shown in fig (6.11). The system for this example is:-

$$\omega_0 = 13.77 \text{ Hz}$$

$$q = 1001/\text{m}$$

$$\zeta = 0.00522$$

$$\text{Modal constant} = 1.0 \text{ I/Kg}$$

using initial velocities of:-

$$\text{i) } \dot{x}(0) = 1.00 \text{ m/s}$$

$$\text{ii) } \dot{x}(0) = 0.10 \text{ m/s}$$

The acceleration response may initially be greater than for the linear system, as shown in fig (6.12), and so if this response was of major interest, using the linear model might not be appropriate. When the response is required as acceleration, or a more accurate response is required, then a non-linear model would be recommended (route (BDE2) from fig (6.1)). It is envisaged that this would be developed in the same fashion as the model for transient response of a system with friction, accounting for the two types of damping and the initial conditions before free decay.

If quadratic viscous damping has been identified in a system, it is recommended that the linear system parameters should be evaluated when predicting displacement and velocity time-histories: the linear model using those system parameters will generate conservative estimates of the response under all initial conditions. It is only necessary to use a non-linear model when a more accurate description of the system is required or when acceleration is the response parameter of interest.

6.7 Discussion

It is clear that when non-linearities are present in a system the prediction of the transient response requires careful consideration, as using the first set of parameters to be evaluated from a model test in a linear model with the 'Fourier transform method' will not necessarily generate a suitable response prediction. The first step will always be to identify the type of non-linearity as this determines the approach to further analysis for transient response. In some cases a linear model may be used for that particular transient response analysis. This is the simplest approach and is easily adapted for further use - eg coupling with other structures. However, the types of non-linearity that this approach can be used on with confidence are limited; the conditions of use in each case, and which set of experimentally determined linear parameters should be used in the model, place severe restrictions on this approach.

The use of a non-linear model is found to be necessary in most cases and applications. These models may vary from an accurate description of the system to specific linearised models which provide conservative estimates suitable for some requirements. It is found that the parameters that are required for non-linear model are generally available from measured FRF data using specifically-adapted reciprocal-of-receptance analysis methods (the variation on the reciprocal-of-receptance technique depends on the non-linearity involved). The solution routes are summarised in fig (6.13) starting with an unknown system from which a transient response prediction is required. The complex non-linear models, whilst providing good approximations to, the transient response, are best used only where absolutely necessary as they increase the calculation times and can be difficult to manipulate.

A non-linear model has been developed for a friction element, but each such type of non-linearity needs individual treatment and this has not been undertaken for other cases. Also, the development of analysis routines to evaluate non-linear parameters once the non-linearity has been identified (for systems other than those with friction or quadratic viscous damping) needs to be addressed.

| System | Gap | force level | Reciprocal-of-receptance analysis using | Natural frequency | Modal constant | Damping loss factor | Average natural frequency | Average modal constant | Average damping loss factor |
|--------|-----------|-------------|---|-------------------|----------------|---------------------|---------------------------|------------------------|-----------------------------|
| linear | 0.00 | 1.00 | Data points above resonance | 13.770 | 0.10000 | 0.02100 | 13.77 | 0.10000 | 0.02100 |
| | | | Data points below resonance | 13.770 | 0.10000 | 0.02100 | | | |
| 1 | a. 000001 | 1.00 | Data points above resonance | 13.758 | 0.09071 | 0.01898 | 13.7595 | 0.10313 | 0.02095 |
| | | | Data points below resonance | 13.761 | 0.10956 | 0.02292 | | | |
| 2 | 0.000001 | 0.50 | Data points above resonance | 13.756 | 0.08120 | 0.01703 | 13.7555 | 0.09979 | 0.02091 |
| | | | Data points below resonance | 13.755 | a. 11831 | a. 02479 | | | |
| 3 | 0.000001 | 0.25 | Data points above resonance | 13.740 | 0.06280 | 0.01290 | 13.7450 | 0.09913 | 0.02031 _B |
| | | | Data points below resonance | 13.742 | 0.13547 | 0.02786 | | | |
| 4 | 0.000005 | 1.00 | Data points above resonance | 13.748 | 0.05318 | 6.01102 | 13.7425 | 0.09874 | 0.0204 _B |
| | | | Data points below resonance | 13.737 | 0.14430 | 0.02994 | | | |

Table 6.1 Data from analysts of systems with backlash type non-linearity subjected to constant-force stepped-sine tests and reciprocal-of-receptance analysis using data points either above or below resonance and averaging the two results

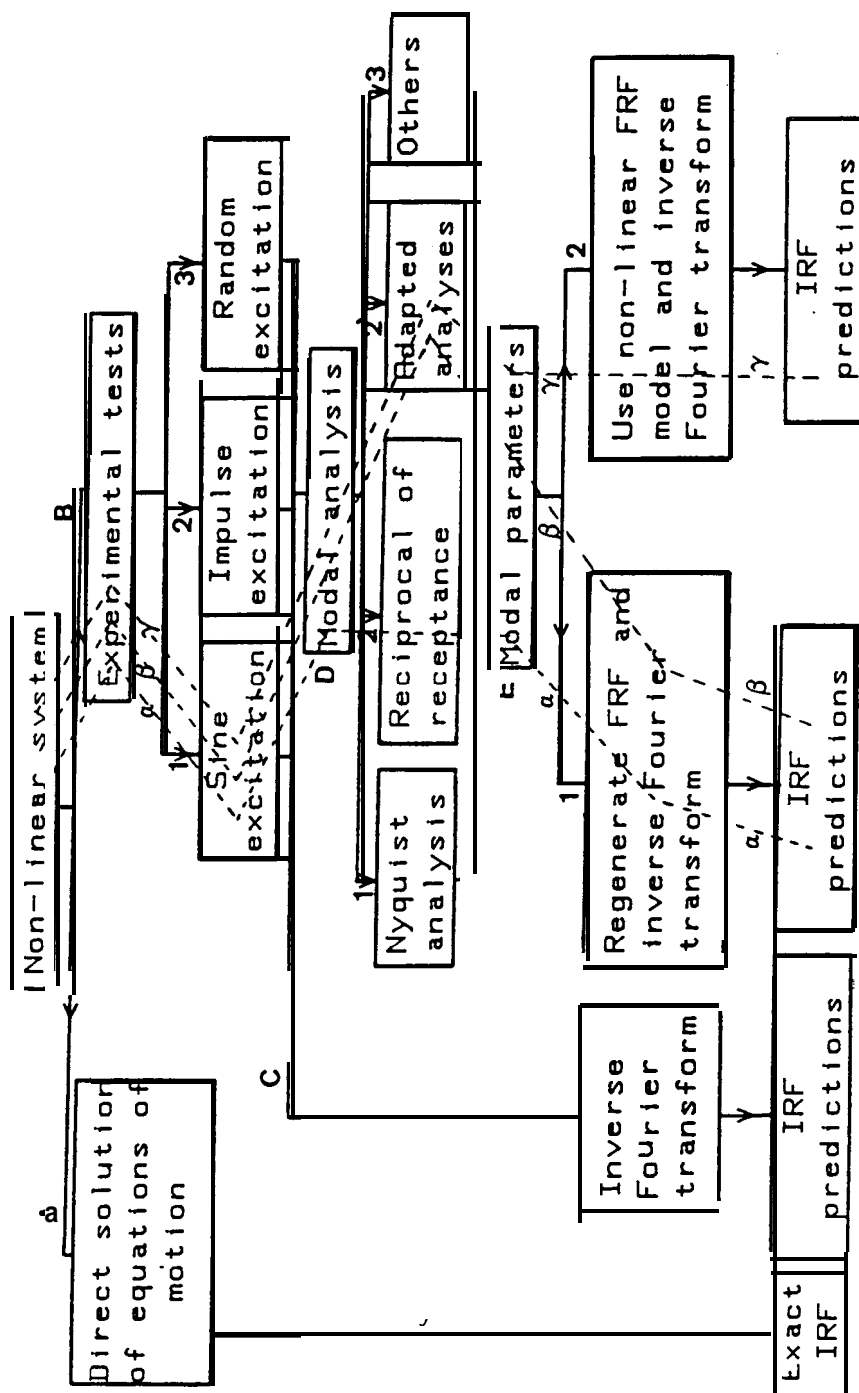


Fig 6.1 Solution routes for impulse response functions (IRFs) of non-linear systems

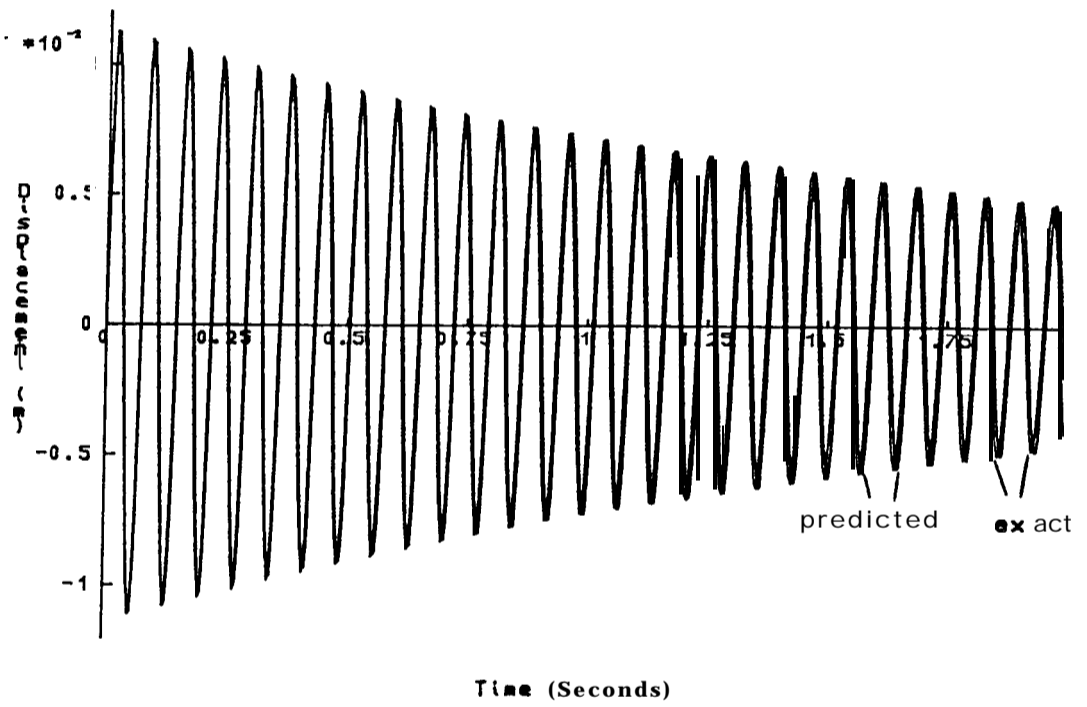
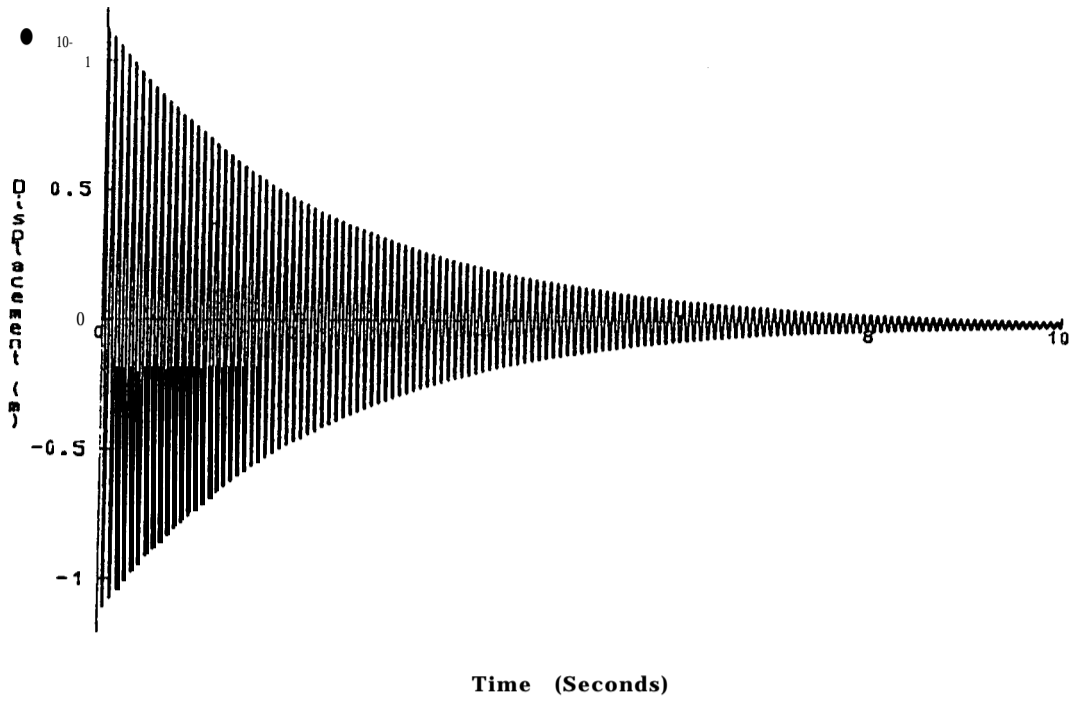


Fig 6.2 Exact and predicted transient response of a system with cubic stiffness; $v(0)=1.0\text{ m/s}$
 a Full response
 b Expanded view of first 2 seconds

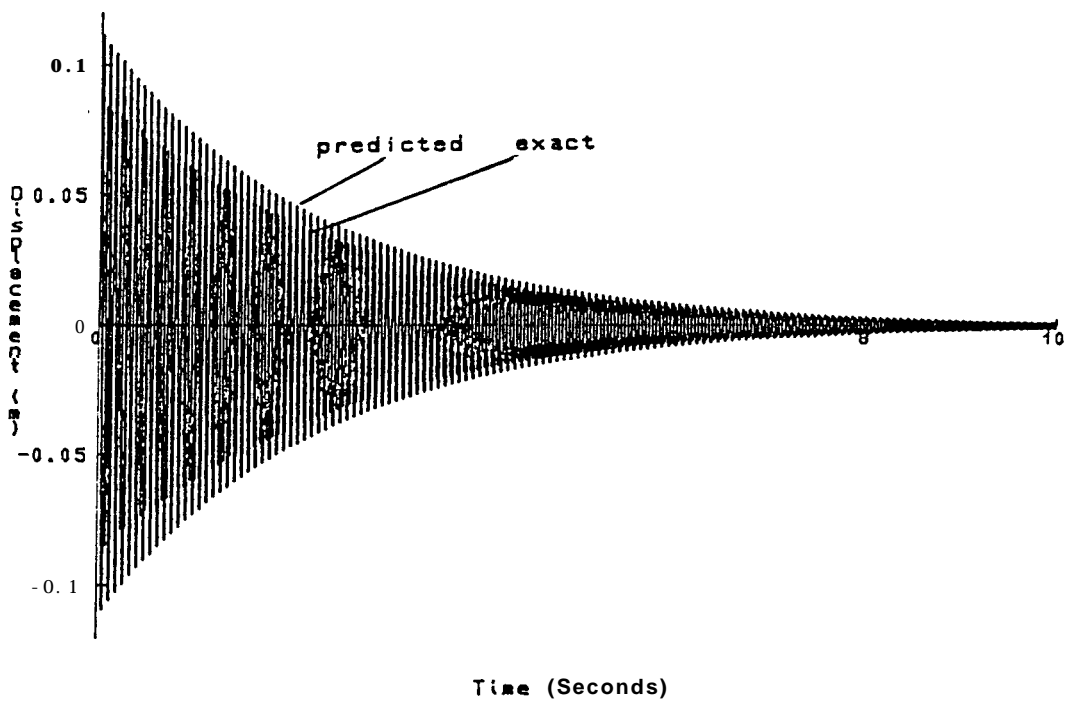
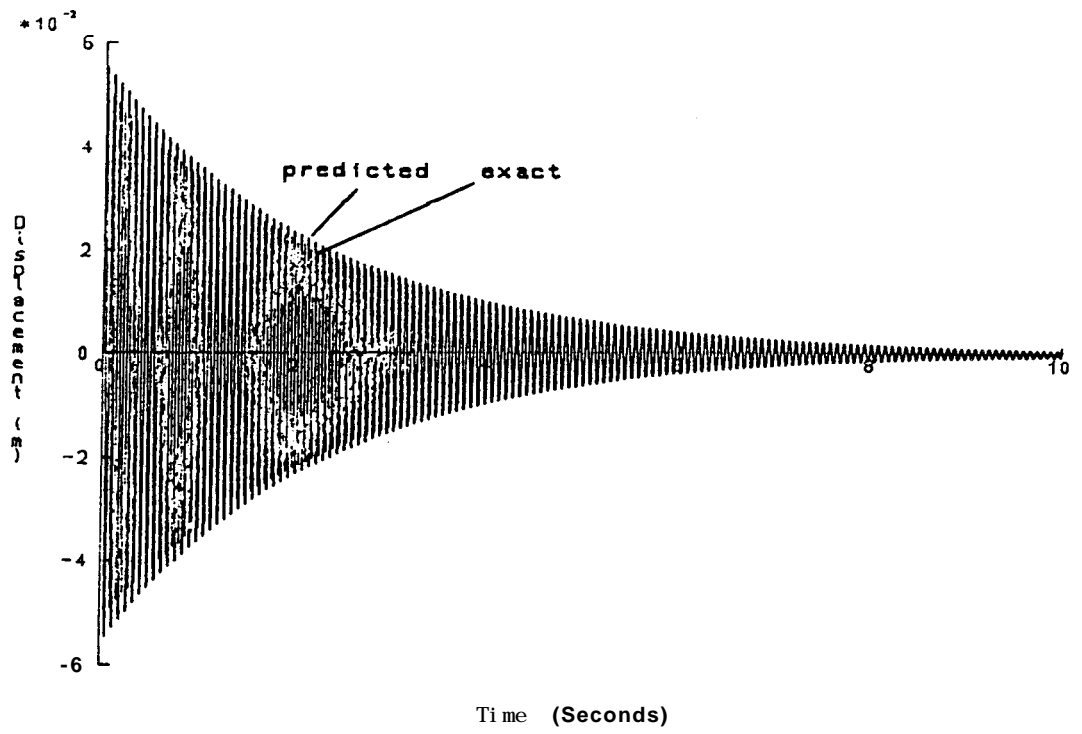


Fig 6.3 Exact and predicted transient response of a system with cubic stiffness
 a $v(0) = 5.0$ m/s
 b $v(0) = 10.0$ m/s

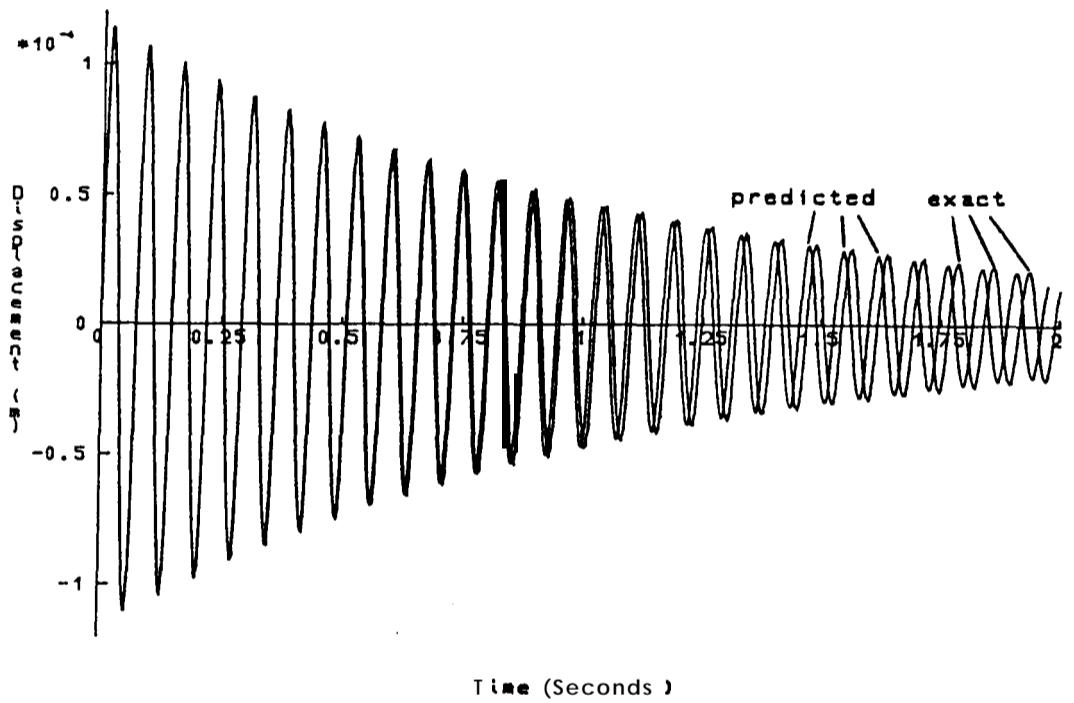
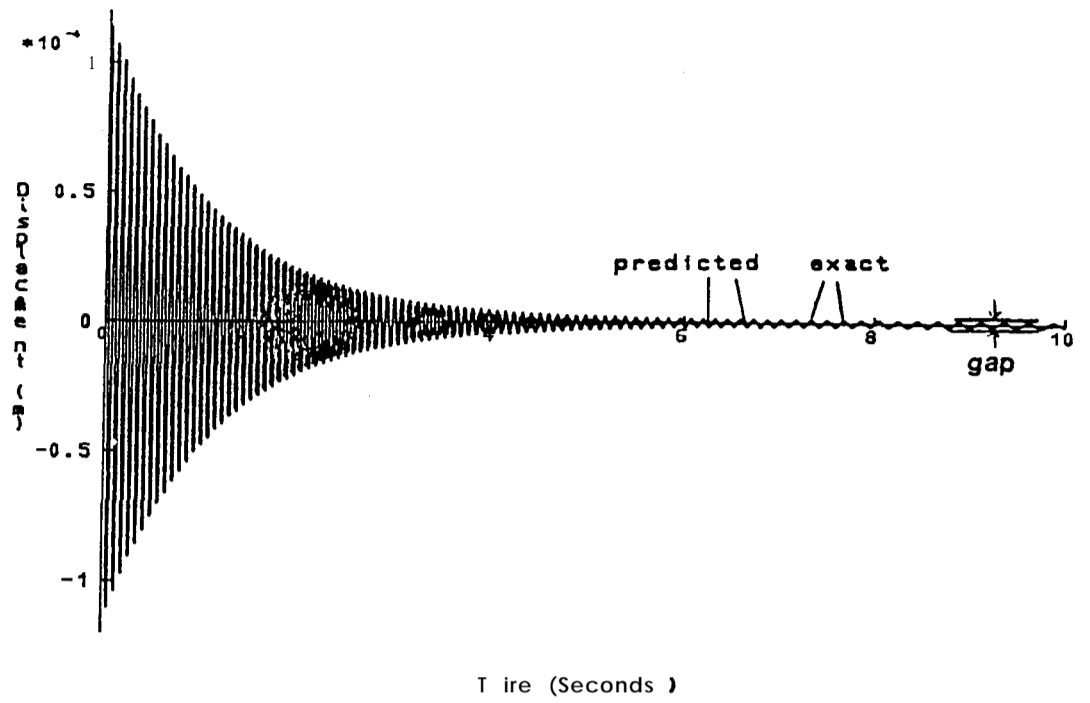


Fig 6.4 Exact and predicted transient response of a system with backlash; gap is approx. 1% of max. disp.
a Full response
b Expanded view of first 2 seconds

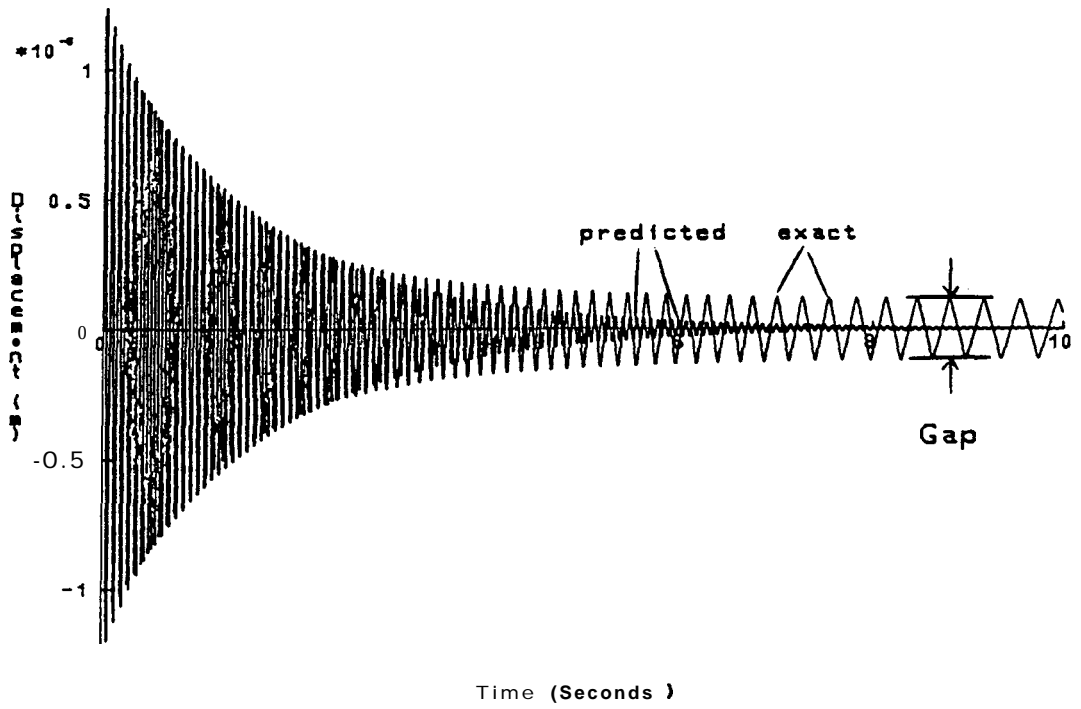
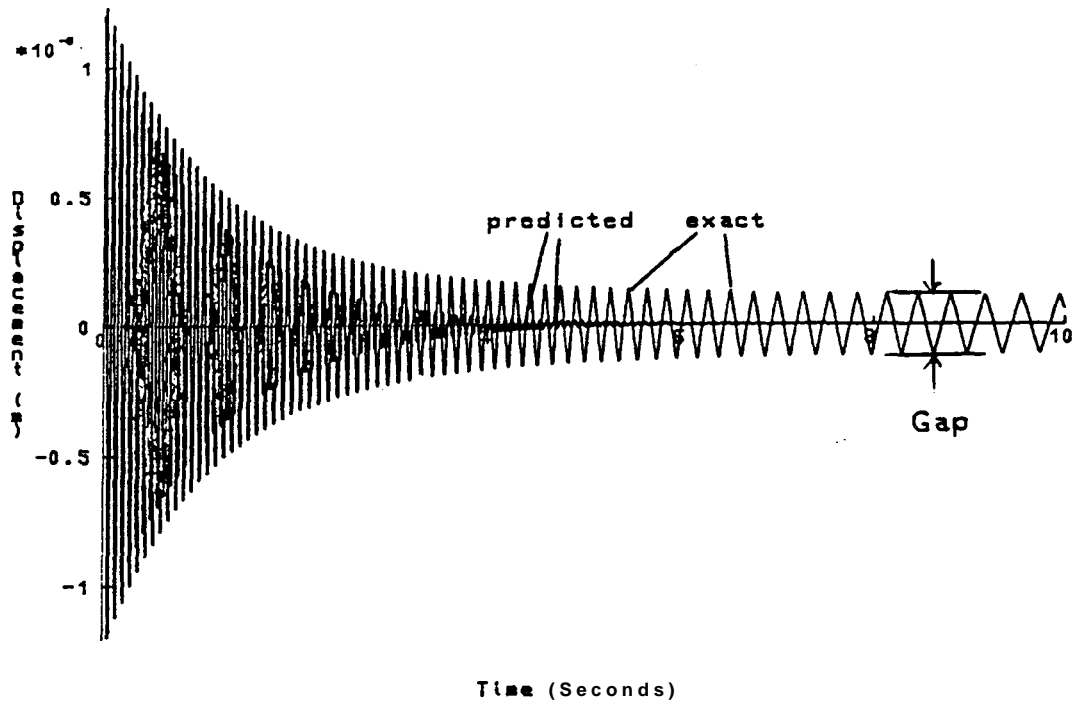


Fig 6.5 Exact and predicted transient *response* of a system with backlash; gap is approx. 10% of max. disp.
 a Prediction using underlying linear parameters
 b Prediction using apparent initial damping ratio

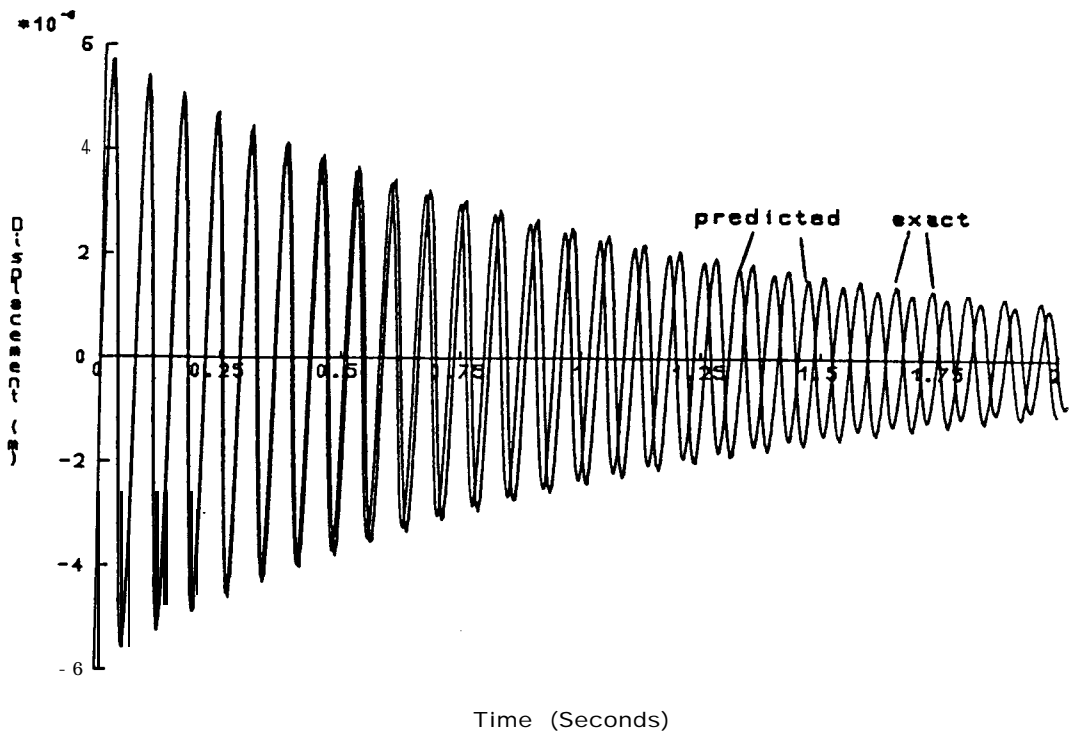
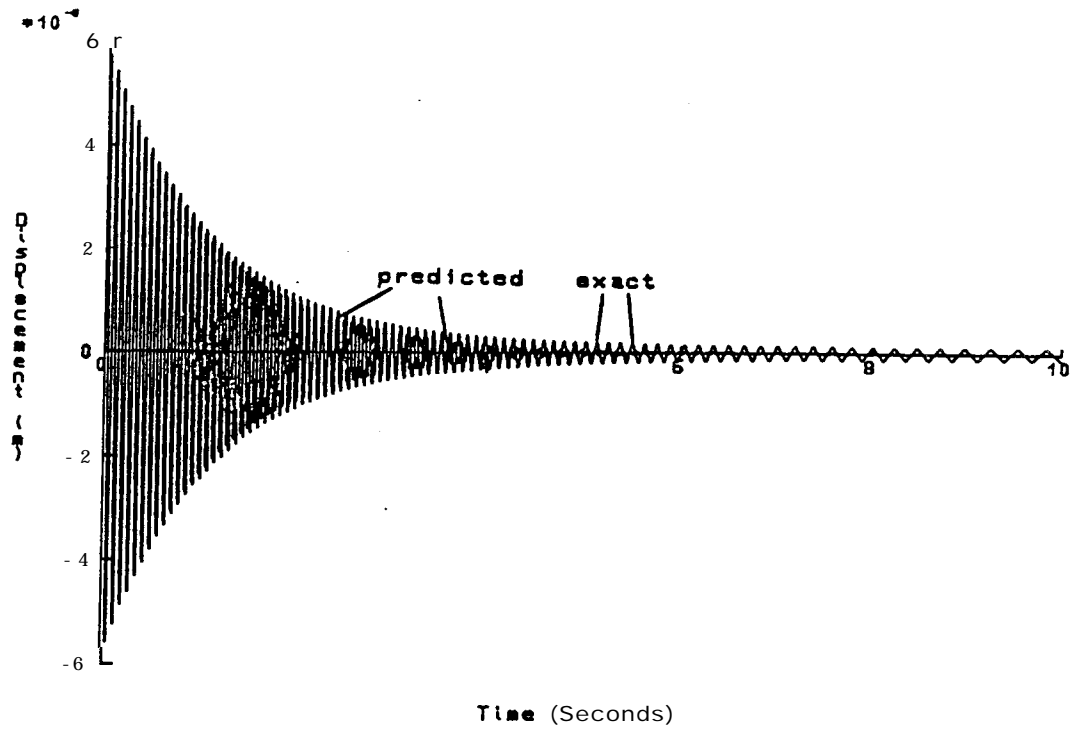


Fig 6.6 Exact and predicted transient response of a system with backlash; gap is approx. 5% of max. disp.
a Full response
b Expanded view of first 2 seconds

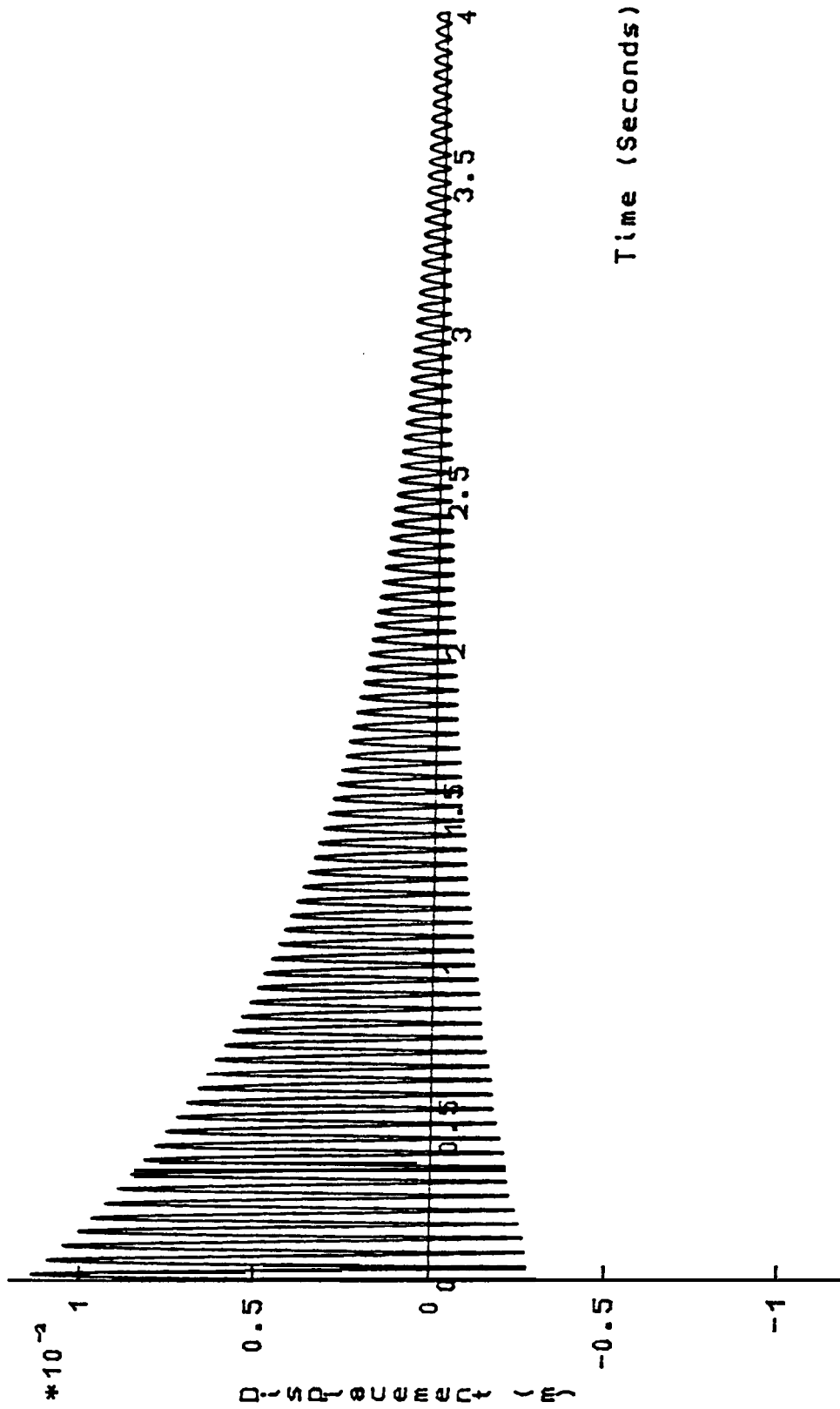


Fig 6.7 Example of the IRF of a system with bi-linear stiffness;
Spring ratio 1:16

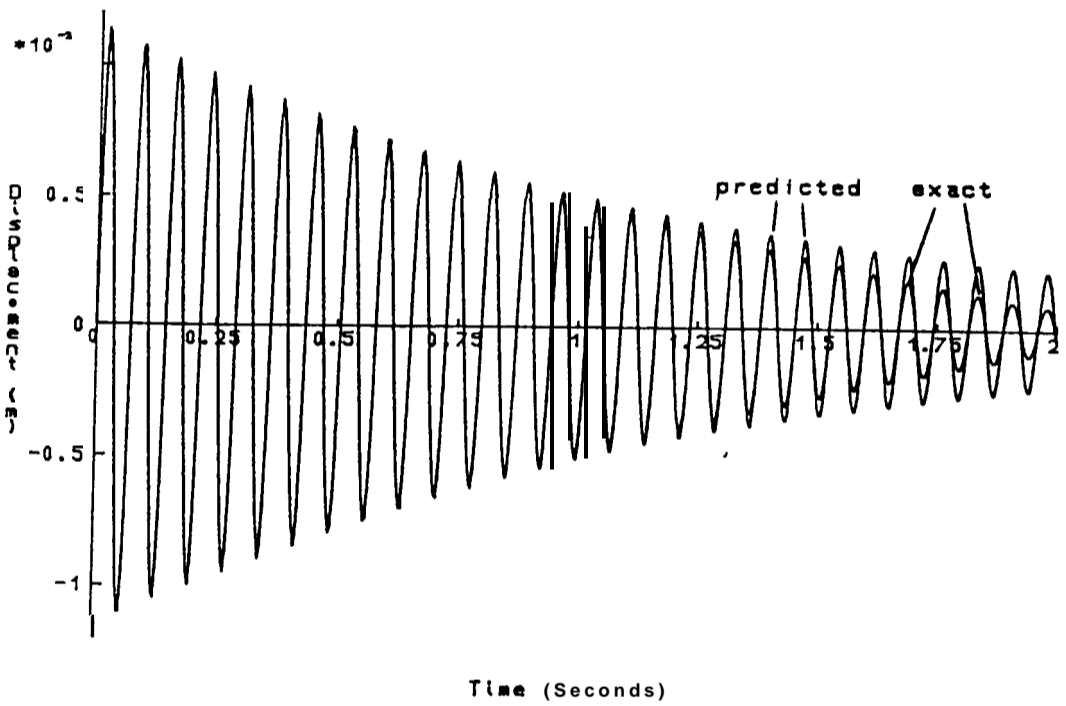
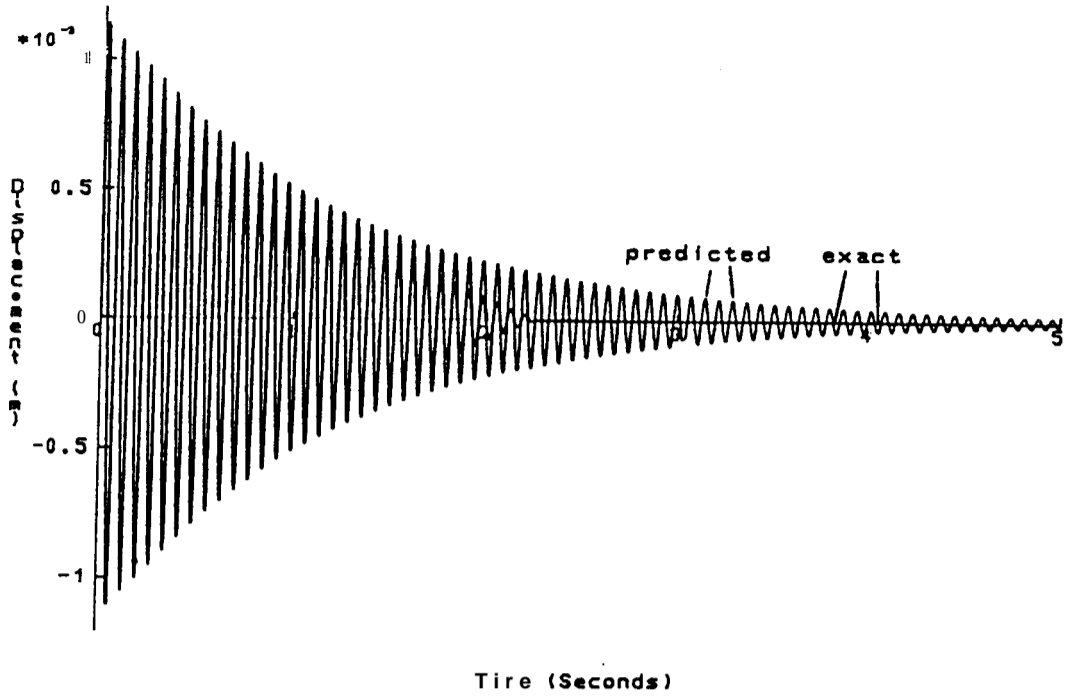
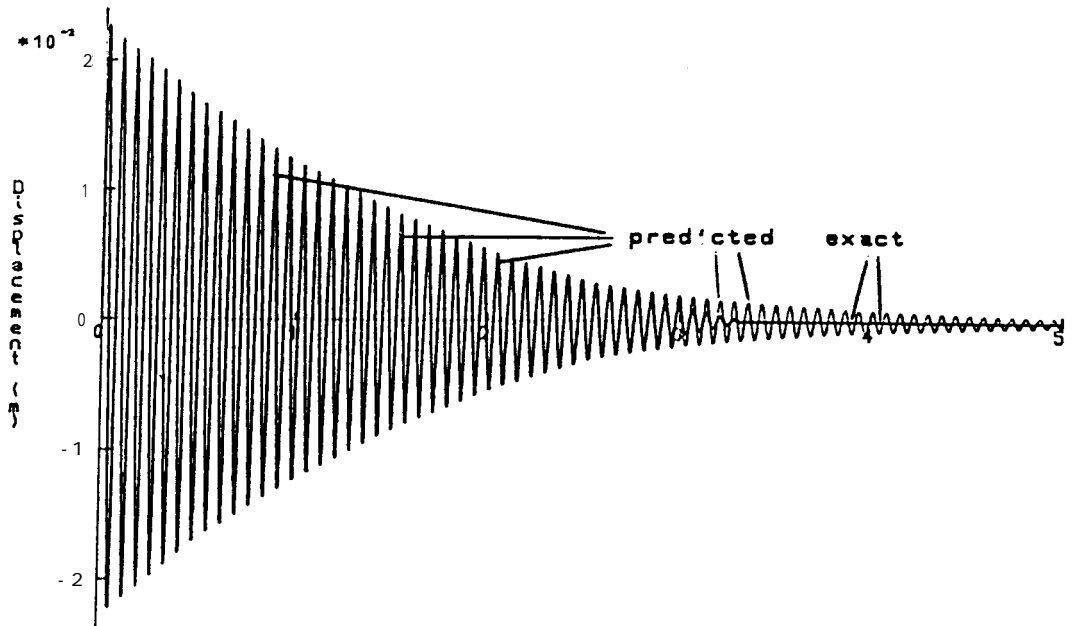
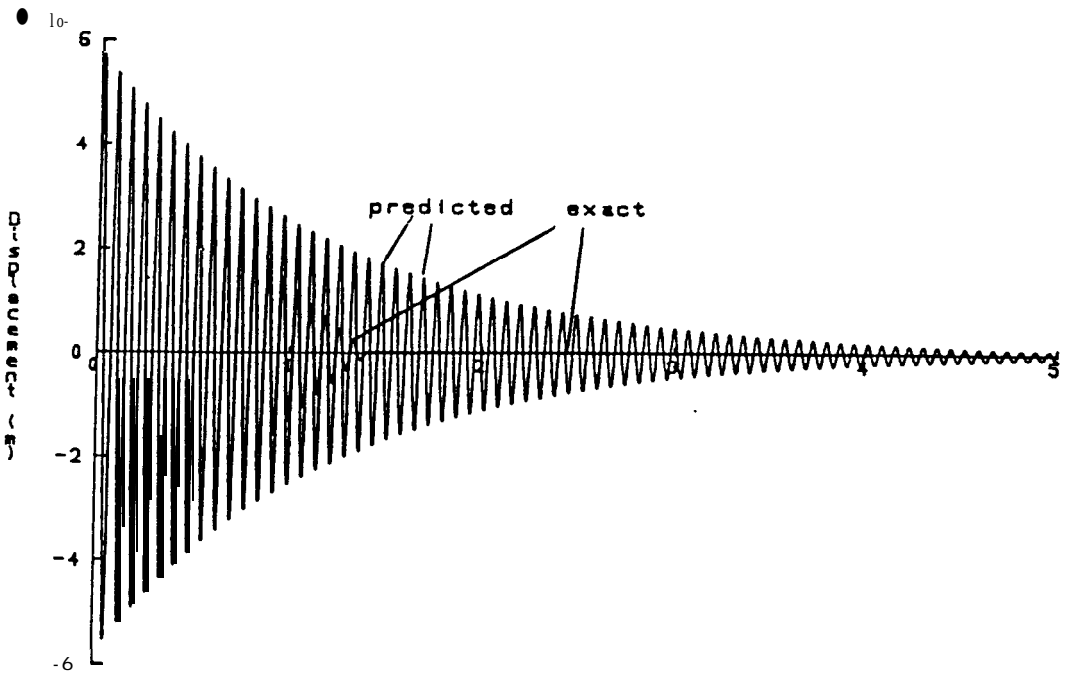


Fig 6.8 Exact **and** predicted transient response of a system with friction; using a linear model; $v(0)=1.0$ m/s
a Full response
b Expanded view of first 2 seconds



Time (Seconds)



Time (Seconds)

Fig 6.9 Exact and predicted transient response of a system with friction; using a *linear* model
 a High initial velocity; $v(0)=2.0$ m/s
 b Low initial velocity; $v(0)=0.5$ m/s

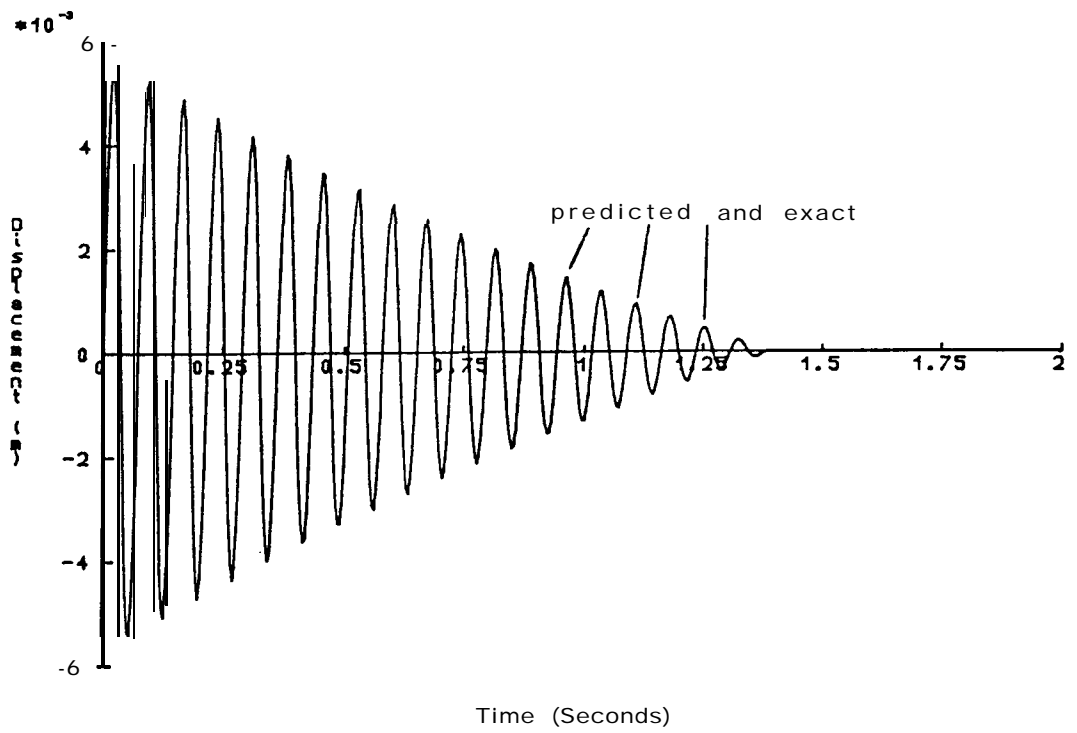
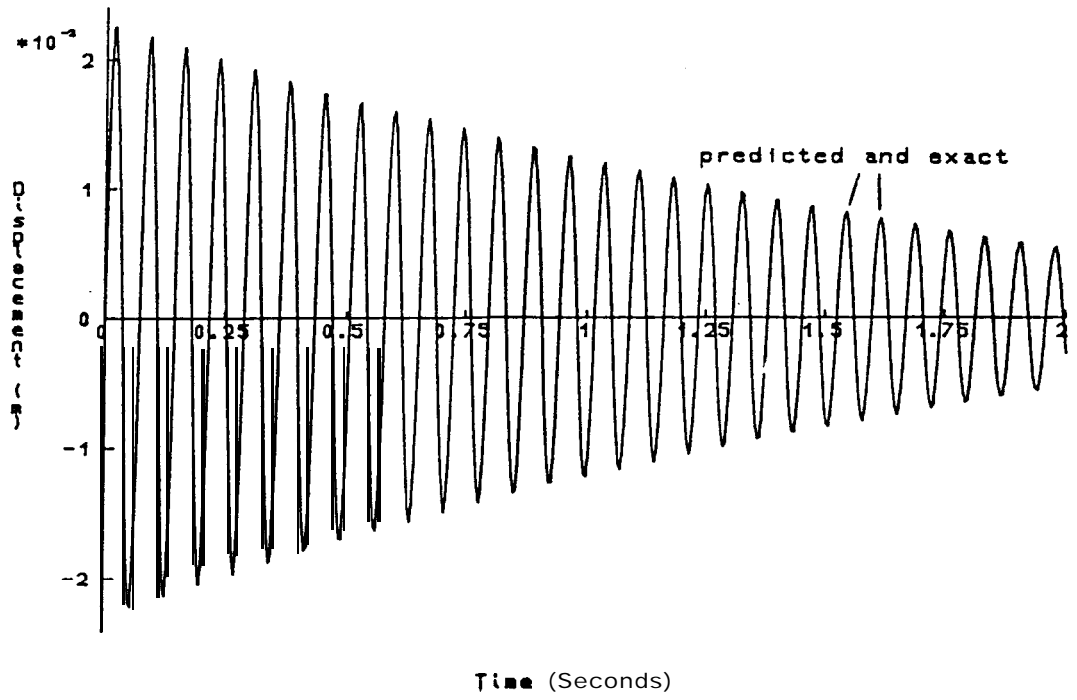
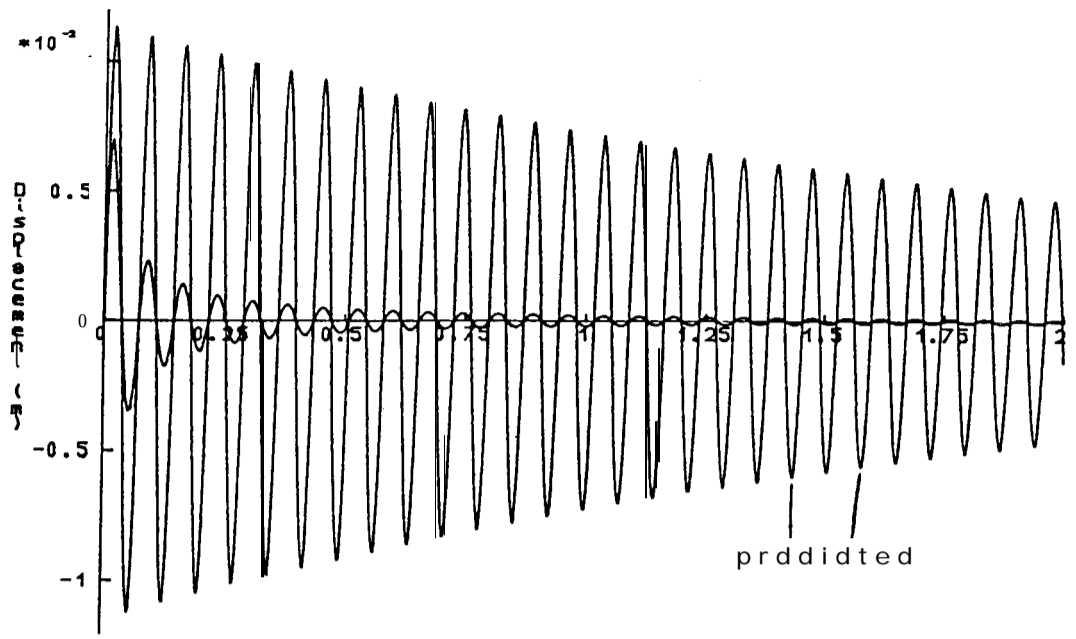
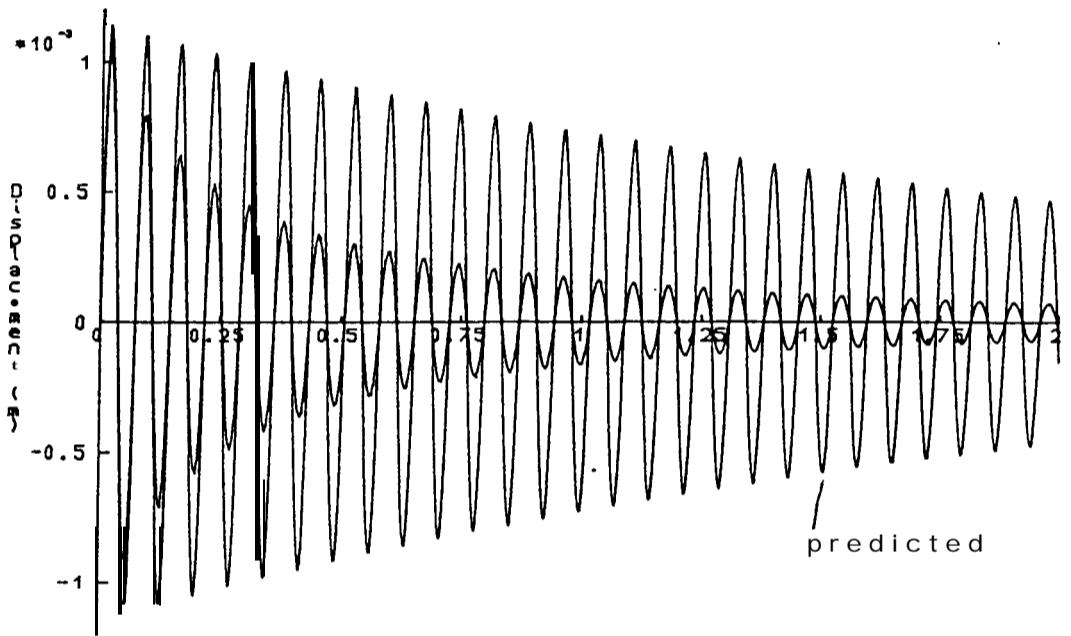


Fig 6.10 Exact and predicted transient response of a system with friction; using a non-linear model
 a $v(0)=2.0$ m/s (compare with fig 6.9a)
 b $v(0)=0.5$ m/s (compare with fig 6.9b)



Time (Seconds)



Time (Seconds)

Fig 6.11 Exact and predicted transient response of a system with quadratic viscous damping; using a linear model

- a $v(0) = 1.0 \text{ m/s}$
- b $v(0) = 0.1 \text{ m/s}$

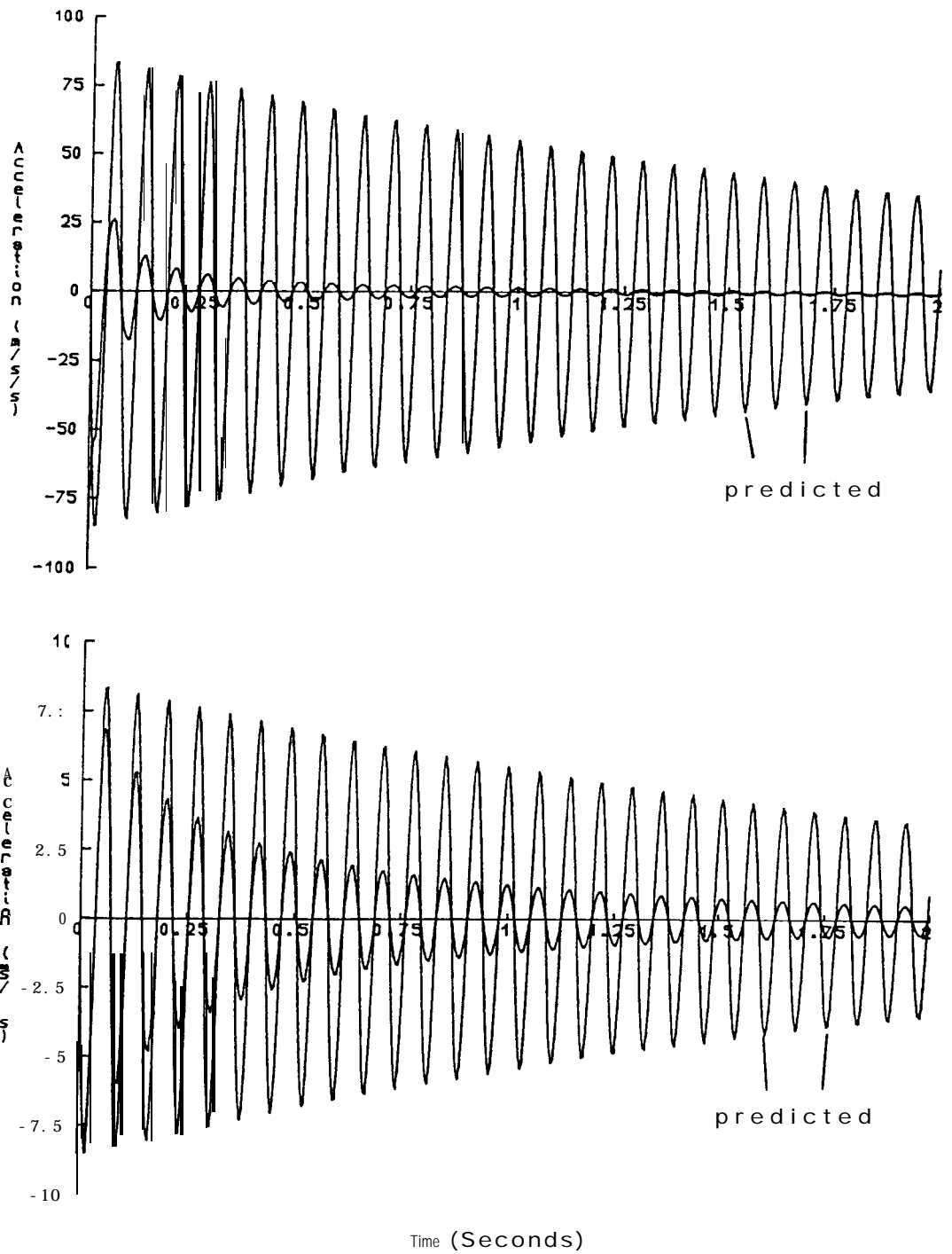


Fig 6. 12 Exact and predicted acceleration transient response of a system with quadratic viscous damping; using a linear model
 a $v(0)=1.0$ m/s; large initial acceleration
 b $v(0)=0.1$ m/s; response less than prediction

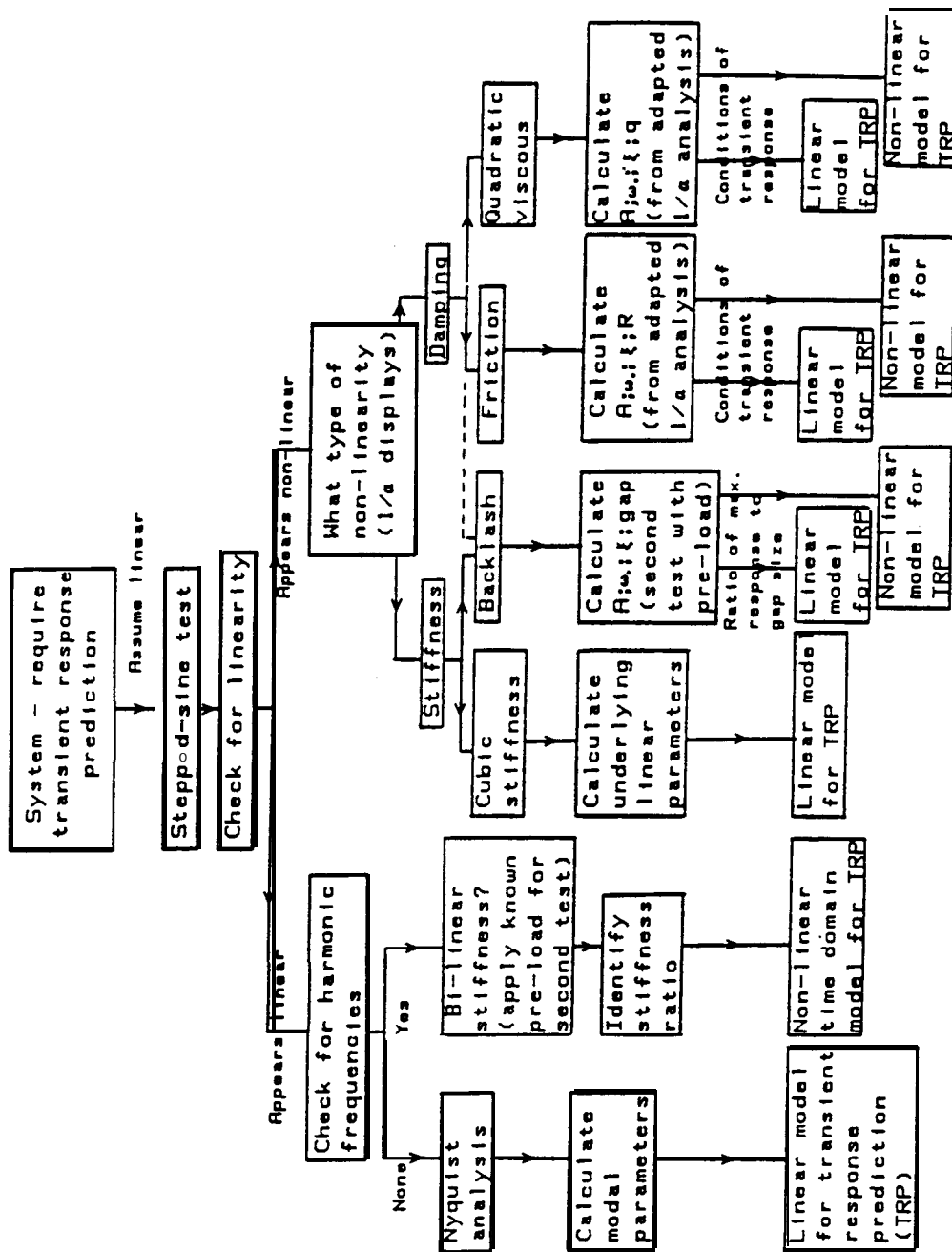


Fig 6.13 Solution routes for transient response predictions of various non-linear systems

7 RESPONSE ANALYSIS OF MDOF SYSTEMS WITH A NON-LINEAR ELEMENT

7.0 Introduction

The response of a single-degree-of-freedom (SDOF) system with a non-linear element has been shown to depend on the type and level of excitation. When different analysis techniques are applied to the frequency response functions (FRFs) measured in different ways, a wide range of modal parameters are obtained. The variation in the displays (in either the frequency or the time domain) can be used to identify, and sometimes to quantify, the non-linearity in the system. The approach for transient response prediction of the non-linear element has also been discussed in chapter 6 and different prediction routes recommended for specific non-linearities, depending on the eventual application of the results. It is the aim of this chapter to consider the applicability of the techniques for identifying and quantifying non-linearity in a SDOF element to identifying and quantifying non-linearity in a multi-degree-of-freedom (MDOF) system, and also for predicting the transient response of that type of system.

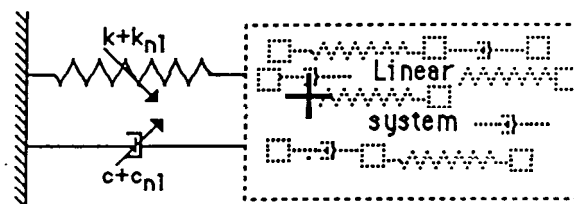
A linear model with a single non-linear element 'added' on is used in this chapter to examine the effect of non-linear elements on an MDOF system. This non-linear system is then excited using constant-force sine tests and the Nyquist and reciprocal-of-receptance analyses performed to study the extent of the effect of different non-linear elements on the remaining linear system. The responses are also inspected to determine if the trends that have been identified in SDOF non-linear elements are also applicable to MDOF systems. The transient responses of the systems are then compared with the linear response for various initial conditions to examine the effect of the non-linear element on the time-history of an MDOF system.

The chapter begins with a description of the system used for the illustrations followed by a brief summary of existing methods for the transient response prediction of non-linear MDOF structures. The basic system is then analysed in the frequency domain with various non-linear elements in place and finally the transient responses are examined.

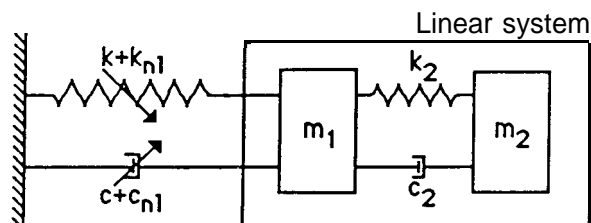
7.1 System definition

In many practical systems the non-linearity is often limited to one part of the structure, such as a joint, and is therefore concentrated in one element of the spatial model. The non-linearity will, however, affect the response of all the structure, thereby classifying the whole structure as non-linear. It is found in practice that the effect of a non-linearity is usually most noticeable in the low-frequency resonances where the response amplitude is generally largest.

As non-linearities tend to be concentrated in one element of the real structure, the system that is to be used for theoretical analysis in this chapter is, in terms of the spatial model, an MDOF linear system with one non-linear element. This is shown below where either k_{nl} or c_{nl} can be non-linear



This non-linear system will be used to initiate study into the effect of a single non-linear element coupled to a linear system and will explore ways of analysing the resulting non-linear system, with particular attention on the use of the evaluated parameters for the transient response prediction of such a system. For the specific examples in this chapter, the linear system consists of two masses connected by a single linear spring and damper as shown below.



7.2 Application of prediction techniques for transient response of MDOF non-linear systems

The techniques that exist and are adapted for non-linear transient response prediction all require knowledge of the basic system parameters - including the non-linearity - in either spatial or modal form. The methods are all mentioned in chapter 2 and are briefly recalled in this section. The solution route that will be used as the reference transient response for comparison later in this chapter is the direct solution of the equations of motion. This requires the spatial model of the system which, as stated previously, is often difficult to derive from experimental data even for a simple linear component, and when non-linear elements are included this solution route is totally inappropriate. However, for our examples the spatial model is known and provides a suitable reference solution as the number of degrees-of-freedom are small.

The Newmark- β method (eg ref [9]) has received attention and is adapted for use with non-linear systems. This is a method of solving the equations of motion, but one in which the modal parameters of the system can be used in place of the spatial properties. Again, the non-linearity needs to be quantified - which is possible for damping type non-linearities, but difficult for stiffness type non-linearities - and for large numbers of degrees of freedom the equations become difficult to manipulate.

The hybrid method by Lyons et al [14] combines the necessity for a time-marching solution for the non-linear systems with the more efficient linear transform technique for transient response prediction. This hybrid technique has been tested to find where the non-linearities are most evident and concludes that they are only noticeable around the low frequency modes. Other work (eg ref [12]) also suggests that only the first few modes affect the displacement response to a transient - in many cases only the first three modes - in which case the second stage of this hybrid method is unnecessary, particularly as the recommendation is that the first ten modes are used to ensure that all the non-linear effects are accounted for. If the response required is displacement, and the non-linear effects can be quantified, then it is possible to use any of the methods that have been adapted for non-linear systems

representing the structure by the first few modes only. With velocity or acceleration response, the number of modes required to describe the system adequately for a transient excitation increases, thereby making the numbers of equations large and any manipulation or solution inefficient and time-consuming.

In summary, there are a limited number of techniques available for the transient response prediction of non-linear systems. Each method requires information on the system parameters, which necessitates the ability to evaluate these parameters from a non-linear component. The assumption that these parameters are available using any of the linear analysis methods on a non-linear structure is not necessarily valid.

7.3 Modal analysis, of non-linear systems

The MDOF system described in section 7.1 has been analysed for the five different types of non-linearity previously discussed, and for various forcing levels. The physical description of each system is given in table (7.1), and the results of analyses of data from simulated constant-force sine tests are presented in tables (7.2) to (7.9). When the non-linearity is evident, the trends that emerge in **all** systems are the same as for the equivalent SDOF non-linear element discussed in chapter 6. In most examples, the second mode is found to be linear, and only at high effective non-linearities does this mode begin to appear non-linear. Often, the system is more non-linear when the excitation is applied to mass 2, and reciprocity does not hold for the non-linear examples - ie FRF (2,1) is not the same as FRF (1,2). Examples of the Bode plot sets are shown in figs (7.1) to (7.6), including the linear system and one example from each non-linear element.

For the example with cubic stiffness (fig (7.2), the second mode has not been affected by the non-linearity at the chosen forcing levels, but the first resonance could be identified as a SDOF cubic stiffness element. The reciprocal-of-receptance analysis is performed using data above that resonance but, while the results show less variation than those from a Nyquist analysis, some of the parameters are not as close to the linear system as was obtained for the SDOF elements - a difference mainly confined to those cases with very high non-linear effects.

With the backlash examples the non-linearity is evident in both resonances (fig (7.3)). The trends are the same in the two resonances as seen in the SDOF non-linear element study. For the reciprocal-of-receptance analysis, the average parameters from the above and below resonance regions have been calculated for both resonances when non-linearity is apparent. The modal parameters obtained using this method are more consistently close to the linear system than are those from Nyquist analysis, but the resonance frequency estimated from the average is usually low.

The results for the bi-linear stiffness in these examples are particularly interesting (fig (7.4)). There are, as expected, two modes with frequencies slightly shifted from those of the original linear system (26.95Hz and 66.78Hz as compared with the linear system natural frequencies of 24.45Hz and 63.41Hz), but there is also a 'harmonic' natural frequency showing through near 54Hz. For FRFs (1,1) (2,1) and (1,2), this is only a single point disturbance in the Bode plot, and would probably be ignored in analysis. However, for FRF (2,2), the corresponding response is quite large and a modal analysis performed on the full data generated the results shown in table (7.10). A small disturbance of this nature is often seen in Bode plots from measurements and it is recommended to check if the 'resonant' frequency is a harmonic component of any of the more dominant modes to consider the possibility that the system has a bi-linear stiffness characteristic.

For the friction (fig (7.5)) and quadratic viscous damping (fig (7.6)) examples, only the first resonance appears to be affected by the non-linearity. With both types of non-linearity, the trends in the Nyquist circle, 3-D damping plots and the reciprocal-of-receptance displays are very similar to those from the corresponding SDOF non-linear elements.

For the examples presented in this section, the effect of the single non-linear element is usually only obvious in the first resonance of the system, unless the effective non-linearity is high when the effect can also be seen in the second resonance. This is essentially as expected due to the larger displacements of the lower frequency resonances. The results from the second mode when there is no indication of non-linearity present are similar to those from the linear system, indicating that analysing that resonance as a linear mode for that particular excitation condition is valid. This will aid system modelling if the FRF can sensibly be analysed as linear with 'non-linear modes' rather than having to undertake an analysis of the full response as a non-linear system. One problem that emerged, and was particularly noticeable in FRF (2,2), is when the modes that are effectively linear are noticeably influenced by the 'non-linear' modes. For the linear FRF (2,2), analysis by iterations on the circle-fit method is necessary in order to remove the effects of mode 1 from the resonance of mode 2. In the non-linear examples it is assumed that, as the Nyquist plot for mode 2

is similar to that plot from the linear system, the interaction of 'non-linear' mode 1 on mode 2 is 'linear'. However, a problem now exists in that clearly mode 2 cannot be sensibly analysed without the effects of 'non-linear' mode 1 being first removed, but this requires the interaction to be identified. This aspect of modal analysis of non-linear systems is an area of work that requires further attention.

In addition to the identification of non-linearities in MDOF non-linear systems, the location of non-linear elements within a structure using experimental modal analysis is an area that also requires exploring. There are several possibilities, but as an individual linear element cannot necessarily be quantified from modal analysis - and only modal parameters are available - the concept of 'modal non-linearity' needs exploring. Returning to the non-linear systems analysed in this section, the effect of the non-linear element is more noticeable in the first resonance than in the second, so in these examples the 'modal non-linearity' would be greater for the lower frequency resonance than for the higher resonance.

If a component that is to be coupled to others to form a complete system model has been identified as non-linear, there will be concern about the validity of continuing with a linear coupling technique. This is one application area of modal data in which the effect that non-linear components have on the results has to be examined in detail. There is the possibility of using an iterative technique for including the non-linearity which effectively uses non-linear amplitude dependent frequency or time domain models. For this application, the non-linearity needs to be quantified and the response dependence of the non-linearity determined, and this returns to the problem of accurately analysing non-linear data for the required parameters.

7.4 Transient response of non-linear systems via the frequency domain

Once the problems of modal analysis of a MDOF non-linear system have been addressed, and a set of modal parameters obtained, the transient response prediction via the frequency domain of the same system can be considered. In this section the validity of using a linear model for transient response prediction of a non-linear system is assessed. As for the SDOF elements discussed in chapter 6, a non-linear model is still required for some applications and those non-linear models need developing such that they now also account for the influence of the other elements in the system.

For cubic stiffness (figs (7.7) to (7.9)) the linear model clearly provides a good prediction for the smaller initial velocity (fig (7.7)) with the discrepancies in amplitude increasing with increasing non-linear effects as seen in figs (7.8) & (7.9) where the non-linear effects are increased in the higher figure numbers. For most of the trace, the linear prediction provides a conservative estimate. However, as can be seen in the expanded view of fig (7.9), the prediction does on two occasions underestimate the response of minor maxima and minima. It is also anticipated that for softening cubic stiffness the linear prediction will underestimate the response.

Backlash (fig (7.10) to (7.12)) shows a satisfactory prediction using the linear system for up to 2% gap-to-initial-displacement ratio. The response for a ratio value of 3.5% is shown in fig (7.13a) and demonstrates an irregular response when the mass remains almost totally within the gap, although the trend of an ever-increasing period is similar to that from the SDOF backlash element. The transient response prediction for the initial response of this example is shown in fig (7.13b).

The response for a system with the bi-linear stiffness element is shown in fig (7.14). The linear responses using the softer spring, the stiffer spring, and the average spring stiffness are shown in figs (7.15) to (7.17) and should be compared with the exact response shown in fig (7.14). To ensure that the maximum values are not underestimated the softer spring should be used, but

the final decay is better represented by the stiffer linear system. The response from the average spring stiffness is approximately the response that would be estimated using parameters evaluated from a modal test on a system with bi-linear stiffness.

In both of the damping type non-linearities the linear system overestimates the response and thus provides a conservative estimate, but not necessarily a good prediction. For friction (figs (7.18) to (7.20)), the difference between the predicted and the exact responses is more noticeable later in the response, and in the examples shown the initial responses are very similar. With quadratic viscous damping, figs (7.21) & (7.22), the overestimation in the first part of the response is significant, and the amplitudes of the two time-histories converge at later times. As damping type non-linearities increase the overall damping in a system, the use of the underlying linear parameters to estimate a transient response prediction will produce a conservative estimate for any damping type non-linearity.

7.5 Discussion

Existing techniques for transient response prediction of non-linear systems require information on the system parameters. This involves evaluating the parameters from experimental tests when details of the structure are not available as a theoretical model. From the examples discussed in this chapter and other undocumented experimental modal analysis on non-linear structures, the initial indications are that trends in the data from a MDOF non-linear system correspond to the SDOF non-linear element, facilitating non-linear identification in MDOF systems. Also, any modes that appear to be linear can be analysed as such, but it must be remembered that as the whole structure is non-linear and if the effective non-linearity is increased then the non-linear effect may also be apparent those modes, thereby invalidating the initial analysis. When a non-linearity - eg friction - is quantified from the analysis, just as the viscous damping term evaluated is a modal quantity, then the non-linearity is not necessarily represented as a spatial quantity and will generally be the modal contribution of that non-linearity. This aspect of 'modal non-linearity' is a topic that requires further research.

One other area of modal analysis for MDOF non-linear systems that requires further attention is the influence of one mode on another. If a structure has two coupled modes, and the dominant mode appears to be linear, then its effects can be removed from the 'non-linear mode'. However, it is not necessarily valid to assume that the effect of the linear mode on the 'non-linear' mode is a linear relationship - the resulting change in response amplitude of the 'non-linear mode' due to the effect of 'linear modes' will result in a change in the effective non-linearity. When the situation is reversed, and the 'non-linear mode' is dominant, it appears that the effects of the 'non-linear mode' on the linear mode have a 'linear' relationship - or distortions would occur making both modes appear non-linear - but the influence of different types of 'non-linear modes' on the linear mode has yet to be determined. This problem will be extended when the coupling becomes stronger as the modes move closer together in frequency. In these cases, a situation is easily envisaged when both modes are clearly non-linear, and the effect of one mode on the other may also now be non-linear. The problem of decoupling two 'non-linear modes' to be able to

analyse each one separately with SDOF non-linear identification techniques, needs to be examined. It may be that this linear approach of separating the resonances is not applicable, and where there are two strongly coupled 'non-linear modes' the approach may be to analyse that section of the FRF as a whole.

Using the linear parameters of the system for transient response prediction of a non-linear system via the frequency domain has been examined for accuracy and applicability. For systems with only damping-type non-linearities, the underlying linear system always overestimates the response and provides an easy-to-use conservative estimate. This is particularly useful for friction and quadratic viscous damping where the viscous damping term can be isolated from the damping non-linearity by using a reciprocal-of-receptance type analysis on measured FRF data. Stiffness-type non-linearities affect the natural frequency, and hence the phase relationship in MDOF systems. In these cases, it is possible that the time-history at a specific point in time has two modes in phase with each other, whilst the linear prediction for the same point in time has the modes out of phase; this would result in a gross underestimation of the response from the linear model. In the examples shown, the linear predictions for cubic stiffness and backlash are reasonable, and it is envisaged that serious underestimation of maximum responses will only occur with large displacements or large non-linear elements in a system. For the response not to be underestimated in a system with bi-linear stiffness, the softer of the two springs should be used in the linear model. Any non-linear model - in either the frequency or the time domain - needs developing for MDOF systems with possibly an iterative process to account for the effects of the other elements in the system. It may be necessary to develop a non-linear model when a conservative estimate is not sufficient and a good transient response prediction is required.

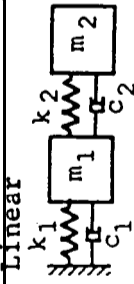
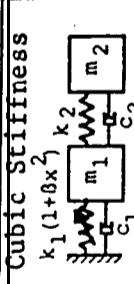
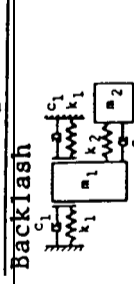
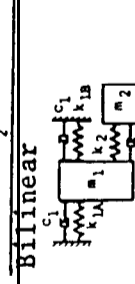
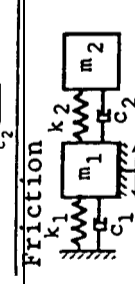
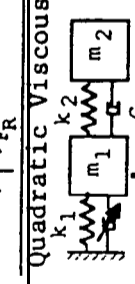
| | Non-Linearity | m_1/kg | m_2/kg | $k_1/\text{N/m}$ | $k_2/\text{N/m}$ | $C_1/\text{Ns/m}$ | $C_2/\text{Ns/m}$ | Forcing Conditions (Amplitude) |
|---|-----------------------------|-----------------|-----------------|------------------|------------------|-------------------|-------------------|--------------------------------|
|  | - | 1 | 1 | 62500 | 60000 | 10 | 10 | 1 |
|  | $\beta = 400 \text{ 1/m}^2$ | 1 | 1 | 62500 | 60000 | 10 | 10 | 50, 75, 100 |
|  | Gap = 0.000005 m | 1 | 1 | 62500 | 60000 | 10 | 10 | 1, 0.5 |
|  | K1B = 125000 N/m | 1 | 1 | 62500 | 60000 | 10 | 10 | 1, 2 |
|  | $R = F = 0.1 \text{ N/kg}$ | 1 | 1 | 62500 | 60000 | 10 | 10 | 5, 1, 2 |
|  | $q = \frac{d}{m}$ | 1 | 1 | 62500 | 60000 | 10 | 10 | 1, 2 |

Table 7.1 Physical description of each 2 degree-of-freedom system

| Non-linearity (Non-linearity and forcing amplitude see table 7.1) | Analysis | Natural Frequency | Modal Constant | Damping Loss Factor | Phase |
|--|---|-------------------|----------------|------------------------|--------|
| Linear | Nyquist | 24.450 | 0.26852 | 0.02466 | +1.01 |
| | Reciprocal-of- Receptance | 24.442 | 0.26781 | 0.02458 | 0.00 |
| Cubic 50 | Nyquist | 24.450 | 0.26888 | 0.02486 | +1.11 |
| | Reciprocal-of- Receptance | 24.442 | 0.26783 | 0.02477 | 0.00 |
| Cubic 75 | Nyquist | 26.150 | 0.25631 | 0.02679 | -61.61 |
| | Reciprocal-of- Receptance (pts above) | 24.783 | 0.21305 | 0.02143 | 0.00 |
| Cubic 100 | Nyquist | 26.750 | 0.24636 | 0.02790 | -63.23 |
| | Reciprocal-of- Receptance (pts above) | 24.929 | 0.20145 | 0.02236 | 0.00 |
| Backlash 1 | Nyquist | 24.395 | 0.25191 | 0.02273 | -25.68 |
| | Reciprocal-of- Receptance above | 24.425 | 0.16021 | 0.01472 | 0.00 |
| | below | 24.389 | 0.37161 | 0.03385 | 0.00 |
| | average | 24.407 | 0.26591 | 0.02428 | 0.00 |
| Backlash 5 | Nyquist | 24.335 | 0.21395 | 0.01895 | -51.72 |
| | Reciprocal-of- Receptance above | 24.403 | 0.05936 | 0.00538 | 0.00 |
| | below | 24.315 | 0.45697 | 0.04151 | 0.00 |
| | average | 24.359 | 0.25816 | 0.02344 | 0.00 |
| Bi-linear 1 | Nyquist | 26.955 | 0.20797 | 0.02678 | +1.31 |
| | Reciprocal-of- Receptance | 26.950 | 0.20729 | 0.02665 | 0.00 |
| Bi-linear 2 | Nyquist | 26.955 | 0.20791 | 0.02678 | +1.29 |
| | Reciprocal-of- Receptance | 26.950 | 0.20728 | 0.02664 | 0.00 |
| Friction 1 | Nyquist | 24.450 | 0.24863 | 0.02765 | +0.74 |
| | Reciprocal-of- Receptance | 24.443 | 0.27011 | 0.02888 | 0.00 |
| Friction 2 | Nyquist | 24.450 | 0.25958 | 0.02638 | +1.23 |
| | Reciprocal-of- Receptance | 24.443 | 0.26977 | 0.02700 | 0.00 |
| Friction 5 | Nyquist | 24.450 | 0.26484 | 0.02562 | +1.46 |
| | Reciprocal-of- Receptance | 24.443 | 0.26794 | 0.02569 | 0.00 |
| Quadratic Viscous 100 | Nyquist | 24.450 | 0.30009 | 0.03994 | -0.36 |
| | Reciprocal-of- Receptance | 24.444 | 0.2637 | 0.03827 | 0.00 |
| Quadratic Viscous 200 | Nyquist | 24.435 | 0.31792 | 0.05031 | +1.26 |
| | Reciprocal-of- Receptance | 24.442 | 0.26809 | 0.04681 | 0.00 |

Table 7.2 Parameters from Mode 1 point 1,1

| Non-linearity | Analysis | Natural Frequency | Modal Constant | Damping Loss Factor | Phase |
|-----------------------|--|-------------------|----------------|---------------------|--------|
| Linear | Nyquist | 63.415 | 0.72369 | 0.06516 | +0.56 |
| | Reciprocal-of-Receptance | 63.387 | 0.73411 | 0.06579 | 0.00 |
| Cubic 50 | Nyquist | 63.475 | 0.72745 | 0.06550 | -1.56 |
| | Reciprocal-of-Receptance | 63.418 | 0.73519 | 0.06602 | 0.00 |
| Cubic 75 | Nyquist | 63.500 | 0.72951 | 0.06524 | -0.83 |
| | Reciprocal-of-Receptance (pts above) | 63.459 | 0.73462 | 0.06559 | 0.00 |
| Cubic 100 | Nyquist | 63.690 | 0.72726 | 0.06502 | -7.84 |
| | Reciprocal-of-Receptance (pts above) | 63.514 | 0.73306 | 0.06556 | 0.00 |
| Backlash 1 | Nyquist | 62.995 | 0.69554 | 0.06242 | -24.29 |
| | Reciprocal-of-Receptance above below average | 62.515 | 0.69774 | 0.6373 | 0.00 |
| Backlash 5 | Nyquist | 62.620 | 0.58588 | 0.05235 | -51.96 |
| | Reciprocal-of-Receptance above below average | 61.728 | 0.62401 | 0.05781 | 0.00 |
| Bi-linear 1 | Nyquist | 66.785 | 0.78576 | 0.06199 | -0.27 |
| | Reciprocal-of-Receptance | 66.765 | 0.79110 | 0.06235 | 0.00 |
| Bi-linear 2 | Nyquist | 66.785 | 0.78575 | 0.06199 | -0.27 |
| | Reciprocal-of-Receptance | 66.765 | 0.79110 | 0.06235 | 0.00 |
| Friction 1 | Nyquist | 63.410 | 0.63597 | 0.07021 | +1.05 |
| | Reciprocal-of-Receptance | 63.393 | 0.73629 | 0.07584 | 0.00 |
| Friction 2 | Nyquist | 63.445 | 0.68271 | 0.06769 | -1.02 |
| | Reciprocal-of-Receptance | 63.396 | 0.73644 | 0.07061 | 0.00 |
| Friction 5 | Nyquist | 63.415 | 0.71337 | 0.06660 | +0.39 |
| | Reciprocal-of-Receptance | 63.396 | 0.73642 | 0.06791 | 0.00 |
| Quadratic Viscous 100 | Nyquist | 63.320 | 0.79413 | 0.07685 | +4.44 |
| | Reciprocal-of-Receptance | 63.391 | 0.73635 | 0.07419 | 0.00 |
| Quadratic Viscous 200 | Nyquist | 63.495 | 0.81298 | 0.08446 | -2.91 |
| | Reciprocal-of-Receptance | 63.393 | 0.73724 | 0.08065 | 0.00 |

Table 7.3 Parameters from Mode 2 point 1.1

| Non-linearity | Analysis | Natural Frequency | Modal Constant | Damping Loss Factor | Phase |
|-----------------------|--------------------------------------|--|----------------|---------------------|--------|
| Linear | Nyquist | 24.450 | 0.44368 | 0.02476 | +1.00 |
| | Reciprocal-of-Receptance | 24.453 | 0.44190 | 0.02475 | 0.00 |
| Cubic 50 | Nyquist | 26.700 | 0.444736 | 0.02623 | -70.73 |
| | Reciprocal-of-Receptance | 24.464 | 0.46664 | 0.03039 | 0.00 |
| Cubic 75 | Nyquist | 27.750 | 0.43913 | 0.02868 | -67.39 |
| | Reciprocal-of-Receptance (pts above) | 24.318 | 0.49113 | 0.03787 | 0.00 |
| Cubic 100 | Nyquist | | | | - |
| | Reciprocal-of-Receptance (pts above) | 24.173 | 0.50873 | 0.04602 | 0.00 |
| Backlash 1 | Nyquist | 24.395 | 0.43687 | 0.02430 | -10.99 |
| | Reciprocal-of-Receptance above | 24.397 | 0.36125 | 0.02014 | 0.00 |
| | below | 24.393 | 0.52283 | 0.02916 | 0.00 |
| | average | 24.395 | 0.44204 | 0.02465 | 0.00 |
| Backlash 5 | Nyquist | 24.375 | 0.41602 | 0.02289 | -28.16 |
| | Reciprocal-of-Receptance above | 24.386 | 0.25576 | 0.01414 | 0.00 |
| | below | 24.340 | 0.60106 | 0.03337 | 0.00 |
| | average | 24.363 | 0.42842 | 0.02375 | 0.00 |
| Bi-linear 1 | Nyquist | 26.955 | 0.39795 | 0.02674 | +1.17 |
| | Reciprocal-of-Receptance | 26.961 | 0.39933 | 0.02677 | 0.00 |
| Bi-linear 2 | Nyquist | | | | |
| | Reciprocal-of-Receptance | (Not measured - the same as Bi-linear 1) | | | |
| Friction 1 | Nyquist | 24.450 | 0.42412 | 0.02664 | +1.38 |
| | Reciprocal-of-Receptance | 24.453 | 0.44398 | 0.02722 | 0.00 |
| Friction 2 | Nyquist | 24.450 | 0.43486 | 0.02582 | +1.45 |
| | Reciprocal-of-Receptance | 24.454 | 0.44467 | 0.02612 | 0.00 |
| Friction 5 | Nyquist | | | | |
| | Reciprocal-of-Receptance | (Not measured - as linear) | | | |
| Quadratic Viscous 100 | Nyquist | 24.440 | 0.51519 | 0.04687 | +1.62 |
| | Reciprocal-of-Receptance | 24.452 | 0.44437 | 0.04423 | 0.00 |
| Quadratic Viscous 200 | Nyquist | 24.415 | 0.55377 | 0.06133 | +3.66 |
| | Reciprocal-of-Receptance | 24.446 | 0.44461 | 0.05574 | 0.00 |

Table 7.4 Parameters from Model Point 1,2

| Non-linearity | Analysis | Natural Frequency | Modal Constant | Damping Loss Factor | Phase |
|--------------------------|---|---------------------------------|----------------|---------------------|---------|
| Linear | Nyquist | 63.390 | 0.44686 | 0.06572 | -178.30 |
| | Reciprocal-of- Receptance | 63.414 | 0.45463 | 0.06604 | +180.00 |
| Cubic 50 | Nyquist | 63.340 | 0.45289 | 0.06612 | -175.04 |
| | Reciprocal-of- Receptance | 63.607 | 0.45191 | 0.06712 | +180.00 |
| Cubic 75 | Nyquist | 63.400 | 0.45341 | 0.06600 | -177.93 |
| | Reciprocal-of- Receptance (pts above) | 63.622 | 0.45187 | 0.06708 | +180.00 |
| Cubic 100 | Nyquist | 63.495 | 0.45146 | 0.06564 | +178.94 |
| | Reciprocal-of- Receptance (pts above) | 63.642 | 0.45088 | 0.06685 | +180.00 |
| Backlash 1 | Nyquist | 62.590 | 0.42005 | 0.05639 | +153.49 |
| | Reciprocal-of- Receptance above | 62.579 | 0.23007 | 0.03285 | +180.00 |
| | below | 62.593 | 0.61787 | 0.08819 | +180.00 |
| | average | 62.586 | 0.42397 | 0.06052 | +180.00 |
| Backlash 5 | Nyquist | 62.100 | 0.23707 | 0.03010 | +84.48 |
| | Reciprocal-of- Receptance above | (Too much distortion) | | | |
| | below | 61.499 | 0.65712 | 0.09159 | +180.00 |
| Bi-linear 1 | Nyquist | 66.790 | 0.40941 | 0.06234 | -178.40 |
| | Reciprocal-of- Receptance | 66.996 | 0.41383 | 0.06319 | +180.00 |
| Bi-linear 2 | Nyquist | (Not measured - as Bi-linear 1) | | | |
| | Reciprocal-of- Receptance | | | | |
| Friction 1 | Nyquist | 63.430 | 0.36188 | 0.07427 | +176.55 |
| | Reciprocal-of- Receptance | 63.663 | 0.45723 | 0.08616 | +180.00 |
| Friction 2 | Nyquist | 63.400 | 0.40733 | 0.06994 | +179.62 |
| | Reciprocal-of- Receptance | 63.633 | 0.45632 | 0.07598 | +180.00 |
| Friction 5 | Nyquist | (Not measured - as Bi-linear 1) | | | |
| | Reciprocal-of- Receptance | | | | |
| Quadratic Viscous 100 | Nyquist | 63.440 | 0.48012 | 0.07340 | +178.92 |
| | Reciprocal-of- Receptance | 63.619 | 0.45545 | 0.07316 | +180.00 |
| Quadratic Viscous 200 | Nyquist | 63.400 | 0.50135 | 0.07943 | +179.51 |
| | Reciprocal-of- Receptance | 63.633 | 0.45585 | 0.07760 | +180.00 |

Table 7.5 Parameters from Mode 2 point 1,2

| Non-linearity | Analysis | Natural Frequency | Nodal Constant | Damping Loss Factor | Phase |
|--------------------------|---|-------------------|----------------|---------------------|--------|
| Linear | Nyquist | 24.450 | 0.44283 | 0.02467 | +0.99 |
| | Reciprocal-of- Receptance | 24.453 | 0.44408 | 0.02472 | 0.00 |
| Cubic 50 | Nyquist | 24.450 | 0.44344 | 0.02487 | +1.08 |
| | Reciprocal-of- Receptance | 24.453 | 0.44412 | 0.02491 | 0.00 |
| Cubic 75 | Nyquist | 26.150 | 0.43047 | 0.02496 | -62.45 |
| | Reciprocal-of- Receptance (pts above) | 24.517 | 0.45327 | 0.02780 | 0.00 |
| Cubic 100 | Nyquist | 26.750 | 0.42330 | 0.02562 | -64.15 |
| | Reciprocal-of- Receptance (pts above) | 24.466 | 0.46676 | 0.03099 | 0.00 |
| Backlash 1 | Nyquist | 24.395 | 0.40797 | 0.02252 | 25 77 |
| | Reciprocal-of- Receptance above | 24.404 | 0.20074 | 0.01556 | 0.00 |
| | below | 24.370 | 0.57506 | 0.03196 | 0.00 |
| | average | 24.387 | 0.42790 | 0.02376 | 0.00 |
| Backlash 5 | Nyquist | 24.340 | 0.32739 | 0.01787 | 54.27 |
| | Reciprocal-of- Receptance above | 24.391 | 0.10276 | 0.00560 | 0.00 |
| | below | 24.274 | 0.68529 | 0.03787 | 0.00 |
| | average | 24.332 | 0.39402 | 0.02173 | 0.00 |
| Bi-linear 1 | Nyquist | 26.955 | 0.39848 | 0.02679 | +1.23 |
| | Reciprocal-of- Receptance | 26.961 | 0.39933 | 0.02683 | 0.00 |
| Bi-linear 2 | Nyquist | 26.955 | 0.39839 | 0.02679 | +1.20 |
| | Reciprocal-of- Receptance | 26.961 | 0.39931 | 0.02683 | 0.00 |
| Friction 1 | Nyquist | 24.450 | 0.41027 | 0.02768 | +0.79 |
| | Reciprocal-of- Receptance | 24.452 | 0.44385 | 0.02878 | 0.00 |
| Friction 2 | Nyquist | 24.450 | 0.42820 | 0.02640 | +1.21 |
| | Reciprocal-of- Receptance | 24.453 | 0.44252 | 0.02687 | 0.00 |
| Friction 5 | Nyquist | 24.450 | 0.43678 | 0.02563 | +1.43 |
| | Reciprocal-of- Receptance | 24.454 | 0.44417 | 0.02583 | 0.00 |
| Quadratic Viscous 100 | Nyquist | 24.450 | 0.49512 | 0.03996 | +0.26 |
| | Reciprocal-of- Receptance | 24.453 | 0.44485 | 0.03849 | 0.00 |
| Quadratic Viscous 200 | Nyquist | 24.440 | 0.52502 | 0.05034 | +1.33 |
| | Reciprocal-of- Receptance | 24.449 | 0.44439 | 0.04707 | 0.00 |

Table 7.6 Parameters from Mode 1 point 2,1

| Non-linearity | Analysis | Natural Frequency | Modal Constant | Damping Loss Factor | Phase |
|--------------------------|---|-------------------|--------------------|---------------------|--------------------|
| Linear | Nyquist | 63.400 | 0.44249 | 0.06538 | -179.4 |
| | Reciprocal-of- Receptance | 63.413 | 0.45016 | 0.06565 | +180.00 |
| Cubic 50 | Nyquist | 63.475 | 0.45293 | 0.06615 | +178.53 |
| | Reciprocal-of- Receptance | 63.628 | 0.45268 | 0.06744 | +180.00 |
| Cubic 75 | Nyquist | 63.500 | 0.45860 | 0.06639 | +179.26 |
| | Reciprocal-of- Receptance (pts above) | 63.669 | 0.454744 | 0.06729 | +180.00 |
| Cubic 100 | Nyquist | 63.540 | 0.45525 | 0.06639 | -179.49 |
| | Reciprocal-of- Receptance (pts above) | 63.724 | 0.45230 | 0.06744 | +180.00 |
| Backlash 1 | Nyquist | 62.600 | 0.47892 | 0.06652 | +178.15 |
| | Reciprocal-of- Receptance above below average | 62.720 | 0.46426 | 0.06722 | +180.00 |
| Backlash 5 | Nyquist | 62.400 | 0.44476 | 0.05770 | +144.50 |
| | Reciprocal-of- Receptance above | 62.029 | 0.33624 | 0.04751 | +180.00 |
| | Reciprocal-of- Receptance below average | 62.102 62.065 | 0.60125 0.46874 | 0.06556 0.06653 | +180.00 +180.00 |
| Bi-linear 1 | Nyquist | 66.785 | 0.40412 | 0.06190 | -179.59 |
| | Reciprocal-of- Receptance | 66.975 | 0.41616 | 0.06367 | +180.00 |
| Bi-linear 2 | Nyquist | 66.785 | 0.40413 | 0.06190 | -179.59 |
| | Reciprocal-of- Receptance | 66.975 | 0.41616 | 0.06375 | +180.00 |
| Friction 1 | Nyquist | 63.420 | 0.39885 | 0.07105 | +179.77 |
| | Reciprocal-of- Receptance | 63.636 | 0.45249 | 0.07712 | +180.00 |
| Friction 2 | Nyquist | 63.455 | 0.42522 | 0.06827 | +178.14 |
| | Reciprocal-of- Receptance | 63.621 | 0.45232 | 0.07183 | +180.00 |
| Friction 5 | Nyquist | 63.415 | 0.44325 | 0.06713 | -179.68 |
| | Reciprocal-of- Receptance | 63.612 | 0.45239 | 0.06916 | +180.00 |
| Quadratic Viscous 100 | Nyquist | 63.320 | 0.49950 | 0.07790 | -176.19 |
| | Reciprocal-of- Receptance | 63.631 | 0.45471 | 0.07592 | +180.00 |
| Quadratic Viscous 200 | Nyquist | 63.400 | 0.51869 | 0.08632 | +179.14 |
| | Reciprocal-of- Receptance | 63.657 | 0.46004 | 0.08324 | +180.00 |

Table 7.7 Parameters from Mode 2, point2,1

| Non-linearity | Analysis | Natural Frequency | Modal Constant | Damping Loss Factor | Phase |
|-----------------------|--------------------------------------|-------------------|---------------------------------|---------------------|--------|
| Linear | Nyquist | 24.450 | 0.73121 | 0.02472 | +0.98 |
| | Reciprocal-of-Receptance | 24.454 | 0.73317 | 0.02477 | 0.00 |
| Cubic 50 | Nyquist | 26.700 | 0.76101 | 0.02418 | -71.65 |
| | Reciprocal-of-Receptance | 24.641 | 0.68375 | 0.02424 | 0.00 |
| Cubic 75 | Nyquist | 27.750 | 0.78562 | 0.02559 | -68.39 |
| | Reciprocal-of-Receptance (pts above) | 24.695 | 0.68170 | 0.02626 | 0.00 |
| Cubic 100 | Nyquist | 28.665 | 0.75195 | 0.02491 | -75.43 |
| | Reciprocal-of-Receptance (pts above) | 24.796 | 0.67152 | 0.02787 | 0.00 |
| Backlash 1 | Nyquist | 24.395 | 0.71221 | 0.02416 | -11.03 |
| | Reciprocal-of-Receptance | | | | |
| | above | 24.417 | 0.56235 | 0.01916 | 0.00 |
| | below | 24.397 | 0.86769 | 0.02945 | 0.00 |
| average | 24.407 | 0.71502 | 0.02430 | 0.00 | |
| Backlash 5 | Nyquist | 24.375 | 0.67067 | 0.02262 | -28.22 |
| | Reciprocal-of-Receptance | | | | |
| | above | 24.418 | 0.37979 | 0.01290 | 0.00 |
| | below | 24.367 | 1.02081 | 0.03464 | 0.00 |
| average | 24.392 | 0.70030 | 0.02377 | 0.00 | |
| Bi-linear 1 | Nyquist | 26.955 | 0.76208 | 0.02674 | +1.08 |
| | Reciprocal-of-Receptance | 26.957 | 0.76424 | 0.02672 | 0.00 |
| Bi-linear 2 | Nyquist | | | | |
| | Reciprocal-of-Receptance | | (Not measured - as Bi-linear 1) | | |
| Friction 1 | Nyquist | 24.450 | 0.69898 | 0.02664 | +1.36 |
| | Reciprocal-of-Receptance | 24.450 | 0.73068 | 0.02718 | 0.00 |
| Friction 2 | Nyquist | 24.450 | 0.71667 | 0.02582 | +1.43 |
| | Reciprocal-of-Receptance | 24.451 | 0.73165 | 0.02608 | 0.00 |
| Friction 5 | Nyquist | | | | |
| | Reciprocal-of-Receptance | | (Not measured - as linear) | | |
| Quadratic Viscous 100 | Nyquist | 24.445 | 0.84949 | 0.04687 | +1.51 |
| | Reciprocal-of-Receptance | 24.455 | 0.73150 | 0.04413 | 0.00 |
| Quadratic Viscous 200 | Nyquist | 24.425 | 0.91387 | 0.06137 | +3.49 |
| | Reciprocal-of-Receptance | 24.458 | 0.73426 | 0.05560 | 0.00 |

Table 7.8 Parameters from Mode 1, point 2.2

| Non-linearity | Analysis | Natural Frequency | Modal Constant | Damping Loss Factor | Phase |
|-----------------------|--------------------------------------|---------------------------------|----------------|---------------------|--------|
| Linear | Nyquist | 63.390 | 0.26879 | 0.06542 | +1.80 |
| | Reciprocal-of-Receptance | 63.413 | 0.25738 | 0.06457 | 0.00 |
| Cubic 50 | Nyquist | 63.350 | 0.26823 | 0.06541 | +4.54 |
| | Reciprocal-of-Receptance | 63.423 | 0.25830 | 0.06466 | 0.00 |
| Cubic 75 | Nyquist | 63.440 | 0.26663 | 0.06516 | +0.40 |
| | Reciprocal-of-Receptance (pts above) | 63.442 | 0.25524 | 0.06414 | 0.00 |
| Cubic 100 | Nyquist | 63.495 | 0.26863 | 0.06535 | -0.99 |
| | Reciprocal-of-Receptance (pts above) | 63.462 | 0.25615 | 0.06419 | 0.00 |
| Backlash 1 | Nyquist | 62.880 | 0.26960 | 0.05593 | -42.26 |
| | Reciprocal-of-Receptance above | 62.690 | 0.15175 | 0.03164 | 0.00 |
| | below | 62.408 | 0.40663 | 0.08577 | 0.00 |
| | average | 62.549 | 0.27919 | 0.05870 | 0.00 |
| Backlash 5 | Nyquist | 62.090 | 0.20841 | 0.03854 | -90.01 |
| | Reciprocal-of-Receptance above | (Too much distortion) | | | |
| | below | 61.695 | 0.58502 | 0.10949 | 0.00 |
| | average | | | | |
| Bi-linear 1 | Nyquist | 66.780 | 0.20786 | 0.06187 | +2.87 |
| | Reciprocal-of-Receptance | 66.822 | 0.19789 | 0.06112 | 0.00 |
| Bi-linear 2 | Nyquist | (Not measured - as Bi-linear 1) | | | |
| | Reciprocal-of-Receptance | | | | |
| Friction 1 | Nyquist | 63.450 | 0.22843 | 0.07613 | -6.27 |
| | Reciprocal-of-Receptance | 63.312 | 0.20730 | 0.07284 | 0.00 |
| Friction 2 | Nyquist | 63.455 | 0.24938 | 0.07054 | -3.70 |
| | Reciprocal-of-Receptance | 63.378 | 0.23325 | 0.06865 | 0.00 |
| Friction 5 | Nyquist | (Not measured - as linear) | | | |
| | Reciprocal-of-Receptance | | | | |
| Quadratic Viscous 100 | Nyquist | 63.390 | 0.28027 | 0.07236 | +1.07 |
| | Reciprocal-of-Receptance | 63.401 | 0.26610 | 0.07120 | 0.00 |
| Quadratic Viscous 200 | Nyquist | 63.390 | 0.20824 | 0.07792 | +0.38 |
| | Reciprocal-of-Receptance | 63.388 | 0.27127 | 0.07633 | 0.00 |

Table 7.9 Parameters from Mode 2, point 2,2

| Mode | Frequency (Hz) | Modal Constant (1/kg) | Phase (deg) | Damping Loss Factor |
|------|-------------------|-----------------------------|----------------|------------------------|
| 1 | 27 | 0.7839 | 0 | 0.02764 |
| 2 | 54 | 0.0142 | 0 | 0.00898 |
| 3 | 67 | 0.23078 | 0 | 0.06348 |

Table 7.10 Results from using 'Ident' type analysis of Point (2,2) of the 2 degree-of-freedom system with bi-linear stiffness (fig 7.3d)

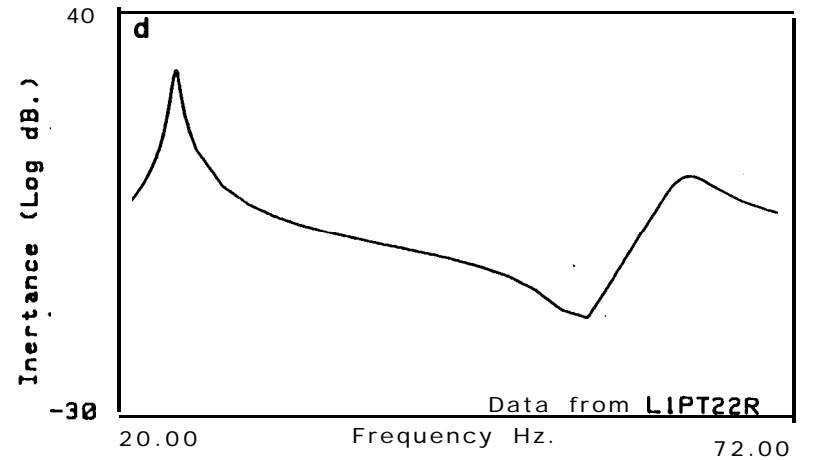
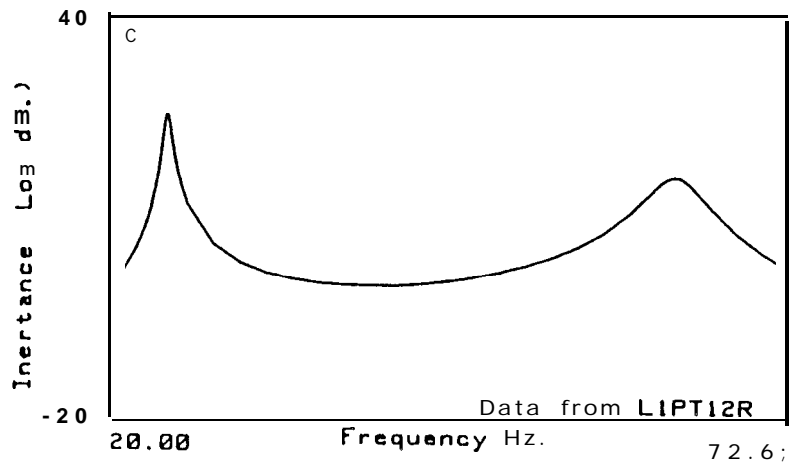
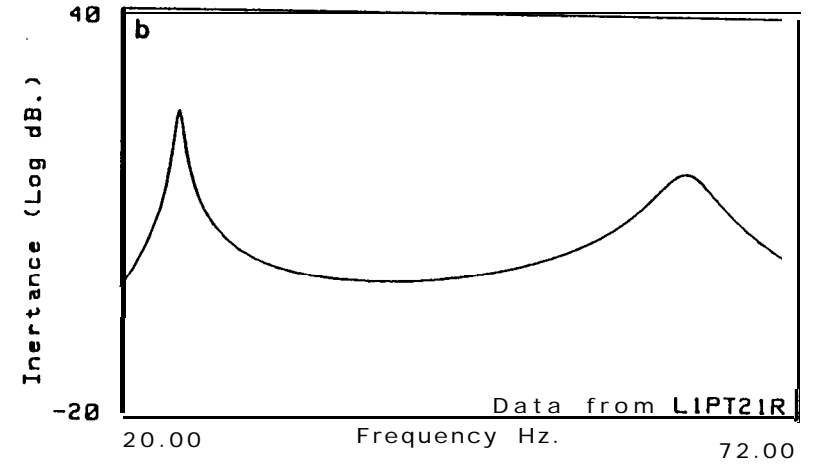
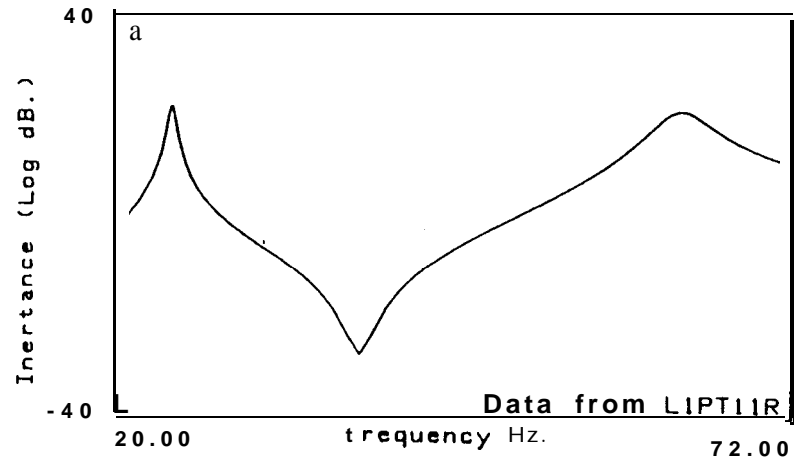


Fig 7.1 FRFs from a linear system
a FRF (11); b FRF (21)
c FRF (12); d FRF (22)

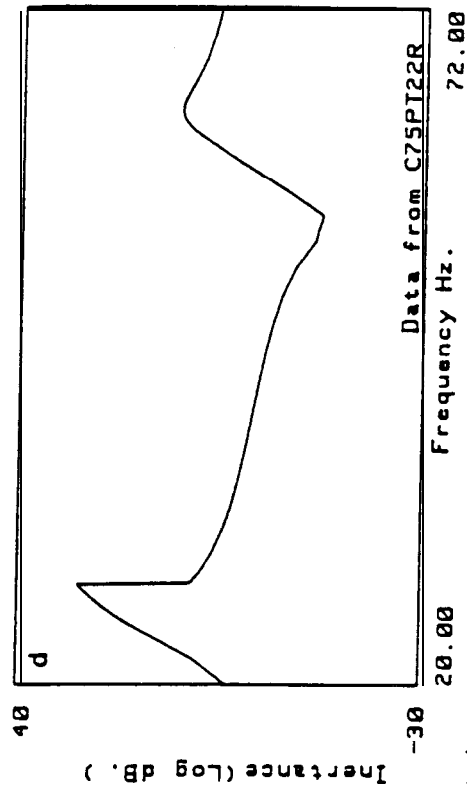
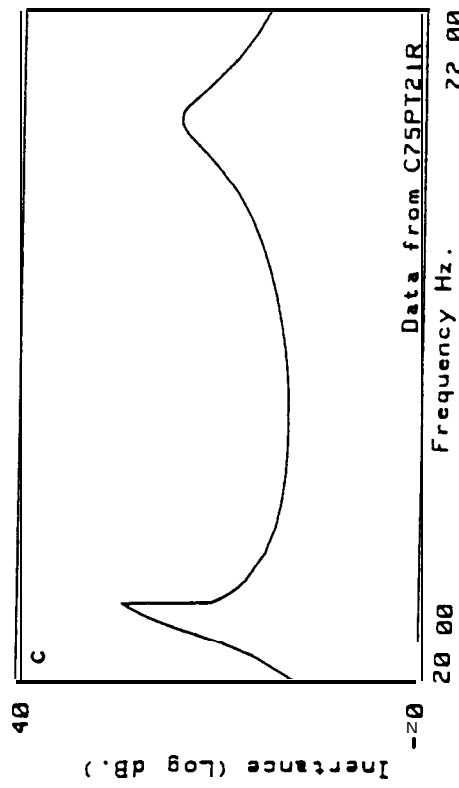
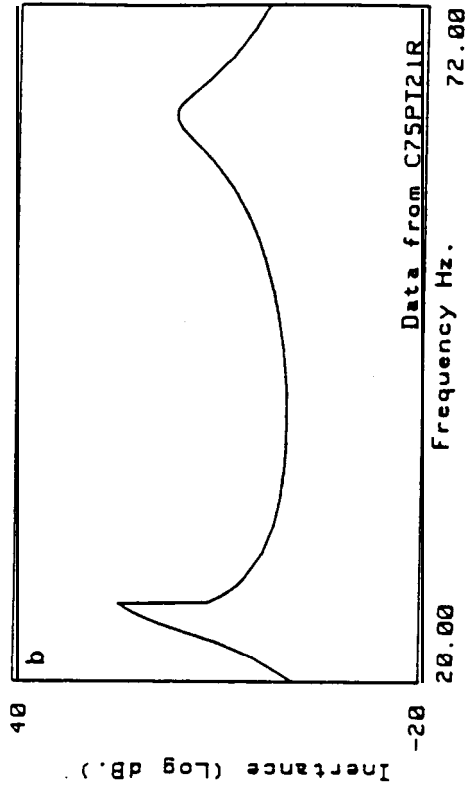
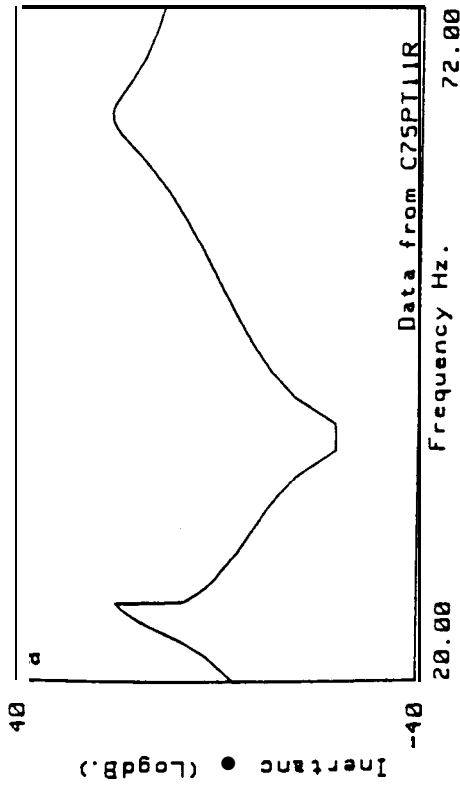


Fig 7.2 FRFs from a system with cubic stiffness subjected to a constant-force sine test (force amplitude 75)
 a FRF (1 1); b FRF (2 1)
 c FRF (1 2); d FRF (2 2)

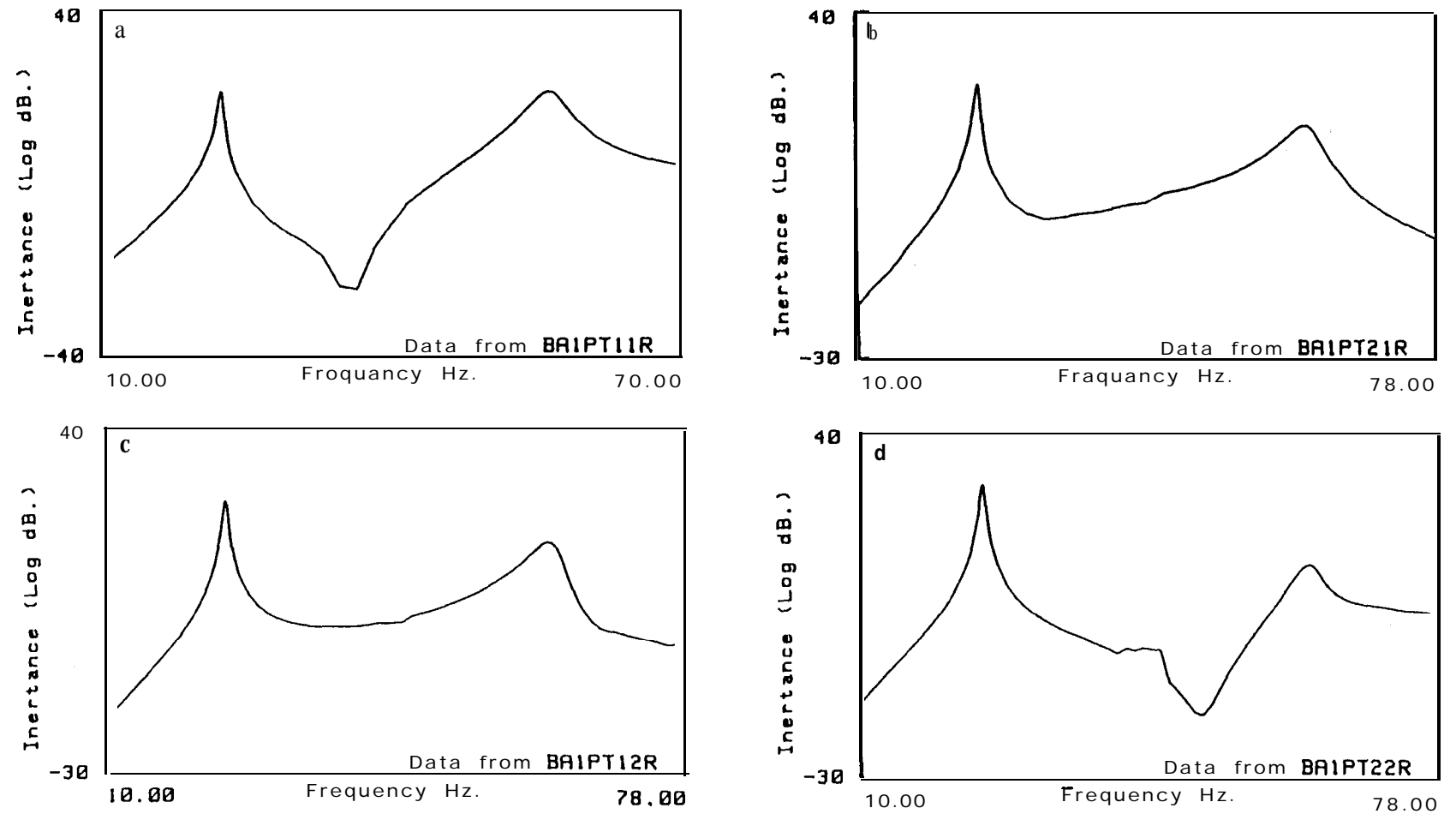


Fig 7.3 FRFs from a system with back1 ash subjected to a constant-force sine test (force amplitude1)
 a FRF (11); b FRF (21)
 c FRF (12); d FRF (22)

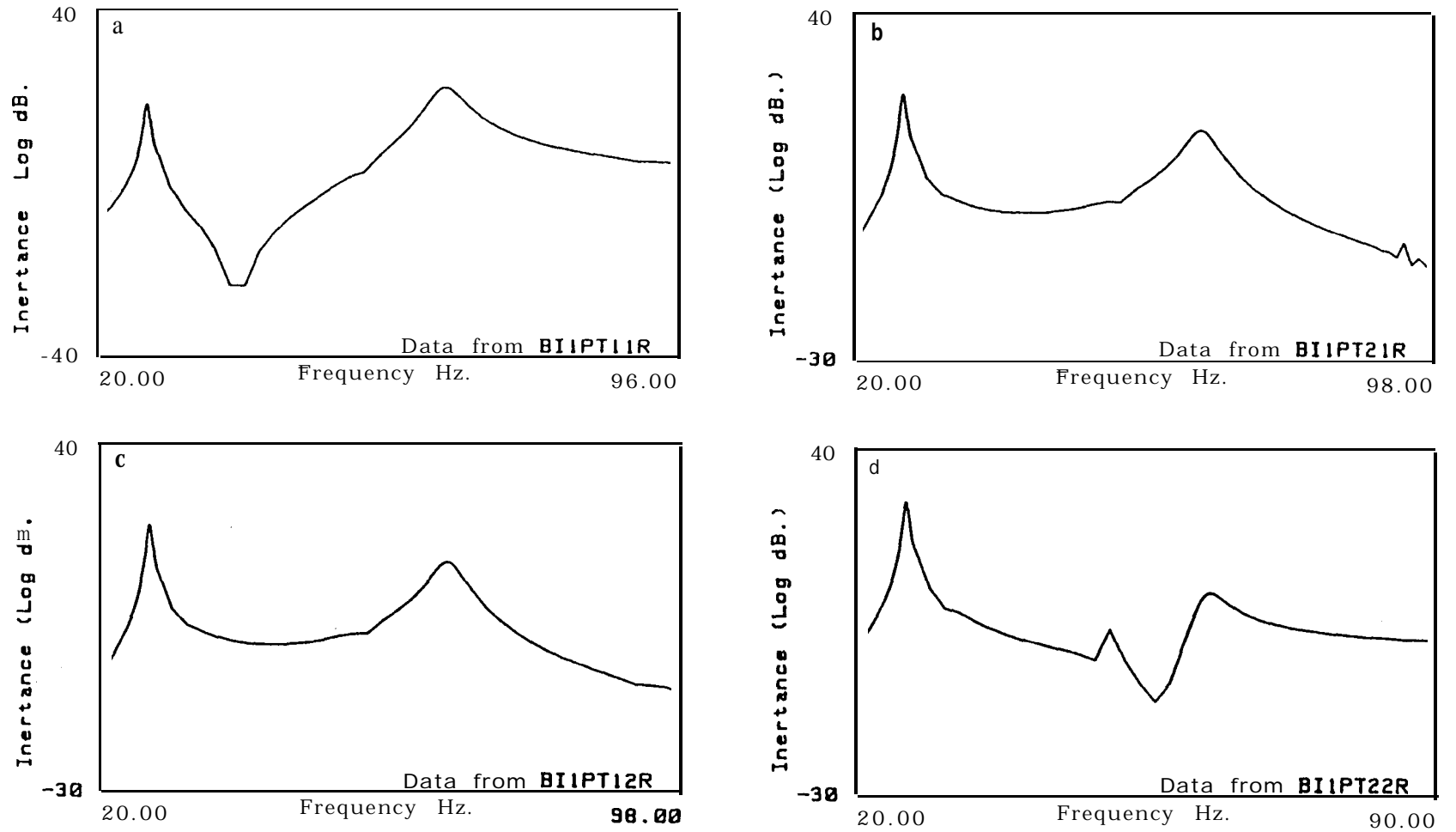


Fig 7.4 FRFs from a system with bi-linear stiffness subjected to a constant-force sine test
 a FRF (11); b FRF (21)
 c FRF (12); d FRF (22)

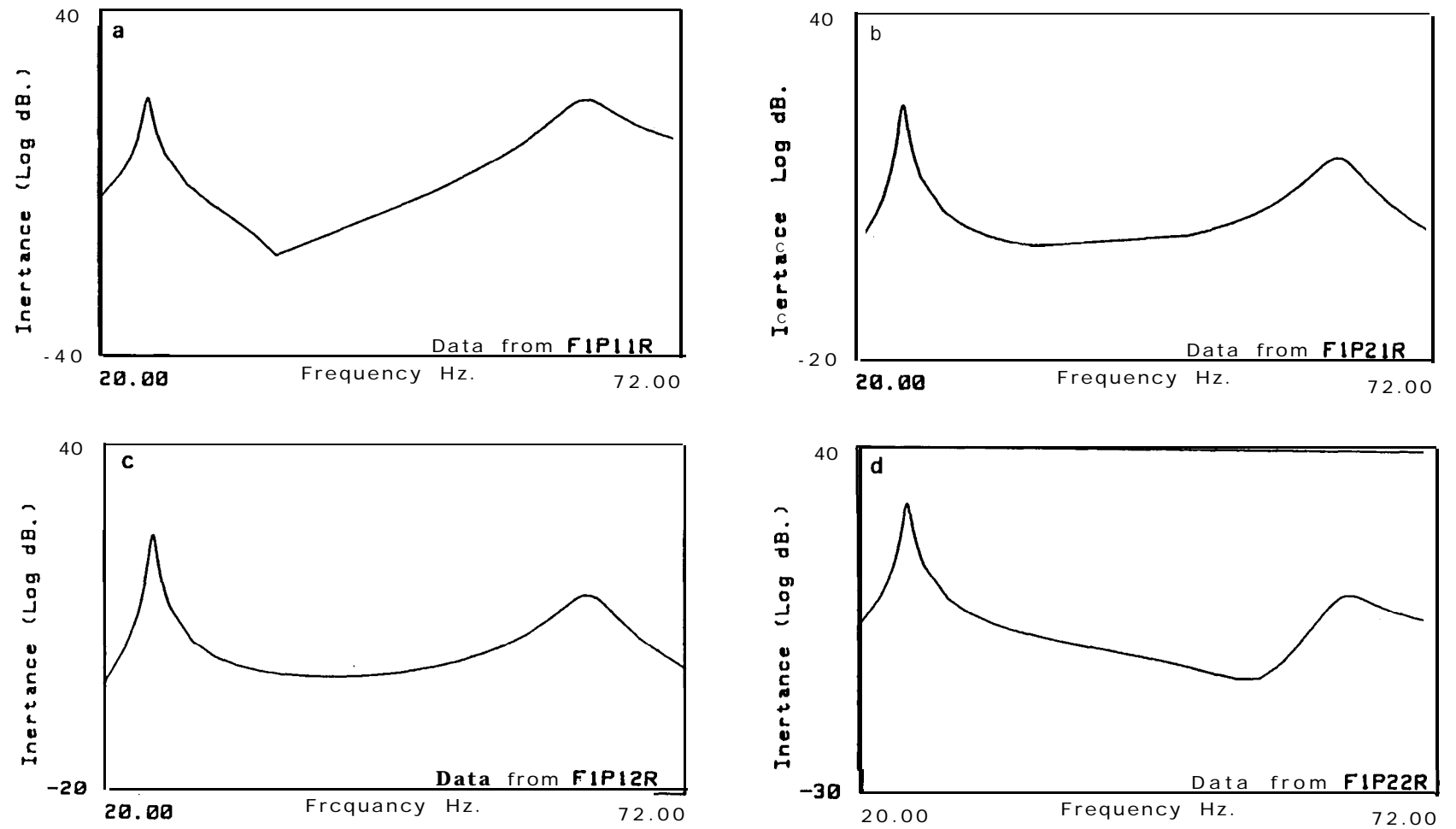


Fig 7.5 FRFs from a system with friction subjected to a constant-force sine test (force amplitude 0.1)
 a FRF (1 1); b FRF (2 1)
 c FRF (1 2); d FRF (2 2)

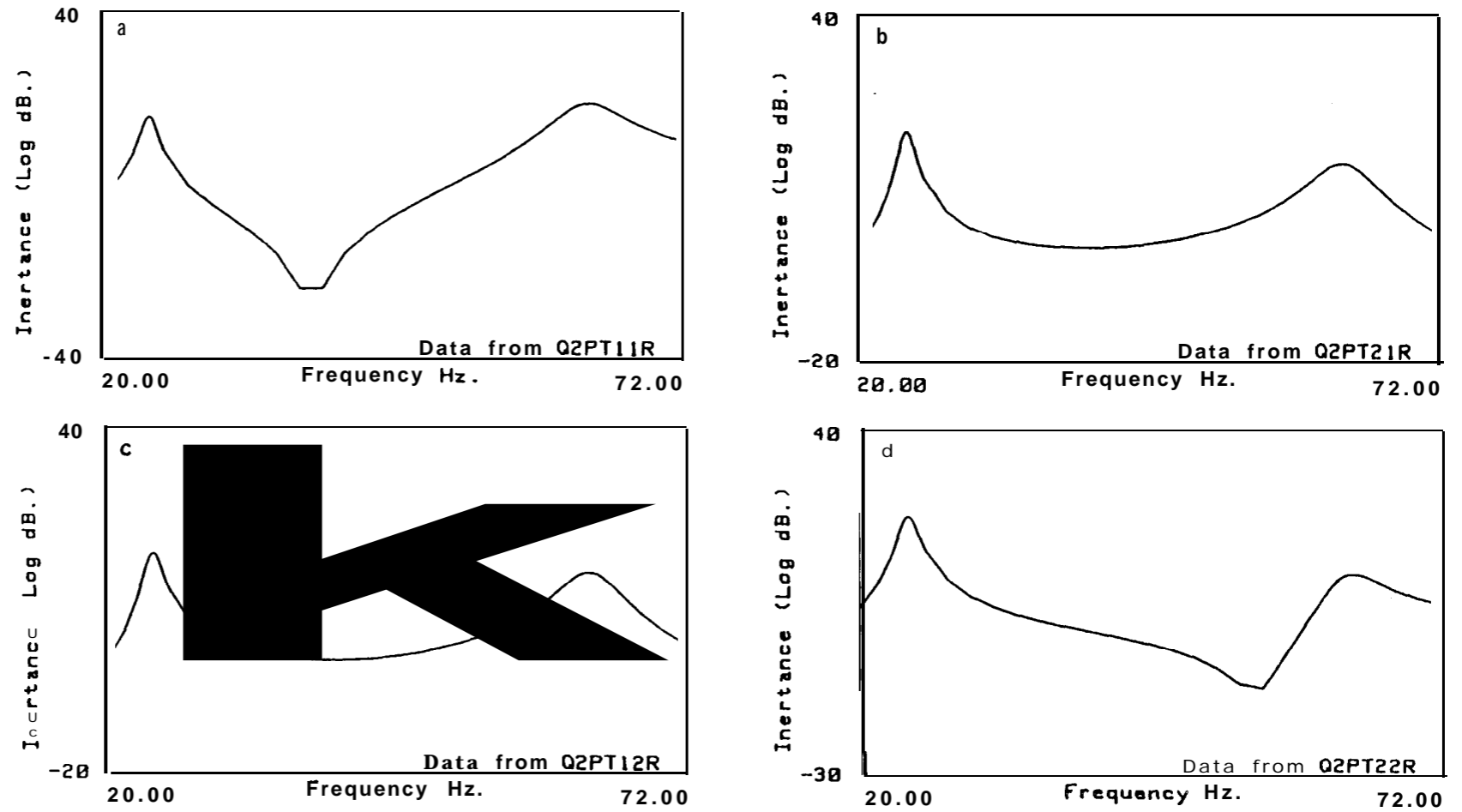


Fig 7.6 FRFs from a system with quadratic viscous damping
 subjected to a constant-force sine test (force amplitude 2)
 a FRF (11); b FRF (21)
 c FRF (12); d FRF (22)

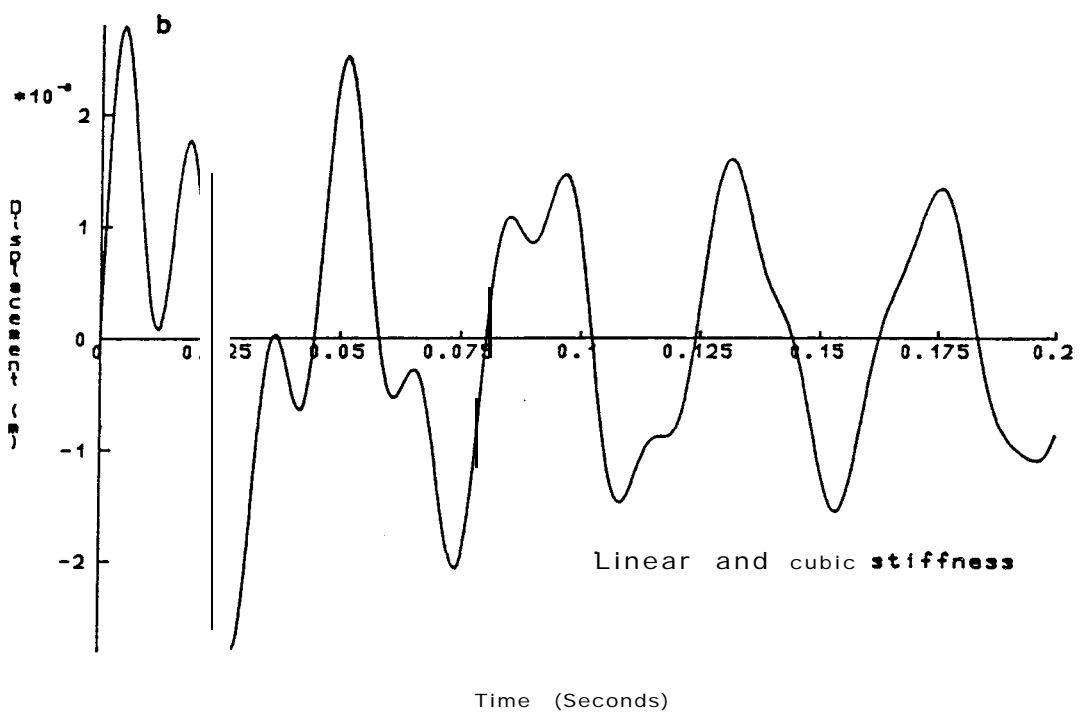
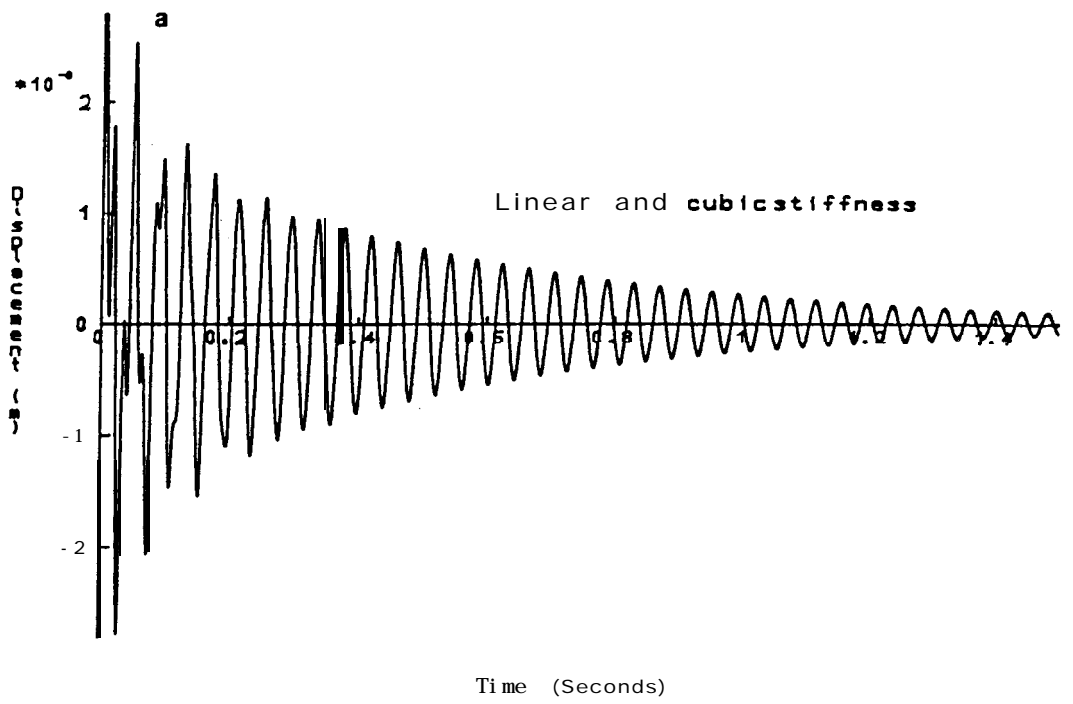


Fig 7.7 IRFs from a system with cubic stiffness and a linear system: $v(0) = 1.0$ m/s
a Response up to 1.5 seconds
b Expanded response for first 0.2 seconds

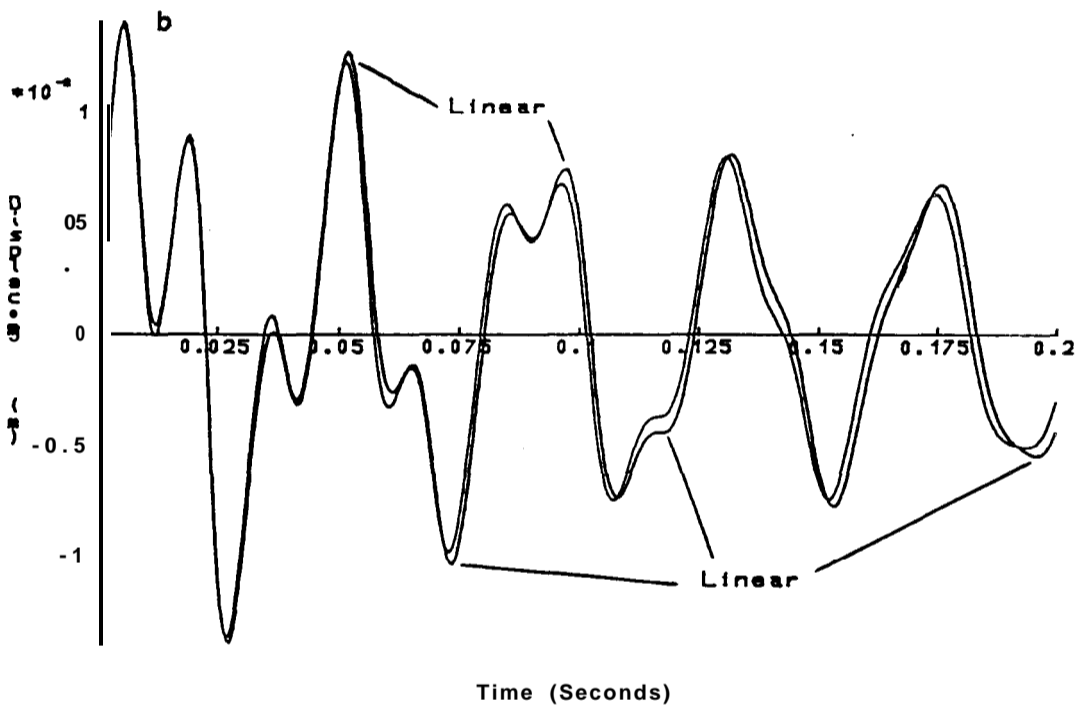
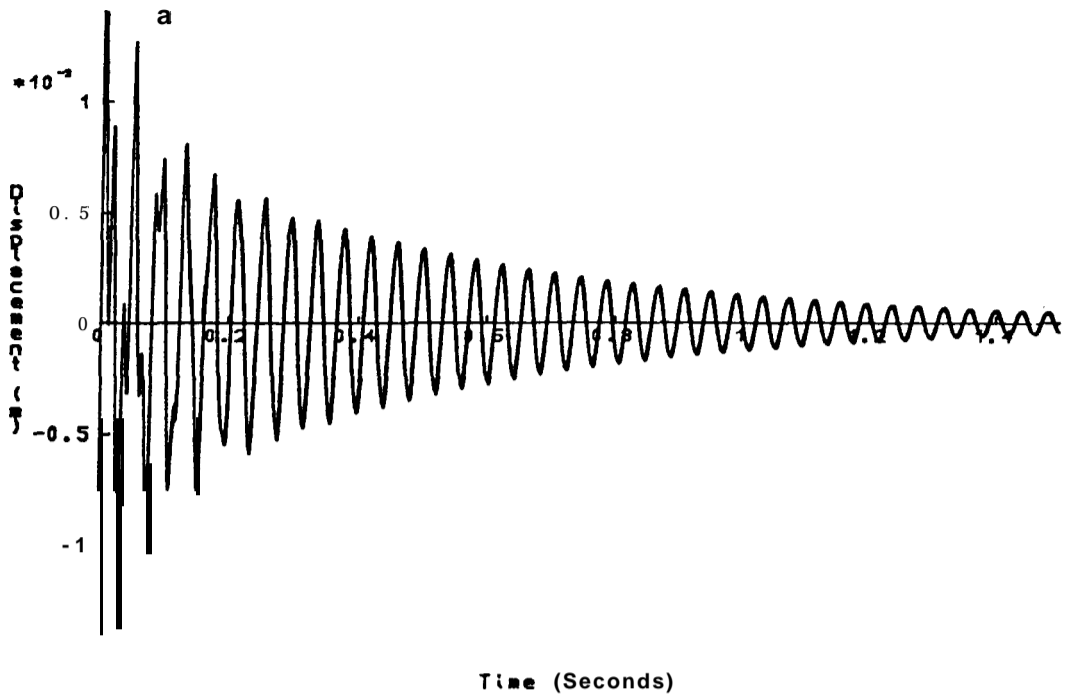


Fig 7.8 IRFs from a system with cubic stiffness and a linear system; $v(0) = 5.0$ m/s
 a Response up to 1.5 seconds
 b Expanded response for first 0.2 seconds

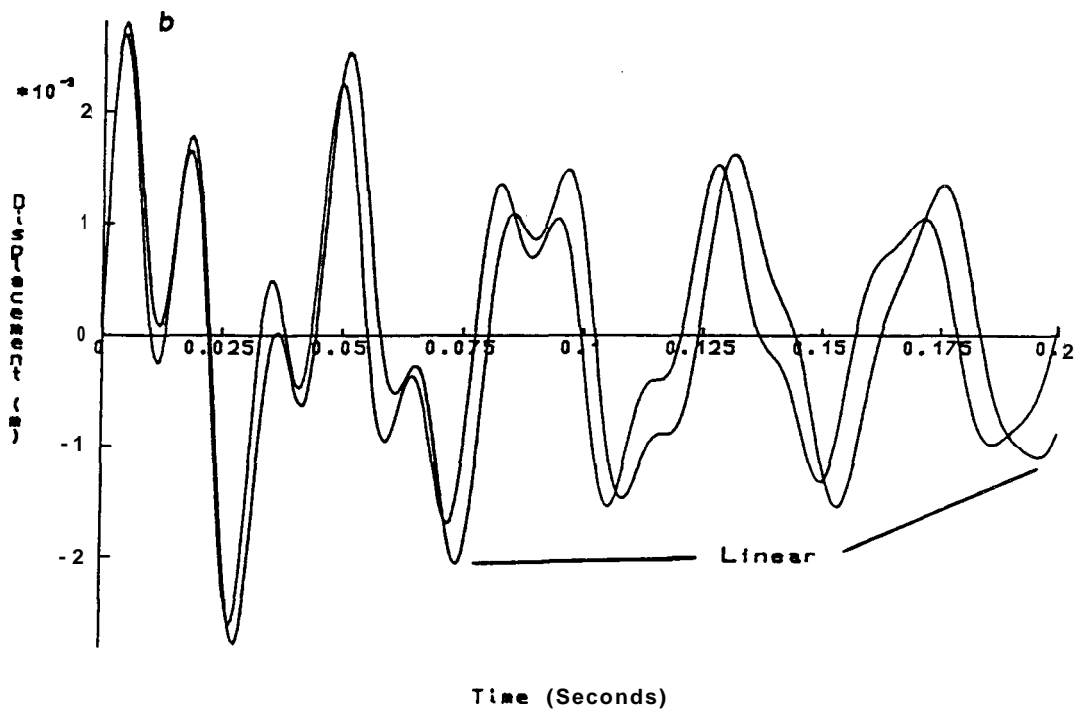
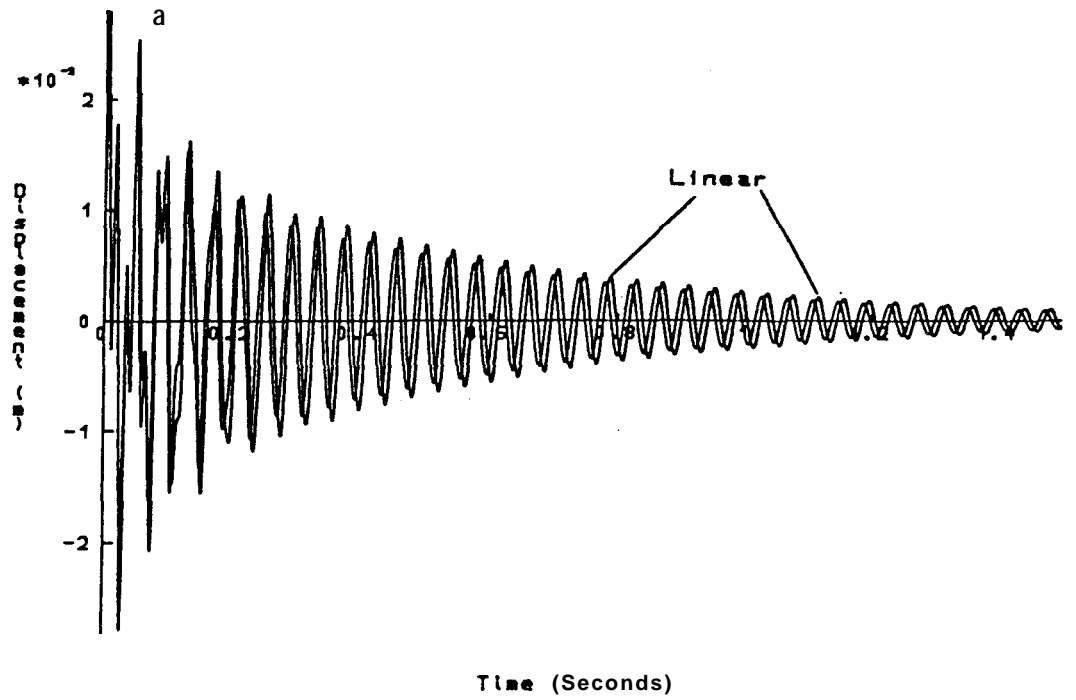


Fig 7.9 IRFs from a system with cubic stiffness and a linear system; $v(0)=10.0$ m/s
a Response up to 1.5 seconds
b Expanded response for first 8.2 seconds

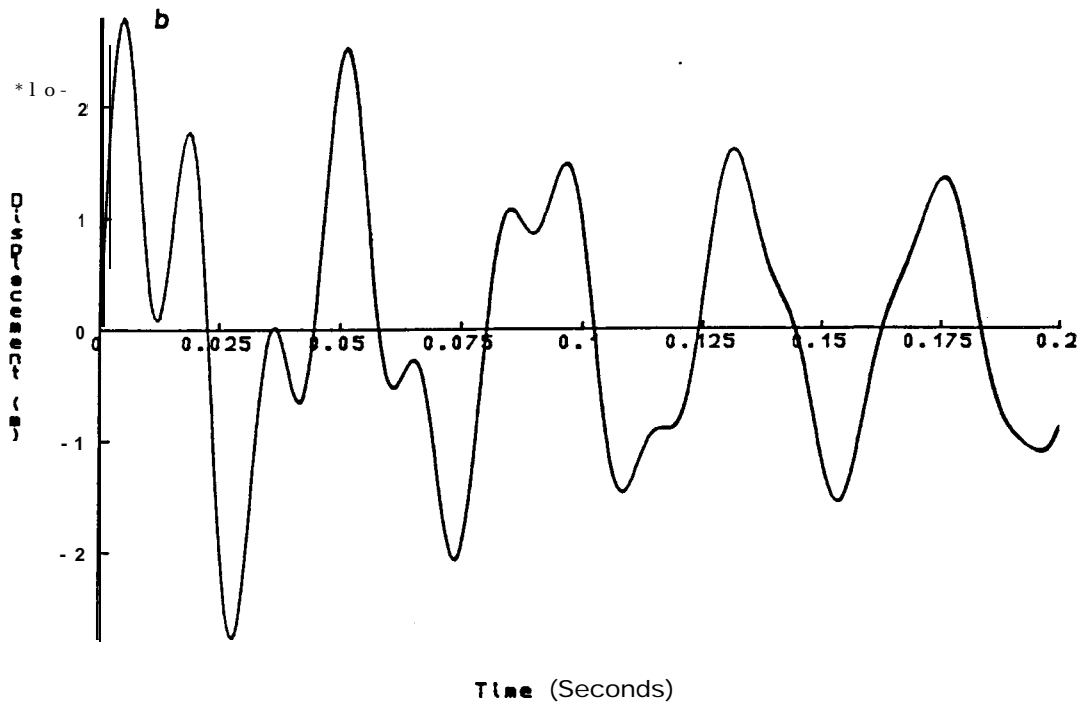
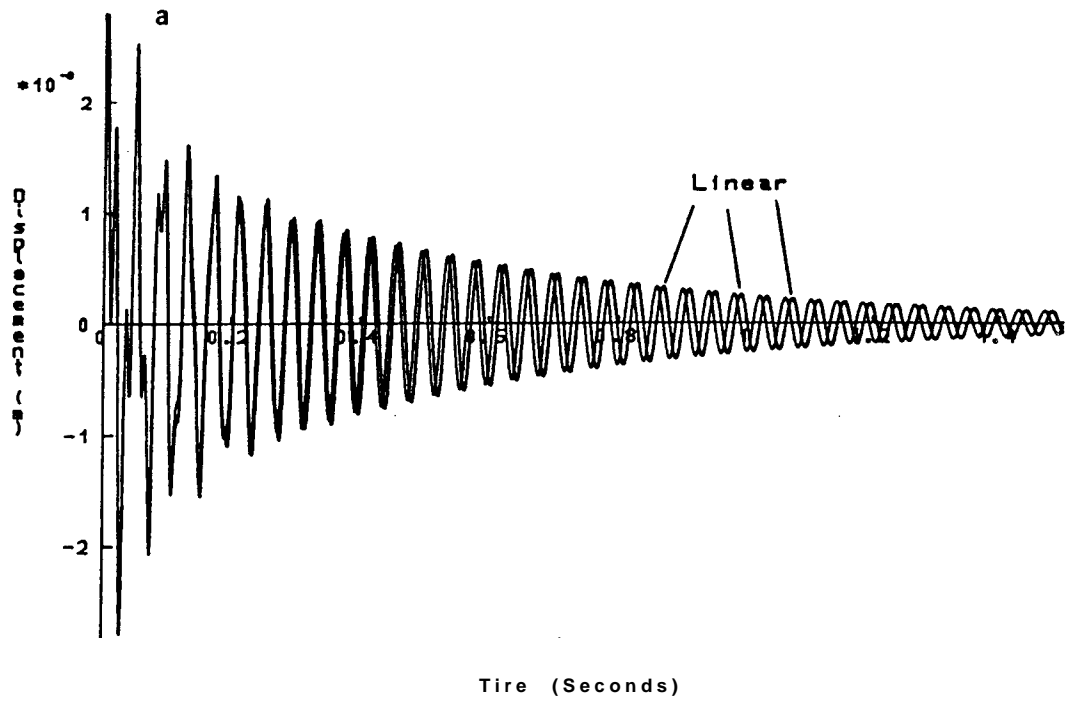


Fig 7.10 IRFs from a system with backlash and a 1 insar system: $v(0) = 1.0$ m/s
 a Response up to 1.5 seconds
 b Expanded response for first 0.2 seconds

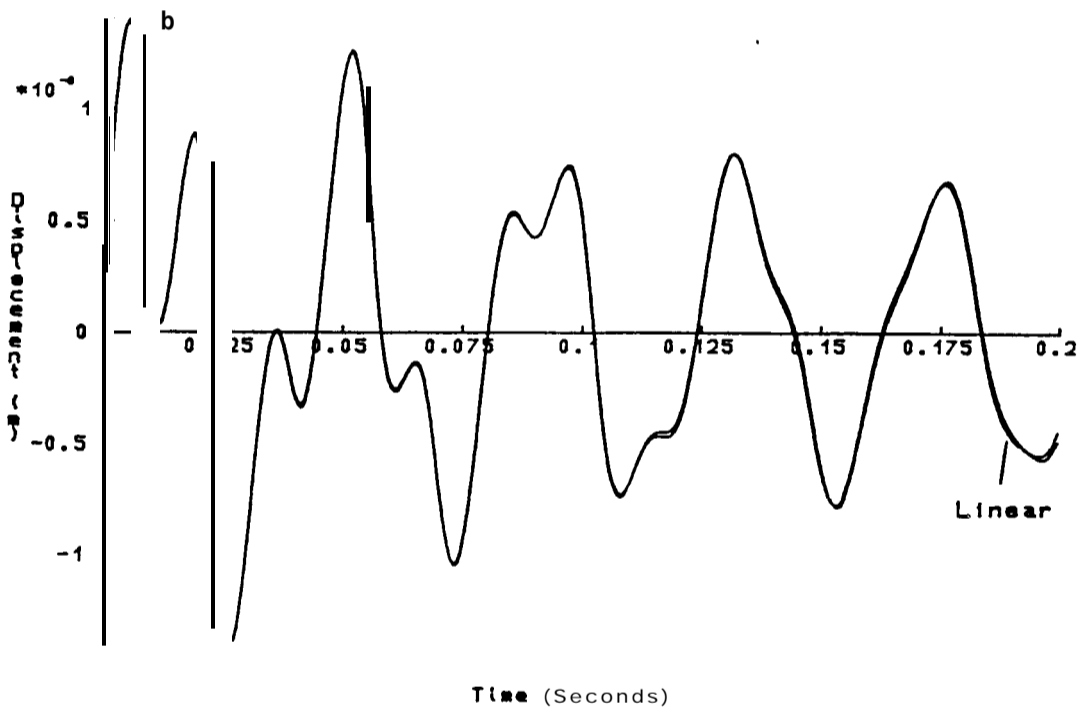
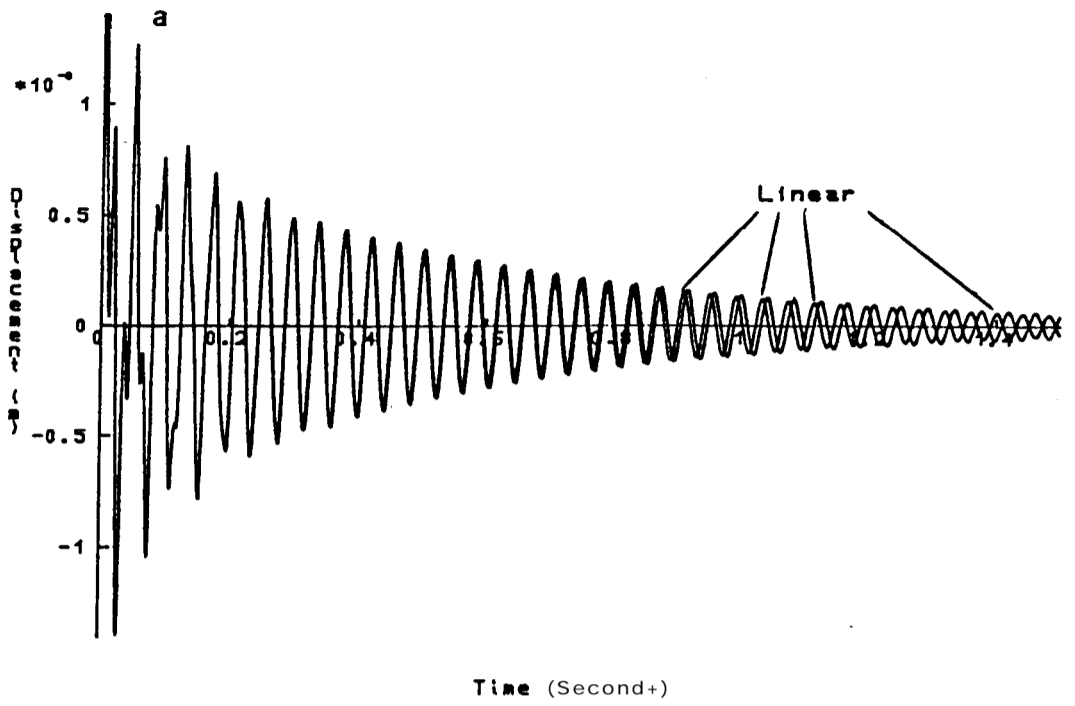


Fig 7.11 IRFs from a system with backlash and a linear system: $v(0) = 5.5$ m/s
 a Response up to 1.5 seconds
 b Expanded response for first 0.2 seconds

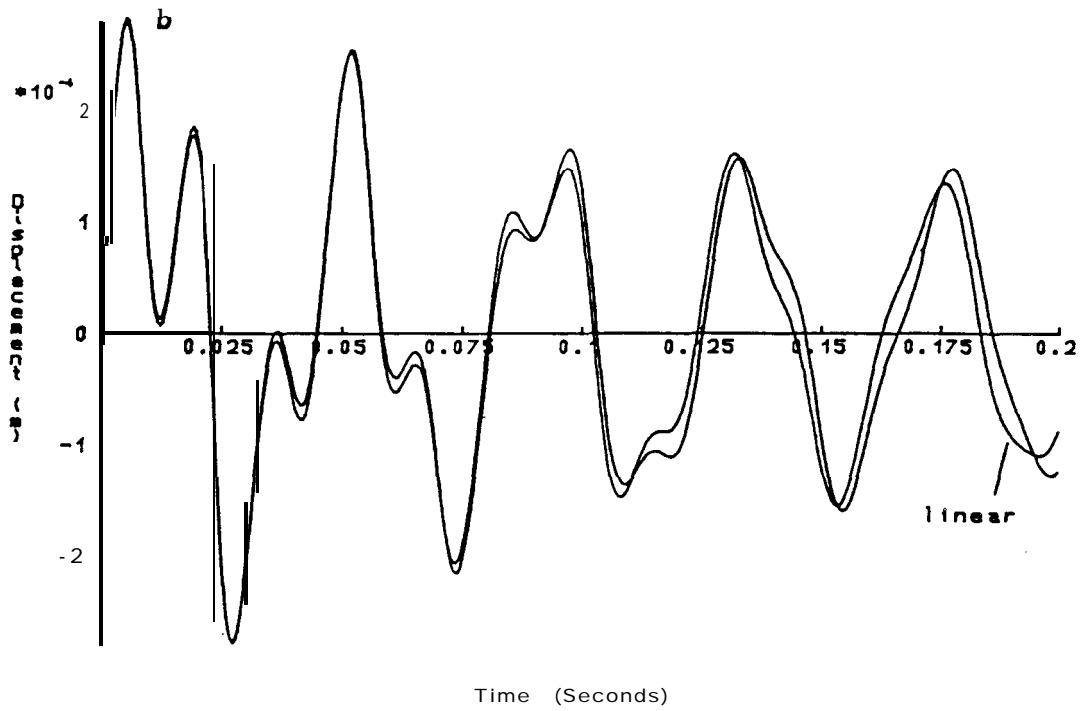
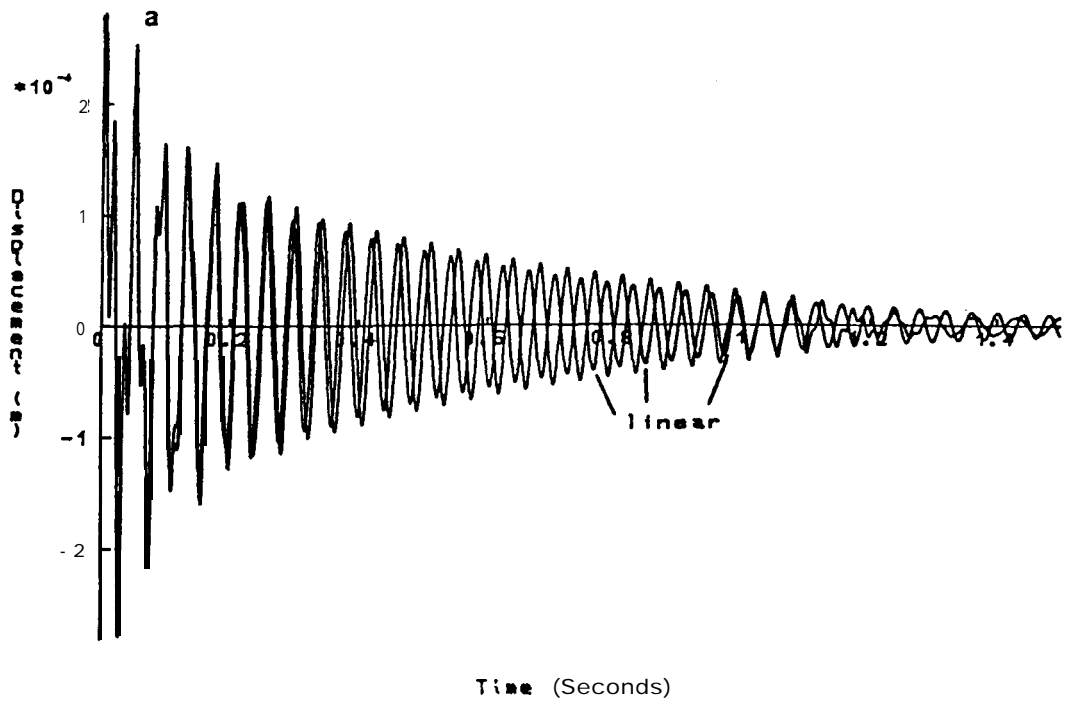


Fig 7.12 IRFs from a system with backlash and a linear system: $v(0) = 0.1 \text{ m/s}$
 a Response up to 1.5 seconds
 b Expanded response for first 0.2 seconds

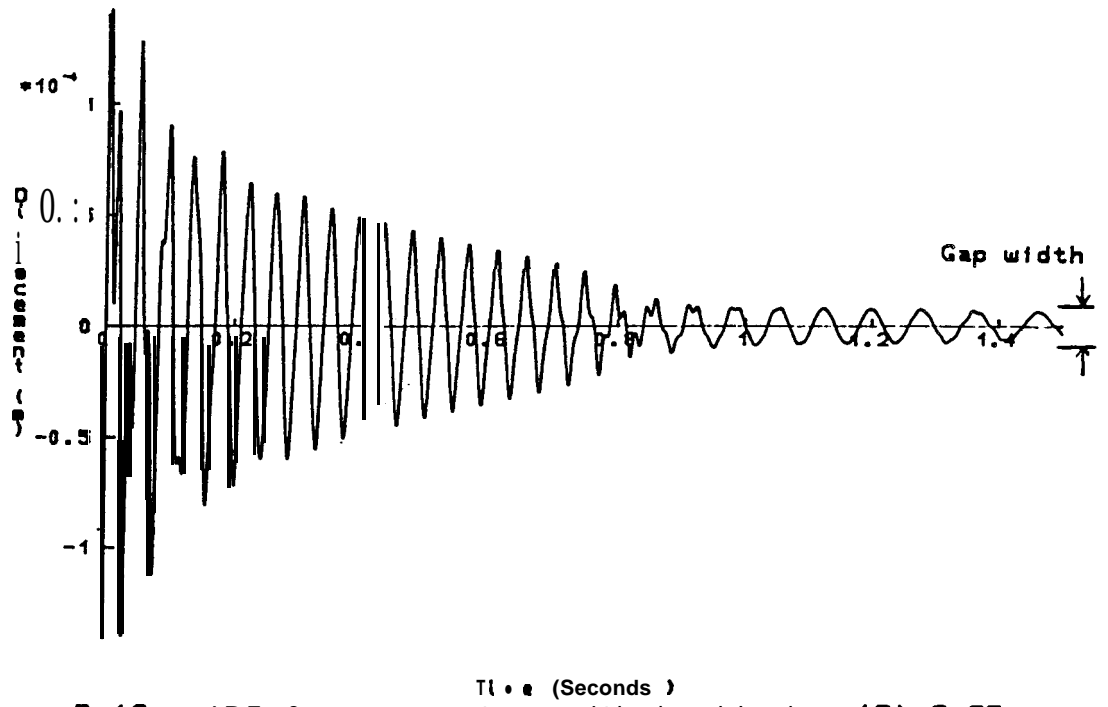


Fig 7.13a IRF from a system with backlash; $v(0) = 0.05 \text{ m/s}$

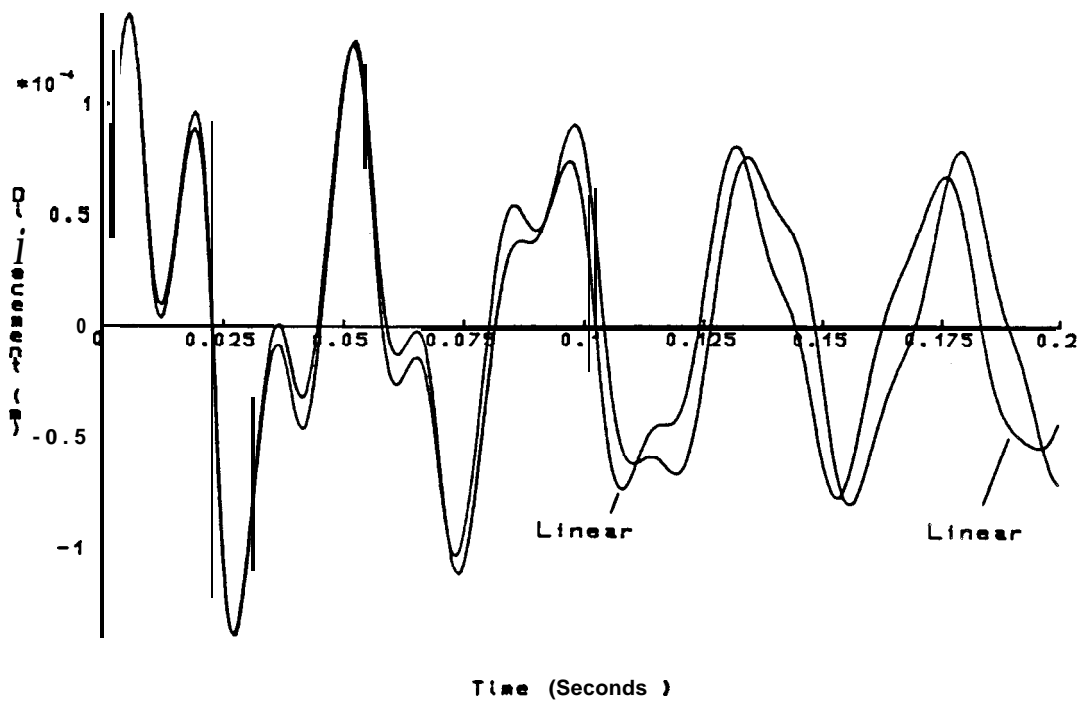


Fig 7.13b Expanded view (up to 0.2 seconds) of IRFs from a system with backlash and a linear system; $v(0) = 0.05 \text{ m/s}$

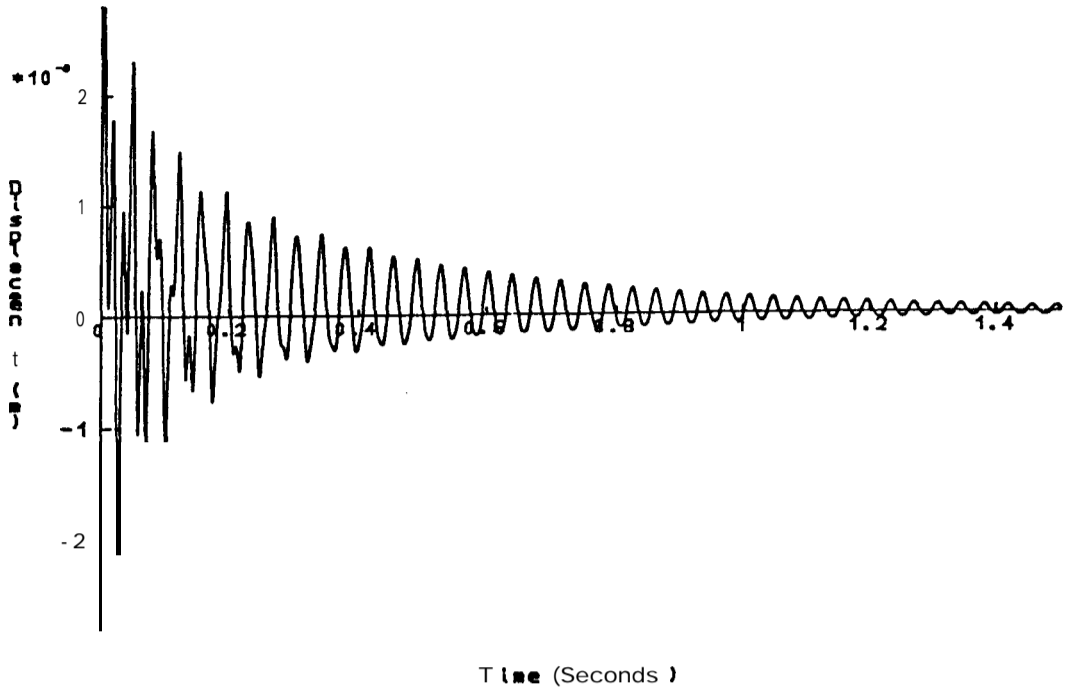


Fig 7.14 IRF from a system with bi-linear stiffness

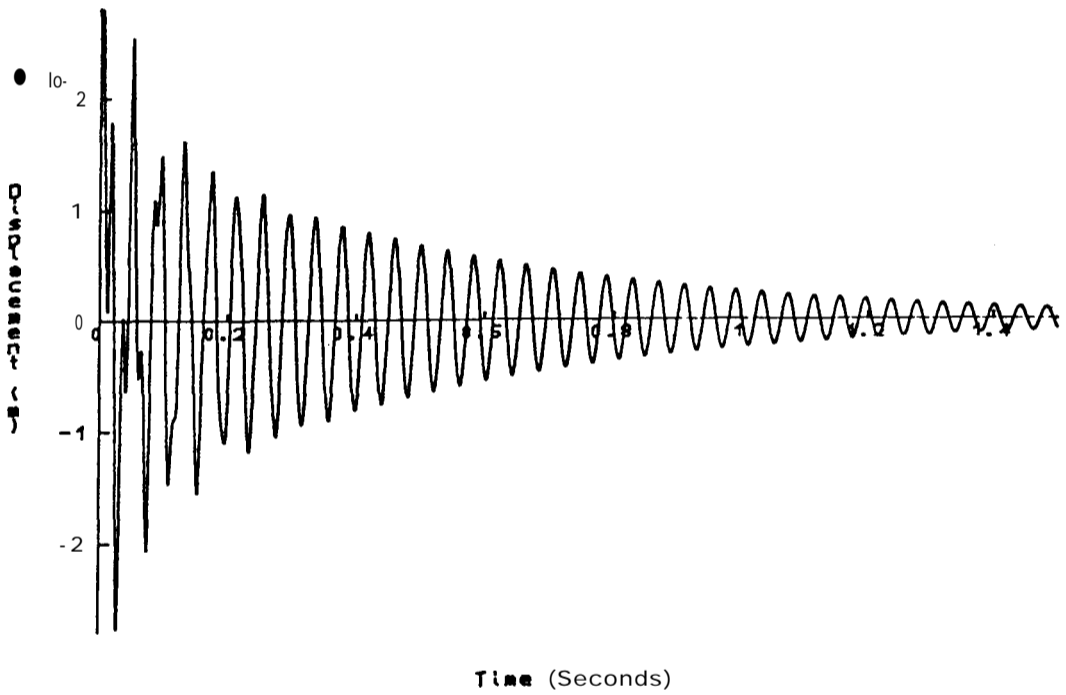


Fig 7.15 Predicted IRF for a system with bi-linear stiffness using a linear model with the softer of the two springs

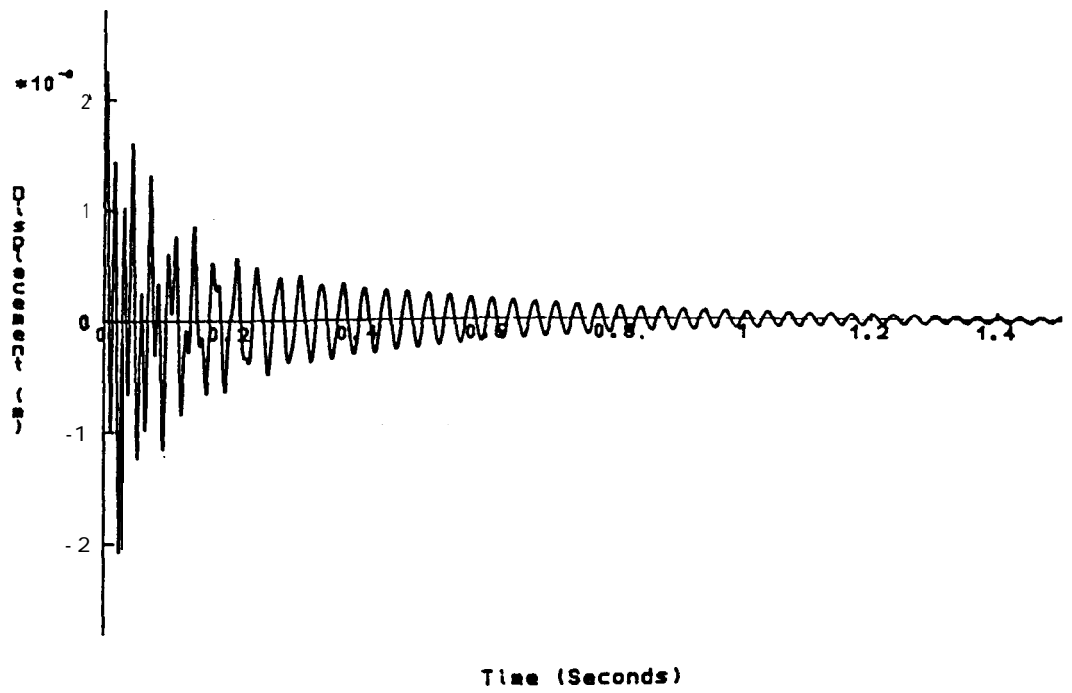


Fig 7.16 Predicted IRF for a system with bi-linear stiffness using a linear model with the **stiffer** of the two spring

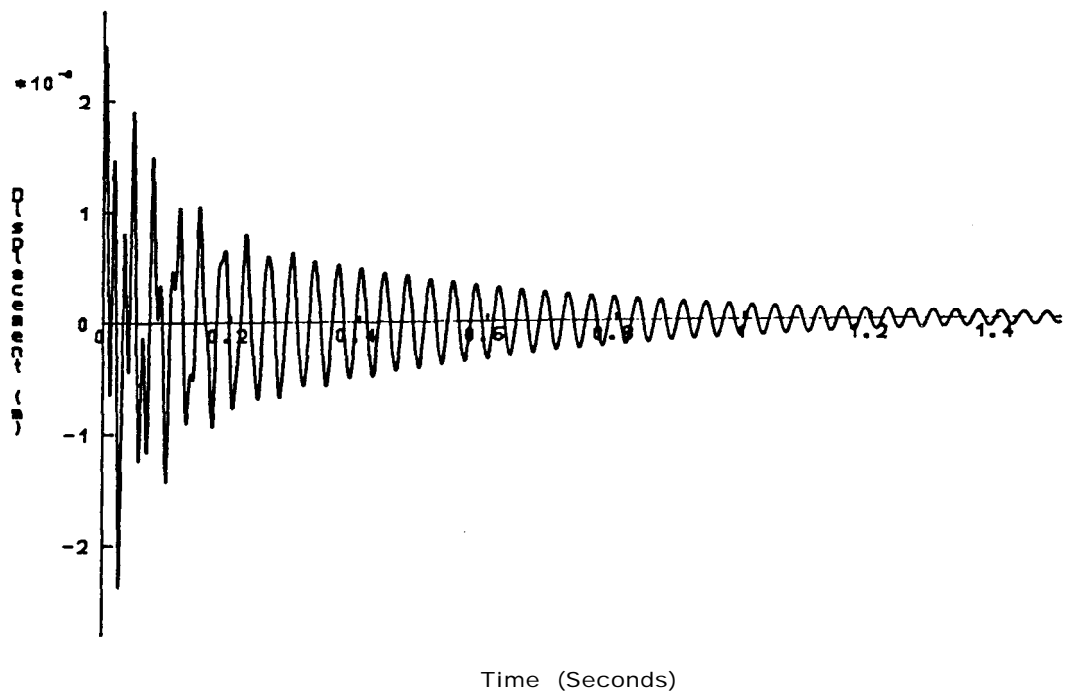


Fig 7.17 Predicted IRF for a system with bi-linear stiffness using a **linear** model with the average of the two springs

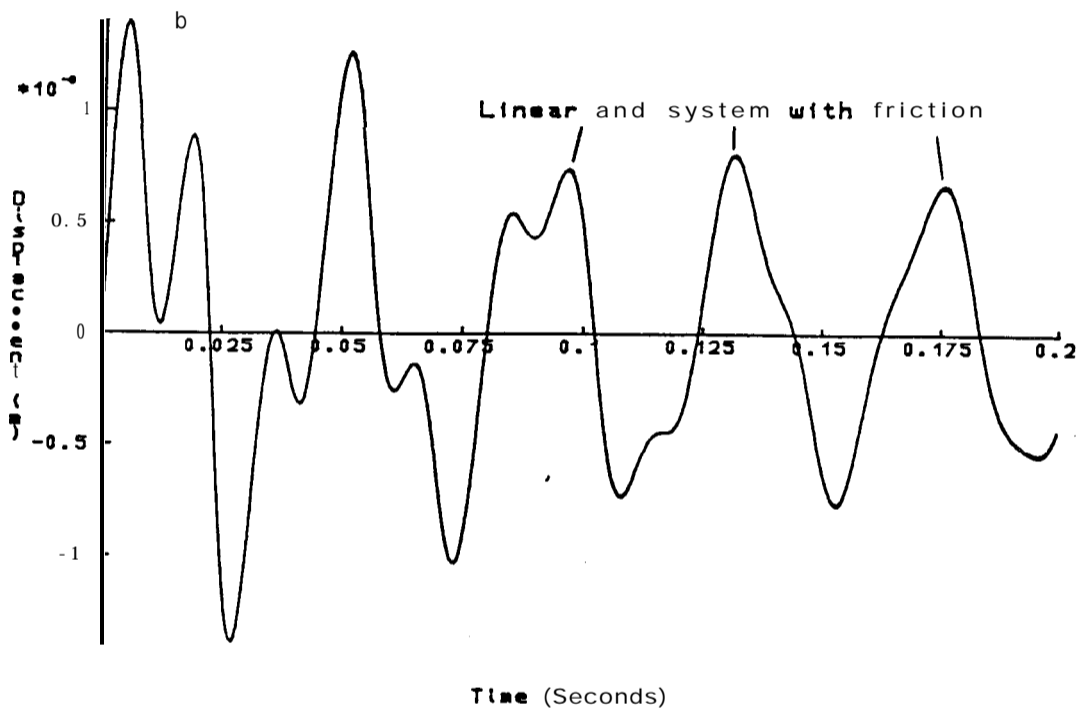
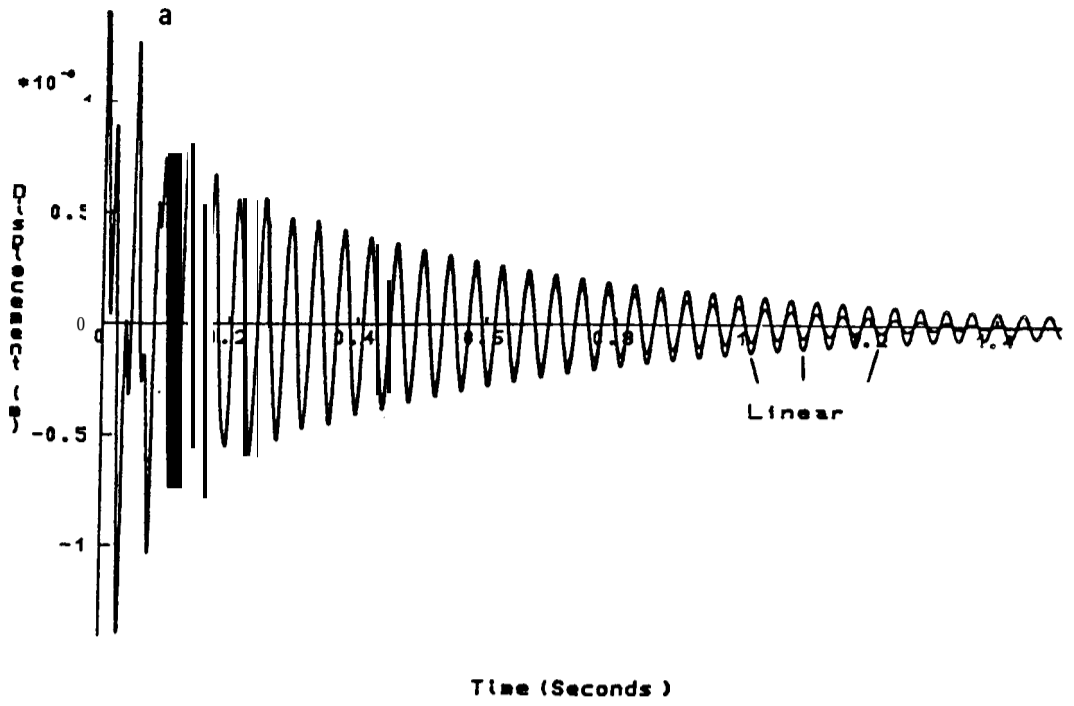


Fig 7.18 IRFs from a system with friction and a linear system; $v(0) = 0.5$ m/s
 a Response up to 1.5 seconds
 b Expanded response for first 0.2 seconds

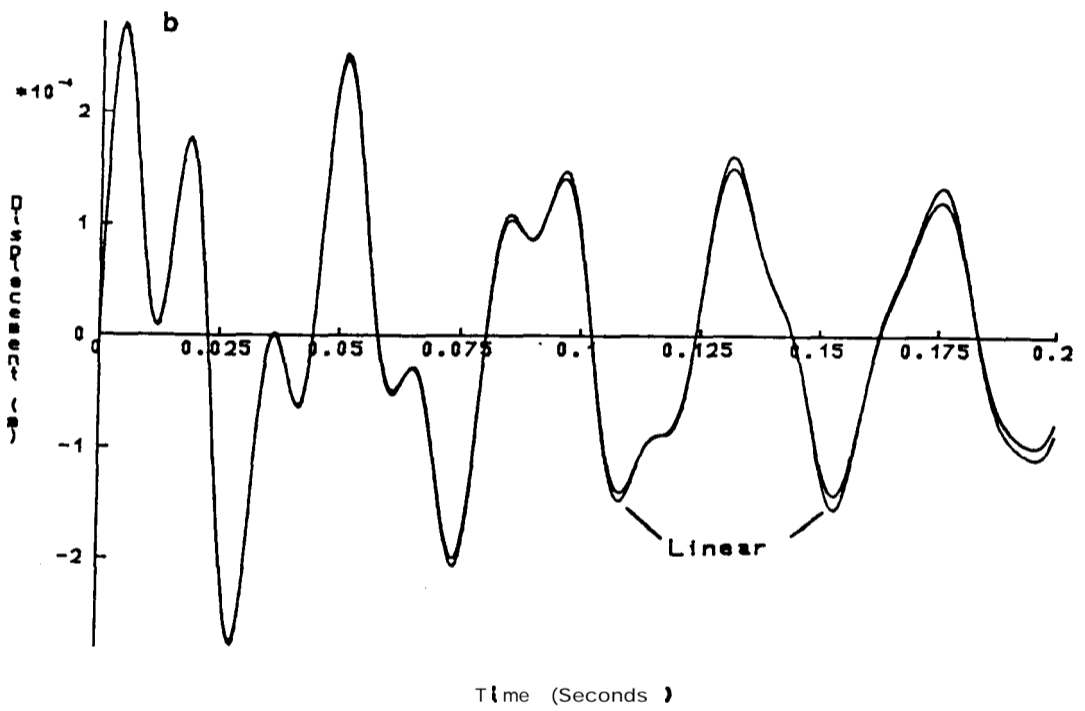
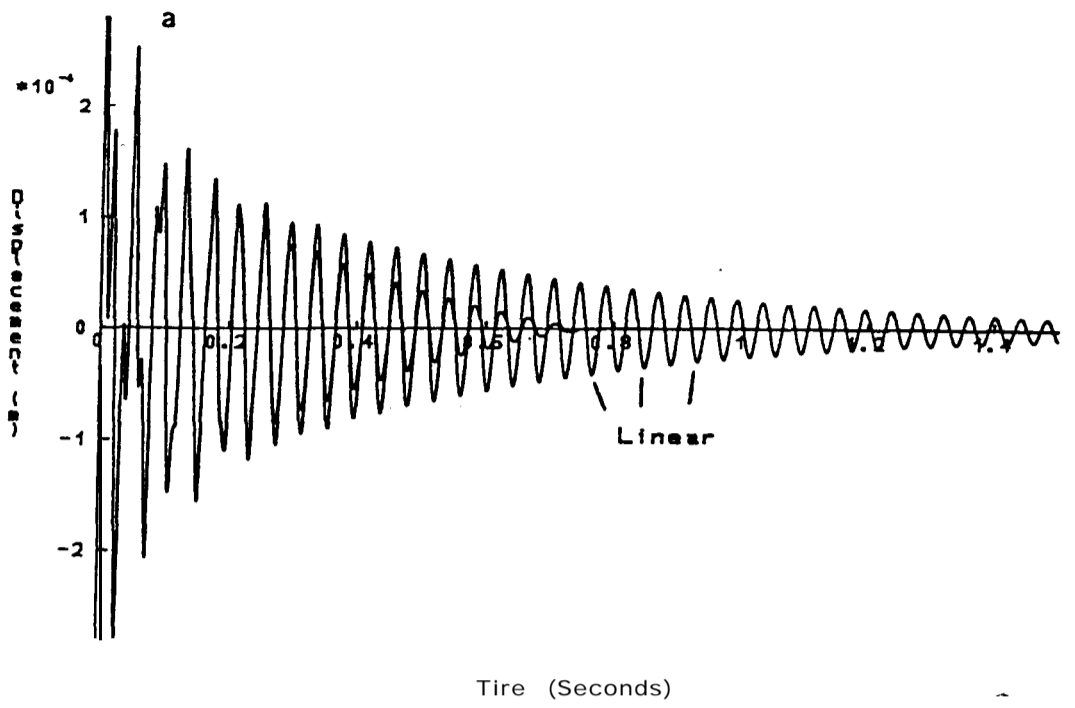


Fig 7.19 IRFs from a system with friction and a linear system; $v(0)=0.1$ m/s
a Response up to 1.5 seconds
b Expanded response for first 0.2 seconds

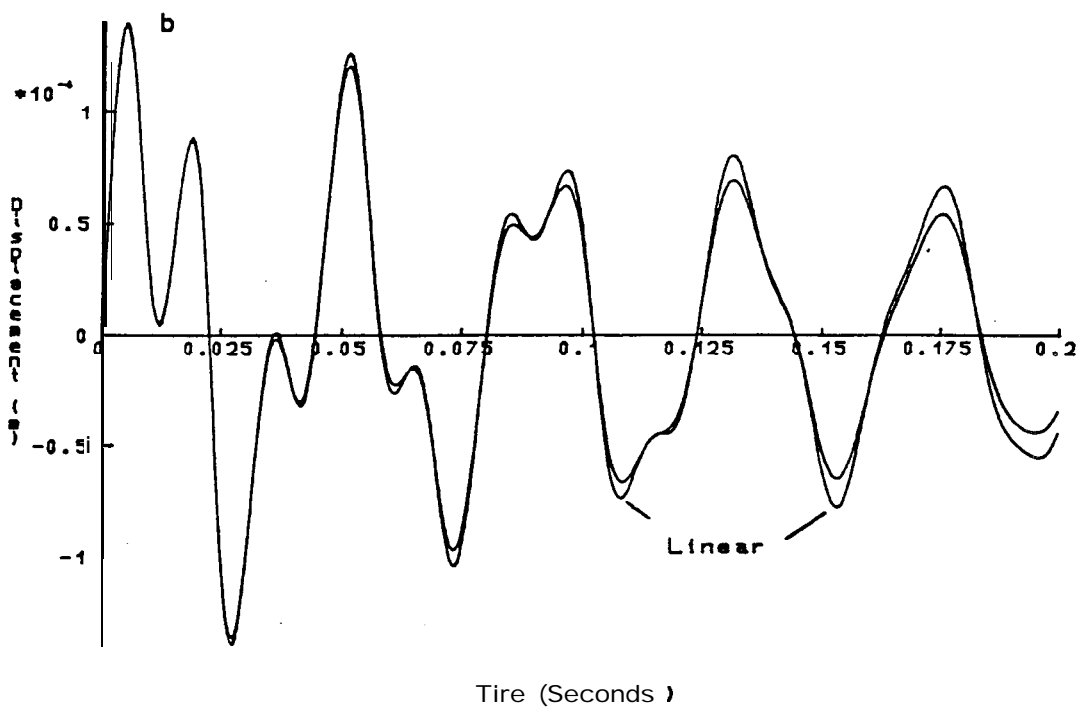
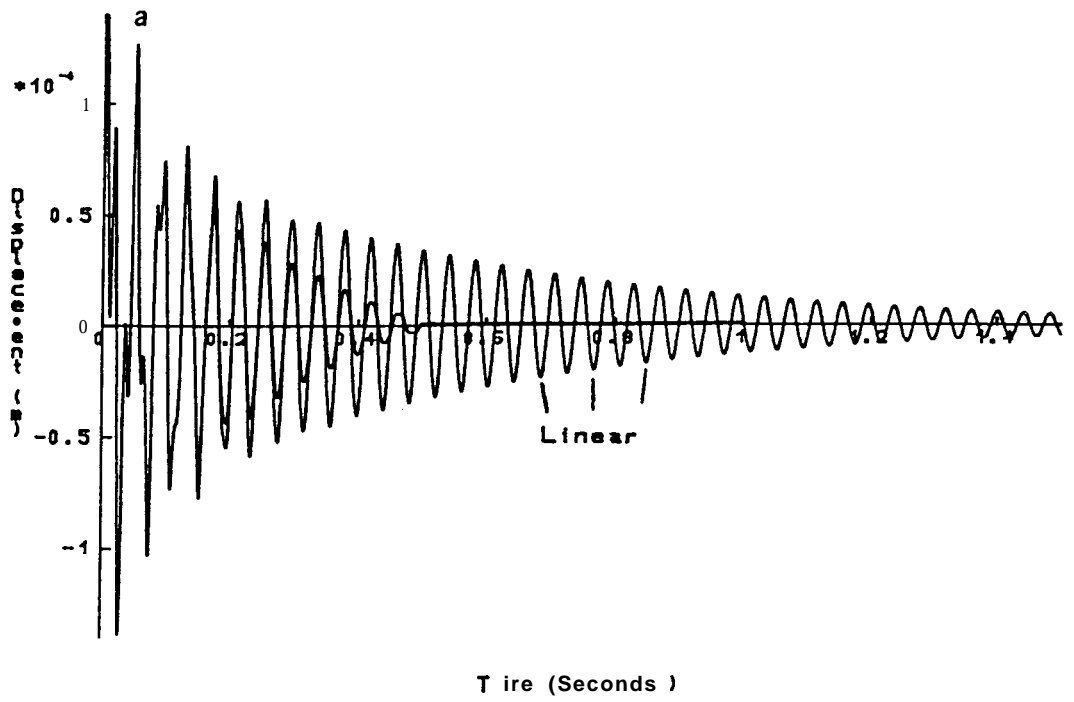


Fig 7.26 IRFs from a system with friction and a linear system; $v(0)=0.05$ m/s
a Response up to 1.5 seconds
b Expanded response for first 0.2 seconds

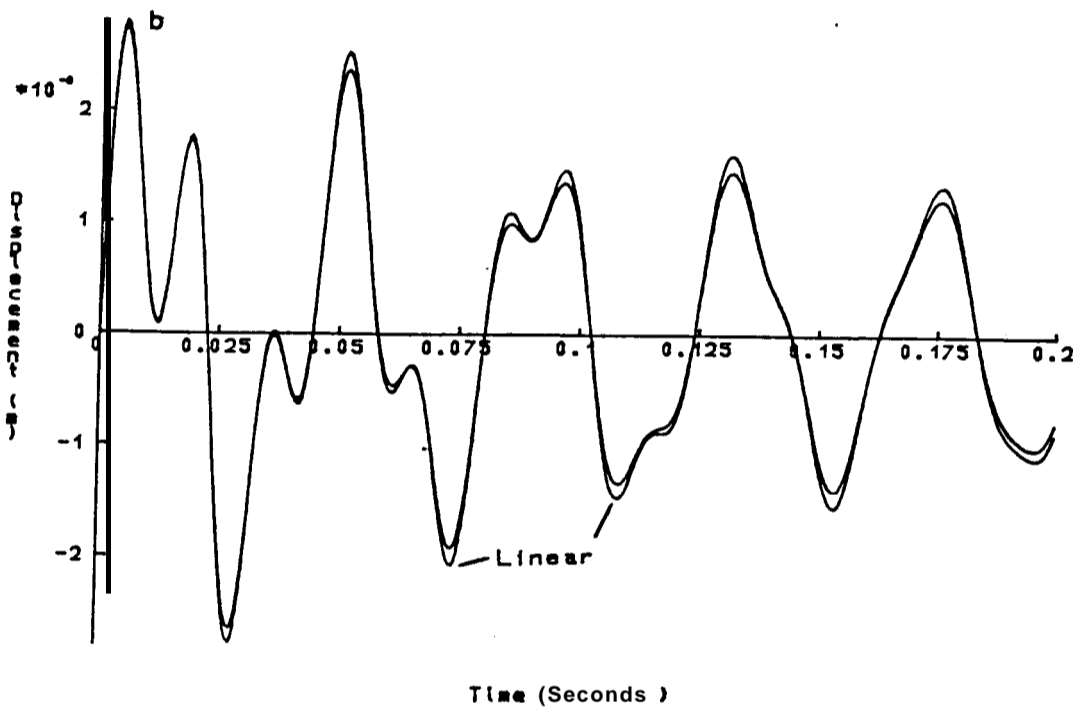
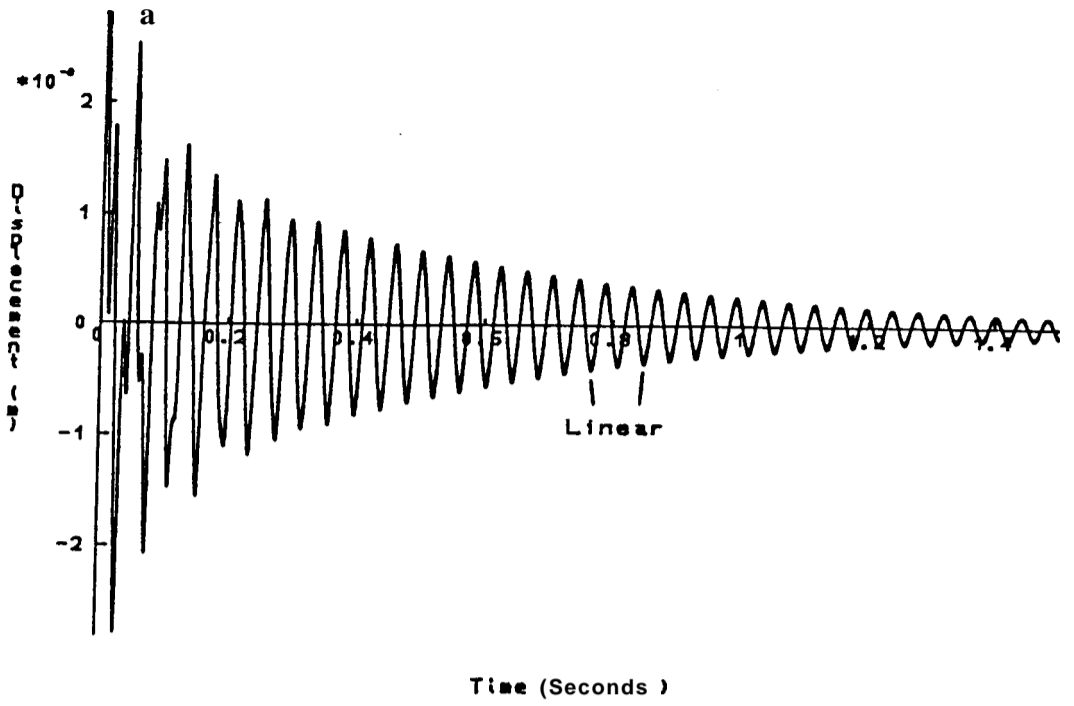


Fig 7.21 IRFs from a system with quadratic viscous damping and a linear system; $v(0)=1.0$ m/s
 a Response up to 1.5 seconds
 b Expanded response for first 0.2 seconds

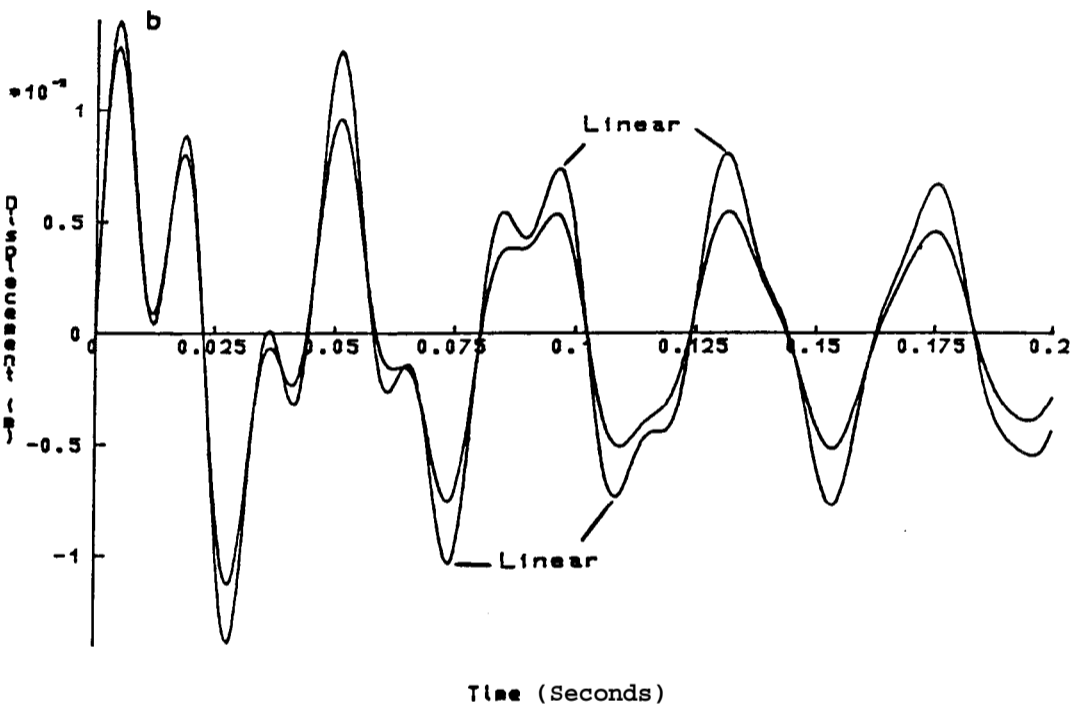
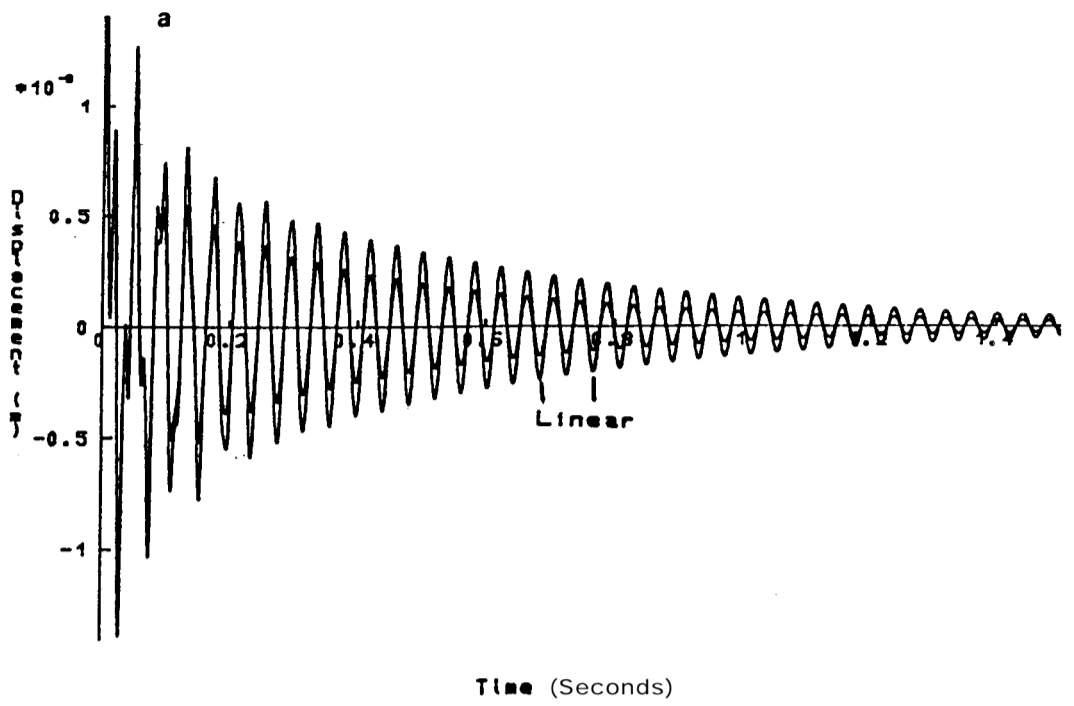


Fig 7.22 IRFs from a system with quadratic viscous damping and a linear system: $v(0) = 5.0$ m/s
 a Response up to 1.5 seconds
 b Expanded response for first 0.2 seconds

8 CONCLUDING DISCUSSION

8.0 Introduction

The aim of this research work has been to explore the use of experimental modal analysis techniques for application to the transient response prediction of structures. Particular attention has been paid to the accuracy required of the modal analysis methods. In addition to examining techniques for transient response of linear structures, the implications of using these techniques on non-linear systems has also been considered in some detail since most practical structures are to some degree non-linear and transient responses do tend to cover a wide range of amplitudes, thereby exposing amplitude-dependent effects.

The conclusions and discussions on the limitations and accuracy of experimental modal analysis and Fourier transform methods are summarised first in this chapter. This is followed by recommendations of how to use experimental modal analysis in transient response predictions, and conclusions about the limitations within the procedure. Finally, there are suggestions for further research.

8.1 Discussion

Various techniques that are available for transient response prediction have been examined in this thesis with the focus on their applicability to physical structures rather than to mathematical models of systems. It is found that most of the methods require a mathematical description of the structure - usually in terms of its mass, stiffness and damping elements. Such formulations are difficult to obtain by experimental description and the method that exhibits most potential for use with experimental data is that referred to as the 'Fourier transform method' - which takes the frequency response of the structure and the input force spectrum and then transforms the product to the time domain using the discrete Fourier transform. In practice, whilst many structures can now be modelled theoretically, there are still some systems that, due to their complexity, can only realistically be determined via experimental procedures. It is concluded that this 'Fourier transform method' is the most appropriate

technique to be used for a transient response prediction of those structures that may not be modelled analytically with sufficient reliability or confidence.

The methods available for experimentally determining the properties of a structure in the frequency domain are generally known as 'experimental modal analysis' and have been reviewed in chapter three. There are several excitation techniques and analysis procedures that can be used in undertaking an experimental modal analysis, all of which will generate accurate results provided that care is taken in the measuring of the data and that the most suitable analysis method for the available data is used. The structural properties evaluated using experimental modal analysis techniques are frequently in the form of 'modal parameters' from which the physical system parameters most often required by transient prediction techniques cannot usually be evaluated because of the incompleteness of the measured data. This enforces the need to develop the 'Fourier transform method', which uses the frequency response of the structure available through experimental modal analysis.

The relevant forms of Fourier transform theory have been examined in order to determine the limitations that the discrete Fourier transform places on the quality of modal data used and on the accuracy of the resulting response time-histories. The Fourier transform technique uses measured frequency response data, or frequency response data regenerated using parameters evaluated from modal analysis of the measured data. There is much literature available on the subject of Fourier transforms, and the minimum sample rate required in digitising signals to avoid frequency aliasing. Corresponding to this minimum sample rate to avoid frequency aliasing, a maximum frequency spacing relationship has been derived to avoid time-aliasing. This frequency spacing is related to the largest possible error in the maximum amplitude of the transformed signal, and is expressed in terms of the natural frequency and the damping in the mode.

Most practical structures are non-linear to some degree, and for that reason the application of the aforementioned techniques has also been examined in relation to a number of the more commonly occurring non-linearities. The application of

'standard' experimental modal analysis to individual non-linear elements was considered first, where it was shown how trends in measured data (either from constant-force sine tests or from impulse excitation) can identify clearly the type of non-linearity. It has also been shown that for damping-type non-linearities, it is possible to separate non-linear damping terms from the linear viscous damping in the system using reciprocal-of-receptance type analysis. Comparison in both the frequency and time domains is then made between the measured and transformed responses from impulse excitation and from constant-force sine tests. It was found that for any given non-linearity the plots and trends are often dissimilar from the two types of excitation, and may in fact agree with the trends of another non-linearity excited using the other technique. Transforming frequency response data measured using a constant-force stepped-sine test does not generally result in an acceptable prediction of the impulse response function, and it is concluded that different approaches need to be considered for predicting the impulse response function of non-linear systems using data from experimental modal analysis. The different frequency response functions (FRFs) for a system with a given non-linearity, obtained using various force levels or types of excitation, can all be used with any of the analysis techniques to evaluate modal parameters. The resulting sets of 'modal' parameters do not necessarily agree. By careful choice of the data to be analysed and the method used, it was found that consistent parameters - close to the underlying linear system - could be determined from some of the non-linear elements. These included:

- i) cubic stiffness - using data away from resonance with reciprocal-of-receptance analysis produced a good estimate to the underlying linear system;
- ii) backlash - using two reciprocal-of-receptance analyses on data above resonance then data below resonance. The average of the two sets of parameters are close to the underlying linear system; and
- iii) friction and quadratic viscous damping - with an adapted version of reciprocal-of-receptance analysis, the linear parameters can be evaluated and also the non-linear damping term.

Consideration is given to the application of the techniques of the single-degree-of-freedom (SDOF) non-linear system to multi-degree-of-freedom (MDOF) systems. For the example used in chapter 7 of a linear system plus a non-linear element, the non-linearity appears to affect the resonances of MDOF systems in much the same way as in those of the SDOF elements. In these cases, any trends in a MDOF system can be related to the corresponding SDOF element and hence the type of non-linearity identified. For small non-linear effects in the symmetric non-linearities considered in this study, only the first resonance is noticeably different to a linear response, but as the effective non-linearity increases - by changing the force level or the non-linear component - the second resonance sometimes becomes affected. However, there is no reason to believe that the parameters chosen for the examples used in this study emphasise a particular characteristic, and the results from undocumented experimental modal analysis on non-linear structures have also appeared to exhibit one 'non-linear mode' with the other modes behaving in a linear manner. The 'non-linear modes' in these cases also possess the same characteristics of known non-linear elements. The first resonance of a system will generally be vibrating at the largest displacement amplitude (hence a variation in amplitude through resonance), and as many of the non-linearities are amplitude-dependent, it is felt that this causes the first resonance to be more pronouncedly non-linear. When subsequent resonances are excited to the same level and with the same range of displacements, then it is assumed that they too will exhibit similar non-linear characteristics to the initial resonance.

Bi-linear stiffness appeared almost linear in the example used (the 'extra' resonance would not be identified as 'extra' from a structure of unknown degrees of freedom), and the response was not amplitude-dependent. As this non-linearity is not amplitude-dependent, it does not follow in this case that the first mode is where the non-linearity is most evident. The effect - most noticeable in the time domain - will affect all the modes that the particular spring element is active in. However, as the time-history of a MDOF system with bi-linear stiffness may be too complex to identify any discrepancies in the positive and negative responses, it may no longer be feasible to use it as a method of identifying and quantifying this non-linearity. Bi-linear stiffness appears to be harder to detect in MDOF systems than SDOF systems.

8.2 Recommendations for transient response predictions

For practical structures that are modelled using experimental techniques, and that may be treated as linear, the most suitable approach to transient response prediction is found to be using frequency response data from experimental modal analysis together with the Fourier transform, as all other transient response prediction methods require the mass, stiffness and damping properties of the structure explicitly. To satisfy the accuracy required of modal parameters when they are to be used in transient response prediction, the structure should be tested with sufficient data around resonance so that an accurate value of damping can be estimated. Also, the limitations of the process of discrete Fourier transforming data are such that a minimum sample rate and a maximum frequency spacing are stipulated for a given structure to avoid both frequency and time aliasing. Provided that these conditions are met both in the modal analysis stage and in the transformation of the data, the predictions will provide an accurate description of the transient response of the structure. However, large deviations from the true response can be introduced in the prediction if any of the modal parameters are in error, or if time aliasing occurs in the transform to the time-history. In summary, experimentally-derived structural models can be used for transient response analysis provided the following conditions are observed:

- i) data must be measured as accurately as possible to enable good estimates of the modal parameters to be evaluated. Particular care is required over the damping loss factor and in determining the phase of a modal constant, implying the need to use Nyquist circle-fit type modal analysis; and
- ii) the measured or regenerated frequency response functions should have sufficient points around resonance to avoid time aliasing, and the force input should be sampled rapidly enough to avoid frequency aliasing.

The choice of linear damping model is a topic of discussion. For frequency response functions, hysteretic damping is a better representation than viscous damping in most cases of the dissipation mechanism in structures - but neither is an accurate model of the damping. In terms of the mathematics, viscous damping provides a rigorous solution, but the equations for hysteretic damping are often easier to manipulate and can be related by engineering interpretation to the solutions for free vibration even though hysteretic damping is only strictly defined for forced vibrations. Most modal analysis routines calculate the damping loss factor at resonance, and this can be changed to an equivalent viscous damping ratio using the relationship derived from energy considerations at resonance. It was shown that this relationship also holds with light damping for the decay rate of the time-history. If a hysteretic damping model is used in an FRF which is then subjected to a Fourier transform, a non-causal response - which is usually associated with non-linear systems - will result. It is recommended therefore, that a viscous damping model is used for transient response prediction to avoid this apparent non-linearity in the system, which will hinder the detection of any non-linear elements present.

It was noted in the previous section that for any given non-linearity the trends in the response depend on the type of excitation. These differences in trends for the same non-linearity have a two-fold significance. The first is that exciting a non-linear structure using an impulsive or other transient excitation will not necessarily generate the FRF for the required excitation level (the FRF represents the response frequency by frequency for steady-state excitation), and as such, a constant-force sine test should be used to measure the FRF. However, the second point is that using the modal parameters evaluated from **FRFs** measured using constant-force sine tests for predicting the transient response of a non-linear model may yield incorrect results. Clearly, in this second case, what is required is a frequency response model that closely matches the transformed impulse response, and not the measured FRF. Such a non-linear model, using parameters evaluated from data measured using a constant-force sine test, has been developed for friction non-linearity. The model was very complex, and led to the conclusion that it should only be used if an alternative solution using a linear frequency response model could not be derived.

For a specific non-linear system, several different sets of modal parameters can be calculated and, thus, several different impulse response predictions can be estimated for the same system using the 'Fourier transform method'. By examination of the resulting time-histories it has been shown which answers are acceptable, and under what conditions, and therefore which experimentally derived modal parameters should be used. However, for some applications, the use of a non-linear model rather than a linear model is still recommended. It is obviously a much easier approach if a linear model can be used, both in terms of computational time and in the determination of the required parameters. Thus, wherever possible it is recommended that a linear model is used.

For damping-type non-linearities the linear approximations to the transient response of MDOF systems are valid for the same situations as the SDOF elements; using the underlying linear system parameters will always provide an overestimation of the response. In situations where a non-linear model is recommended for good approximations in the SDOF elements, the model would now have to account for the influence of other modes on the amplitude of response. For the symmetric stiffness-type non-linearities, the techniques for evaluating the underlying system parameters are still valid, but not always as accurately as from the SDOF element. Also, the linear model does not over-predict the response at all times due to the now continually changing phase relationship of the modes caused by the natural frequency changing with amplitude.

The main difficulties are with detecting non-symmetric stiffness non-linearities, where the force due to positive response does not equal the magnitude of the force due to negative displacements. For the example used - bi-linear stiffness - it is difficult to detect the non-linearity in the frequency domain from any type of excitation, but the effect is very noticeable in the transient response time-history. For an accurate time-history prediction, time domain models need to be developed which require the identification of the different spring stiffnesses. However, a linear model using the softer of the two springs can be used for transient response analysis which will generate an overestimation of the result.

In general, the conditions for steady-state response prediction and transient response prediction vary considerably with non-linearities, and one response cannot necessarily be predicted from the measurement of the other. A few of the many alternative linear models that can be calculated using modal analysis techniques on non-linear structures can be used in some applications of transient response prediction when conservative estimates of the response is the requirement. However, where accurate predictions are required, non-linear models will have to be developed, but as these models will increase the work involved in obtaining a transient response prediction, their use should be restricted to cases for which they are absolutely necessary.

8.3 Suggestions for further research

While many of the questions raised at the outset of this research have now been answered, this study has highlighted a number of problems that require further research. These topics are all related to the analysis and treatment of non-linear systems.

In using modal analysis techniques on non-linear structures, the main problem at present lies in identifying and quantifying a non-symmetric non-linearity from frequency domain data. If the presence of this non-linearity is detected, then there are methods of quantifying the different non-linear parameters for SDOF elements but corresponding methods for quantifying the parameters need to be examined for MDOF systems as the effect of applying an off-set to the structural component will change more than one resonance. Using the other technique of visual inspection of signals, it may become increasingly difficult to identify non-symmetry in the response, in which case the implication is that for MDOF systems the non-symmetry in non-linearities can be ignored in the transient response prediction of such systems. This is another aspect that needs further research, which may make the initial problem to be addressed - that of detecting this type of non-linearity - unnecessary.

For symmetric non-linearities, further investigation is required into the evaluation of consistent parameters from experimental tests on MDOF structures, with a more comprehensive study of such systems than was recorded in this study. Related to this is the interpretation of any non-linear parameter evaluated from the frequency response of a MDOF system, where the possibility of physically locating a non-linearity from modal analysis, or expressing the non-linearity in modal terms requires further research.

In the transient response prediction of non-linear structures, where a non-linear model is recommended, one would have to be created for the specific non-linearity and application (except in the case of a friction element where a non-linear model has already been developed in this work), but any requirement for accurate predictions balanced against the extra time and effort involved in developing and using a non-linear model.

8.3 Suggestions for further research

While many of the questions raised at the outset of this research have now been answered, this study has highlighted a number of problems that require further research. These topics are all related to the analysis and treatment of non-linear systems.

In using modal analysis techniques on non-linear structures, the main problem at present lies in identifying and quantifying a non-symmetric non-linearity from frequency domain data. If the presence of this non-linearity is detected, then there are methods of quantifying the different non-linear parameters for SDOF elements but corresponding methods for quantifying the parameters need to be examined for MDOF systems as the effect of applying an off-set to the structural component will change more than one resonance. Using the other technique of visual inspection of signals, it may become increasingly difficult to identify non-symmetry in the response, in which case the implication is that for MDOF systems the non-symmetry in non-linearities can be ignored in the transient response prediction of such systems. This is another aspect that needs further research, which may make the initial problem to be addressed - that of detecting this type of non-linearity - unnecessary.

For symmetric non-linearities, further investigation is required into the evaluation of consistent parameters from experimental tests on MDOF structures, with a more comprehensive study of such systems than was recorded in this study. Related to this is the interpretation of any non-linear parameter evaluated from the frequency response of a MDOF system, where the possibility of physically locating a non-linearity from modal analysis, or expressing the non-linearity in modal terms requires further research.

In the transient response prediction of non-linear structures, where a non-linear model is recommended, one would have to be created for the specific non-linearity and application (except in the case of a friction element where a non-linear model has already been developed in this work), but any requirement for accurate predictions balanced against the extra time and effort involved in developing and using a non-linear model.

9 REFERENCES

- 1 Comparison of Numerical Methods for Analysing the Dynamic Response of Structures.
Chan S. P. & Newmark N. M. US Navy Contract N6-orn-71.
- 2 Linear Vibration Theory: Generalised Properties and Numerical Methods.
Vernon J. B. J. Wiley. (1967).
- 3 Numerical Analysis.
Macon N. J. Wiley.
- 4 Differential Equations (2nd ed.).
Agnew R. P. McGraw-Hill. (1960).
- 5 Numerical Solution of Differential Equations.
Milne W. E. J. Wiley. (1970).
- 6 Numerical Methods for Scientists and Engineers.
Hamming R. W. McGraw-Hill. (1962).
- 7 The Numerical Solution of Ordinary Differential Equations.
Miller J. C. P. Contrib. to Numerical Analysis:
An Introduction ed. Walsh J.
Academic Press. (1967).
- 8 A Method of Computation for Structural Dynamics.
Newmark N. M. Jnl. Engineering Mechanics
Division. Proc. ASCE. pp67-94.
(July 1959) .

- 9 The **Newmark** Beta Method of Transient Response Analysis.
Dobson B. J. RNEC Manadon, Plymouth. Rept.
No RNEC-TR-82003.
(Feb. 1982).
- 10 Transient Analysis of Complex Structural Mechanical Systems.
Chan S. P., Cox H. L. & **Benfield** W. A. Jnl. Royal Aeronautical Soc. v66
pp457-460. (July 1962).
- 11 The Transient Analysis of a Structure Using a Modal Model.
Gaught T. M. & Dobson B. J. Int. Jnl. Modal Analysis ppl I-I 6
(Jan. 1986).
- 12 The **Newmark** and Mode Superposition Methods for the Transient Analysis of
a Linear Structure: A Case Study.
Dobson B. J. RNEC Manadon, Plymouth. Rept.
No RNEC-TR-83011.
(June 1983).
- 13 Dynamic Structural Modelling and Time Domain Analysis.
Ratcliffe C. P. RNEC Manadon, Plymouth. Rept.
No RNEC-TR-82014.
(Oct. 1982).
- 14 Dynamic Simulation of Structural Systems with Isolated Non-linear
Components.
Lyons J. A., Minnetyan L. & **Gerardi** T. G. Air Force Office of Scientific
Research USAF AFOSR-82-0216
(1982).
- 15 Concepts in Shock Data Analysis.
Rubin S. Ch. 23 Contrib. to Sound &
Vibration Handbook v2 ed. Harris
C. M. & Crede C. E. (1976).

- 26 Response of an Elastically Non-Linear System to Transient Disturbances.
Evaldson R. L., Ayre R. E. & Jnl. Franklin Inst. **v248**
Jacobsen L S. **pp473-484** (1949).
- 27 On a General Method of Solving Second-Order Ordinary Differential Equation
by Phase-Plane Displacements.
Jacobsen L. S. Jnl. Applied Mechanics **v19**
 pp543-553 (Dec 1952).
- 28 Nonlinear Vibrations.
Abramson H. N. Ch. 4 Contrib. to Sound &
 Vibration Handbook vi ed. Harris
 C. M. & Crede C. E. (1976).
- 29 A Comparative Study of Pulse and **Step-Type** loads on a Simple Vibratory
System.
Jacobsen L. S. & Ayre R. S. US Navy Contract **N6-on-154**.
- 30 A Theory of the Greatest Maximum Response of Linear Structures.
Youssef N. A. N., & Popplewell N. Jnl. Sound & Vibration **v56(1)**
 pp21-33 (1978).
- 31 Shock Response Spectra and **Maximax** Response.
Matsuzaki Y. Shock & Vibration Digest
 pp11-15.
- 32 A Review of Shock Response Spectrum.
Matsuzaki Y. Shock & Vibration Digest **v9(3)**
 pp3-12 (1977).
- 33 Some Shock Spectra Characteristics and Uses.
Fung Y. C. & Barton M. V. J Applied Mechanics
 (Sept. 1958).

- 34 The **Maximax** Response of Discrete Multi-Degree-of-Freedom Systems.
Youssef N. A. N. & Popplewell N. Jnl. Sound & Vibration v64(1)
pp1-15 (1979).
- 35 A Comparison of **Maximax** Response Estimates.
Popplewell N. & Youssef N. A.N. Jnl. Sound & Vibration v62(3)
pp339-352 (1979).
- 36 Earthquake Response of Structures.
Clough R. W. Ch. 12 Earthquake Engineering
Ed. Wiegel R. L. Prentice Hall.
(1970).
- 37 Understanding and Measuring the Shock Response Spectrum, Part I.
Heiber G. M. & Tustin W. Sound & Vibration pp42-49
(March 1974).
- 38 Understanding and Measuring the Shock Response Spectrum, Part II.
Heiber G. M. & Tustin W. Sound & Vibration pp50-54
(April 1975).
- 39 Vibrations and Shock in Damped Mechanical Systems.
Snowden J. C. J. Wiley. (1968).
- 40 Transform Methods in Linear System Analysis.
Aseltine J. A. McGraw-Hill. (1958).
- 41 The Fourier Transform and Its Application.
Bracewell R. McGraw-Hill. (1965).
- 42 Frequency Analysis.
Randall R. B. **Bruell & Kjær** publications.
(1977).

- 43 Shock and Vibration in Linear Systems.
Crafton P. A. Harper. (1961).
- 44 Vibration Testing and Signal Analysis.
Hammond J. K. et al. **ISVR Univ. Southampton. Course notes** (Feb. 1982).
- 45 Digital Signal Processing.
Oppenheim A. V. & Schafer R. W. Prentice-Hall. (1975).
- 46 Modal Testing: Theory and Practice.
Ewins D. J. Research Studies Press. (1984).
- 47 Mechanics of Vibration.
Bishop R. E. D. & Johnson D. C. Cambridge Univ. Press. (1960).
- 48 Dynamic Response of Materials in Vibrations.
Rogers J. D. **Proc. SEM Fall Conf.**
'Computer-aided testing with
Modal Analysis' Milwaukee
(4-7 Nov. 1984).
- 49 Modal Vector Estimation for Closely-Spaced Frequency Modes.
Craig R. R., Yung-Tseng Chung & **Proc. Int. Modal Analysis Conf.**
Blair M. A. Orlando, Fl. (Jan. 1985).
- 50 Modal analysis of Large Structures - Multiple Exciter Systems.
Zaveric K. Bruell and Kjaer Publication.
(1984).
- 51 Multi-Point Transient Modal Testing.
Lauffer P., Tucker M. D. & **Proc. Int. Modal Analysis Conf.**
Smallwood D. O. London (1987).

- 52 A State-of-the-Art Implementation of Multiple input Sine Excitation.
Hunt D. L., Mathews J. & Williams R. **Proc. Int. Modal Analysis Conf.**
London (1987).
- 53 International Organisation for Standardisation (**ISO**) Methods for the
Experimental Determination of Mechanical Mobility.
Part 1 - Basic Definitions.
Part 2 - Measurement using Single-Point Translation Excitation.
Part 3 - Measurement of Rotational Mobility.
Part 4 - Measurement of the Complete Mobility Matrix Using Attached
Shakers.
Part **5** - Measurement Using Impact Excitation which is not Attached to the
Structure.
- 54 Frequency Response - An Effective Solution to a Complex Problem.
Cogger N. D. **Noise & Vibration Control**
Worldwide (March 1982).
- 55 An Introduction to Random Vibration and Spectral Analysis.
Newland D. E. Longman. (1975).
- 56 The Reduction of Bias Error in Transfer Function Estimates Using FFT Based
Analysis.
Cawley P. **Jnl. Vibration Acoustics, Stress
Reliability in Design v104
pp29-35 (Jan. 1984).**
- 57 The Improved Frequency Response Function and its Effect on Modal Circle
Fits.
Elliot K. B. & Mitchell L. D. **ASME Jnl. Applied Mechanics v51
pp657-663 (Sept. 1984).**

- 58 An Unbiased Frequency Response Function Estimator.
 Mitchell L. D., Cobb R. E., **Proc. Int. Modal Analysis Conf.**
Deel J. C. & Luk Y. W. London (1987).
- 59 A Comparison of Methods for Aircraft Ground Vibration Testing.
 Hunt D. L. **Proc. Int. Modal Analysis Conf.**
 Orlando, **Fl.** (Jan.1 985).
- 60 Impulse Techniques for Structural Frequency Response Testing.
 Halvorsen W. G. & Brown D. L. **Sound & Vibration pp8-21**
 (Nov. 1977).
- 61 Practical Application of the Rapid Frequency Sweep Technique for
 Structural Frequency Response Measurement.
 White R. G. & Pinnington R. J. **Aeronautical Journal**
 (May 1982).
- 62 Mobility Measurement Using the Rapid Frequency Sweep Technique.
 Westland P. G. **AUWE Portland WLTM 412/82**
 (Nov. 1982).
- 63 Improved Technique for the Valuation of Structural Dynamic Response.
Bolton J. S. & Dyne M. **Mechanique Materiaux Electricite**
pp71-73 (Mar./April 1984).
- 64 A Review of Modal Parameter Estimation Concepts.
 Allemang R. J. & Brown D. L. **Proc 1 1th Int. Seminar on Modal**
Analysis (1986).
- 65 Survey of Parameter Estimation Methods in Experimental Modal Analysis.
 Fullekrug U. **Proc. Int. Modal Analysis Conf.**
 London (1987).

- 66 Modal Analysis Bibliography - 1979 - 1984.
 Mitchell L. D. & Mitchell L. D. Proc. Int. Modal Analysis Conf.
 London (1987).
- 67 Modal Parameter Estimation Using Difference Equations.
 Dobson B. J. RNEC Manadon, Plymouth. Rept.
 No RNEC-TR-85014.
 (July 1985).
- 68 Parameter Estimation Techniques for Modal Analysis.
 Brown D. L, Allermang R. J., SAE Technical Paper Series
 Zimmerman R. & Mergeay M. 790221 (1979).
- 69 Critical Assessment of the Accuracy of Modal Parameter Extraction.
 Ewins D. J & He J. Imperial College, Dept. Mech. Eng.
 Dynamics Section Rept. No 85003
 (Oct. 1985).
- 70 A Weighted Least Squares Method for Circle Fitting to Frequency Response
 Data.
 Brandon J. A. & Cowley A. Jnl. Sound & Vibration v89(3)
 pp419-424 (1983).
- 71 Modal Analysis Using Dynamic Stiffness Data.
 Dobson B. J. RNEC Manadon, Plymouth. Rept.
 No RNEC-TR-84015.
 (June 1984).
- 72 Reciprocals of Mobility and Receptance - Applications in Modal Analysis
 Study of Linear and Non-linear Systems.
 Peccatte L. Univ. of Manchester Simon
 Engineering Lab. End of studies
 Technical Report. (Oct. 1984).

- 66 Modal Analysis Bibliography - 1979 - 1984.
 Mitchell L. D. & Mitchell L. D. Proc. Int. Modal Analysis Conf.
 London (1987).
- 67 Modal Parameter Estimation Using Difference Equations.
 Dobson B. J. RNEC Manadon, Plymouth. Rept.
 No RN EC-TR-85014.
 (July 1985).
- 68 Parameter Estimation Techniques for Modal Analysis.
 Brown D. L, Allermang R. J., SAE Technical Paper Series
 Zimmerman R. & Mergeay M. 790221 (1979).
- 69 Critical Assessment of the Accuracy of Modal Parameter Extraction.
 Ewins D. J & He J. Imperial College, Dept. Mech. Eng.
 Dynamics Section Rept. No 85003
 (Oct. 1985).
- 70 A Weighted Least Squares Method for Circle Fitting to Frequency Response
 Data.
 Brandon J. A. & Cowley A. Jnl. Sound & Vibration **v89(3)**
 pp419-424 (1983).
- 71 Modal Analysis Using Dynamic Stiffness Data.
 Dobson B. J. RNEC Manadon, Plymouth. Rept.
 No RNEC-TR-84015.
 (June 1984).
- 72 Reciprocals of Mobility and Receptance - Applications in Modal Analysis
 Study of Linear and Non-linear Systems.
 Peccatte L. Univ. of Manchester Simon
 Engineering Lab. End of studies
 Technical Report. (Oct. 1984).

- 73 Global Parameter Estimation using Rational Fraction Polynomials.
Jones R. & Kobayashi Y. **Proc. Int. Modal Analysis Conf. Los Angeles, CA (1986).**
- 74 Global Frequency and Damping Estimates from Frequency Response Measurements.
Richardson M. H. **Proc. Int. Modal Analysis Conf. Los Angeles, CA (1986).**
- 75 A Simultaneous Frequency Domain Technique for Estimation of Modal Parameters from Measured Data.
Coppolino R. N. **SAE Technical Paper Series 811046 (1981).**
- 76 A Global Technique for Estimation of Modal Parameters from Measured Data.
Coppolino R. N. & Stroud R. C. Proc. Int. Modal Analysis Conf. Los Angeles, CA (1986).
- 77 A Method for Modal Identification of Lightly Damped Structures.
Ewins D. J. & Gleeson P. T. **Jnl. Sound & Vibration v84(1) pp57-79 (1982).**
- 78 On Predicting Point Mobility Plots from Measurements of Other Mobility Parameters.
Ewins D. J. **Jnl. Sound & Vibration v70(1) pp69-75 (1980).**
- 79 A Recursive Approach to Prony Parameter Estimation.
Davis P. **Jnl. Sound & Vibration v89(4) pp571-583 (1983).**
- 80 A Parametric Study of the Ibrahim Time Domain Modal Identification Algorithm.
Pappa R. S. & Ibrahim S. R. Sound & Vibration Bulletin v51(3) pp43-72 (1981).

- 81 Modal Identification Techniques Assessment and Comparison.
Ibrahim S. R. Sound &Vibration (Aug. 1985).
- 82 The Polyreference Time Domain Technique.
Deblaws F. & Allemang P. J. Univ. of Cincinatti Report
- 83 Application and Evaluation of Multiple Input Modal Parameter Estimation.
Lembregts F., Snoeys R. & Leuridan J. **Proc. Int. Modal Analysis Conf.**
London (1987).
- 84 Global Modal Parameter Estimation Methods.
Leuridan J., Van der Auweraer H., **Proc. Int. Modal Analysis Conf. Los**
Lipkens J. & Lembregts F. Angeles, CA (1986).
- 85 A Multi-Input Modal Estimation Algorithm for Mini-Computers.
Vold H., Kundrat J., Rocklin G. T. & **SAE Technical Paper Series**
Russell R. 820194 (1982).
- 86 Time Domain Modal Parameter Identification and Modelling of Structures.
Ibrahim S. R. **Proc. American Control San**
Fransisco CA **pp989-996**
(1983).
- 87 Identification of Mechanical System Modal Parameters Using Time Series
Approach.
Zhas X. **Proc. Int. Modal Analysis Conf.**
Orlando, Fl. (Jan.1985).
- 88 Comparative Results from Time Domain Modal Parameter Estimation
Algorithms.
Galtardt D. & **Quantz C.** **Proc. Int. Modal Analysis Conf.**
London (1987).

- 89 An Alternative Time Domain Method for Modal Analysis.
Liang Z. & Inman D. J. Proc. Int. Modal Analysis Conf.
London (1987).
- 90 Improved Time Domain Polyreference Method for Modal Identification.
Zhang L., Yao Y. & Lu M. Proc. Int. Modal Analysis Conf.
London (1987).
- 91 Modification of Finite Element Models Using Experimental Modal Analysis.
Dobson B. J. Proc. Int. Modal Analysis Conf.
Orlando, Fl. (Feb.1 984).
- 92 Correlation of Finite Elements and Modal Test Studies of a Practical
Structure.
Sidhu J. & Ewins D. J. Proc. Int. Modal Analysis Conf.
Orlando, Fl. (Feb.1 984).
- 93 Structural Dynamics Modification - An Extension to Modal Analysis.
Formenti D. & Welaratna S. SAE Technical Paper Series
811043 (1981).
- 94 Methods and Applications of Structural Modelling from Measured Frequency
Response Data.
Goyder H. G. D. Jnl. Sound & Vibration v68(2)
pp209-230 (1980).
- 95 Identification of Physical Mass, Stiffness and Damping Matrices using
Pseudo-Inverse.
Luk Y. W. Proc. Int. Modal Analysis Conf.
London (1987).

- 96 Measurement Techniques and Data Analysis, Dynamics Measurements, Vibrations and Acoustics.
Ewins D. J., Silva J. M. M. & Maleci G. Sound & Vibration Bulletin v50. (Sept. 1980).
- 97 Coupled Structure Analysis.
Ewins D. J., Silva J. M. M. & Maleci G. Sound & Vibration Bulletin v50. (Sept. 1980).
- 98 Modelling Vibration Transmission Through Coupled Vehicle Sub-Systems Using Mobility Matrices.
Hemingway N. G. Proc. Institution Mechanical Engineers v200 No D2 (1986).
- 99 Structural Modification and Coupling Dynamic Analysis using Measured FRF Data.
Imregun M., Robb D. A. & Ewins D. J. Proc. Int. Modal Analysis Conf. London (1987).
- 100 Introduction to Fourier Analysis and Generalized Functions.
Lighthill M. J. Cambridge University Press.
- 101 Fourier Series and Boundary Value Problems.
Churchill R. V. Mc Graw Hill. (1941).
- 102 Discourse on Fourier Series.
Lanczos C. Oliver and Boyd. (1966).
- 103 The Fourier Integral and it's Applications.
Papoulis A. Mc Graw Hill. (1962).
- 104 An Introduction to Fourier Analysis.
Stuart R. D. Chapman and Hall. (1961).

- 105 Fourier Transforms and the Theory of Distribution.
Arsac J. Prentice-Hall. (1966).
- 106 Outline of Fourier Analysis.
Hsu H. P. Illife Books Ltd. (1967).
- 107 The Interpretation of Discrete Fourier Transforms.
Furber A. M. RAE Farnborough Rept. No. RAE
TR 73127 (Nov. 1973).
- 108 An Introduction to the Fast Fourier Transform.
Richards L. J. RAE Farnborough Tech. Memo
RAD-NAV (Feb. 1979).
- 109 Guidelines for the Reduction of Random Modal Test Data.
Au-Yang M. K. & Maynard K. P. Proc. Int. Modal Analysis Conf.
Orlando, Fl. (Jan.1 1985).
- 110 Time Aliasing: A Digital Data Processing Phenomenon.
Thornhill R. J. & Smith C. C. ASME Jnl. Dynamic Systems,
Measurement & Control v105
pp232-237 (Dec. 1983).
- 111 Discrete Fourier Transform Methods for Transient Structural Dynamic
Analysis.
Burgess A. Imperial College, Dept. Mech.Eng.
Dynamics Section Rept. No
860011 (May 1986).
- 112 Forming the Fast Fourier Transform of a Step Response in Time Domain
Metrology.
Nicolson A. M. Electronic Letters 12
(July 1973).

- 113 The Impulse Response Function of a Single-Degree-of-Freedom system with Hysteretic Damping.
Milne H. K. J. Jnl. Sound & Vibration v100(4)
pp590-593 (1985).
- 114 An introduction to the Analysis and Processing of Signals.
Lynn P. A. Macmillan Press (1977).
- 115 Estimation of Damping from Response Spectra.
Seybert A. F. Jnl. Sound & Vibration v75(2)
pp199-206 (1981).
- 116 Reconciliation of Non-Linearity and Measured Modal Properties of Structures.
Sidhu J. Imperial College, Dept. Mech. Eng.
Dynamics Section Contract Rept.
No 8303 (Oct. 1983).
- 117 Simulation of Nonlinearity on an Analogue Computer.
He J. Imperial College, Dept. Mech. Eng.
Dynamics Section Rept. No 84004
(Sept. 1984).
- 118 The Modal Analysis of Non-Linear Structures Employing the Hilbert Transform.
Kirk N. E. PhD Thesis Univ. Manchester
(1985).
- 119 Modal Testing and the Linearity of Structures.
Ewins D. J. & Sidhu J. *Mechanique Materiaux Electricite*
(May, June, July 1982).

- 120 Comparison of Excitation Signals: Sensitivity to Non-Linearity and Ability to Linearize Dynamic Behaviour.
Frachebourg A. & Gygan P. E. Int. Seminar on Modal Analysis (1985).
- 121 Experimental Determination of the Effect of Non-Linear Stiffness on the Vibration of Elastic Structures.
Mayman G. & Rechfiel L. W. 26th Israel Annual Conf. on Aviation & Aeronautics (8/9 Feb. 1984).
- 122 A Simple Theoretical and Experimental Study of the Force Characteristics from **Electrodynamic** Exciters on Linear and Non-Linear Systems.
Tomlinson G. R. Proc. Int. Modal Analysis Conf. London (1987).
- 123 Vibration Analysis and Identification of Non-Linear Structures.
Tomlinson G. R., Vinh T. & D Goyder H. G. D. Univ. Manchester SEL Short Course Notes (23-25 Sept. 1985).
- 124 Experimental Modal Analysis of Non-Linear Systems: A Feasibility Study.
Busby H. R., Nopporn C. & Singh R. Jnl. Sound & Vibration v108(3) pp415-427 (1986).
- 125 Detection, Identification and Quantification of Nonlinearity in Modal Analysis - A Review.
Tomlinson G. R. Proc Int. Modal Analysis Conf. Los Angeles, CA (1986).
- 126 A New Method of Interpretation for the Modal Analysis of Non-Linear Systems.
He J. Imperial College, Dept. Mech. Eng. Dynamics Section Rept. No 86008 (Oct. 1986).

- 127 Modal Tests on Vibration Isolators.
Robb D. A., Hillary B. Ewins D. J. & Imperial College, Dept. **Mech.** Eng.
Dynamics Section Contract Rept.
No 8402 (March 1984).
- 128 Identification, Classification and Treatment of Non-Linear Systems.
Burgess A. Imperial College, Dept. **Mech.** Eng.
Dynamics Section Rept. No 86010
(March 1986).
- 129 Dynamic Non-Linear Behaviour of Mechanical Structures.
Chouychai T. These de Docteur-Ingenieur
ISMCM (Paris 1986).
- 130 Some Applications of the Hilbert Transform to Non-Linear Systems.
Haoui A., Vinh T., Simon M. & ISMCM Paris and Univ.
Tomlinson G. R. Manchester
- 131 Application of Hilbert Transform in the Analysis of Non-Linear Structures.
Haoui A., Vinh T. & Chevalier Y. Research Note ISMCM, Paris.
- 132 Use of the Hilbert Transform in Modal Analysis of Linear and Non-Linear
Structures.
Simon M. & Tomlinson G. R. Jnl. Sound & Vibration **v96(4)**
pp421-436 (1984).
- 133 On the Identification of Non-Linearities in Modal Testing Employing the
Hilbert Transform.
Tomlinson G. R. and Kirk N. E. 8th International Seminar on
Modal Analysis, Leuven (1983).

- 134 Modal Analysis and the Identification of Structural Non-Linearity.
Tomiinson G. R., Kirk N. K. & Blair M. A. **Proc.** 2nd Int. Conf. on recent advances in structural dynamics I.S.V.R Univ. Southampton (April 1984).
- 135 Transient Response of a Friction Element.
Burgess A. **ARE(Portland) DN(UJI)86157** (Oct. 1986).
- 136 Numerical Transient Predictions of Forced, Non-Linear Single Degree of Freedom Systems.
Thompson R. M. & Burgess A. **ARE(Portland) DN(UJI)86158** (Nov. 1986).

APPENDIX 1 Summary of essential modal theory

The theory presented in this appendix is a brief summary of the development of modal analysis, and is found in literature on the subject. This section has been included to support the sections in the thesis where these methods have been used.

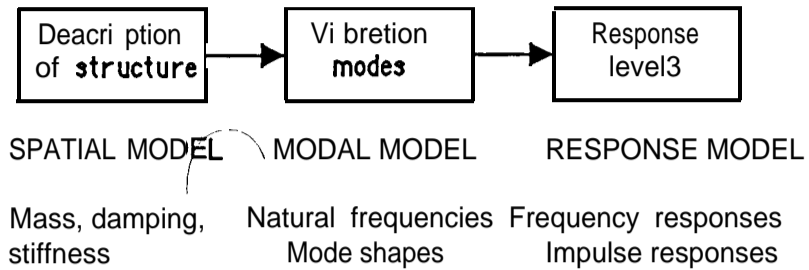


Fig (A1.1) Theoretical route to vibration analysis

Fig (A1.1) sets out the steps in theoretical modal analysis. This procedure will now be followed for a single-degree-of-freedom (SDOF) undamped model, with extensions for the damped models and multi-degree-of-freedom (MDOF) systems.

SDOF undamped spatial model



Fig (A1.2) SDOF undamped spatial model

First consider the system with no external forcing

$$m\ddot{x} + kx = 0$$

SDOF undamped modal model

The solution $x(t) = xe^{i\omega t}$ leads to the requirement that $(k - \omega^2 m) = 0$. The modal model for this system consists of a single mode of vibration with a natural frequency ω_0 given by $(k/m)^{1/2}$.

SDOF undamped response model

Consider now the forced system where $f(t) = fe^{i\omega t}$:

$$m\ddot{x} + kx = fe^{i\omega t}$$

and a solution of the form $x(t) = xe^{i\omega t}$, where x and f are complex to accommodate both phase and amplitude information.

$$(k - \omega^2 m)x e^{i\omega t} = fe^{i\omega t}$$

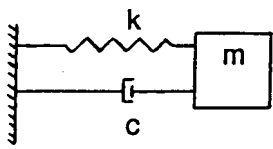
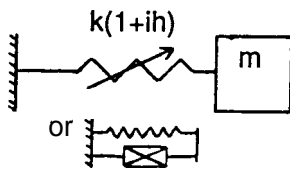
The frequency response function (FRF) is the response model and takes the form:-

$$\frac{x}{f} = \frac{1}{k - \omega^2 m}$$

= $\alpha(\omega)$ the system receptance FRF

Damped SDOF models

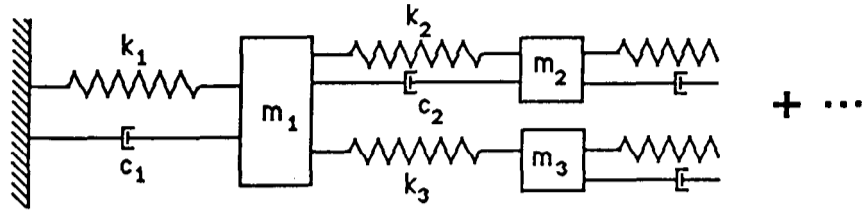
There are two linear damping models ^{that} can be used in vibration analysis. These are viscous and hysteretic (or structural) damping

| | Viscous | Hysteretic |
|----------------|---|---|
| Spatial model |  $m\ddot{x} + c\dot{x} + kx = f(t)$ |  $m\ddot{x} + k(1+ih)x = f(t)$ |
| Modal model | setting $f(t) = 0$ leads to $x = e^{-\zeta\omega_0 t} e^{i\omega_d t}$ where $\omega_d = \omega_0 \sqrt{1 - \zeta^2}$ $\omega_0 = \sqrt{k/m}$ $\zeta = c / (2\sqrt{km})$ | |
| Response model | using $f(t) = fe^{i\omega t}$ leads to $\alpha(\omega) = \frac{1}{(k - \omega^2 m) + i(\omega c)}$ | using $f(t) = fe^{i\omega t}$ leads to $\alpha(\omega) = \frac{1}{(k - \omega^2 m) + i(h)}$ |

MDOF systems

The solutions for MDOF systems are similar in appearance to a SDOF system, but the elements are replaced by matrices.

Spatial model



$$[M]\{\ddot{x}(t)\} + [C]\{\dot{x}(t)\} + [K]\{x(t)\} = \{f(t)\}$$

Modal model

To obtain the modal model ($f(t)$ is set to zero). The solution takes the form $\{x(t)\} = \{x\}e^{i\omega t}$ and for the undamped system ($[C]=0$) this leads to the condition

$$\det [[K] - \omega^2[M]] = 0$$

For an N DOF system, N values of ω^2 are obtained and also N sets of relative values for $\{x\}$ can be calculated. These can be usually written as two matrices

$$\left. \begin{array}{l} [\omega_r^2] \text{ Natural frequency squared (eigenvalues)} \\ [\psi] \text{ Mode shapes (eigenvectors)} \end{array} \right\} \begin{array}{l} \text{Modal} \\ \text{model} \end{array}$$

Response models

Using the function $\{f(t)\} = \{f\}e^{i\omega t}$ and assuming a solution of the form $\{x(t)\} = \{x\}e^{i\omega t}$, for the undamped case the equations are:-

$$([K] - \omega^2[M])\{x\} = \{f\}$$

$$\text{or } \{x\} = ([K] - \omega^2[M])^{-1} \{f\}$$

Now $([K] - \omega^2[M])^{-1}$ can be written as $[a(\omega)]$ and is known as the response model. By matrix manipulation the individual parameters of the response model can be expressed as:-

$$\alpha_{jk}(\omega) = \sum_{r=1}^N \frac{rA_{jk}}{\omega_r^2 - \omega^2}$$

where rA_{jk} is the r^{th} modal constant and is the product of the r^{th} mode shape vectors from coordinates j and k .

If proportional damping is introduced (ie $[\text{damping}] = \beta[K] + \gamma[M]$) then the general FRF expressions are:-

$$\alpha_{jk}(\omega) = \sum_{r=1}^N \frac{rA_{jk}}{(k_r - \omega^2 m_r) + i(\omega c_r)} \quad \text{Viscous damping}$$

$$\alpha_{jk}(\omega) = \sum_{r=1}^N \frac{rA_{jk}}{(k_r - \omega^2 m_r) + i(h_r)} \quad \text{Hysteretic damping}$$

where the denominator is now complex ie complex eigenvalues, but the mode shapes are the same as the undamped model.

For general damping the expressions are similar, but in both cases the numerator is complex, and for viscous damping the modal constant is also a function of frequency.

Different forms of the FRF

The three main forms of FRF use displacement, velocity or acceleration.

$$\frac{\text{Displacement}}{\text{Force}} = \text{Receptance} = [\alpha(\omega)]$$

$$\frac{\text{Velocity}}{\text{Force}} = \text{Mobility} = i \omega [\alpha(\omega)] = [Y(\omega)]$$

$$\frac{\text{Acceleration}}{\text{Force}} = \text{Accelerance} = i \omega [Y(\omega)] = -\omega^2 [\alpha(\omega)] = [A(\omega)]$$

In all three cases the definition for a single element also states that all other forces to the system must be zero, ie

$$\alpha_{jk} = \left(\begin{array}{c} x_j \\ f_k \end{array} \right)_{f=0, m=1, N; \neq k}$$

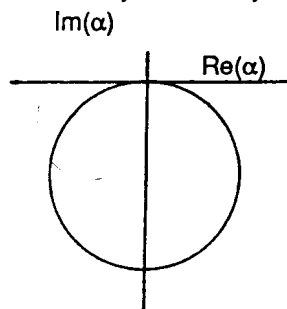
APPENDIX 2 Summary of SDOF modal analysis methods

This appendix covers the theoretical development of two SDOF modal analysis methods. These are the Nyquist circle fit method, and the reciprocal-of-receptance analysis. The Nyquist method is covered in much of the literature on modal analysis (eg ref [64] to [66] & [69]) and is included for information. The techniques behind the reciprocal-of-receptance method are exploited in some of the applications to non-linear analysis.

Nyquist circle fit

The Nyquist circle for two particular cases - mobility for the viscously damped system and receptance for a hysteretically damped system - trace out exact circles for SDOF systems.

For the hysteretically damped case:-



$$a(\omega) = \frac{1}{k - \omega^2 m + ih} = \frac{k - \omega^2 m - ih}{(k - \omega^2 m)^2 + h^2}$$

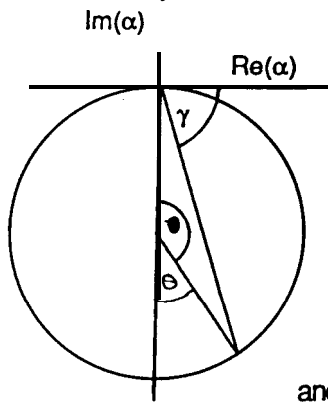
$$\text{Re}(\alpha) = \frac{k - \omega^2 m}{(k - \omega^2 m)^2 + h^2} ; \text{Im}(\alpha) = \frac{-h}{(k - \omega^2 m)^2 + h^2}$$

$$\Rightarrow (\text{Re}(\alpha))^2 + (\text{Im}(\alpha) + 1/2h)^2 = (1/2h)^2$$

Hence plots of $\text{Re}(\alpha)$ against $\text{Im}(\alpha)$ will trace out a circle of radius $1/2h$ and centre $(0, -1/2h)$. Similar analysis can be made for the system with viscous damping using the mobility FRF data and results in a circle of radius $(1/2c)$ and centre $(1/2c, 0)$.

Natural frequency estimation

For the system with hysteretic damping:-



$$a(\omega) = \frac{1}{\omega_r^2(1-(\omega/\omega_r)^2)+i\eta_r}$$

(The modal constant scales the circle, and rotates it if complex)

$$\tan \gamma = \frac{\eta_r}{1-(\omega/\omega_r)^2}$$

$$\tan (90-\gamma) = \tan (e/2) = (1-(\omega/\omega_r)^2)/\eta_r$$

$$\omega^2 = \omega_r^2 (1 - \eta_r \tan (\theta/2))$$

and
$$\frac{d\omega^2}{d\theta} = \frac{-\omega_r^2 \eta_r}{2} (1 + (1-(\omega/\omega_r)^2)^2 / \eta_r^2)$$

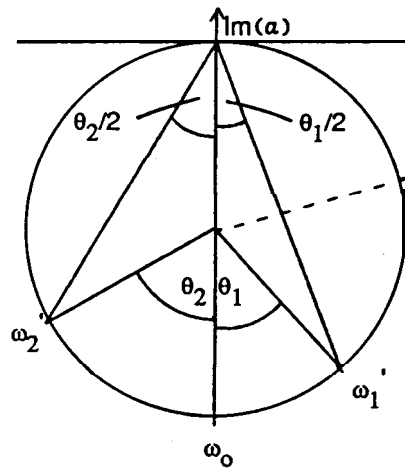
The reciprocal of this quantity - which is a measure of the rate at which the locus sweeps around the arc - may be shown to reach a maximum value (maximum sweep rate) when $\omega = \omega_r$. The natural frequency of the system. This is shown by further differentiation, this time with respect to frequency:-

$$\frac{d}{d\omega(d\omega^2/d\theta)} = 0 \text{ when } (\omega_r^2 - \omega^2) = 0$$

This property can be used to estimate the natural frequency by examining the relative spacing of linearly spaced data points around resonance. A similar analysis can be made for viscous damping on the mobility plot.

Damping estimates

Once the natural frequency has been located at the position of maximum sweep rate, the damping can be estimated. Working through with hysteretic damping and using the receptance plot:-



$$\text{Re}(\alpha) \quad \alpha(\omega) = \frac{1}{k - \omega^2 m + ik\eta}$$

$$\text{Now } \tan(\theta_1/2) = \frac{k - (\omega_1')^2 m}{k\eta}$$

$$\text{and } -\tan(\theta_2/2) = \frac{k - (\omega_2')^2 m}{k\eta}$$

which leads to

$$\eta = \left(\frac{(\omega_2')^2 - (\omega_1')^2}{(\omega_0)^2} \right) \left(\frac{1}{\tan(\theta_1/2) + \tan(\theta_2/2)} \right)$$

As can be seen different combinations of frequency points above and below resonance can be used to provide a damping estimate. For a linear system these values will all be the same, but by examining the 3-D damping plot, any errors are easily classified as random (for instance due to noise on the signals) or systematic (for example due to incorrect location of the natural frequency or non-linearities in the system). The values obtained for the damping ratios can be averaged to find a single value or, after examining the 3-D damping plot, a weighted average can be used.

Summary of Nyquist analysis procedure

Locate the natural frequency: $(\omega_0 = (k/m)^{1/2})$

Calculate damping ratio: $(\eta = h/k)$

Find the Nyquist circle radius: (diameter = l/h)

Hence all values can be determined. In the case of the SDOF system these m , k and h relate to the physical model, but in the MDOF systems they relate to the modal model, and usually the modal constant is calculated from the Nyquist diameter which can also be expressed as:-

$$A/\omega_0^2\eta$$

This procedure can also be followed for systems with viscous damping. In this case the damping expression in terms of frequency points above and below resonance is:-

$$\zeta = \frac{(\omega_2')^2 - (\omega_1')^2}{2\omega_0} \left(\frac{1}{\omega_1' \tan(\theta_1/2) + \omega_2' \tan(\theta_2/2)} \right)$$

and the mobility Nyquist circle radius is:-

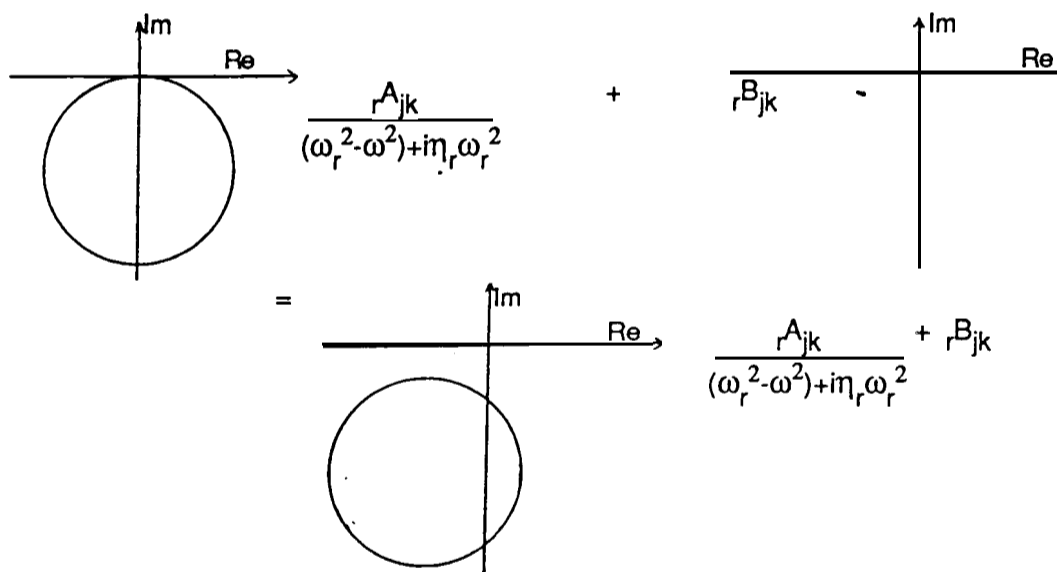
$$A/2\omega_0\zeta$$

MDOF systems

Applying this SDOF technique to MDOF systems the assumption is made that in the vicinity of resonance the response is dominated by that single mode. For the r^{th} mode this means that-

$$\alpha_{jk}(\omega) = \frac{rA_{jk}}{(\omega_r^2 - \omega^2) + i\eta_r\omega_r^2} + rB_{jk} \quad (\text{in the vicinity of the } r^{\text{th}} \text{ mode})$$

The contribution of other modes in this region is approximated by a single term which has the effect of displacing the Nyquist circle for the r^{th} mode. This is shown in pictorial form.



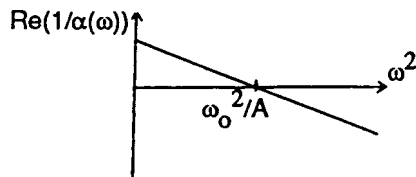
Reciprocal-of-receptance analysis

Using the receptance FRF;

$$a(o) = \frac{A}{(\omega_o^2 - \omega^2) + 2i\omega\omega_o\zeta}$$

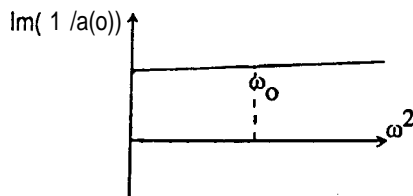
$$\frac{1}{\alpha(\omega)} = \frac{(\omega_o^2 - \omega^2) + 2i\omega\omega_o\zeta}{A}$$

$$\text{Re}(1/\alpha(\omega)) = \frac{(\omega_o^2 - \omega^2)}{A}$$



Which on a plot of $\text{Re}(1/\alpha(\omega))$ against ω^2 has a slope of $-1/A$ and crosses the axis at ω_o^2/A

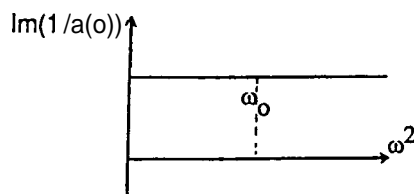
$$\text{Im}(1/\alpha(\omega)) = \frac{2\omega\omega_o\zeta}{A}$$



In the vicinity of resonance this approximates to a straight line when plotted against ω^2 , and at $\omega = \omega_o$ the value is $2\omega_o^2\zeta/A$; ω_o and A being calculated from the $\text{Re}(1/\alpha(\omega))$ plot hence η can be evaluated.

For hysteretic damping

$$\text{Im}(1/\alpha(\omega)) = \frac{\omega_o^2\eta}{A}$$



Which is a straight line, and knowing ω_o^2 and A from the $\text{Re}(1/\alpha(\omega))$ plot, η can be calculated.

APPENDIX 3 MDOF curve fitting for lightly damped structures

This appendix describes the theory behind an MDOF curve fitting routine for lightly damped structures (ref [77]), that is often referred to as 'Ident' analysis.

Starting with an undamped model:-

$$\alpha_{ij}(\omega) = \sum_{r=1}^N \frac{P_{ij}}{\omega_r^2 - \omega^2}$$

The receptance can be recorded at specific frequency values from the FRF curve, and the resonance frequencies can also be located. The receptance can then be written as:-

$$\alpha_{ij}(\Omega_1) = \left\{ (\omega_1^2 - \Omega_1^2)^{-1} \quad (\omega_2^2 - \Omega_1^2)^{-1} \quad \dots \right\} \begin{Bmatrix} 1A_{ij} \\ 2A_{ij} \\ \dots \\ \dots \\ \dots \end{Bmatrix}$$

Once the resonances have been located, N other FRF measurements are chosen where N is the number of resonances plus 2 (to account for the residuals).

$$\begin{Bmatrix} \alpha_{ij}(\Omega_1) \\ \alpha_{ij}(\Omega_2) \\ \dots \\ \dots \\ \dots \\ \alpha_{ij}(\Omega_N) \end{Bmatrix} = \begin{vmatrix} (\omega_1^2 - \Omega_1^2)^{-1} & (\omega_2^2 - \Omega_1^2)^{-1} & \dots \\ (\omega_1^2 - \Omega_2^2)^{-1} & (\omega_2^2 - \Omega_2^2)^{-1} & \dots \\ \dots & \dots & \dots \\ \dots & \dots & \dots \\ \dots & \dots & \dots \\ (\omega_1^2 - \Omega_N^2)^{-1} & (\omega_2^2 - \Omega_N^2)^{-1} & \dots \end{vmatrix} \begin{Bmatrix} 1A_{ij} \\ 2A_{ij} \\ \dots \\ \dots \\ \dots \\ NA_{ij} \end{Bmatrix}$$

Now all of the $\alpha(\Omega)$ values are known and the corresponding frequency also, the resonance frequencies are known. This leads to :-

$$[A_{ij}] = [R]^{-1}[\alpha_{ij}(\Omega)]$$

from which the modal constants can be calculated.

Returning to the damped model - using a generalised damping term:

$$\alpha_{ij}(\omega) = \sum_{r=1}^N \frac{P_{ij}}{\omega_r^2 - \omega^2 + iD_r}$$

at resonance assume that the response is due to that mode only

$$\alpha_{ij}(\omega_r) = \frac{rA_{ij}}{\omega_r^2 - \omega_r^2 + iD_r}$$

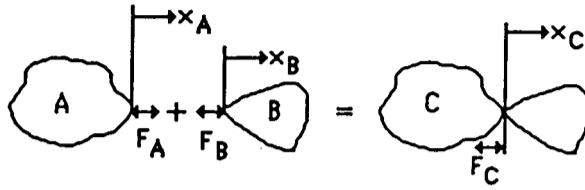
which is:-

$$\alpha_{ij}(\omega_r) = \frac{rA_{ij}}{iD_r}$$

rA_{ij} has been calculated, and $\alpha_{ij}(\omega_r)$ has been recorded from the FRF curve, so the damping term can now be calculated.

APPENDIX 4 Basic impedance coupling theory

The theory behind impedance coupling is briefly summarised in this appendix to provide a reminder to the parameters required when using this technique to form a single response model from several models from different components.



The excitations and responses are related by:-

$$x_A = F_A \alpha_A$$

$$x_B = F_B \alpha_B$$

$$x_C = F_C \alpha_C$$

When A and B are connected

$$x_A = x_B = x_C$$

and

$$F_A + F_B = F_C$$

which leads to

$$\frac{1}{\alpha_C} = \frac{1}{\alpha_A} + \frac{1}{\alpha_B}$$

This can be extended to MDOF systems for coupling, and this now becomes:-

$$[\alpha_C]^{-1} = [\alpha_A]^{-1} + [\alpha_B]^{-1}$$

APPENDIX 5 Free decay for systems with viscous or hysteretic damping

This section is included to show how the two different forms of linear damping have the same relationship for free decay as they do at resonance for steady state response.

Starting with the equation of motion for viscous damping:

$$\ddot{x} + 2\zeta\omega_0\dot{x} + \omega_0^2x = (\text{forcing function})$$

assume a solution of the form $\{x\} = \{X\}e^{st}$

which leads to the familiar solution

$$s = -\zeta\omega_0 \pm i\omega_0\sqrt{1-\zeta^2}$$

or

$$\{x\} = \{X\}e^{-\zeta\omega_0 t} (\cos(\omega_0\sqrt{1-\zeta^2}t) + i \sin(\omega_0\sqrt{1-\zeta^2}t))$$

The same procedure can be followed for hysteretic damping even though the solution evaluated is for free vibration and hysteretic damping is only defined for forced harmonic vibration.

Starting with the equation of motion for hysteretic damping:

$$\ddot{x} + \omega_0^2(1+i\eta)x = (\text{forcing function})$$

assume a solution of the form $\{x\} = \{X\}e^{\lambda t}$

where λ is complex.

This leads to

$$\lambda^2 + \omega_0^2(1+i\eta) = 0$$

or

$$\lambda = \pm i\omega_0\sqrt{1+i\eta}$$

Now let $\lambda = a + ib$

$$\therefore \lambda^2 = a^2 - b^2 + 2iab$$

Also

$$\lambda^2 = -\omega_o^2(1+i\eta)$$

$$\therefore a^2 - b^2 = -\omega_o^2$$

$$\text{and } 2ab = -\omega_o^2\eta$$

from which

$$b = -\omega_o^2\eta/2a$$

$$\therefore 4a^4 + 4a^2\omega_o^2 - \omega_o^4\eta^2 = 0$$

$$\Rightarrow a = -\omega_o \left(\frac{\sqrt{1+\eta^2} - 1}{2} \right)^{1/2}$$

Expanding this equation leads to

$$a = -\omega_o\eta/2 + \omega_o\eta^3/16 - \dots\dots\dots$$

The estimated value of damping in most structures is such that the second term is negligible. This leads to:-

$$a \approx -\omega_o\eta/2 \quad (0.125\% \text{ error with } \eta = 0.1)$$

and

$$b = \omega_o \text{ from above } \quad (0.125\% \text{ error with } \eta = 0.1)$$

Substituting the values for a and b in the solution leads to

$$\{x\} \approx \{X\}e^{-(\eta/2)\omega_o t}(\cos \omega_o t + i \sin \omega_o t)$$

Comparing this with the solution for viscous damping shows that for the decay

$$\text{term } -\zeta\omega_o = -(\eta/2)\omega_o$$

$$\therefore \zeta = \eta/2$$

This is the same relationship as is derived for the two forms of damping using energy considerations for systems subjected to steady state vibration and at resonance frequency.

APPENDIX 6 Determination of friction damping from reciprocal-of-receptance analysis

This section is included to demonstrate how different forms of damping can be determined from a single frequency response measurement, when the input force level is known, using an adaption of the reciprocal-of-receptance analysis method.

Starting with the receptance equation for a system with friction from the equivalent linearised equation of motion:-

$$\alpha(\omega) = \frac{A}{\omega_0^2 - \omega^2 + 2i\zeta\omega\omega_0 + 4Ri\omega/\pi\omega_0}$$

Examining the inverse of this equation and splitting into real and imaginary parts leads to:

$$\text{Re}(1/\alpha) = (\omega_0^2 - \omega^2) / A \quad (\text{as in linear case})$$

$$\text{Im}(1/\alpha) = \frac{2\omega\omega_0\zeta}{A} + \frac{4R\omega}{A\pi\omega_0 a}$$

Now 'a', the amplitude, can be written as αF (where F is the input force level).

If two values of $\text{Im}(1/\alpha)$ are taken from a single plot from a constant input force stepped-sine excitation then R can be calculated as follows:

$$\text{Im}(1/\alpha)_1 = \frac{2\omega_1\omega_0\zeta}{A} + \frac{4R\omega_1}{A\pi\omega_0\alpha_1 F} \quad (\text{a6.1})$$

similarly

$$\text{Im}(1/\alpha)_2 = \frac{2\omega_2\omega_0\zeta}{A} + \frac{4R\omega_2}{A\pi\omega_0\alpha_2 F} \quad (\text{a6.2})$$

Multiply 1 by ω_2 and 2 by ω_1 then subtract to give:-

$$\omega_2 \operatorname{Im}(1/\alpha)_1 - \omega_1 \operatorname{Im}(1/\alpha)_2 = \frac{4R\omega_1 \omega_2}{A\pi\omega_0 F} \left(\frac{1}{a} - \frac{1}{\alpha_2} \right)$$

where F is the constant excitation force amplitude

and $1/\alpha_1$ and $1/\alpha_2$ are the reciprocals of the magnitude of receptance (not just the real or the imaginary part).

This information is available from one receptance curve. Having calculated R using the equation above, this value can then be used to calculate the viscous damping in the system from either (a6.1) or (a6.2). A similar analysis can be performed for systems with quadratic viscous damping which again enables the two forms of damping in a system to be evaluated separately.

APPENDIX 7 Development of non-linear model for the transient response prediction of a friction element (ref [135])

This is a brief summary of the results developed in ref [135] for the transient response prediction of a friction element.

The results were obtained by observation of the time-histories of a system with friction and viscous damping subjected to an impulse, and an equation derived that uses the system parameters that can be calculated (modal constant, natural frequency, viscous damping, friction and the initial conditions). This equation was then analytically transformed to the frequency domain to provide the non-linear frequency response function for use in the transient response prediction of a system with friction. The equation is:-

$$\begin{aligned} \alpha(\omega) = & \frac{1}{\omega_d} \left[\frac{A\omega_d}{(\omega_o^2 - \omega^2 + 2i\omega\omega_o\zeta)} + \frac{Ae^{(-i\omega - \zeta\omega_o)T} ((-i\omega - \zeta\omega_o) \sin \omega_d T - \omega_d \cos \omega_d T)}{(\omega_o^2 - \omega^2 + 2i\omega\omega_o\zeta)} \right. \\ & - \frac{BTe^{(-i\omega - \zeta\omega_o)T} ((-i\omega - \zeta\omega_o) \sin \omega_d T - \omega_d \cos \omega_d T)}{2(\omega_o^2 - \omega^2 + 2i\omega\omega_o\zeta)} + \frac{B\omega_d(-i\omega - \zeta\omega_o)}{(\omega_o^2 - \omega^2 + 2i\omega\omega_o\zeta)^2} \\ & + \frac{Be^{(-i\omega - \zeta\omega_o)T} ((\omega_o^2 - \omega^2 + 2i\omega\omega_o\zeta - 2\omega_d^2) \sin \omega_d T - 2(-i\omega - \zeta\omega_o)\omega_d \cos \omega_d T)}{2(\omega_o^2 - \omega^2 + 2i\omega\omega_o\zeta)^2} \\ & - \frac{B(1-2\pi\zeta)2i\omega\omega_d}{2(\omega_d^2 - \omega^2)^2} - \frac{B(1-2\pi\zeta)Te^{-i\omega T}(-i\omega \sin \omega_d T - \omega_d \cos \omega_d T)}{2(\omega_d^2 - \omega^2)} \\ & \left. - \frac{B(1-2\pi\zeta)e^{-i\omega T}((\omega_d^2 + \omega^2) \sin \omega_d T - 2i\omega\omega_d \cos \omega_d T)}{2(\omega_d^2 - \omega^2)^2} \right] \end{aligned}$$

where $a(0)$ is the response divided by the input force

ω_0 is the undamped natural frequency

ζ is the damping ratio

ω_d is the damped natural frequency ($\omega_d = \omega_0 \sqrt{1 - \zeta^2}$)

A is the modal constant multiplied by the initial velocity

A is friction force/stiffness (m); the 'dead zone'

B is $2\omega_0^2 \Delta / \pi$ multiplied by the modal constant

and T satisfies $2Ae^{-\zeta\omega_0 T} - BTe^{-\zeta\omega_0 T} - BT + 2\pi B\zeta T = 0$

Using the 'Fourier transform method' with this non-linear frequency response function generates good predictions, and examples are shown in chapter 6 in fig (6.10).